Contribution of Glucose Metabolism to the B Lymphocyte Responses

Author: Fay Josephine Dufort

Boston College

The Graduate School of Arts and Sciences

Department of Biology

CONTRIBUTION OF GLUCOSE METABOLISM TO THE B LYMPHOCYTE RESPONSES

by

FAY JOSEPHINE DUFORT

submitted in partial fulfillment of the requirements

for the degree of

Doctor of Philosophy

August 2012

Title: CONTRIBUTION OF GLUCOSE METABOLISM TO THE B LYMPHOCYTE RESPONSES.

Author: Fay J. Dufort

Advisor: Thomas C. Chiles, PhD.

Abstract

B-lymphocytes respond to environmental cues for their survival, growth, and differentiation through receptor-mediated signaling pathways. Naïve B-lymphocytes must acquire and metabolize external glucose in order to support the bioenergetics associated with maintaining cell volume, ion gradients, and basal macromolecular synthesis. The up-regulation of glycolytic enzyme expression and activity via engaged B-cell receptor mediated-events was glucose-dependent. This suggests an essential role for glucose energy metabolism in the promotion of B cell growth, survival, and proliferation in response to extracellular stimuli. In addition, the activity of ATP-citrate lyase (ACL) was determined to be crucial for *ex vivo* splenic B cell differentiation to antibody-producing cells wherein B cells undergo endomembrane synthesis and expansion. This investigation employed knockout murine models as well as chemical inhibitors to determine the signaling components and enzymes responsible for glucose utilization and incorporation into membrane lipids. These results point to a critical role for phosphatidylinositol 3-kinase (PI3K) in orchestrating cellular glucose energy metabolism and glucose-dependent *de novo* lipogenesis for B lymphocyte responses.

Table of Contents

Acknowledgements

Much thanks to my family, the BC biology department, and the many members of the Chiles' laboratory that have made this experience a wonderful one. Most especially, I would like to thank Tom for his support, patience, and advice throughout the years. It has been a blessing and I am deeply grateful to have worked in his laboratory. Thank you all for all your kindness, support, and generosity.

Abbreviations

2-DOG: 2-deoxy-$_D$-glucose
2DG: 2-deoxy-$_D$-glucose
5TG: 5-thioglucose
6-ANA: 6-aminonicotinamide
^{13}C-U-glucose: ^{13}C-uniformly labeled-glucose
^{13}C-U-glutamine: ^{13}C-uniformly labeled-glutamine
[^{14}C]-U-glucose: [^{14}C]-uniformly labeled-glucose
18S rRNA: 18 Svedberg units ribosomal RNA
A549: adenocarcinomic human alveolar basal epithelial cells
Ab: antibody
ACC: acetyl-CoA carboxylase
Aceto-acyl CoA: acetoacetyl-coenzyme A
Acetyl-CoA: acetyl-coenzyme A
ACL: ATP citrate lyase
αIg: fragment antigen-binding region F(ab')$_2$ of Immunoglobulin M
Akt: alpha-ketoglutarate mouse strain spontaneous thymic lymphoma protein
Anti-hsp90: antibody recognizing heat shock protein 90
AP1: activator protein 1
ATP: adenosine-5'-triphosphate
au: arbitrary unit
B-1: peritoneal B lymphocytes
B_{reg}: regulatory B lymphocytes
B-2: conventional splenic B lymphocytes
B220: a molecular form of CD45
BAD: Bcl-2-associated death promoter protein
Bax: Bcl-2–associated X protein
bcl-2: B-cell lymphoma 2 gene
bcl-xl: B-cell lymphoma-extra large gene
BCR: B-cell receptor
Bfl-1: B-cell leukemia/lymphoma 2 related protein A1a
Blimp-1/PRDM1: B lymphocyte-induced maturation protein-1/positive regulatory domain I element binding protein
BLNK: B-cell linker protein
β-ME: beta-mercaptoethanol
BP: 3-bromopyruvate
bp: base pair
BSA: bovine serum albumin
BTK: Bruton's tyrosine kinase
C: cholesterol
C14:0: myristic acid
C16:0: palmitic acid
C16:1: palmitoleic acid

C17:0: heptadecanoic acid or margaric acid
C18:0: stearic acid
C18:1: oleic acid
C18:2: linoleic acid
C20:0: arachidic acid
C-9: compound-9, 2-hydroxy-*N*-arylbenzenesulfo-namide 9
c-myc: myelocytomatosis oncogene
CB: cerebroside
CD23: cluster of differentiation marker number 23, also known as Fc epsilon-receptor II
CD34: cluster of differentiation marker for hematopoietic progenitor cell antigen number 34
CD40: cluster of differentiation marker number 40
CD40L: cluster of differentiation marker number 40 ligand
CD45: cluster of differentiation marker number 45 for leukocyte-common antigen of nucleated haematopoietic cells
CDP: cytidine diphosphate
CE: cholesterol ester
CEPT: choline/ethanolamine-phosphotransferase
CH12.lx: inducible murine lymphoma cell line
CL: cardiolipin
CM: ceramide
CoA: coenzyme A
cpm: counts per minute
CPT/CPT-1A: Carnitine palmitoyltransferase I isoform A
C_T: cycle threshold
D-J: Diverse and Joining gene segments recombination of the heavy chain locus
DAG: diacylglycerol
ΔΔCT: DeltaDeltaC_T= C_t for an RNA or DNA from the gene of interest divided by C_t of RNA/DNA from a housekeeping gene
DEAE-Sephadex: diethylaminoethanol-Sepharose
dpm: disintegrations per minute
DT40: avian leukosis virus-transformed chicken immature B lymphocyte cell line
DTT: dithiothreitol
ECL: enhanced chemiluminescence
EDTA: ethylenediaminetetraacetic acid
EGTA: ethylene glycol tetraacetic acid
eIF4E: eukaryotic translation initiation factor 4E
ER: endoplasmic reticulum
FAMES: fatty acid methyl esters
FAS: fatty acid synthase
Fc: fragment crystallizable region
FCS: fetal calf serum
FFA: free fatty acid
FITC: fluorescein isothiocyanate

FL5.12: IL-3-dependent mouse pro/pre-B cell line
Foxo1: forkhead box protein O1
FSC-A: forward scatter–area
G1: Gap 1 phase of the cell cycle
g6pd: glucose-6-phosphate dehydrogenase
GA2: monosialo-ganglioside
γc chain: common gamma chain receptor sub-unit
GC-MS: gas chromatography-mass spectrometry
glut-1: facilitated glucose transporter member 1
GSK3: glycogen synthase kinase-3
GSL: glycosphingolipids
H-2^k: mouse histocompatibility locus (H2) class II genes mapped to *H2K*
H-2^d: mouse histocompatibility locus (H2) class II genes mapped to *H2D*
HEPES: 4-(2-hydroxyethyl)-1-piperazineethanesulfonic acid
HepG2: hepatocellular carcinoma cell line
hk: hexokinase
HMG-CoA: 3-hydroxy-3-methyl-glutaryl- coenzyme A
HP-TLC: high performance-thin layer chromatography
hr: hour
HRP: horseradish peroxidase
IAN: iodoacetamide
IAP1/2: inhibitors of apoptosis 1 and 2
IC_{50}: half maximal inhibitory concentration
ICC: fluorescent immunocytochemistry
IFNβ: interferon-beta
IgA: immunoglobulin isotype A
Igα/β: immunoglobulin alpha and beta heterodimers associated with mIg to form the intracellular portion of BCR
IgG: immunoglobulin isotype G
IgG1: immunoglobulin isotype G 1
IgH: immunoglobulin heavy chain subunit of an antibody
IgE: immunoglobulin isotype E
IgM: immunoglobulin isotype M
IgL: immunoglobulin light chain kappa and lambda chains of an antibody
IκB: inhibitor of kappa B protein
IKK: inhibitory protein inhibitor of kappa B protein kinase
IL1R: interleukin-1 receptor
IL-4: cytokine interleukin-4
IL-4/13Rα: interleukin-4 or interleukin-13 receptor alpha chain
IL-10: cytokine interleukin-10
IL-13: cytokine interleukin-13
Iono: ionomycin
IP3: inositol 1,4,5-trisphosphate
IRAK1: interleukin-1 receptor-associated kinase 1

IRAK4: interleukin-1 receptor-associated kinase 4
IRF1: interferon regulatory factor 1
IRF3: interferon regulatory factor 3
IRF4: Interferon regulatory factor 4
IRS2: insulin receptor substrate 2
ITAMs: immunoreceptor tyrosine activation motifs
JAK1/3: janus kinase isoform 1 or 3
JNK: c-jun N-terminal kinases
Ki: binding affinities, dissociation constant
KO: knock-out
ldh: lactate dehydrogenase
LPC: lysophosphatidylcholine
LPS: lipopolysaccharide
LY: LY294002, 2-morpholin-4-yl-8-phenylchromen-4-one
LYN: lck/yes-related novel protein tyrosine kinase of the SRC-family
μ: microns
mAb: monoclonal antibodies
malonyl-CoA: malonyl-coenzyme A
MAP: mitogen-activated protein
mcl-1: ML-1 human myeloid leukemia cell line bcl-2 protein
MDH: malate dehydrongenase
Mg-ATP: magnesium-adenosine triphosphate
MHCII: major histocompatibility factor class II molecule
mIg: membrane-associated immunoglobulin, portion of BCR
mTOR: mammalian target of rapamycin
MyD88: myeloid differentiation primary response gene 88 protein
NAD+: nicotinamide adenine dinucleotide
NADH: nicotinamide adenine dinucleotide, hydrate
NADP+: nicotinamide adenine dinucleotide phosphate
NADPH: nicotinamide adenine dinucleotide phosphate, hydrate
Na^+K^+ pump: sodium-potassium adenosine triphosphatase pump
NF-κB: nuclear factor kappa-light-chain-enhancer of activated B cells
OD_{340}: optical density at 340 nm wavelength
p38 MAPK: protein 38 mitogen-activated protein kinase
p52: active DNA-binding protein of NF-κB heterodimer
p65: subunit of NF-κB, also called RelA
p85: regulatory subunit of PI3K
p110: catalytic subunit of PI3K
pax5: gene of Paired box protein family of transcription factors
PA: phosphatidic acid
PBS: phosphate buffered saline
PC: phosphatidylcholine
pdh: pyruvate dehydrogenase
pdk: pyruvate dehydrogenase kinase

PE: phosphatidylethanolamine
PE-A: phycoerythrin-area
pfk: phosphofructokinase
PG: phosphatidylglycerol
pgam: phosphoglycerate mutase
PH domain: pleckstrin homology domain
phospho-serine^{454} ACL: phosphorylated-serine^{454} residue of ACL enzyme
phospho-serine^{473} Akt: Akt phosphorylated at serine^{473} residue
PI: phosphatidylinositol
PI: propidium iodide
PI3K: phosphatidylinositol 3-kinase
Pim: proto-oncogene serine/threonine-protein kinase
PKC: protein kinase C
PLC: phospholipase C-gamma
PMA: phorbol 12-myristate 13-acetate
PMSF: phenylmethylsulfonyl fluoride
PNGase F: peptide-N4-(N-acetyl-beta-glucosaminyl)asparagine amidase-F
PPP: pentose phosphate pathway/shunt
PS: phosphatidylserine
PtdInsP2: phosphatidylinositol (4,5)-bisphosphate
PtdInsP3: phosphatidylinositol (3,4,5)-triphosphate
pu.1: gene of purine-rich sequence transcription factor number 1
PVDF: polyvinylidene fluoride
Rap: rapamycin 23,27-Epoxy-3H-pyrido[2,1-c][1,4]oxaazacyclohentriacontine
RAG: recombination activating gene protein
RIPA: radioimmunoprecipitation assay buffer
RNAi: RNA interference
RPMI-1640: Roswell Park Memorial Institute medium
RTK: receptor tyrosine kinase
S phase: DNA synthesis phase of the cell cycle
SB201076: 2(R*)-[8-(2,4-dichlorophenyl)-2(S*)-hydroxyoctyl]-2-hydroxybutanedioic acid
SDS-PAGE: sodium dodecyl sulfate polyacrylamide gel electrophoresis
sec: seconds
siRNA: small interfering RNA
SM: sphingomyelin
SP: sphingosine
sq-rtPCR: semi-quantitative real time polymerase chain reaction
SRC: sarcoma tyrosine kinase
SREBP-1: sterol regulatory element-binding proteins
SSC-A: side scatter-area
STAT6: signal transduction and activators of transcription family member 6
Sub-G1: DNA content below G_1 phase DNA content
SYK: spleen tyrosine kinase
TAT: Trans-activator of transcription

TBS-T: Tris-buffered saline and Tween 20
TCA: tricarboxylic acid cycle
Tdt: terminal deoxynucleotidyltransferase
TG: triglyceride
TGFβ: transforming growth factor beta
TI-1: T cell independent activation type 1
TI-2: T cell independent activation type 2
TLR4: toll-like receptor 4
TRAF6: tumor necrosis factor-receptor associated factor protein 6
TRAM: Toll-interleukin 1 receptor (TIR) domain-containing adaptor-inducing interferon-β-related adaptor molecule
TRIF: Toll/interleukin-1 receptor domain-containing adapter-inducing interferon-beta protein
TSC2: Tuberous sclerosis protein 2
UPR: unfolded protein response
VDAC: voltage-dependent anion channels
V-J: Variable and Joining gene segment recombination of the light chain locus
VT: active form of STAT6 in which amino acids at valine^{547}/threonine^{548} were substituted by alanine residues
Wort: wortmannin, (1alpha,11alpha)-11-(Acetyloxy)-1-(methoxymethyl)-2-oxaandrosta-5,8-dieno(6,5,4-bc)furan-3,7,17-trione
WT: wild-type
XBP1: X-box binding protein 1
XLA: human X-linked agammaglobulinemia
XID: murine X-linked immunodeficiency

Introduction

The immune system comprises of a multitude of cells classified as lymphocytes. Responsible for the humoral response, B-lymphocytes (B cells) are a major cellular subset of the immune system residing in the peritoneum, tonsils, spleen, and lymph nodes. The B cell subset includes peritoneal (B-1), regulatory B (B_{reg}), and splenic (B-2) (naïve mature, germinal center, follicular, plasma, and memory B cells): our interest lies in examining the regulation of immune responses of B cells isolated from the spleen (1).

An immune response is a highly regulated process controlled by extrinsic signals and conditions of the cellular environment. From origin to elimination, developing B cells undergo many tightly regulated stages to become functional and mature lymphocytes, *i.e.* antigen-presenting cells and antibody-producing plasma cells. B cells have specific receptors on their cell surface (surface immunoglobulin) that upon engagement, and with the addition of co-stimulatory molecules, activate an immune response to induce survival, proliferation, and differentiation. B cells as efficient antigen-presenting cells provide cytokines (interleukin-4, -10, TGFβ) and MHCII peptides necessary to evoke lymphocyte activation. The humoral response provides the defense against foreign substances. Antigens through their recognition and presentation by antigen-presenting cells (primarily T-lymphocytes and macrophages) induce formation of highly specific antibodies. In response to environmental cues and receptor-mediated signal transduction pathways, B cells

differentiate into plasma cells, providing host protection through secretion of high-affinity immunoglobulin.

B cell activation

A major signaling complex in the plasma membrane, the B cell antigen receptor (BCR) plays a central role in the development and functional responses of B cells. This complex is made up of immunoglobulin heavy (IgH) and light (IgL) chains (mIg) which associate with two Igα and Igβ heterodimers (see Figure 1) (2-6). IgH and IgL are responsible for ligand binding, while Igα/Igβ heterodimers are signaling components responsible for intracellular signal transduction.

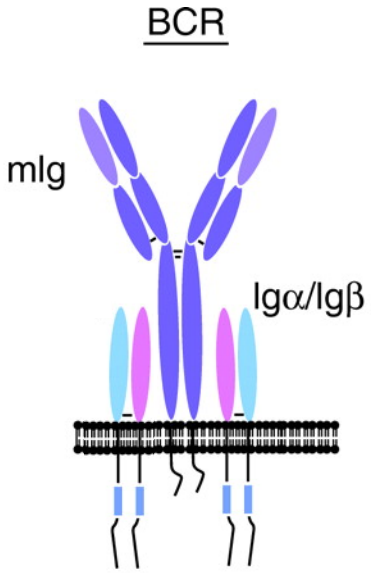

Figure 1: The B cell receptor, adapted image from (7). The BCR is composed of a membrane-bound immunoglobulin (mIg) flanked by two immunoglobulin α/β (Igα/Igβ) heterodimers. The tails of Igα/Igβ heterodimers extend into the cytosol and are responsible for transducing the activation signal incurred by engaged mIg.

The process through which a B cell responds to environmental cues is termed activation. BCR engagement with antigen "cross-linking" initiates the clustering of multiple BCRs into lipid rafts, cholesterol-rich microdomains of the plasma membrane (5; 8-11). An activation signal is transduced intracellularly by subsequent phosphorylations of Igα/Igβ heterodimers at immunoreceptor tyrosine-rich activation motifs (ITAMs)

via receptor protein tyrosine kinases (RTKs), spleen tyrosine kinase (SYK) and sarcoma-related kinase (SRC)-family protein tyrosine kinase, LYN (see Figure 2) (12, 15-17, 21). Additional SYK and SRC-family kinases, Bruton's tyrosine kinase (BTK), and the guanine-nucleotide exchange factor Vav are recruited to augment the activation signal (17, 18, 20, 21). A series of signal cascades ensues to prevent cellular death and to amplify the activation signal (13, 14, 17, 25, 29, 31). Delineation of signaling pathways involved in activation have been accomplished by a variety of means including chemicals, natural genetic mutations, and use of transgenic mouse models; defects in BCR structural components or RTKs lead to developmental deficiencies and severely diminished lymphocyte number in murine models (22, 25-27). Of particular interest to this investigation, mutation of BTK leads to X-linked agammaglobulinemia (XLA) in humans, otherwise called X-linked immunodeficiency (XID) in mice, wherein the phenotype is decrease in B cell population and lack of immune response to antigen (18, 23, 24, 30, 48).

Multiple kinase cascades modulate the activation signal to elicit growth, survival, and maturation of B cells for an immune response. Two crucial and essential pathways initiated from BCR are the phosphatidylinositol-3 kinase (PI3K) and phospholipase Cγ2 (PLC) pathways (see Figures 2 and 3) (12, 23, 24, 29, 32, 35, 47). Both PI3K and PLC are effecter enzymes that generate second messengers in BCR signaling. Active BTK and SYK recruit the adaptor protein BLNK to activate PLC (33-35, 49). PLC enzymatically cleaves phosphatidylinositol-4, 5-bisphosphate (PtdInsP2) to generate inositol-1,4,5-trisphosphate (IP3) and diacylglycerol (DAG),

second messengers required for the release of intracellular calcium and activation of protein kinase C (PKC) (32, 37-42).

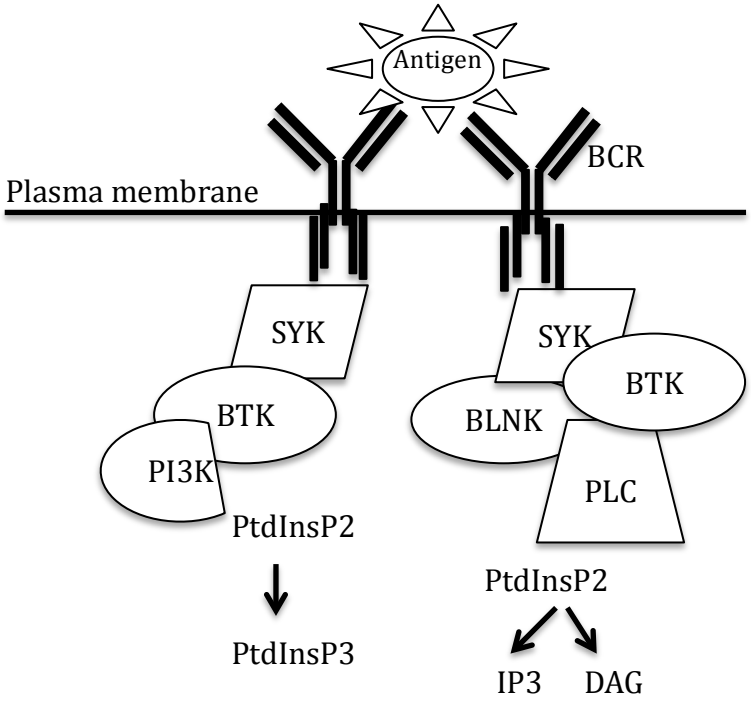

Figure 2: B cell activation. The B cell recognizes antigen through the BCR and responds through activation of Igα/Igβ at their ITAMs (immunoreceptor tyrosine-rich activation motifs) and association of the receptor tyrosine kinases (spleen tyrosine kinase, SYK). Additional SYK kinases, Bruton's tyrosine kinase (BTK), and adaptor molecule BLNK are recruited to augment the activation signal. Two major pathways activated are the phosphatidylinositol-3 kinase (PI3K) and phospholipase Cg (PLC) pathways.

Various PKC isoforms are activated through DAG, which have different functional roles in B cells (43, 51). In particular PKCβ is activated through PLC signaling and further perpetuates the activation signal, as mice deficient of the β isoform demonstrate impaired humoral responses (34, 35, 44, 50). PKCδ is another isoform activated by PLC signal pathway, however its function is to regulate the proliferation and survival of B cells as murine B cells deficient of this isoform have increased

proliferative response and autoimmunity (36, 45, 46). In addition to PKCs, DAG activates the nuclear factor of kappa light chain gene enhancer in B cells (NF-κB) cascade (37-42). Active NF-κB translocates into the nucleus to regulate transcription of pro-survival and proliferation genes, such as *bcl-2*, *bcl-xl*, and *c-myc* (52-55). Deficiency of PLC, BLNK, impairs early B cell development and proliferation such that murine models are severely immune-compromised, displaying phenotypes similar to the XID mouse model (33, 34). The knockout phenotypes of the NF-κB family members, p65 and p52, are both survival and growth deficiencies; B cells herein are incapable to express *c-myc* and do not increase in size or continue into S phase of the cell cycle (56, 57).

A dimer of a regulatory subunit (p85α) and an active subunit (p110), PI3K phosphorylates PtdInsP2 to produce phosphatidylinositol-3,4,5-triphosphate (PtdInsP3). Through pleckstrin homology (PH) domain interaction with PtdInsP3, additional signal transduction molecules are recruited to the plasma membrane, thus extending the activation signal further (58, 59, 60). Loss of p85α or p110γ impairs B cell development and reduces numbers of B cells, and as a result mice bearing these deficiencies lack of humoral immunity similar to XID mice (61, 62).

A target of PI3K is α-ketoglutarate thymoma protein (Akt) (see Figure 3), also known as protein kinase B. This serine/threonine kinase is activated by phosphorylation and interaction of PH domains. In many cell types, Akt phosphorylates a myriad of cellular targets involved in survival, growth, and proliferation. Among many targets, Akt inhibits the activation of pro-apoptotic BCL-

2 family member BAD (63), promotes the degradation of IκB kinase (IKK) for nuclear factor kappa B (NF-κB) translocation to the nucleus for gene transcription (64, 70), phosphorylates and inhibits glycogen synthase kinase 3 (GSK3) (66), and phosphorylates and destabilizes myc and cyclin D for cell cycle progression (67, 68). To support adipocyte and T-lymphocyte cellular growth, Akt induces glucose transporter expression and translocation to the cellular surface (69, 70). In

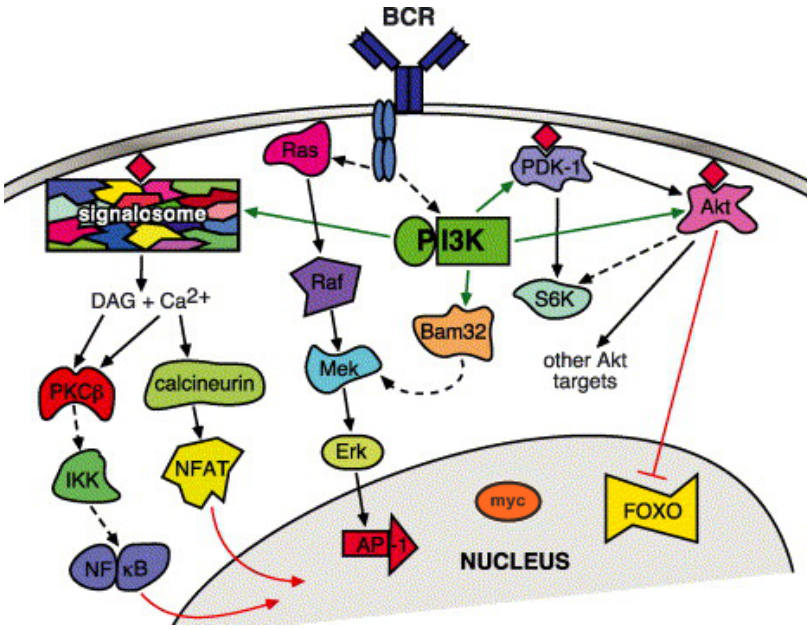

Figure 3. Multiple pathways activated in BCR signaling (adapted from ref. 59). Through the Ras/Raf, PI3K and PLC (signalosome) pathways, B cells activate multiple transcription factors for an activation response. PI3K mediates signalosome assembly for robust PLC activity (mobilization of Ca^{2+} and production of DAG) for the activation and translocation of NF-κB (and probably NFAT) into the nucleus. Activation of Akt downstream of PI3K results in the phosphorylation and inhibition of FOXO family transcription factors, and may also promote NF-κB activation. PI3K might also play a role in the activation of AP-1, as the novel PI3K effector Bam32 contributes to activation of the MAPK cascade. Hatched arrows indicate one or more steps omitted for simplicity, or unknown intermediates. Green arrows represent 3-phosphoinositide-mediated membrane recruitment. Red lines indicate translocation into the nucleus. *A.C. Donahue, D.A. Fruman / Seminars in Cell & Developmental Biology 15 (2004) 183–197.*

addition, Akt has been shown in non-B cells and cancer cell lines to activate the glycolytic enzymes, hexokinase and phosphofructokinase, and promotes protein synthesis through signaling to mammalian target of rapamycin (mTOR) (71-72). Akt also promotes *de novo* lipogenesis in hematopoietic cell lines by phosphorylation and activation of ATP citrate lyase (ACL) and inhibition of fatty acid β-oxidation via inhibition of carnitine palmitoyltransferase (CPT)-1A expression (77-79).

Multiple isoforms of Akt exist which likely permits the diversity of its targets. Akt1-null mice have reduced organismal size (80-82). In contrast, mice deficient of Akt2 have mild growth deficiency and display a diabetic phenotype (83). The role of Akt3 is less clear as Akt3 knockout mice display impaired brain development (84, 85). Furthermore, the disruption of Akt in an immature B cell line (DT40) promoted apoptosis in response to BCR engagement, illustrating the role of Akt in cellular growth and survival (66).

Development of B cells

B cell development is a sequential and orderly process that proceeds by the production of a functional antigen receptor (Figure 4) (87-90). In the bone marrow, B cells begin their development as stem cell progenitors (expressing CD34), cued by interleukin-7 and stromal cell interaction (91). DNA polymerase terminal deoxynucleotidyl transferase (Tdt) and recombination activating gene product (RAG) are synthesized and initiate antigen-receptor gene rearrangement (92). Additionally, genes encoding *pax5*, *pu.1* and *ikaros* are transcriptionally expressed

thereby committing the stem cell to B cell lineage (93, 94). Progenitor cells undergo diversity-joining gene segment (D-J) joining on the Ig heavy chain (IgH) chromosome to become early pro-B cells. At the pro-B cell stage, cells express the identifying surface recognition markers CD45/B220 and MHCII (95).

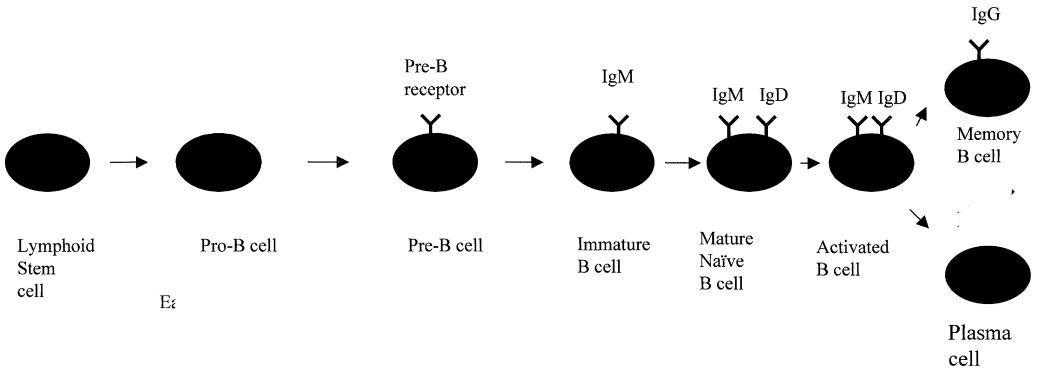

Figure 4: Development of B cells, adapted from (86). B cells begin their development in the bone marrow as stem cells. Progression through the maturation and development process is controlled by the expression of the BCR. During the immature stage, the B cell exits the bone marrow and travels through the blood stream to take up residency in lymphoid organs, specifically the spleen. Upon encounter with antigen a B cell may progress to the plasma cell or memory B cell stage.

Pre-B cells are characterized when membrane μ chains and surrogate light chains associate with the pre-B cell receptor (1, 91). Following a burst of proliferation, variable–joining gene segment (V-J) joining on the light chain (IgL) occurs. Synthesized and expressed on the cell surface, the membrane IgM characterizes the B cell as being at the immature stage. Efficient elimination of potentially harmful, self-reactive B cells occurs at the immature stage in one of three ways: negative selection (BCR-induced cell death), inactivation (anergy), or revision

of the specificity of their BCRs (receptor editing). If not self-reactive, the immature B cell will emerge from the bone marrow and circulate through the periphery.

Mature B cells reside in the spleen and are naïve until recognition of antigen. BCR cross-linking of B cells during the transition from immature to mature induces their differentiation to follicular mature B cells (8, 96). Upon stimulation by a T cell, B cells in the germinal center of a spleen differentiate into memory B cells or plasma cells. Alternatively, B cells may be stimulated polyclonally by T-dependent or independent antigenic stimulation. Lipopolysaccharide (LPS) is a polyclonal T-independent (TI-I) stimulation (87, 97, 98); BCR cross-linking with interleukin-4 (IL-4) is a TI-2 stimulation (99), whereas Cluster of Differentiation 40 ligand (CD40L) is a T-dependent antigenic stimulus (87, 100-104). BCR cross-linking induces proliferation without maturation, whereas addition of IL-4 induces maturation without proliferation. CD40L induces proliferation, differentiation (Ig class switching), and maturation (99, 100, 105). This differentiation process termed affinity-maturation requires BCR engagement, positive selection, and presence of cytokines (including interleukin-10 (IL-10) or IL-4). Dependent upon the transcription factors Blimp-1/PRDM1 and IRF4B, cells will divide rapidly becoming plasmablasts, and eventually plasma cells, and begin producing large volumes of antibodies (106). Once the plasma cell stage is achieved, B cells may be eliminated by apoptosis or relocate to the bone marrow as memory B cells.

Throughout life, from fetal to adult, B cells continue to be generated in the bone marrow at a rate of 5×10^7 cells per day in the mouse. Of which 2-5 % become

mature, surface Ig positive cells of the periphery; most B cells die by apoptosis (91, 96). Autoimmune diseases where proliferation of B cells or activity is uncontrolled correlate with human diseases include systemic lupus erythematosus, rheumatoid arthritis, scleroderma, type 1 diabetes, and multiple sclerosis (107). Commonly researched leukemias of plasma cells are plasmacytoma, multiple myeloma, and Waldenström macroglobulinemia (108, 109).

B cell growth and glucose utilization

Resting lymphocytes primarily metabolize aerobically by glycolysis and oxidative phosphorylation, and shift to generate energy in large part by up-regulating aerobic glycolysis with stimulation (110, 111). B cells in response to antigen will enter the cell cycle from quiescence (G_0) and undergo a period of extensive growth (increased size and volume). Cell growth and DNA synthesis are tightly coupled and regulated. B cells increase in cell size and protein synthesis through the Akt and NF-κB pathways and activation of the transcription factors, eIF4E and c-myc, to develop into antibody-secreting plasma cells (67, 112, 113). Dependent on increased glucose metabolism, the research focus of the Chiles' laboratory has been in examining the regulation of glycolysis through the PI3K-Akt pathway in activated B cells (114).

Glucose and its metabolites are utilized as a carbon source for the synthesis of amino acids and phospholipids and in addition, its metabolism generates ATP and NADPH and regulates apoptosis, via the Bcl-2 family (115, 116, 120). The activation

of FL5.12B cells stimulates glucose uptake and glycolysis to promote macro-molecular synthesis of lipids and proteins (79, 117, 118). In B cells, intracellular glucose is converted into two molecules of pyruvate, that are converted primarily to lactate, generating ATP and NAD from NADH (111, 114, 119). Progression in the cell cycle to DNA synthesis in lymphocytes elicits a shift in catabolism to include the pentose phosphate pathway. This pathway has several purposes including providing reduced coenzyme NADPH for reductive biosynthesis and ribose 5-phosphate for nucleotide synthesis.

Glucose utilization in cells includes its ability to be a source of carbon for the biosynthesis of lipids (121, 124). The glycolytic product, pyruvate, directs glucose carbons into lipid synthesis by way of the mitochondria (79, 122-124). In the Kreb's cycle, pyruvate is de-carboxylated and converted to acetyl-CoA by pyruvate dehydrogenase complex, upon which citrate synthase catalyzes the condensation of acetyl-CoA with oxaloacetate to produce citrate. The mitochondrial citrate is then translocated into the cytosol where ATP citrate lyase converts the molecule to oxaloacetate and acetyl-CoA, a precursor for fatty acids and cholesterol (120, 125-127, 134). Glutamine is an additional nutrient required for *in vitro* culture of B cells (121, 128-133); thus the possibility of glutamine as an alternative source of carbon for lipid synthesis in B cells was considered, as it may be metabolized to enter the TCA cycle and in addition yield acetyl-CoA.

ATP citrate lyase and acetyl-CoA synthesis

ATP citrate lyase (ACL) is a regulated cytoplasmic enzyme responsible for the generation of extra-mitochondrial acetyl-CoA (125, 135, 136). ACL produces acetyl-CoA by a sequential reaction: with Mg-ATP bound first to histidine 760/765, followed by binding of citrate and CoA, the phospho-enzyme intermediate forms oxaloacetate and acetyl-CoA (137-141). Thus, ACL is critical for the conversion of glucose to cytosolic acetyl-CoA and therefore glucose-dependent lipogenesis. Through glycolysis, acetyl-CoA is generated as previously mentioned, and enters the *de novo* lipid synthesis pathway. Alternative sources for acetyl-CoA synthesis include: acetate acquired through ethanol or from the extracellular environment, amino acid degradation (leucine or isoleucine), or β-oxidation of lipids of lysosomal membranes or acquisition from the extracellular sources (142-148). These alternative sources of acetyl-CoA are degradative or scavenger pathways and likely not employed during cell growth.

ACL enzyme activity has been shown to be dependent upon its phosphorylation status and the presence of phosphorylated sugars (135, 149-153). Of interest to this investigation, Berwick *et al.* (2002) reported the serine/threonine kinase Akt to direct phosphorylate ACL at its active site on serine 454, which in turn increased its enzymatic activity (150). ACL may be regulated allosterically; the formation of an active enzymatic site requires the joining of four homomeric subunits into a stable tetramer. The expression of ACL is regulated by the sterol response element binding protein-1 (SREBP-1) transcription factors; Akt up-

regulates ACL mRNA through SREBP-1 activation (154-156). Additionally the regulation of ACL may be mediated by three phosphorylation events: 1) phosphorylation of histidine 760/765 to maintain tetrameric structure (138, 157), 2) phosphorylation of ACL at serine 450 and threonine 446 by glycogen synthase kinase 3 (GSK3) for reduced enzymatic activity (158, 159) 3) and an activating phosphorylation event mediated by Akt at serine 454 (150).

Much of the functional inhibition studies of ACL have been conducted in cells wherein ACL is highly expressed. ACL deficiency in mice is embryonic lethal so no functional complements of ACL exist within cells (156). ACL knockdown in leukemic FL5.12 and A549 lung adenocarcinoma cells demonstrated the necessity of ACL expression for glucose-dependent lipid synthesis in cellular growth and proliferation of cancerous cells (77, 122, 153, 166). ACL knockdown by siRNA arrests tumor growth. *In vivo* imaging of A549 (non-small cell lung cancer which bears a point mutation in K-Ras, which activates the PI3K-Akt pathway) of siRNA transfected and statin-treated tumors significantly decreased in volume and growth, as well as in cell cycle (160). The chemical inhibition of ACL through radicicol (non-competitive inhibitor) or hydroxycitrate and SB-201076 (competitive inhibitor) reduces insulin secretion and membrane synthesis in pancreatic β cells (161). ACL inhibition also reduces cholesterol and fatty acid synthesis in liver and adipose tissue (162, 163). It is not known if ACL plays a role in the regulation of lipid biosynthesis in B cells. A novel cell-permeable inhibitor, compound-9 (C-9) (also termed BMS-303141) was used in this current investigation (see Figure 5) (164). C-

9 is a synthetic organic compound (of the 2-hydroxy-N-arylbenzenesulfon-amides class), structurally deviate of citrate, designed for *in vivo* bioavailability and specifically inhibits ACL (K_i is 0.13 μM) (164, 165). Oral treatment with C-9 reduces plasma cholesterol and triglycerides in serum of canines fed a high-fat diet. Additionally in cancerous HepG2 cells, C-9 reduces synthesized cholesterol levels (166).

Figure 5: Annotated Compound-9 structure (164).

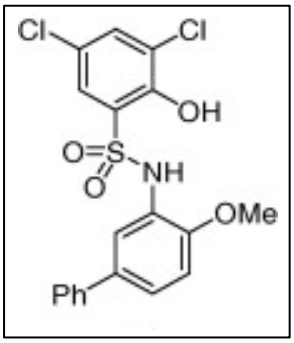

Interleukin-4

Interleukin-4 (IL-4) is a pleiotropic cytokine predominantly generated during the immune response by T-lymphocytes that regulates gene expression for growth and survival in B cells. IL-4 promotes B cell maturation through MHCII peptide and CD23 expression, and immunoglobulin class switching to IgG1 and IgE (99). As a co-stimulant, IL-4 increases glycolysis and up-regulates Bcl-$_X$L, an anti-apoptotic protein (167-169).

Binding of IL-4 to its cognate receptor (IL-4/13Rα and γc) results in the activation of several signal transduction cascades, including the Janus kinase 1 (JAK1) and JAK3 tyrosine kinases (see Figure 6) (167, 170). JAK1/3 phosphorylates

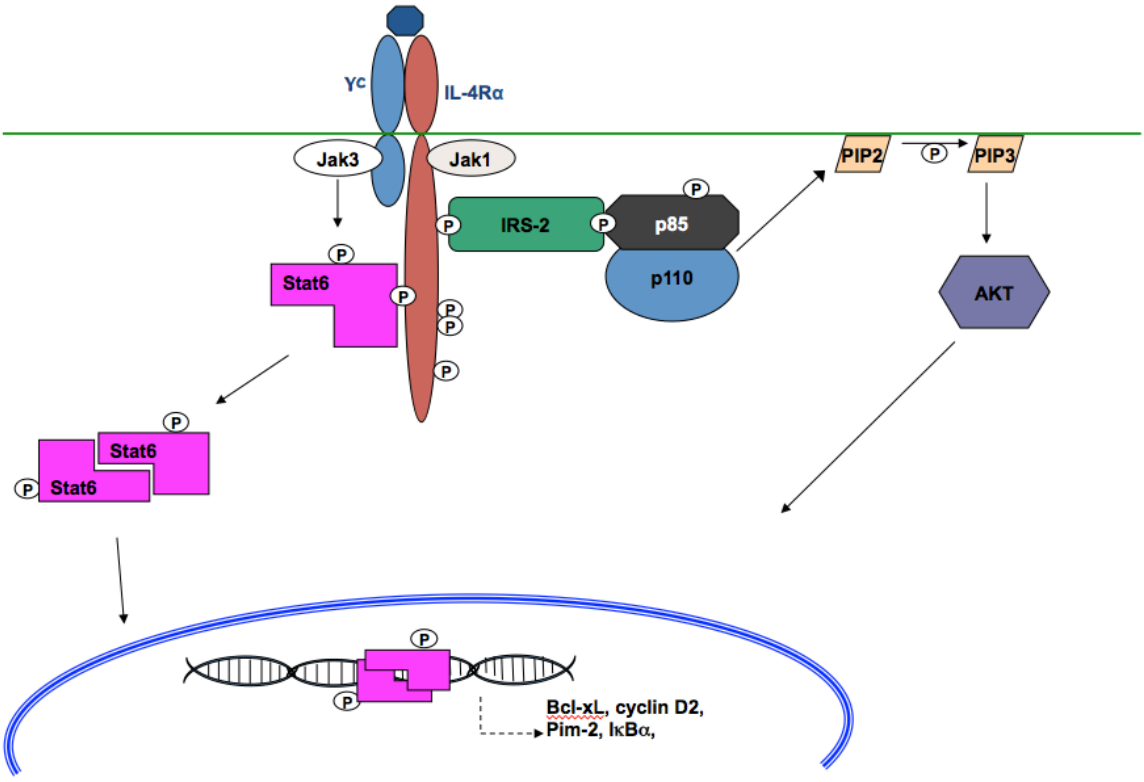

Figure 6: IL-4 Receptor Signaling. The JAK/STAT6 pathway and PI3K-Akt pathway are activated in B cells in response to the cytokine, IL-4.

tyrosine residues in the cytoplasmic domain of the IL-4Rα that serve as docking sites for signal transducer and activator of transcription 6 (STAT6) (167, 171). Tyrosine phosphorylation of STAT6 promotes its homo-dimerization and the subsequent nuclear translocation for gene expression (171). The IL-4Rα chain also recruits and promotes the insulin receptor substrate-2 (IRS-2) association with PI3K (p85α subunit) for subsequent generation of phosphoinositides (167, 171).

Inhibition of PI3K activity or deficiency in p85α, STAT6, or IRS-2 blocks the ability of IL-4 to prevent apoptosis in hematopoietic cells (169, 172-174). Studies of IL-4, IL-13, IL-4Rα, or STAT6 knockout animals have demonstrated the important

role of this signal transduction pathway in the development of protective immunity against most nematode parasites and pathogenesis of allergic diseases (99, 175-178).

Mitogenic activation through lipopolysaccharide

A bacterial membrane component, lipopolysaccharide (LPS) is a polyclonal activator of B cells that is recognized by the toll-like receptor-4 (TLR4). Despite low expression, TLR4 is a pattern recognition receptor that executes a host defense response for growth, proliferation and maturation of B cells to secrete immunoglobulins (179-182, 184). The importance of LPS recognition to TLR4 is demonstrated in mice lacking TLR4 (C3H/HeJ mouse strain) (183); $TLR4^{-/-}$ B cells demonstrate severe impairment of MHCII expression and hypo-responsiveness to LPS, wherein the splenic B cells do not respond to the mitogen by proliferation (180).

LPS engagement with TLR4 triggers the recruitment of the adaptor proteins, myeloid differentiation primary-response protein 88 (MyD88) or Toll-Interleukin-1 receptor domain-containing adaptor protein inducing IFN-β (TRIF) (186). Classical nuclear factor-κB and MAP kinase pathways are activated in both adaptor protein-mediated pathways, leading to AP1 transcription factor-mediated gene transcription (185, 187). MyD88 recruits the complex of interleukin-1 receptor (IL1R)-associated kinase 4 (IRAK4) and IRAK1 to an engaged TLR4 receptor whereby IRAK1 is phosphorylated, dissociates from the receptor, and proceeds to

interact with the TNFR-associated factor 6 (TRAF6). The IRAK1/TRAF6 complex signals to activate IκB kinase complex (IKK), which in turn phosphorylates and targets IκB for degradation, permitting the nuclear translocation of NF-κB for gene transcription. The IRAK1/TRAF6 complex can also activate the Jun N-terminal kinase (JNK) and p38 mitogen-activated protein kinase (MAPK) pathways. Additionally, TLR4 engagement induces activation of MyD88-independent pathways, which involve TRIF and TRIF-related adaptor molecule (TRAM). This signal branch point in the LPS-activated pathway results in the activation of interferon-responsive factor 3 (IRF3), which mediates transcription of the IFN-inducible genes and activates a second delayed wave of NF-κB transcription.

Deficiency of MyD88 or IRAK4 has been identified in a few human patients. Individuals possess an increased proportion of auto-reactive B cells and recurrent bacterial infections (188-192). Furthermore, the MyD88 or IRAK4 deficiency in murine models leads to resistance to sepsis by lack of inflammatory response (184, 185).

Endomembrane expansion and lipid synthesis in the generation of plasma cells

Through extrinsic signal, B cells mature into antibody-secreting plasma cells. The differentiation process requires many intracellular changes for the mass-production of highly specific immunoglobulin and is transcriptional controlled, as the inositol-response factor1α (IRF1), B-lymphocyte induced maturation protein 1 (BLIMP-1), and X-box protein1 (XBP1) are activated, others utilized during earlier

developmental stages (Paired box protein, PAX5) are suppressed (193).

Plasma cells generate a secretory apparatus through the expansion of their intracellular membrane networks. This process institutes a re-organization and re-distribution of plasma membrane lipid content as well as induced gene expression for lipogenic enzymes (194-198). In B cells, the unfolded protein response (UPR) pathway initiates the membrane expansion driven by active XBP-1 (194, 199). The UPR is responsible for delaying protein synthesis and inducing the expression of endoplasmic reticulum (ER) resident proteins (chaperones and folding enzymes), as well as promoting phospholipid synthesis (200, 201). The ER and Golgi apparatus are the major endomembrane compartments wherein a majority of *de novo* bulk membrane lipid and protein synthesis occurs (195, 120).

A majority of lipids in membranes are phospholipids, glycerophospholipids and sphingolipids (202). In the murine B cell lymphoma cell model (CH12.lx), differentiation via LPS stimulation induces the synthesis of three major membrane lipids: phosphatidylcholine (PC), phosphatidylethanolamine (PE), and cholesterol (C) (203). The cytoplasmic leaflet of mammalian plasma membrane is highly enriched in PS and PE, whereas the outer leaflet is enriched with PC. To synthesize PC, the cytidine diphosphate (CDP)–choline pathway is elicited in a PI3K-Akt-dependent manner (204-206). Phosphatidylserine (PS) synthesis occurs in the ER, to which a decarboxylation event occurs to produce PE (207, 208). Additional lipids synthesized in the ER and transferred to the Golgi are phosphatidylinositol (PI), phosphatidylglycerol (PG), sphingosine (and the modification to sphingomyelin), and ceramide (CM) (209, 210). Cardiolipin (CL), a lipid present only in

mitochondria and inner mitochondrial membrane, is synthesized *de novo* as mitochondrial numbers increase in response to LPS (211). Interestingly XBP-1 has been shown to increase mitochondrial mass and function, as well as the size of the ER and its proteins (200); XBP-1 deficiency in B cells reduces lipid synthesis of PC, SM, and PI (198).

The production of cholesterol through *de novo* synthesis or acquisition from extracellular sources is required for differentiation and proliferation of lymphocytes (212). Occuring in the ER, the synthesis of cholesterol (C) utilizes acetyl-CoA subunits. Two acetyl-CoA units are condensed to form aceto-acyl CoA, which is further condensed to another acetyl-CoA to form 3-hydroxy-3-methylglutaryl-coenzyme A (HMG-CoA). HMG-CoA reductase in the ER reduces HMG-CoA to mevalonate for its conversion to isoprene units. The condensation of six activated isoprenes forms squalene, which is through a series of many more reactions modify and rearrangement the structure for the resulting product of cholesterol. The ability to block cholesterol biosynthesis with lovastatin has been shown to inhibit cancer cell growth (126, 213, 214).

As previously described, the cytoplasmic enzyme ATP-citrate lyase (ACL) converts oxaloacetate and citrate to acetyl-CoA (127). In *de novo* lipogenesis, acetyl-CoA is the building block through which lipids such as cholesterol and fatty acids are synthesized. In a committed step of fatty acid synthesis pathway, acetyl-CoA carboxylase (ACC) irreversibly carboxylates acetyl-CoA to form malonyl-CoA. Malonyl-CoA and acetyl-CoA combine to form long chain fatty acids primarily palmitate (C16) or stearate (C18), by fatty acid synthase (FAS) to be utilized in

cholesterol synthesis or glycerolipid synthesis (215). Additionally glycerol 3-phosphate, acquired from the glycolytic pathway, combines with malonyl-CoA to form phosphatidic acid (PA). PA can be modified to generate glycerophospholipids with amino head group attached (serine, choline, ethanolamine, etc.) or hydrolyzed to triacylglycerols. Of note, due to high expression in cancers, the selective inhibition of FAS leads to cancerous cell apoptosis *in vitro* and *in vivo* (216, 217).

B cells in the process of differentiation mature to the plasma cell stage by undergoing periods of growth (*i.e.* cell mass accompanied with size and *de novo* macromolecular synthesis) and proliferation to expand intracellular membrane networks, and undergo organelle biosynthesis for Ig synthesis and assembly (196, 195, 203, 218). The extent to which the essential and regulated enzyme ACL contributes to the regulation of lipid biosynthesis in B cells is not known and was the subject of this investigation (156).

In a previous report, cell cycle progression of B cells correlated with membrane synthesis (203). In B cell lymphoma cells (CH12.lx), the expansion of ER and Golgi has been shown to expand in response to LPS for proliferation and differentiation to and IgM secreting plasma cell (203). In addition to elevation of phospholipid synthesis, CH12.lx cells stimulated with LPS cells elevated gene expression (lipin1, elongase, and choline phosphotransferase) for FA synthesis, elongation, and desaturation. The essential membrane lipids (*i.e.* glycolipids, cholesterol, and phospholipids) were synthesized in activated B cells to support membrane expansion and notably organelle biosynthesis (120, 211, 219). In previous reports, *de novo* lipogenesis increases in B cells stimulated with LPS,

coinciding with reported membrane and organelle biosynthesis. The lipids were phosphatidylcholine (PC), phosphatidylethanolamine (PE), cardiolipin (CL), and cholesterol (C) (120, 203). B cells also synthesized ceramides (CM) phosphatidylglycerol (PG), phosphatidylserine (PS), phosphatidylinositol (PI) and sphingolipids (SM), lipids reported to be maturation markers, components of membrane structure and lipid rafts, as well as signal transducers in apoptosis (202, 220-222). *c-myc*, previously mentioned as a target of the PI3K-Akt pathway, has been shown to be responsible for phosphatidylcholine (PC) synthesis and necessary for biogenesis of mitochondria. Akt has also been shown to directly down-regulate β-oxidation through inhibition of carnitine palmitoyltransferase (CPT1α) activity, stimulating PC and fatty acid (FA) synthesis (79). Therefore, the putative connection between activation signal pathway and *de novo* lipogenesis in B cells was investigated.

The synthetic pathways of lipids are interconnected and *de novo* lipogenesis may commence with ACL activity to generate acetyl-CoA (Figure 7) (204, 223, 224).

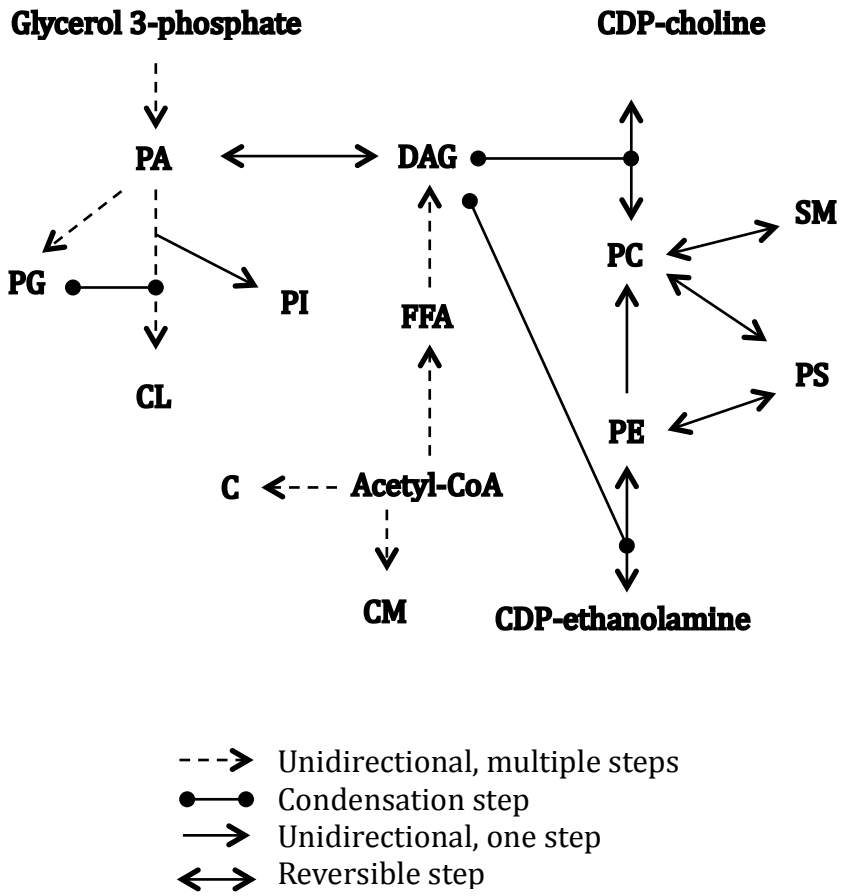

Figure 7: Interconnected conversion of synthesized lipids, adapted from Hermansson *et al*., (2011) (223); [^{14}C]-acetyl-CoA is incorporated into diacylglycerol (DAG) and fatty acids (FA) by fatty acid synthase. Newly synthesized fatty acids are incorporated into DAG, ceramide (CM), and cholesterol (C). Condensation of DAG and glycerol 3-phosphate (an intermediate of glycolysis) synthesizes phosphatidylglycerol (PG), that can be converted to phosphatidic acid (PA), or condense with DAG for the formation of the mitochondrial associated lipid, cardiolipin (CL). Phosphatidylinositol (PI) also can be generated at this branch in lipid biosynthesis through modification of PA. The observed incorporation of glucose carbon in phosphatidylcholine (PC) in response to B cell stimulation may be distributed into additional lipid species via active CDP-choline and CDP-ethanolamine pathways (220). As illustrated, PC can be converted to sphingolipids (sphingomyelin, SM) or phosphatidylserine (PS), while phosphatidylethanolamine (PE) can be synthesized through PS or by ethanolamine and DAG condensation.

The most abundant glycerophospholipid specie, PC is synthesized in the ER and Golgi from diacylglycerol via the Kennedy–CEPT pathway or CPT (222). PC serves as a precursor to the membrane lipids, SM and PE (225, 203). PE is the second most abundant lipid, formed through lipid head group exchange from PS. PS has been shown to play a role in apoptosis and serve as a cofactor to activate PKC, and associates with dynamin and Na^+K^+ ATPase (209, 226-228). PE has been shown in hepatic tissue to promote secretion and maturation of lipoprotein as well as enriched in the cleavage furrow during cytokinesis (229-231). The major free fatty acids are C14:0 [myristic], C16:0 [palmitic], C18:0 [stearic], C18:1 [oleic], C18:2 [linoleic], and C20:0 [arachidic]) (129, 130, 232-234). These free fatty acids may contribute to lipid tail moieties of PE, PG, and PC in B cells. In addition, FA have been shown to serve as structural components of membrane and signaling molecules such as sphingolipids, cholesterol, and glycosylphosphatidylinositol anchored proteins (210, 220).

The role of glucose metabolism in the immune response to extracellular stimuli suggests its requirement for cellular growth, survival, and differentiation. This investigation sought to examine the regulation of glucose in the synthesis of lipids in B cells.

Materials and methods

B cell isolation and culture

BALB/cAnNTac mice and p85α-deficient mice (BALB/cAnNTac-Pik3r1 N12) were obtained from Taconic Farms (Germantown, NY). CBA/CaHN-*Btk*^{xid}/J, CBA/CaJ, C.129S2-*Stat6*^{tm1Gru}/J, and BALB/cJ were obtained from the Jackson Laboratory (Bar Harbor, ME). Housed at Boston College, mice were cared for and handled at all times in accordance with National Institutes of Health and Boston College guidelines. C57BL/6 X 129x1/SvJ and PKCδ-deficient (PKCδ$^{-/-}$) were a generous gift from Dr. Thomas Rothstein, Boston University Medical School, Division of Immunology and Infectious Disease, Boston, MA. The strains of 129xSV and BLNK$^{-/-}$-deficient mice were a generous gift from Dr. Anne Satterthwaite, UT Southwestern Medical Center, Department of Internal Medicine, Dallas, TX. Splenic tissues of age-matched C57BL/6 and BTK-deficient (BTK$^{-/-}$) mice were a generous gift from Dr. Robert Woodland and Sarah Kenward of University of Massachusetts Medical School, Dept. of Molecular Genetics and Microbiology, Worcester, MA.

Splenic B cells from mice at 8 to 12 weeks were isolated and purified by negative selection using the B Cell Isolation Kit, a MidiMACS™ Separator, and an LS Column (Miltenyi Biotec Inc. Auburn, CA). CD43^{+} B cells, T cells, NK cells, dendritic cells, macrophages, granulocytes, and erythroid cells are labeled with a cocktail of biotin-conjugated antibodies against CD43 (Ly-48), CD4 (L3T4), and Ter-119, as well as Anti-Biotin MicroBeads. Purified B cells were cultured in RPMI-1640 medium (Mediatech, Inc. Manassas, VA) plus 10 % FCS (Atlanta Biologicals, Inc.

Lawrenceville, GA), 2 mM L-glutamine, 10 mM HEPES, pH 7.4, 50 μM β-mercaptoethanol, 50 U/mL penicillin, 50 μg/mL streptomycin. Small dense B cells were isolated following centrifugation through a discontinuous 72 % /65 % /50 % Percoll gradient (Sigma-Aldrich Co, St. Louis, MO).

$F(ab')_2$ fragments of goat anti-mouse IgM were obtained from Jackson ImmunoResearch Laboratories, Inc. (West Grove, PA). Murine IL-4 was from EMD Millipore Corporation (Billerica, MA) or R&D Systems, Inc. (Minneapolis, MN). Lipopolysaccharide (LPS O111:B4 or *S. typhosa*) was from Sigma-Aldrich (St. Louis, MO). CD40L/CD8 was a kind gift from Dr. Tom Rothstein. LY294002, wortmannin, rapamycin, and rottlerin were from CalBiochem-NovaBiochem Corp. (San Diego, CA). Compound-9 (C-9) was synthesized by AsisChem Inc. (Watertown, MA) according to methods described by Li *et al.* 2007 (164). All other reagents, unless otherwise noted, were obtained from Fisher Scientific (Pittsburgh, PA).

Cell extraction and Western blotting

Stimulated as specified in the figure legends, B cells were solubilized for whole cell extracts in Triton X-100 buffer (20 mM Tris, pH 7.4, 100 mM NaCl, 0.1% Triton X-100) containing protease inhibitor cocktail (Sigma- Aldrich, St. Louis, MO), 10 μM β-glycerophosphate, 1 μM phenylmethylsulfonyl fluoride (PMSF), 1 μM NaF, 1 μM okadaic acid, 1 mM dithiothreitol (DTT), and 1 μM Na_3VO_4. For glut-1 extraction, B cells were solubilized in membrane protein extraction buffer (0.1 % sodium dodecylsulfate (SDS), 1 % Triton X-100, and protease inhibitor cocktail). Insoluble

debris was removed by centrifugation at 14,000 x *g* for 15 min (4°C). Lysate protein was separated by electrophoresis through 7.5 % polyacrylamide SDS gel with 2X Laemelli buffer or 2.5X glut-loading buffer (5 % SDS, 8 M Urea, 0.16 M DTT, 50 μM βME, 37°C 15 min), or 5X loading buffer (1.56 mL 2 M Tris-HCL pH 6.8, 1 g SDS, 5 mL glycerol, 2.5 mL βME, 5 mg bromophenol blue, 25°C 30 min) transferred to an Immobilon-PVDF membrane (EMD Millipore Corp. Billerica, MA).

For membrane-integrated protein, extracts were prepared in glut-1 lysis buffer (50 mM HEPES, pH 7.5, 150 mM NaCl, 0.5 mM EDTA, 1 mM DTT, 1 mM benzamidine, 1 mM PMSF). After one hour on ice, insoluble debris was pelleted by centrifugation 500 x *g*, 5 min. Supernatants were collected stored at -80°C or PNGase F-treated (New England BioLabs, Inc. Ipswich, MA). Samples were separated on 10 % polyacrylamide SDS gel after addition of 2.5X glut-loading buffer (5 % SDS, 8 M Urea, 0.16 M DTT, 50 μM βME, 37°C 15 min), transferred to an Immobilon-PVDF membrane (EMD Millipore Corporation, Billerica, MA).

The membranes were blocked in TBS-T (20 mM Tris (pH 7.6), 137 mM NaCl, and 0.05 % Tween 20) containing 5 % nonfat dry milk for 60 min and then incubated overnight (4°C) with described primary Ab. The membrane was washed several times in TBS-T, incubated with a 1:2500 dilution of anti-rabbit or anti-mouse IgG-coupled HRP Ab (60 min, Santa Cruz Biotechnology Inc. Santa Cruz, CA) and developed by ECL (Kirkegaard & Perry Laboratories, Inc. Gaithersburg, MD). Autoradiograms were scanned with Adobe Photoshop 7.0 (Adobe Systems, Inc., San Jose, CA). The mean density of each band was analyzed by the ImageJ program

(NIH, Bethesda, MD).

The primary antibodies used were raised against phosphorylated ACL (serine 454) and total ACL (obtained from Cell Signaling Technology, Inc. Danvers, MA), phosphorylated Akt (serine 473) (Upstate/EMD Millipore Corporation, Billerica, MA), glut-1 (Research Diagnostics, Inc. Flanders, NJ), Na^+K^+ pump (sodium potassium ATPase alpha 1, Abcam plc. Cambridge, MA), and heat shock protein 90 (Enzo Life Sciences, Inc. Farmingdale, NY).

Glucose transporter staining by flow cytometry

B cells stimulated as specified in the figure legends were washed twice in staining buffer (1 mL PBS containing 1 % FCS/0.1 % NaN_3) and then incubated for 20 min (4°C) with the anti-CD16/CD32 (2.4G2) mAb Fc block reagent (1:500 v/v Pharmingen). Cells were washed twice in 0.1 mL staining buffer and re-suspended in 250 μL Cytofix/Cytoperm solution (4°C, Pharmingen). After 20 min, cells were washed twice in 0.5 mL Perm/Wash solution, re-suspended in 0.1 mL Perm/Wash solution, and incubated with 1:500 dilution of anti-glut-1 Ab (Research Diagnostics, Inc. Flanders, NJ) or isotype control Ab (4°C). After 60 min, cells were washed 3 times in 0.1 mL Perm/Wash solution and then incubated with PE-conjugated $F(ab)'_2$ fragments of goat anti-rabbit IgG (1:800 CalTag Laboratories (Burlingame, CA) for 1 hr (4°C). Cells were then washed in 0.1 mL Perm/Wash solution, and glut-1 staining was measured by flow cytometry on a BD FACSCanto cytometer and the data analyzed by FACSDiva software (BD Biosciences).

For surface glut-1 staining, B cells were simply not re-suspended in fix or permeabilizing solutions.

Immunocytochemistry

Stimulated as specified in the figure legends splenic B cells (1×10^5) in suspension 200 μL BioWhite fixative (Bioview Ltd. New Zion, Israel) were centrifuged onto glass slides using a Cytospin (Thermo Electron, Pittsburgh, PA). Slides were incubated in 3.7 % (v/v) formaldehyde (20 min), permeabilized with 0.5 % (v/v) Triton X-100 (5 min), and subsequently blocked in 2 % (w/v) BSA (30 min). Slides were incubated with anti-glut-1 antibody (ab14683, Abcam plc. Cambridge, MA) for 18 hr, followed by a 1 hr incubation with FITC-conjugated goat anti–rabbit IgG (Jackson ImmunoResearch Laboratories, Inc. West Grove, PA). After 4 washes with PBS, slides were mounted with Aqua-Poly/Mount (Polysciences, Inc. Warrington, PA) and analyzed by confocal laser scanning microscopy at 488 nm excitation (Leica TCS SP5 confocal microscope; Leica Microsystems, Wetzlar, Germany). A 100x/0.53 numeric aperture objective was used to visualize the images. Leica Confocal Software version 2.61 was used to acquire the images.

Assessment of cell cycle and viability

Approximately 5×10^5 cells stimulated as described in the figure legends were collected, washed in PBS, and then re-suspended in PBS containing 0.1 % Triton X-100, 50 μg/mL propidium iodide (PI) and 50 μg/mL RNase IIIA. After incubating

for 30 min (37^0C), DNA content was measured by flow cytometry using a FACSCanto cytometer and BDFACS Diva software (BD Biosciences San Jose, CA). Acquired data were analyzed with Modfit LT V3.0 (Verity Software House, Topsham, ME).

To assess viability, 5 x 10^5 cells were incubated in PBS containing 0.5 % FCS and 1 μg/mL PI, and exclusion of PI assessed by flow cytometry.

Assessment of relative cellular size

B cells (4 x 10^6/ml) were stimulated as specified in the figure legends and were collected, washed in PBS containing 0.5 % FCS, and evaluated under FSC-A parameter on FACSCanto cytometer and BDFACS Diva software (BD Biosciences, San Jose, CA). Flow rate and parameters (FSC, SSC) were held constant for duration of experiment.

Alternatively, B cells (0.4 x 10^6) in culture were collected, diluted in 200 μL PBS, and analyzed for size and volume by Scepter 2.0 cell counter with 40 μM sensors (EMD Millipore Corporation, Billerica, MA)

ATP determination

Stimulated as specified in the figure legends, B cells (4 x 10^6) were harvested, washed twice in PBS, centrifuged (500 x *g*, 8 min, 4°C) and cellular pellets were re-suspended in 500 μL deionized distilled H_2O. Using the bioluminescence kit available from Molecular Probes (Invitrogen, A22066), the amount of ATP was calculated in triplicate samples from a standard curve on a Lumat LB 9507

luminometer (EG&G Berthold Bad Wildbad, Germany).

Glucose transport measurements

Glucose transport was measured by monitoring the uptake of ^{3}H-labeled 2-deoxy-D-glucose (2-DOG) (Amersham Biosciences Corp. Piscataway, NJ) as described and adapted from Edinger and Thompson (2002) (73). B cells were stimulated as specified in the figure legends and re-suspended at 3 x 10^{7}/mL in uptake buffer (10 mM HEPES (pH 7.4), 136 mM NaCl, 4.7 mM KCl, 1.25 mM $CaCl_2$, and 1.25 mM $MgSO_4$). Transport was initiated by mixing 200 μL B cells with 200 μL uptake buffer containing 200 μM 2-deoxy-D-glucose (2-DOG) and 2 μCi (7.4 x 10^{4} Bq)/mL [^{3}H]2-DOG (Amersham Biosciences Corp. Piscataway, NJ). At the indicated times, 50 μL of the transport mixture was loaded onto a discontinuous gradient of 200 μL bromododecane per 40 μL 20 % perchloric acid, and the gradient was then centrifuged at 14000 x *g* (90 sec). Following centrifugation, the upper aqueous and bromododecane layers were decanted and the perchloric acid phase collected and placed into a vial containing 5 mL scintillation cocktail. The radioactivity was then quantitated by liquid scintillation spectrometry. To assess the contribution of glucose uptake mediated by glucose transporters, uptake of [^{3}H]2-DOG was measured in the presence of 10 μM cytochalasin B, a potent inhibitor of glucose transporter activity.

Glucose utilization (glycolysis) measurements

B cells (10^6 cells/0.5 mL) were stimulated as specified in the figure legends and incubated with 5-[^{3}H]-D-glucose (Amersham Biosciences) for 90 min. The initial rate of anti-Ig-induced glycolysis remained linear for 180 min. Adapted from Fitzpatrick *et al*. 1993 (128), at the indicated times, 100 μL of cells was removed and placed in 1.5 mL free-standing microcentrifuge tubes containing 50 μL 0.2 N HCl. The tubes were then placed in 20 mL scintillation vials containing 0.5 mL water and the vials capped and sealed. [^{3}H]-OH was separated from non-metabolized [^{3}H]-D-glucose by evaporation diffusion for 48 hr. The amount of diffused and non-diffused tritium was quantitated by liquid scintillation spectrometry and compared with parallel vials containing 5-[^{3}H]-D-glucose only and [^{3}H]$_2$O alone.

BrdU incorporation

2 x 10^6 B cells were stimulated as specified in the figure legends and were pulsed for 24 hr with 20 μM bromodeoxyuridine (BrdU). Proliferation was measured and quantified on BD FACSCanto as amount of FITC-BrdU labeling with steps following protocol within Pharmingen FITC-BrdU Flow kit (San Jose, CA).

RT-PCR

Subsequent to stimulation as specified in the figure legends, total RNA was isolated from B cells using the RNeasy mini RNA isolation kit (QIAGEN Inc., Valencia, CA), following the manufacturer's protocol. Following DNase-I treatment, 2 μg RNA was

reverse-transcribed to cDNA using MMLV reverse transcriptase (Ambion Inc., Austin, TX). Real-time PCR was performed with the RealMasterMix SYBR (5Prime Inc., Gaithersburg, MD) on a Mastercycler eGradient realplex^2 Real-time PCR detection system (Eppendorf, Germany). Amplification conditions were as follows: ldh2: 95^{o}C 2 min, followed by 40 cycles of 95^{o}C 15 sec, 55^{o}C 20 sec, 72^{o}C 20 sec. hk2: 95^{o}C 2 min, followed by 40 cycles of 95^{o}C 15 sec, 58^{o}C 20 sec, 72^{o}C 20 sec. pfk1: 95^{o}C 2 min, followed by 40 cycles of 95^{o}C 15 sec, 58^{o}C 20 sec, 72^{o}C 20 sec. glut-1: 95^{o}C 5 min, followed by 40 cycles of 95^{o}C 45 sec, 60^{o}C 45 sec, 72^{o}C 45 sec. Real-time primers contained a specified amplicon length of between 150 and 200 bp. Primers were as follows: forward (F) reverse (R) in 5' to 3' format

β2microglobulin	F-CACCCGCCTCACATTGAAATA	R-CATGCTTAACTCTGCAGGCGT
18S	F-GGTGGTGGTCGTTGGTGTG	R-ACAGGGCGGTGGGTTGG
ldh2	F-CATCGTGGTTTCCAACCCA	R-CGGAATCGAGCAGAATCCA
ldh3	F-AGTGGTGTAAACGTTGCTGGC	R-CCACCACCTGCTTGTGAACAT
hk2	F-TGGAGATTTCTAGGCGGTTCC	R-CATCCGGAGTTGACCTCACAA
pfk1	F-TCCGAGGAAGGCGTTTTGA	R-TGACGGCTACATTGCAGTTGC
glut-1(2)	F-GAGCCCATCCCATCCACCAC	R-TAAGCACAGCAGCCACAAAGG
glut-1 (D/E)	F-CTAGAGCTTCGAGCGCAGCGC	R-AGGCCAACAGGTTCATCATC

Relative expression of RNA was determined as the relative expression = 2^(DDCT), where DDCT = (cycle threshold (CT) of gene of interest): (CT of β2-microglobulin or 18S). Real-time SYBR-green dissociation curves show one species of amplicon for each primer combination (data not shown).

Lipid isolation and HP-TLC

B cells (75 x 10^6) were stimulated as specified in the figure legends in medium containing 1 μCi/mL [^{14}C]-U-D-glucose (MP Biomedicals, LLC. Solon, OH) for indicated time points, washed in PBS, and pellets were stored -80^{o}C. Cellular lipids were extracted in methanol: chloroform (1:1) overnight (25^{o}C). Neutral and acidic lipids were separated using DEAE-Sephadex (A-25, Pharmacia Biotech, Upsala, Sweden) column chromatography. Briefly, DEAE-Sephadex was prepared in bulk by washing the resin three times with solvent B ($CHCl_3$: CH_3OH: 0.8 M Na acetate, 30: 60: 8 by volume), equilibrating in solvent B overnight, followed by washing three times with solvent A ($CHCl_3$: CH_3OH: dH_2O, 30: 60: 8, by volume) until neutral. The total lipid extract, isolated in chloroform-methanol (1:1), was suspended in solvent A and applied to a solvent A-equilibrated DEAE-Sephadex column (1.2 mL bed volume). The column was washed twice with 15 mL solvent A and the entire neutral lipid fraction, consisting of the initial eluent plus washes, was collected. This fraction contained cholesterol, phosphatidylcholine, phosphatidylethanolamine and plasmologens, sphingomyelin, and neutral GSLs to include cerebrosides and GA2. Next, acidic lipids were eluted from the column with 35 mL solvent B. The acidic lipid fraction containing gangliosides was dried by rotary evaporation and transferred to a 15 mL graduated conical glass tube using $CHCl_3$: CH_3OH (1:1, by volume) and adjusted to 7 mL using the same solvent. Water was added and the mixture was inverted, vortexed, and centrifuged for about 10 min at 1200 *x g* to partition gangliosides in the upper phase (235, 236). The upper aqueous phase was

removed and the lower organic phase was washed once with 4.5 mL of the Folch 'pure solvent upper phase' ($CHCl_3$: CH_3OH: dH_2O, 3:48:47, by volume). The combined upper phases, containing gangliosides, were adjusted to 11 mL using CH_3OH. The acidic phospholipid fraction (Folch lower phase) was evaporated under a stream of nitrogen and re-suspended in 1 mL of $CHCl_3$: CH_3OH (1:1, by volume). This fraction contained fatty acids, cardiolipin, phosphatidylserine, phosphatidylinositol, sulfatides. Neutral lipids were dried by rotary evaporation and re-suspended in 1 mL $CHCl_3$: CH_3OH (2:1, by volume). An internal standard (oleoyl alcohol) was added to the neutral and acidic lipid standards and samples as loading controls (237). Purified lipid standards were either purchased from Matreya Inc. (Pleasant Gap, PA, USA), Sigma (St. Louis, MO, USA), or were a gift from Dr. Robert Yu (Medical College of Georgia, Augusta, GA, USA). For extraction controls, B cell samples were spiked with 10 μg lysophosphocholine and cerebrosides (Avanti Polar Lipids, Inc. Alabaster, Alabama) as both lipids were not seen in preliminary bulk lipid isolation of B cell used the method described here. Separated by thin-layer chromatography, plates were developed first to 4.5 cm (of 10 cm total length) in chloroform: methanol: acetate: formate: water (35: 15: 6: 2: 1 volumes), and then to 10 cm with hexane: diisopropyl ether: acetate (65: 35: 2 volumes). [^{14}C]-labeled lipids were visualized on phosphoimager (Storm820, Amersham Biosciences) or by film exposure, minimum 1 week. Total lipids were then visualized by charring in the presence of a solution of 3 % $Cu(OAc)_2$ and 8 %

H_3PO_4. Densitometry was conducted with ImageQuant and LamagTCL scanner with winScan softwares.

ACL enzymatic activity measurements

[^{14}C]-citric acid and MicroScint-O were obtained from Perkin Elmer (Waltham, MA). All other reagents are from Sigma-Aldrich (St. Louis, MO). Approximately 5 x 10^6 B cells, stimulated as specified in the figure legends, were lysed in 150 μL lysis buffer (10 mM Tris, pH 8.0, 150 mM NaCl, 23 mM deoxycholate, 1 % NP-40, 0.1 % SDS) supplemented with 1 mM PMSF, protease inhibitor cocktail. The lysate was centrifuged at 14,000 x *g* for 10 min. The supernatant assessed for ACL activity using the method of Ma *et al.* 2009 (238). The enzymatic reaction of B cell extracts was carried out in 17.5 μL of reaction buffer (87 mM Tris, pH 8.0, 20 μM $MgCl_2$, 10 mM KCl, 10 mM DTT) containing substrates 100 μM CoA, 400 μM ATP, 150 μM [^{14}C]-citrate (specific activity: 2 μCi/μmol) at 37^{o}C for 3 hr. The reaction was terminated by the addition of 1 μL 0.5 M EDTA. An aliquot of 60 μL MicroScint-O was then added to the reaction mixture and incubated at room temperature overnight with gentle shaking. The samples were centrifuged 14000 x *g*, 15 min. Aliquots of supernatant were collected in triplicate (10 μL) and [^{14}C]-acetyl CoA was detected with a Packard Bioscience Tri-Carb 2900 liquid scintillation analyzer (PerkinElmer, Inc. Waltham, MA). The count time was 5 min and the unit of signal is expressed as CPM.

ACL activity was also measured via the malate dehydrogenase coupled method,

described by Linn and Srere 1979 (239). B cells (8 x10^6) were stimulated as specified in the figure legends and solubilized in RIPA buffer (25 mM Tris (pH 7.6), 150 mM NaCl, 1 % NP-40, 1 % sodium deoxycholate, 0.1 % SDS) containing 2.5 μg/mL leupeptin/aprotinin, 10 mM β-glycerophosphate, 1 mM PMSF, 1 mM NaF, and 1 mM Na_3VO_4. Insoluble debris was removed by centrifugation at 15,000 x *g* for 15 min (4°C). Whole cell lysates were added at a 1:19 ratio to the reaction mixture containing 100 mM Tris-HCL (pH 8.7), 20 mM potassium citrate, 10 mM $MgCl_2$, 10 mM DTT, 0.5 U/mL malate dehydrogenase, 0.33 mM CoASH, 0.14 mM NADH, and 5 mM ATP. Change in absorbance at 340 nm was read every 30 s over 12 min on SpectraMax M5 Spectrophotometer with SoftMax Pro v5.4 (Molecular Devices, LLC Sunnyvale, California). Change in absorbance in the absence of exogenous ATP was subtracted from change in absorbance in the presence of ATP. These experiments were carried out in collaboration with Dr. Maria Gumina, Department of Biology, Boston College, Chestnut Hill, MA.

Lactate assay

B cells stimulated and cultured as described in figure legend. Post-centrifugation (500 x *g*), culture media was collected as cell-free supernatant and assessed for lactate concentrations. Lactate was measured in supernatants using an assay kit according to the manufacturer's instructions (Pointe Scientific, Inc. Detroit, MI).

Glucose Consumption/ CO_2 Capture

Stimulated as specified in the figure legends, B cells (4 x 10^6/mL) were cultured in media without bicarbonate with (1 μCi/mL) [$^{14}C_1$]-D-glucose or [$^{14}C_6$]-D-glucose. The method was adapted from procedure detailed by Taber *et al.* 1976 (240). In brief, aliquots of 250 μl cell suspension were placed in a 96 well Falcon tissue culture plate and immediately the plate was covered with prepared filter paper impregnated with 12 N $Ba(OH)_2$ and a plastic lid. The lid was sealed with Parafilm and secured with rubber bands. The plate was then wrapped in aluminum foil to limit exposure to light and incubated at 37°C, 48 hr. The paper was then removed and briefly immersed in acetone, allowed to air-dry, and heated for 5 min at 110°C. The paper is exposed on X-ray film for 1 to 7 days to examine the amount of capture CO_2 in form of barium carbonate.

The $Ba(OH)_2$ saturated paper was prepared by dipping pieces of Whatman 3MM paper (11 x 7 cm) with saturated 12 N $Ba(OH)_2$, drying the papers by blotting with filter paper, and storing in a desiccator over a KOH pellets until dry (up to 5 days) to avoid prolonged contact of the paper with atmospheric CO_2.

Gas chromatography/mass spectroscopy

Unstimulated and LPS-stimulated B cells (6.5 x 10^6) were cultured in modified RPMI-1640 containing 10 % dialyzed FCS (Atlanta Biologicals, Mannassas GA) and 50 % ^{13}C-U-glucose (1 g/L) or 50 % ^{13}C-U-glutamine (0.3 g/L) (Cambridge Isotope Laboratories, Inc. Andover, MA) in the absence or presence of compound-9 (35

μM). At 4 hr, 24 hr, 36 hr, and 48 hr, B cells were harvested, centrifuged at 500 x *g*, and the supernatant collected and frozen at -80°C. Cellular pellets were washed in PBS, re-centrifuged and cellular pellets devoid of supernatant frozen at -80°C. Further steps of this method and analysis were conducted by Dr. Adam Richardson and Dr. David Scott of The Cancer Center; Burnham Institute for Medical Research (La Jolla, CA). Cell pellets were extracted with a 1:1:1 mix of H_2O: CH_3OH: $CHCl_3$. The $CHCl_3$ extracts were methylated to produce fatty acid methyl esters (FAMES) and analyzed by GC-MS. C17:0 fatty acid was added to the samples to serve as an internal standard. Relative amounts of fatty acids were calculated based on intensity of methyl ester ions and adjusted for internal standard as needed. The amounts of different fatty acids were based on total ion count peak area. Fatty acid synthesis and labeling of constituent acetyl units in fatty acids were calculated using methods from Lee *et al*. 1994 (234).

Results

I. B cells modulate glucose utilization through growth and survival pathways.

Glucose is a ubiquitous source of energy for mammalian cells and is utilized in a multitude of cellular processes. The steps involved in the metabolism of glucose have been biochemically elucidated for many years, yet I aimed to investigate the regulation and biological importance underlying the utilization of glucose in B cell biology.

A. Regulation of glucose transport in primary splenic B cells

This investigation began by establishing the uptake of glucose in B cells responding to signals that stimulate activation. B cells do not store glucose as glycogen and thus rely on obtaining glucose from external sources (241). B cell receptor (BCR) engagement and signaling is achieved *in vitro* by its cross-linking with F(ab)'$_2$ IgM (αIg) (242). The amount of glucose uptake was measured in quiescent, small dense splenic B cells (Media) and cells stimulated for 15 hr with αIg. The quantity of [^{3}H]-2-deoxy-glucose taken into B cells within 60 sec of exposure in culture increased in lymphocytes stimulated with αIg (Figure 1A). To assure the specificity of the uptake (transporter-mediated versus simple diffusion), cytochalasin B was added to cells, as it is a glucose transporter inhibitor (K_i = 1 μM) (243, 244). The rate at which [^{3}H]-2-deoxy-glucose was taken up by B cells in the presence of cytochalasin B was linear within 90 sec of exposure to glucose in culture (Figure 1A inset); cytochalasin B blocked this increase. Therefore the induced

uptake illustrated with αIg stimulation is mediated through the function of specific glucose transporters in the B cell plasma membrane.

Alternatively, I investigated the effects of other B cell stimuli, including: lipopolysaccharide (LPS) and interleukin-4 (IL-4). LPS is a surface antigen from the surface of Gram-positive bacteria that engages the toll-like receptor (TLR4) and is sufficient to induce B cell proliferation and differentiation (97, 98). IL-4 is a cytokine that upon binding to its receptor (IL-4R) on the B cell surface initiates growth (*i.e.* increased cell size and mass) and survival, but not proliferation of B-lymphocytes (245, 246). I compared glucose uptake in B cells unstimulated (Media) to those cultured with stimuli for 15 hr. Uptake was significantly induced with αIg, LPS, and IL-4 (Figure 1B). The largest increase in uptake was observed in B cells stimulated with αIg. These data indicate that upon activation, B cells increase uptake of extracellular glucose.

Since glucose transport increased with B cell stimulation, I examined the expression of glucose transporters. A constitutively expressed carrier that directs glucose from extracellular to intracellular compartments is glucose transporter-1 (glut-1) (247). Quiescent B cells stimulated with αIg and IL-4 (αIg + IL-4), αIg, IL-4, or LPS were collected at 3 hr, 9 hr, and 20 hr for subsequent protein extraction and glut-1 detection by Western blotting. As shown in Figure 2A, the amount of glut-1 protein recovered in B cell extracts increased with αIg + IL-4 above unstimulated (Media) at 20 hr post-stimulation and to a lesser extent in αIg, IL-4 and LPS extracts. Of note, extracts of LPS stimulation at 3 hr and 9 hr were poorly transferred or the

glut-1 carrier degraded, shown by Ponceau S staining of the PVDF membrane prior to incubation with anti-glut-1 Ab. Typical of glut-1 migration in poly-acrylamide SDS gels, distinct bands were not readily visualized; glut-1 appeared to migrate as smears that increased in intensity as a function of time post-stimulation. I speculated this is due to the inherent features of the glut-1 protein and extraction process since in the literature glut-1 has been shown to be highly glycosylated, comprised of 7-12 membrane spanning domains (248, 249). To reduce the glut-1 smear evident during SDS-PAGE, I incubated B cell protein extracts obtained from IL-4 stimulated (20 hr) and unstimulated B cells with the de-glycosylating enzyme PNGase F and repeated the Western blot (248, 250). Glut-1 was detected as a smear in samples without enzyme treatment, however glut-1 migrated in a distinct band with PNGase treatment in both media and IL-4 stimulated B cell extracts (Figure 2B). Increase in glut-1 expression was apparent with concise band designation on Western blot.

To ensure that my detergent lysis procedure was extracting plasma membrane integral proteins, I examined another membrane-associated transporter-the sodium-potassium ATPase exchange pump (Na^+K^+ pump). The Na^+K^+ pump is responsible for the maintenance of ion gradients necessary for cell volume and potential (251). The Na^+K^+ pump expression was shown to be up-regulated in human T-cells with the stimulation with interleukin-2 (252). B cells stimulated with αIg + IL-4, αIg, IL-4, or LPS were collected and protein extracted at 3 hr, 9 hr, and 20 hr for detection of Na^+K^+ pump by Western blotting. In stimulated B cell extracts

(Figure 2C), an increase in Na^+K^+ pump expression was detected within 3 hr in response to each stimulus. Further increase of Na^+K^+ pump protein was detected at all time points of stimulation with αIg and αIg + IL-4.

T-lymphocytes and myoblasts upon cellular stimulation undergo a process termed "glut-trafficking" wherein glucose transporters migrate from cytoplasmic vesicles to the plasma membrane upon cellular activation (253-256). I sought to investigate the glut-1 localization in naïve and activated B cells, meanwhile confirming the induction of glut-1. Using immunocytochemistry (ICC), first I determined the optimal dose of anti-glut-1 antibody for detection by confocal microscopy. B cells left unstimulated (Media) or stimulated with αIg + IL-4 for 24 hr were fixed, permeabilized, and then stained with increasing concentrations of anti-glut-1 antibody. Indirectly detected by fluorescently tagged secondary antibody (anti-rabbit IgG-FITC), glut-1 in B cells was optimally detected at a dilution of 1:200 (Figure 3). Compared to unstimulated, I was able to observe a clear increase in glut-1 staining in αIg + IL-4 stimulated B cells.

Having established the ability to detect glut-1 by ICC, I proceeded to examine glut-1 expression in B cells stimulated for 43 hr with additional stimuli: αIg, αIg + IL-4, and IL-4. This time point was chosen to allow B cells to respond to stimuli for differentiation and proliferation, without progression through cell division, which occurs at 48 hr, as well as maximizing possible glut-1 expression. B cells were also stimulated with the maturation factor cluster of differentiation 40-ligand (CD40L). CD40 is a receptor on the surface of B cells that recognizes T-lymphocyte CD40

ligand (CD40L) (103). Physiologically relevant, the interaction of CD40L:CD40 permits B cells to mature into plasma cells that produce antibodies of different classes other than immunoglobulin M (IgM), namely immunoglobulin G (IgG), immunoglobulin A (IgA), and immunoglobulin E (IgE) (104). Glut-1 was induced in B cells under a variety of stimuli, including αIg + IL-4, αIg, and CD40L (Figure 4). I was unable to visualize glut-1 localization in the cytosol by ICC despite labeling of glut-1 in αIg + IL-4, αIg, and CD40L stimulated B cells because most of the cytosol is taken up with the nucleus. Low level staining was unexpected given that the levels of glut-1 protein examined by Western blot (Figure 3) demonstrated an increase in glut-1 under IL-4 stimulation at 20 hr.

To further confirm glut-1 induction in activated B cells, I examined its expression by flow cytometry. B cells were harvested at 6 hr and 12 hr after stimulation with αIg, fixed, permeabilized, and incubated with anti-glut-1 antibody. Subsequent addition of phytoerythrin (PE)-conjugated secondary antibody to indirectly label the glut-1 protein permitted quantification of fluorescence by flow cytometry. As illustrated in Figure 5, B cells induced glut-1 expression following αIg stimulation at 6 hr (blue line) and 12 hr (red line). Moreover, glut-1 expression in B cells stimulated with IL-4 was induced at 15 hr (Figure 6). In summary, the results suggest increased surface expression of glut-1 protein in B cells activated by extracellular stimuli.

I next examined if transcription of the *glut-1* gene increased as well. To examine *glut-1* transcript levels, RNA was extracted from B cells stimulated with αIg

or CD40L for 6 hr, 11 hr, and 24 hr and evaluated by semi-quantitative real-time PCR. The ratio of expression of *glut-1* to the housekeeping gene *18S* rRNA transcript was calculated in unstimulated B cells (Media) and served as a standard baseline SYBR green ratio of 1. Comparison of the ratio of *glut-1*:*18S* transcripts for αIg or CD40L stimuli to the relative level of *glut-1*:*18S* in media revealed increased glut-1 mRNA transcripts (Figure 7). In particular, B cells stimulated with αIg for 11 hr increased relative *glut-1* expression 8-fold, whereas CD40L induced relative *glut-1* expression 2-fold at 6 hr and maintained the induced level at 24 hr. These results suggest that the induction of *glut-1* occurs at the transcriptional level in B cells stimulated with αIg or CD40L. It should be mentioned that for mRNA studies, B cells were isolated from an alternative strain, CBA/CaJ mice rather than the previous BALBc/ByJ strain. Despite variation in haplotype ($H\text{-}2^k$) vs. ($H\text{-}2^d$), each inbred strain has routinely and commonly used in the scientific community and no alterations in B cell population or signaling as a result of stimuli used in my experiments were found (257).

In summary, the results have demonstrated that B cells induce not only glucose transport, but also expression of the glut-1 transporter on the cell surface in response to stimulation by activation signals. I next proceeded to examine intracellular signaling pathways activated by stimulation for putative role(s) in the observed induction of glucose uptake and glut-1 expression.

B. Activation of signaling pathways involved in B cell glucose utilization

I sought to identify intracellular signaling pathways that regulate glucose uptake and glut-1 expression in B cells following BCR ligation. Activated by extracellular stimuli, PI3K and its molecular targets have been suggested as major effectors of viability, growth, and proliferation in T cells, though the role of this pathway has yet to be established in B cells (119, 73, 255, 258, 259). PI3K is a dimer comprised of a catalytic and regulatory subunit, predominantly p110δ/γ and p85α in murine B cells, respectively (260). With this in mind, I sought to determine if PI3K activity was necessary for αIg-mediated induction of glucose transport through the use of chemical inhibition of PI3K and in mice deficient in the p85α.

B cells were stimulated with αIg for 15 hr in the presence or absence of two PI3K inhibitors, LY294002 (LY) and wortmannin (Wort), and subsequently evaluated for glucose uptake. LY is a potent, competitive inhibitor of PI3K that irreversibly binds to p110 at the ATP binding site (261-264). Wort is a highly potent, non-competitive, yet irreversible inhibitor that is specific for the catalytic site in p110γ subunit of PI3K (265, 266). The addition of LY or Wort to B cells reduced the αIg-mediated increase in [^{3}H]-2-deoxy-glucose uptake (Figure 8). Wort addition resulted in relatively less inhibition of uptake in comparison to LY treatment. This result was perhaps due to the expression of the alternative isoform of PI3K catalytic subunit, p110δ, in B cells that may require a higher concentration for complete inhibition of its activity (260, 265, 267, 268).

Glucose uptake was also measured in B cells treated with rapamycin (Rap)

for 15 hr. Rap is an inhibitor of mammalian target of rapamycin (mTOR), a complex activated by Akt through PI3K, which has been reported to be involved in regulating glucose metabolism (264, 269, 270). The amount of glucose uptake was not affected by the addition of Rap (Figure 8). These results suggested that BCR-induced glucose uptake requires PI3K activity.

I obtained murine knockout models to further identify the contribution of PI3K activity in glucose uptake of B cells. Mice deficient in the PI3K regulatory subunit p85α (p85$\alpha^{-/-}$) have low splenic B-lymphocyte numbers, smaller body mass, and shorter life span (271). As a consequence, I was unable to obtain sufficient B cell numbers and viability for glucose uptake experiments. I therefore examined glut-1 expression by flow cytometry in these p85$\alpha^{-/-}$ B cells stimulated with αIg. B cells of p85$\alpha^{-/-}$ mice were cultured in the presence of αIg for 12 hr, collected, fixed, and permeabilized. Expression of glut-1 was quantified by flow cytometry after cell samples were incubated with anti-glut-1 antibody and PE-conjugated secondary antibody (Figure 9). The p85$\alpha^{-/-}$ B cells failed to increase glut-1 expression at 12 hr post-αIg stimulation above the amount displayed in control unstimulated B cells (Media).

I next sought to examine additional BCR-associated signaling components mediating BCR-induced glut-1 expression. Bruton's agammaglobulinemia tyrosine kinase (BTK) is a kinase that has been shown to be important for B cell development, differentiation, and signaling (18). Mutations in BTK lead to X-linked immunodeficiency (XID) in mice (19, 30). As previously described in *Introduction*

section, BTK is active following BCR engagement, directly regulated by PH domain interaction with lipids formed by PI3K activity (20, 23, 24, 272). I utilized XID mice to decipher the requirement of BTK activity for induction of glut-1 expression in B cells responding to stimuli. Given the low recovery of B cells from XID splenic tissue, glut-1 expression was monitored by immunocytochemistry (ICC). XID B cells were harvested after 24 hr of αIg stimulation, and examined for glut-1 expression. By ICC, XID B cells did not measurably increase glut-1 expression in response to αIg (Figure 10). In contrast, B cells from CBA/CaJ strain, the control background strain of XID mice, increased glut-1 expression at 24 hr post-αIg stimulation. These results indicate the engagement of the BCR by αIg induced glut-1 expression, at least in part, through BTK function.

In summary, the results have suggested a role for PI3K activity to increase glucose uptake in B cells specifically activated via BCR ligation. Notably, I have established a role for the PI3K subunit, p85α, and BTK activity in mediating BCR-induced glut-1 expression.

C. Growth and viability of splenic B cells in *ex vivo* cultures

I next explored the role of glucose in B cells responding to stimuli that promote growth and survival. Using flow cytometry, I monitored size alterations using the parameter of forward scatter-area (FSC-A). The relative area of light scatter distributed from individual cells passing through laser beam are captured and quantified by electronic sensors to provide a relative size unit (arbitrary unit, au)

for a cell or "event" (273). An increase in FSC-A, *i.e.* induced cellular enlargement, was observed in B cells stimulated with αIg, αIg + IL-4, CD40L, IL-4, or LPS at 20 hr and 40 hr. The greatest increase in FSC-A was displayed in B cells in response to αIg + IL-4 stimulation, increasing to ~200000 au at 48 hr (Figure 11A). Stimulation with CD40L, αIg, or LPS also enlarged B cells at 20 hr and 40 hr, whereas IL-4 only slightly increased the FSC-A of B cells compared to control unstimulated B cells (Media). B cells cultured in medium alone without stimulation (Media) decrease in size within 20 hr.

I also investigated the viability of B cells in response to alternative activating stimuli. Viability was assayed by flow cytometry, as the number of cells (shown in percent PI negative out of 10,000 events) capable of excluding the nucleic acid dye propidium iodide (PI). The viability of unstimulated B cells (Media) over time in culture decreased to 52 % within 24 hr. Without stimulation, B cells apoptose within 24 hr and more so at 48 hr due to removal from the *in vivo* environment and transfer to *in vitro* culture (274, 275). Viability decreased with αIg stimulation over time, with minimum viability of 50 % at 24 hr. B cells were also stimulated with IL-4, CD40L, αIg + IL-4, and LPS for 24 hr and 48 hr, collected and analyzed. Addition of IL-4 to αIg stimulation resulted in survival of B cells (Figure 11B) (168, 169). The viability of B cells was maintained with moderate reduction up to 48 hr under conditions of IL-4, CD40L, αIg + IL-4, and LPS stimulation. Collectively, these results indicated that B cells in response to growth and differentiation stimuli increase size and maintain viability.

D. Requirement of glucose for growth and survival of stimulated B cells

To evaluate the requirement of increased glucose utilization for growth or survival of B cells, I measured cell size and viability in response to IL-4 by flow cytometry in the presence or absence of the glycolytic inhibitors 2-deoxy-glucose (2DG) or iodoacetamide (IAN). A glucose analog, 2DG inhibits hexokinase, whereas IAN is an irreversible inhibitor of cysteine peptidases and inhibits glucose metabolism by interacting with glyceraldehyde 3-dehydrogenase as well as other putative glycolytic enzymes (276-278). IL-4 stimulated B cells were treated with 1 mM 2DG or 10 μM IAN for 18 hr and then assayed for size and viability. Induced cellular size in response to IL-4 was not diminished by the addition of 2DG or IAN. The presence of 2DG with IL-4 stimulation reduced the enlargement of cells to 128000 FSC-A from 131000 FSC-A demonstrated without inhibitor, however this change was not statistically significant (Figure 12A). IAN prevented enlargement of cells similarly reducing FSC-A.

The assessment of viability at 18 hr of IL-4 stimulated B cells with addition of IAN and 2DG was also conducted. Both inhibitors provided similar results wherein a reduction of viability in IL-4 stimulated B cells by 30 % (Figure 12B). Alternatively, I measured cell size and viability in response to IL-4 by flow cytometry in the presence or absence of inhibition of glucose uptake (glucose transporter) with 5-thioglucopyranose (5TG) or inhibition of glycolysis (hexokinase) evaluated with 3-bromopyruvate (BP) (276, 277, 279). Neither 5TG

nor BP had a significant effect on IL-4 stimulated B cell viability or size at 24 hr (Figures 13 and 14, respectively). The results thus suggest B cells respond to IL-4 in a manner dependent on glucose metabolism for viability and not cellular size.

E. Metabolism of glucose in B cells in response to BCR cross-linking

I have shown thus far that B cells respond to a variety of extracellular stimuli that promote growth and/or survival by increasing glucose uptake at least in part via glut-1 transporters. In addition, the glucose response to BCR engagement was mediated by activation of the signal molecules BTK and PI3K. To further explore the utilization of intracellular glucose in activated B cells, I examined the ability of cells to metabolize glucose through glycolysis. By pulsing B cells with [^{3}H]-5-glucose (1 μCi/ml), the glycolytic rate was quantified as the production of tritiated water ([^{3}H]OH) from the penultimate step of glycolysis (280). As shown in Figure 15, B cells upon stimulation with αIg increased the rate of glucose metabolism via glycolysis within 20 hr and maintained a high rate of glycolysis for 48 hr.

I also explored the ability of additional stimuli to enhance the glycolysis of acquired glucose in B cells. Cells were stimulated with CD40L, LPS, αIg + IL-4, IL-4, and for comparison αIg for 20 hr and glycolysis assays performed. An increased rate of glycolysis was observed in all samples, though the increase above unstimulated B cells varied with different stimuli. B cells stimulated with CD40L, LPS, or αIg + IL-4 produced the largest increase in glycolytic rate at 20 hr (Figure 16). IL-4 stimulated B cells in comparison to αIg displayed a lower rate of glycolysis,

despite the increase above unstimulated (Media) B cells. These results indicate that the rate of glycolysis was increased in activated B cells responding to external stimuli and correlate to aforementioned results observing a differential in glucose transport.

I next sought to evaluate putative role(s) of intracellular signal molecules in the regulation of glycolysis. To decipher the role of PI3K in induction of glycolysis, I again used the PI3K inhibitors, LY and Wort. B cells were stimulated with αIg in the presence of LY or Wort for 12 hr and glycolysis assays performed. The increased rate of glycolysis provided by αIg stimulation was significantly reduced in B cells cultured with LY or Wort (Figure 17). The inhibition of PI3K activity resulted in reduced glycolytic rates to levels displayed in control untreated B cells (Media). Therefore PI3K activity is required for induction of glycolysis in the response to cross-linking of the BCR.

The role of PI3K activity in induction of glycolysis of αIg stimulated B cells was also evaluated in p85$\alpha^{-/-}$ mice. B cells of p85$a^{-/-}$ and BALBc/ByJ (WT) mice were stimulated with αIg for 18 hr and 28 hr and glycolytic rates measured. The p85α-deficient B cells failed to increase glycolysis in response to αIg (Figure 18), whereas wild-type B cells stimulated with αIg increased the rate of glycolysis at 18 hr and 28 hr. Taken together, the activity of PI3K is essential for the induction of glycolysis in response to BCR engagement.

In addition, I evaluated the role of functional BTK in the control of BCR-mediated glycolysis. Murine B cells obtained from XID or control wild-type

(CBA/CaJ) strains were stimulated with αIg and glycolytic rates determined. Engagement of the BCR by αIg resulted in a moderate increase in glycolysis in XID B cells within 3 hr with no additional increase at 6 hr, 12 hr, or 22 hr, in comparison to unstimulated XID B cells (Figure 19A). Similarly, CBA/CaJ B cells upon αIg stimulation induced glycolysis at 3 hr, however a significant increase in glycolytic rate was exhibited at 6 hr, 12 hr, and especially at 22 hr. To determine if functionally BTK-deficient B cells respond to extracellular stimuli by increased glycolysis independent of the BCR, glycolysis was monitored in XID and CBA/CaJ B cells stimulated with CD40L for 3 hr, 6 hr, 12 hr, and 22 hr. The increase of glycolysis in response to CD40L was similar in B cells from XID or CBA/CaJ, suggesting a regulatory role BTK in BCR-mediated glycolytic flux. Similar results were obtained in BTK-deficient B cells (Figure 19B) stimulated with CD40L (for 6 hr, 12 hr, and 23 hr) or αIg (for 6 hr, 12 hr, 23 hr, 44 hr, and 72 hr). Therefore BTK is a necessary signaling component involved in activation pathways following BCR engagement, not CD40L, for increased glycolysis.

The B-cell linker protein (BLNK) is an adaptor protein that promotes membrane recruitment, activation, and association of BCR with BTK, PLCγ, and PI3K (281). Defects in BLNK lead to inhibition of B cell maturation and differentiation and cause agammaglobulinemia (282). I examined BLNK for its contribution to the regulation of glucose utilization in BLNK-deficient B cells ($BLNK^{-/-}$). B cells of both $BLNK^{-/-}$ and the control strain (129xSV) were stimulated with αIg, CD40L, and LPS for 5 hr, and glycolysis assays were performed. 129xSV B cells increased glycolysis,

as BLNK$^{-/-}$ B cells were also able to induce glycolysis in response to BCR ligation (Figure 20). 129xSV B cells with LPS or CD40L to have comparable levels of glycolysis at 5 hr. In response to LPS or CD40L, BLNK-deficiency led to an induction of glycolysis in comparison to wild-type B cells. As expected, BLNK$^{-/-}$ B cells increased the glycolytic rate via LPS or CD40L to identical degrees as in wild-type B cells as these stimuli in published reports have been shown to induce proliferation in BLNK–deficient B cells (33, 283, 284).

BCR cross-linking results in the activation of the phospholipase Cγ (PLCγ) pathway in B cells. PLCγ hydrolyzes PIP2 (the membrane phospholipid generated by PI3K) to produce inositol-3,4,5-trisphosphate (IP3) and diacylglycerol (DAG), which in turn increases Ca^{2+} mobilization and activates protein kinase C (PKC), respectively (32, 49, 285). I evaluated the contribution of the PLCγ-PKC pathway in the induction of glucose metabolism via BCR cross-linking. Rottlerin was originally characterized as a selective inhibitor of PKCδ (IC_{50} = 3-6 μM), however recent reports indicate that this inhibitor also acts on additional to members of the PKC family (286, 287). B cells stimulated with αIg were incubated with rottlerin for 3 hr and 6 hr and glycolytic flux measured. An increase in glycolysis was observed with rottlerin to levels similar to B cells stimulated with αIg alone (Figure 21). The combination of αIg and rottlerin (αIg + Rottlerin) amplified the glycolytic rate in B cells further. The results presented here were not expected, as rottlerin appeared to stimulate glycolysis rather than inhibit, perhaps due to the lack of specificity of rottlerin (288). In light of these results, I subsequently evaluated the role of PKCδ in

BCR-induced glycolysis from PKCδ-deficient (PKCδ$^{-/-}$) B cells. B cells of PKCδ$^{-/-}$ and control wild-type background strain (WT: C57BL/6 X 129x1/SvJ) were stimulated for 24 hr with αIg and assayed for glycolysis. PKCδ$^{-/-}$ B cells increased glycolysis within 24 hr at a rate that was only slightly reduced in comparison to WT B cells (Figure 22). These results therefore suggest the role of PKCδ in the down-regulation of glycolysis in B cell responses.

F. Functional studies on the metabolism of glucose in response to IL-4

IL-4 stimulation of *ex* vivo B cells was shown in the aforementioned experiments to increase glucose uptake and utilization via glycolysis. As part of a parallel project, I investigated glucose utilization in B cells activated by IL-4. To this end, I obtained knockout mice with deficiency in a signal transducer and activator of transcription 6 (STAT6) (289). STAT6 is required for IL-4-mediated survival of B-lymphocytes (169, 290). I monitored the glycolytic rate in STAT6-deficient (STAT6 KO) B cells within 48 hr of IL-4 stimulation. Control strain BALBc/ByJ (WT) B cells increased glycolysis in the presence of IL-4, but not STAT6 KO B cells (Figure 23). STAT6 therefore is necessary for the response of B cells to IL-4. To determine if STAT6 was sufficient for the IL-4-mediated induction of glycolysis, I restored STAT6 protein by the addition of cell-permeable protein fusion constructs. Provided by Dr. Abu-Amer, STAT6 protein, wild-type (WT) or constitutively active (VT: valine, threonine substitution) was fused to trans-activating transcriptional activator (TAT) (TAT-STAT6 peptides), to allow efficient transported into cells (291-293). As shown

in Figure 23, the impairment of glycolysis in STAT6 KO B cells responding to IL-4 stimulation was rescued with addition of TAT-STAT6-WT at 48 hr. Furthermore, the addition of STAT6-VT in the absence of IL-4 stimulation enhanced the induction of glycolysis above that observed of IL-4 stimulated WT B cells. Therefore, B cells responding to IL-4 increase glycolysis in a STAT6-dependent manner.

G. Related experiments on glucose metabolism in splenic B cells

Glucose is phosphorylated by hexokinase (HK) to yield glucose-6 phosphate (294-296). Phosphofructokinase (PFK) commits glucose to glycolysis by the phosphorylation of fructose 6-phosphate to fructose 1,6-bisphosphate (297). Lactate dehydrogenase (LDH) converts the end product of glycolysis, pyruvate, to lactate for export out of a cell (298-304). I investigated the expression of these key glycolytic enzymes in αIg stimulated B cells at 24 hr and 48 hr by semi-quantitative real time PCR. Relative levels of gene expression of *pfk*, *ldh*, and *hk* were assessed by comparison of the threshold cycle number of the target gene of interest to the housekeeping gene of *18S rRNA* (68, 305, 306). The levels of enzyme expression increased in response to activation of the B cells within 24 hr, particularly *pfk* (Figure 24). The expression of *hk* was not induced significantly at 24 hr or 48 hr.

Glycolysis may also be modulated by the intracellular localization of glycolytic enzymes. Precedence provided by Gottlob *et al*. 2001 (307) indicated lymphocytes upon activation through Akt, translocate HK from cytosolic fractions to the outer mitochondrial membrane whereby this glycolytic enzyme interacted with the permeability transition pore (the voltage-dependent anion channel (VDAC) and

Bax) to promote cell survival (307-310). Hexokinase by direct interaction with the mitochondria thereby receives preferred access to mitochondrial ATP (311, 312). With the knowledge of its ability to associate with mitochondria, I sought to examine HK localization in B cells. I was unable to reproducibly isolate and purify mitochondrial fractions from primary B cells to monitor HK, by methods described by Gottlob *et al*. 2001 (307).

I next monitored glycolytic metabolite and ATP production in B cells in response to activation stimuli through BCR cross-linking or IL-4. Increased glucose consumption in proliferating cells has been shown to yield lactate; glucose through glycolysis serves as an energy source to provide fuel for increased demand (313). I evaluated the amount of lactate produced in B cells stimulated with αIg. By colorimetric enzyme assay, the amount of lactate secreted into the culture medium was monitored following B cell stimulation with αIg for 16 hr, 24 hr, and 48 hr. As shown in Figure 25, the amount of lactate produced and secreted by stimulated B cells increased over time. To evaluate the glycolytic response elicited through BTK in response to IL-4, I purified B cells from XID and CBA/CaJ mice. The amount of ATP produced from glycolysis or respiration was quantified in B cells stimulated with αIg or IL-4 for 22 hr by bioluminescence assay. I observed the greatest concentration of ATP (nM) in CBA/CaJ B cells stimulated with IL-4 and a significant increase in extracts of αIg stimulation (Figure 26). XID B cells yielded considerably less ATP than CBA/CaJ B cells under all experimental conditions. As expected, the concentration of ATP in XID B cells did not increase with αIg and only slightly with IL-4 stimulation at 22 hr. These results suggest that B cells in response to αIg or IL-

4 increase ATP production and that this increase requires BTK activity.

I next sought to determine the metabolism of intracellular glucose through the pentose phosphate shunt (PPP) and the citric acid cycle (TCA). Through radioactive labeling experiments, I monitored glucose consumption to generate CO_2 (314). The generation of $[^{14}C]O_2$ from [^{14}C]-1-labeled glucose occurs through the PPP whereby glucose-6 phosphate is utilized to generate ribulose-5-phosphate, CO_2 and NADPH (315). Further CO_2 may be generated from C-1 and C-6 when glucose is metabolized by glycolytic pathway, pyruvate dehydrogenase complex, and TCA (316, 317). B cells were cultured in the presence or absence of αIg or IL-4 for 44 hr in bicarbonate-free media and the released $[^{14}C]O_2$ was captured with saturated $Ba(OH)_2$ filter paper sandwiched in a sealed culture plate (240). Autoradiography revealed that B cells stimulated with αIg or IL-4 for 44 hr primarily produced $[^{14}C]O_2$ via decarboxylation at C-1, not significantly from C-6 of glucose (Figure 27). B cells stimulated with αIg produced a greater amount of $[^{14}C]O_2$ than cells stimulated with IL-4 or control unstimulated B cells.

In addition, I monitored $[^{14}C]O_2$ production in B cells in response to additional stimuli. B cells were cultured with αIg or IL-4 alone or in combination, or LPS for 24 hr and monitored for $[^{14}C]O_2$ production from [^{14}C]-1-glucose or [^{14}C]-6-glucose. B cells, stimulated with αIg + IL-4 produced the greatest amount of $[^{14}C]O_2$. A lesser amount of $[^{14}C]O_2$ was produced in B cells cultured with [^{14}C]-6-glucose, as an increase was observed only with αIg + IL-4 stimulation. Of note, B cells stimulated with IL-4, αIg + IL-4, or LPS significantly increased the production of $[^{14}C]O_2$ from [^{14}C]-1-glucose or [^{14}C]-6-glucose compared to unstimulated (Media)

(Figure 28). I alternatively treated B cells with phorbol myristate acetate and ionomycin (PMA + Iono) to bypass receptor dependent signal pathways and mimic the activation of the PLCγ pathway through activation of PKC and elevation of calcium ions (318-321). The B cell response to activation stimuli increased the metabolism of glucose to generate $[^{14}C]O_2$. To confirm the activity of PPP, I added 6-aminonicotinamide (6-ANA), an inhibitor of the PPP (322). B cells were stimulated with αIg for 18 hr were again monitored for the release of $[^{14}C]O_2$ from ^{14}C-1-glucose, but in the presence of 6-ANA for 24 hr. B cells produced less $[^{14}C]O_2$ than αIg B cells without inhibitor (Figure 29), though a minor reduction. In summary, B cells modulate glucose metabolism through BCR mediated signaling events for the production of CO_2, as well as ATP and lactate.

II. ATP Citrate Lyase is a regulatory protein in activated B-lymphocytes

Differentiation of mature B cells via mitogens results in activation and entry into cell cycle as well as immunoglobulin (Ig) production. During the proliferative response, extensive development of the endoplasmic reticulum (ER) network and other membrane organelles occurs in order to support the secretion of Ig. Their assembly requires substantial increases of membrane protein and phospholipid synthesis (120, 323).

In keeping with this, I sought to investigate whether glucose was metabolized in pathways other than glycolysis. Notably, it has been reported that glucose-derived carbons can be shuttled to *de novo* lipid synthesis pathways (119, 134, 324). ATP Citrate Lyase (ACL) is a lipogenic enzyme that catalyzes a critical reaction linking cellular glucose catabolism and lipogenesis (127, 325). On this point the metabolism of citrate is significantly reliant upon ACL. From the glycolytic end-product pyruvate, citrate is formed as an intermediate in the TCA (Krebs) cycle in the mitochondria and transported out and into the cytoplasm (Figure 30). The cytosolic citrate is converted into acetyl-Coenzyme A (acetyl-CoA) by ACL to support lipid synthesis. The function of ACL to control substrate supply for glucose-dependent lipid synthesis has been determined by both siRNA depletion and chemical inhibition in cell lines (122, 130, 153, 162, 164, 326). Down-regulation of ACL activity in cancer cell lines inhibits cell proliferation *in vitro* and *in vivo*, as well as decreases cholesterol, isoprenoid, and fatty acid synthesis.

A. ACL is a phosphorylated in B cells responding to extracellular stimuli

A few reports in the literature suggest a means of regulation of ACL activity is through phosphorylation events; in particular the enzymatic activity increases with phosphorylation at the residue serine 454/455 (150-152, 327). I sought to determine if ACL was phosphorylated during the B cell response to antigenic stimulation. Cellular extracts were prepared from B cells stimulated with IL-4, αIg, or αIg + IL-4 for up to 9 hr. Western blotting of protein extracts with anti-phospho-serine^{454}-ACL antibody (Ab) revealed phosphorylation of ACL at serine 454 (phospho-serine^{454} ACL) (Figure 31). As band intensity relates to the quantity of phospho-serine^{454} ACL in extracts, B cell stimuli increased the phosphorylation of ACL at serine^{454} at 3 hr and was maintained up to 9 hr, in comparison to unstimulated B cells (Media).

In addition, phospho-serine^{454} ACL was examined in extracts prepared from B cells stimulated with αIg, IL-4, alone or in combination for 24 hr, 48 hr, and 72 hr. The phosphorylation of ACL at serine^{454} was maintained up to 72 hr in the extracts of stimulated B cells. Stimulation of B cells with αIg alone at these extended time points displayed a greater amount of phospho-serine^{454} ACL versus αIg + IL-4. The Western blots were stripped and re-probed with anti-hsp90 Ab, for protein loading control. These results suggest that B cells phosphorylate ACL at serine^{454} in response to extracellular stimuli. Of note, two bands were detected by anti-phospho-serine^{454} ACL Ab. Currently, I do not know if the additional bands reflect a cross-reactivity or non-specific interaction of the antibody with an unrelated

protein, an additional isoform of ACL, degradation of the ACL protein, or the phosphorylation of ACL at another phospho-specific site (127).

B. Regulation of the phosphorylation of ACL

The regulation of ACL phosphorylation in tumor cells has been previously reported to be dependent upon several pathways, including the PI3K-Akt pathway (150, 159, 328, 329). Berwick *et al*. (2000) reported in non-immune cells the ability of Akt to induce the enzymatic activity of ACL upon serine^{454} phosphorylation (150). Akt is a downstream target of PI3K, phosphorylated on serine^{473} for its activation, which will activate the mTOR complex (330, 331). To investigate whether PI3K activity was involved in the phosphorylation of ACL on serine^{454}, I treated B cells with the PI3K inhibitors, LY294002 (LY) or wortmannin (Wort) post-6 hr stimulation with αIg, IL-4, or αIg + IL-4. Cellular extracts were prepared and the phosphorylation of ACL at serine^{454} was determined by Western blotting techniques. The phosphorylation of ACL at serine^{454} was reduced following inhibition of PI3K with either LY or Wort (Figure 32). As a control to confirm the activation of the PI3K-Akt pathway, B cells stimulated with αIg and/or IL-4 were treated with rapamycin and the phosphorylation of ACL at serine^{454} evaluated. Rapamycin is an inhibitor of the mTOR complex, a downstream target of Akt, which has not been reported to phosphorylate ACL, but is activated through PI3K-Akt during proliferation (331). By western blot, ACL was phosphorylated at serine^{454} in the presence of rapamycin. Only with PI3K inhibition was the ACL phosphorylation

at serine^{454} reduced, suggestive of signal transduction via active PI3K-Akt for phosphorylation of ACL at serine^{454}, not including mTOR.

To confirm the requirement of PI3K activity for ACL phosphorylation at serine^{454}, we examined ACL phosphorylation on serine^{454} in B cells from mice deficient in the regulatory subunit of PI3K, p85α. As previously mentioned, p85$\alpha^{-/-}$ mice display phenotypes of severe immunodeficiency and agammaglobulemia, similar to XID and BTK knockout mice (271, 332). We isolated B cells from knock-out (p85$\alpha^{-/-}$), heterozygous (p85$\alpha^{+/-}$) and wild-type (p85$\alpha^{+/+}$) BALB/c mice and whole cell extracts were prepared from B cells unstimulated (Media) or stimulated with αIg, IL-4, αIg + IL-4, or LPS for 3 hr and 6 hr. As shown by Western blot, phospho-serine^{454} ACL was present in p85$\alpha^{+/-}$ and p85$\alpha^{+/+}$ B cells at 3 hr and 6 hr; p85$\alpha^{-/-}$ B cells had no detectable phosphorylation of serine^{454} on ACL (Figure 33). In addition, LPS stimulation led to phosphorylation of ACL at serine^{454} at 6 hr in all p85α genotypes. LPS engages the TLR4 receptor on the B cell surface, upon which pathways generally associated with BCR engagement are activated and provide alternative means of activation for B cell response (179, 333, 334). I have not further characterized this phosphorylation event and further studies are required to examine the pathways up-regulating the phosphorylation of ACL in response to LPS in B cells.

C. ACL activity in B cells

I next sought to determine if the activity of ACL was regulated in B cells following receptor stimulation. B cells stimulated with αIg + IL-4 were collected every 6 hr for up to 48 hr and ACL enzyme activity measured by the citrate lyase-malate dehydrogenase coupled enzyme (ACL-MDH) assay (150, 239). The reaction is: $\text{Citrate} + \text{CoA} + \text{ATP} \xrightarrow{\text{ACL}} \text{Acetyl-CoA} + \text{Oxaloacetate} + \text{ADP} + P_i$

$\text{Oxaloacetate} + \text{NADH} + H^+ \xrightarrow{\text{MDH}} \text{Malate} + NAD^+$

ACL activity, monitored by the oxidation of NADH to H^+ and NAD^+, increased over time of B cell stimulation with αIg + IL-4 (Figure 34). Thus, B cell stimulation increased ACL activity.

I further evaluated the role of the PI3K-Akt pathway for ACL enzymatic activity in PI3K-deficient B cells. B cells of p85$\alpha^{-/-}$, p85$\alpha^{+/-}$, and p85$\alpha^{+/+}$ BALB/c mice were stimulated with αIg + IL-4 for 18 hr. Whole cell extracts were prepared and ACL enzymatic activity measured by the ACL-MDH coupled enzyme assay, normalized to change in absorbance in the absence of exogenous ATP. Deficiency of p85α (p85$\alpha^{-/-}$ and p85$\alpha^{+/-}$) in B cells resulted in reduced levels of ACL enzymatic activity equivalent to unstimulated B cell extracts (Figure 35). With αIg + IL-4 stimulation, B cells of p85$\alpha^{+/+}$ displayed an elevated enzymatic activity of ACL within 18 hr. Collectively these results suggest that PI3K (via p85α) regulates serine^{454} phosphorylation and enzymatic activity of ACL in activated B cells.

To corroborate these findings, I performed an alternative ACL enzyme assay. Enzymatic activity of ACL was previously dependent upon the coupling to MDH

enzyme, an indirect measurement, and this limits the measurement of ACL enzyme-inhibitor interactions (238). To avoid this inherent short-coming, I directly measured ACL enzyme activity in whole cell extracts as a function of the amount of [^{14}C]-acetyl-CoA produced from the conversion of [^{14}C]-labeled citrate to acetyl-CoA by ACL, monitored by the differential solubility in MicroScint-O ([^{14}C]-citrate remains in the aqueous phase) (238). I evaluated the enzymatic activity of ACL in B cells over time following αIg + IL-4 or LPS stimulation. B cells were harvested and whole cell extracts prepared every 6 hr during a 48 hr time period. The ACL activity at each time point was then evaluated by formation of [^{14}C]-acetyl-CoA at 180 min and subsequently extracted in MicroScint-O. As shown in Figure 36, the amount of [^{14}C]-acetyl-CoA increased in extracts of B cells stimulated for up to 24 hr to 31 hr, thereafter there was no increase. This confirmed results of increased activity in αIg + IL-4 stimulated B cell samples by ACL-MDH enzyme assay and in addition illustrated the induction of ACL enzyme function in LPS stimulated B cells.

The enzymatic activity of ACL in stimulated B cells was also evaluated by the addition of the ACL-specific chemical inhibitor, compound-9 (C-9). This synthetic compound has been reported to specifically inhibit ACL in HepG2 cells (IC_{50}= 0.13 μM) (164). B cells were stimulated with αIg + IL-4 or LPS for 24 hr in the presence or absence of C-9 (25 μM, 35 μM, and 50 μM). Extracts were prepared and the direct ACL enzyme assay was performed. The amount of [^{14}C]-acetyl-CoA formed decreased with increasing concentrations of C-9 (Figure 37). These results suggested [^{14}C]-acetyl-CoA in LPS or αIg + IL-4 stimulated B cell extracts was

through ACL activity, despite only a reduced and incomplete inhibition of [^{14}C]-acetyl-CoA production. I suggest that the inhibition of ACL enzymatic activity was not complete due to inherent limitations of the modified assay: measured in a crude protein extract of B cells not with purified ACL protein, alternative pathways to generate acetyl-CoA as well as pathways which utilize acetyl-CoA were not inhibited, the amount of C-9 which was incubated with *ex vivo* B cells was the concentration allowed cellular uptake and modification of cellular response, and C-9 was not directly added to extracts in the enzyme assay due to the insolubility of C-9 in enzyme assay buffer (164, 166).

D. Role of ACL in the B cell growth and survival responses

I sought to examine the role of endogenous ACL activity in B cell responding to extracellular stimuli for entry into G_1 phase, characterized by increased cellular size and mass (335, 336). The relative size of B cells stimulated with αIg + IL-4 or LPS in the presence and absence of the ACL inhibitor, C-9, was determined by Scepter technology (Millipore). Cell volume (pL) and size (μ, microns) was measured after 48 hr LPS or αIg + IL-4 stimulation in the presence and absence of C-9 (20-50 μM) (Table I). B cells increased in size from an initial 6.265 μ to 9.040 μ with LPS and to 9.020 μ with αIg + IL-4 stimulation at 48 hr. Volume of B cells stimulated for 48 hr with LPS or αIg + IL-4 also increased from the initial 0.129 pL to 0.386 pL and 0.384 pL, respectively. No effect in cellular size or volume was demonstrated with C-9, up to 50 μM. These results taken together illustrate the

increased cellular size and thus G_1-phase entry of B cells in response to LPS or αIg + IL-4 stimulation was not affected by inhibition of ACL activity.

Next, the role of ACL activity in the survival of B cells was evaluated. The ability of B cells to maintain viability in the presence of C-9 was measured by flow cytometry through PI exclusion. B cells stimulated with αIg + IL-4 maintain viability above 80 % for 48 hr; co-incubation of αIg + IL-4 with 20 μM C-9 or greater (up to 50 μM C-9) reduced B cell survival (Table II). Similar results were obtained in B cells stimulated with LPS. Survival was maintained with LPS, but a time dependent decrease in viability after 24 hr was demonstrated with the addition of C-9 (25 μM, 35 μM, or 50 μM). Therefore the inhibition of ACL activity by C-9 reduced B cell viability in response to extracellular stimuli.

The syntheses of lipids have been shown to be required for plasma membrane generation and daughter cell formation; membrane phospholipid synthesis in response to activation stimuli is coordinated with the cell cycle (268, 337, 338). In B-lymphoma cell lines, changes in lipid metabolism for the acceleration of membrane phospholipid synthesis support the differentiation of activated B cells into antibody-secreting plasma cells, in a manner similar to activated splenic B cells (203). I therefore sought to examine the role of ACL activity in B cells progressing through the cell cycle in the proliferation response. B cells were stimulated with LPS or αIg + IL-4 in the presence and absence of increasing doses of C-9 for up to 72 hr and DNA distribution monitored by flow cytometry. Through cell cycle analysis, treatment with 50 μM C-9 increased the number of LPS

stimulated B cells with sub-G_1 (apoptotic) the DNA content, from 2.7 % at 24 hr to 35 % at 48 hr and 28.3 % at 72 hr (Table III). An increase in sub-G_1 DNA content was also demonstrated in B cells stimulated with αIg + IL-4 in the presence of C-9.

Additionally, I monitored bromo-deoxyuridine (BrdU) incorporation in B cells as a measure of DNA synthesis (S-phase). After 24 hr stimulation with LPS or αIg + IL-4, B cells were treated with C-9 and BrdU was added to culture. At 48 hr and 72 hr post-stimulation, B cells were harvested and BrdU incorporation quantified via anti-BrdU-FITC Ab labeling and flow cytometry. As shown in Table III, the percentage of αIg + IL-4 or LPS stimulated B cells that incorporated BrdU was significantly reduced by the addition of 35 μM or 50 μM C-9. Collectively, these results indicate that the inhibition of ACL activity reduces proliferation of B cells in response to TLR4 or BCR and IL-4 receptor engagement.

E. Role of ACL in *de novo* lipid synthesis of B cells

As B cells differentiate into a plasma cells, the synthesis of glycolipids, sphingosines, and ceramides increases to support cell growth and Ig secretion (203, 337). Notably, phosphatidylethanolamine (PE), phosphatidylcholine (PC), cardiolipin (CL), and cholesterol (C) are synthesized *de novo* in differentiating B cells. Utilizing acetyl-CoA precursors, several pathways for lipid synthesis have been described, including the cytidine diphosphocholine (CDP-choline) pathway and the PE methylation pathway (239, 325, 339-41). With this in mind, I sought to examine the significance of glucose utilization for *de novo* lipogenesis in B cells

responding to stimuli.

Bulk lipid synthesis was examined in B cells responding αIg + IL-4 or LPS for 24 hr, 48 hr, and 72 hr. Lipids were extracted and further purification and separation of the neutral and acidic lipids were conducted through the Bligh-Dyer method, ion exchange chromatography, and Folch partitioning (236). The total lipid fractions (neutral and acidic) were separated on individual silica-60 chromatogram plates by high-performance thin-layer chromatography (HP-TLC) and visualized by charring in the presence of $Cu(OAc)_2$ /H_3PO_4. Standard lipid cocktails and isolated murine brain lipid extracts were spotted in tandem on chromatograms for determination of B cell lipid species based upon migration of known lipid species (236). Comparison of lipid species of unstimulated B cells with that of αIg + IL-4 stimulated for 48 hr revealed a universal increase in the amount of bulk lipid species (Figure 38). The neutral lipid species distinguished were phosphatidylethanolamine (PE), phosphatidylcholine (PC), cholesterol (C), triglycerides (TG), and an unidentified band migrating slightly below sphingomyelin (SM) (Figure 38A). The acidic lipid species also increased, in particular phosphatidylinositol (PI), phosphatidylserine (PS), phosphatidylglycerol (PG, a standard lipid not shown here, whose migration is slightly lower than phosphatidic acid (PA)), cardiolipin (CL), and free fatty acids (FFA) (Figure 38B). A similar increase in bulk lipid synthesis was demonstrated in B cells stimulated with LPS for 24 hr, 48 hr, and 72 hr (Figure 39). Collectively these results illustrate B cells in response to αIg + IL-4 or LPS increase bulk lipid content.

In addition to migration rate, the identities of lipids from αIg + IL-4 stimulated B cells were confirmed by staining HP-TLC plates with colorimetric dyes specific for lipid moieties. First the neutral lipid species of B cells stimulated for 48 hr with αIg + IL-4 was evaluated by migration distance on HP-TLC in comparison to standards (neutral lipids and murine brain neutral lipid fraction). The distribution of B cell lipids coincided with standard lipids, based on migration and charring (Figure 40A). Orcinol-H_2SO_4 reagent spray binds to glycolipids (342); in the neutral lipid fraction of B cells, C, PE, and PC were dyed purple (Figure 40B). Lipids containing amino groups were detected via the ninhydrin reagent (343); PE of the neutral fraction was identified with ninhydrin (Figure 40C). Interestingly, an unidentified band was stained with ninhydrin below sphingomyelin and above lysophosphatidylcholine (LPC) on the neutral plate; further characterization was not completed at this time. Molybdate/H_2SO_4, Dittmer's ester, detects phospholipids by binding to the phosphate group (344). Separated neutral lipids of stimulated B cells that retained the blue dye were PC, PE, C, and cholesterol esters (CE) (Figure 40D). In a similar manner the acidic lipid fraction of 48 hr αIg + IL-4 stimulated B cells was examined for lipid species' identification. First distribution of acidic fraction lipids based on migration was confirmed by charring (Figure 41A). In addition, a single lane was dedicated to phosphatidylglycerol (PG), a precursor to cardiolipin, to identify the band that was corresponding to an unidentified species on the previously charred-only acidic lipid chromatogram, in reference to Figure 36B (223). Orcinol-H_2SO_4 reagent spray did not bind to any lipid species in the

acidic lipid fraction of B cells, however in the murine brain acidic lipid fraction, two purple bands indicating the presence of sulfatides were seen (Figure 41B). A yellow smear was seen in orcinol staining of B cell fractions, migrating along the solvent A front; its characterization is unknown. Ninhydrin spray of the acidic lipid fraction identified PS (Figure 41C). Dittmer's spray was utilized on the acidic fraction chromatogram, staining PI, PS, PG, and CL (Figure 41D). I was thus able to isolate and identify major lipid species of bulk lipid synthesis that were synthesized in B cells in response to extracellular stimuli.

F. Incorporation of glucose-derived carbons in *de novo* lipid synthesis

The contribution of carbons originating from glucose metabolism to *de novo* lipogenesis in response to stimuli was evaluated in B cells by [^{14}C]-U-glucose labeling experiments. In brief, B cells were incubated with [^{14}C]-U-glucose and subsequently stimulated with LPS or αIg + IL-4. At sequential time points, B cells were harvested and lipids extracted and separated by HP-TLC. Autoradiograms analyzed for incorporation of [^{14}C] in lipid species by densitometry, were subsequently charred to identify by migration corresponding lipid species to standards. An increase in band intensity correlated with an increase in incorporation of [^{14}C] originating from supplemented [^{14}C]-U-glucose.

By HP-TLC analysis, B cells stimulated with αIg + IL-4 for 24 hr demonstrated an increase of [^{14}C]-U-glucose incorporation, especially PC and PE (Figure 42A). Furthermore, the distribution of [^{14}C] incorporation was increased at 48 hr, wherein label from [^{14}C]-U-glucose was incorporated in PC and PE, as well as LPC, SM, CE,

and an unidentified band above C (further analysis of this band was not conducted). The acidic lipid species of B cells stimulated with αIg + IL-4 also incorporated label from [^{14}C]-U-glucose at 24 hr, with an increase at 48 hr (Figure 42B). In particular, the acidic lipid species incorporating label from [^{14}C]-U-glucose to the greatest density were PI, PS, PG, and CL, as the band intensity (*i.e.* dpm) enhanced with the extension of stimulation from 24 hr to 48 hr.

Likewise, B cells stimulated with LPS for 24 hr, 48 hr, and 72 hr were evaluated for glucose-dependent *de novo* lipogenesis. The neutral lipid species identified in 24 hr LPS stimulated B cells that incorporated label from [^{14}C]-U-glucose were: LPC, an unidentified band slightly above migration of LPC species (also present in the unstimulated cell sample), PC, and an additional unidentified band below PE species migration (Figure 43A). The extension of LPS stimulation to 48 hr and 72 hr revealed an increase in label from [^{14}C]-U-glucose incorporation into PC, PE, C, and triglycerides (TG) (Figure 43A). The stimulation of B cells with LPS at 24 hr, 48 hr, and 72 hr also increased the distribution and incorporation of label from [^{14}C]-U-glucose in the acidic lipid species (Figure 43B). At each time point, PI was labeled by [^{14}C]-U-glucose incorporation, which increased in intensity at 48 hr to 72 hr. At 48 hr, PS, PG, and CL incorporated label from [^{14}C]-U-glucose, as band intensity increased at 72 hr. Collectively, these [^{14}C]-HP-TLC results revealed B cells respond to proliferating stimuli by increasing *de novo* synthesis of neutral and acidic lipids via the metabolism of extracellular glucose.

G. The role of ACL activity contribution in *de novo* lipogenesis

I next sought to evaluate the role of ACL activity in *de novo* lipogenesis of B cells responding to extracellular stimuli. As previously mentioned, the enzymatic activity of ACL produces acetyl-CoA from citrate and thereby directly links glucose metabolism via glycolysis to lipid synthesis. The contribution of glucose carbons to *de novo* lipogenesis via ACL activity was examined in B cells by targeting ACL with C-9.

Cultured with [^{14}C]-U-glucose, B cells were stimulated with LPS for 24 hr, 48 hr, or 72 hr in the presence or absence of 25 μM, 35 μM, or 50 μM C-9. Lipids were then extracted and separated by HP-TLC. Autoradiogram of LPS stimulated B cells treated with 25 μM C-9 revealed a reduction in label from [^{14}C]-U-glucose incorporation of neutral lipid species at 24 hr, 48 hr, and 72 hr, in particular PE (Figure 44A). The addition of 35 μM and 50 μM C-9 drastically reduced the incorporation of [^{14}C]-U-glucose in the neutral lipid fractions of stimulated B cells at 24 hr and 48 hr. Acidic lipid species of LPS stimulated B cells treated with C-9 was also evaluated by [^{14}C]-HP-TLC. Less incorporation of label from [^{14}C]-U-glucose was seen in lipid species identified in LPS stimulated B cells with C-9 treatment (Figure 44B). A particular reduction of PG, CL, and PI was illustrated in LPS stimulated B cells treated with 25 μM C-9 at 48 hr and 72 hr. Overall, LPS stimulated B cells incorporated less [^{14}C] from [^{14}C]-U-glucose in both acidic and neutral lipid fractions with the inhibition of ACL activity.

Moreover, B cells stimulated for 24 hr and 48 hr with αIg + IL-4 in the presence or absence of 20 μM, 35 μM, or 50 μM C-9 were evaluated for *de novo* lipid

synthesis by addition of [^{14}C]-U-glucose. In αIg + IL-4 stimulated B cells, a universal reduction of *de novo* synthesized lipid species incorporating [^{14}C]-label was demonstrated with the addition of C-9 (Figure 45). Both neutral and acidic lipids fractions at 24 hr, contained decreased [^{14}C]-U-glucose incorporation (Figure 45). In addition the total bulk lipid content of αIg + IL-4 stimulated B cells decreased with C-9 treatment, as shown by charring. The reduction of *de novo* lipids was less pronounced at 48 hr as incorporation of [^{14}C]-label decreased in neutral lipid species of B cells incubated with C-9 (Figure 45A). The acidic lipid fraction of αIg + IL-4 B cells treated with 50 μM C-9 revealed the most pronounced reduction in incorporation of [^{14}C]-label (Figure 45B). Of note, the lane containing the acidic lipid fraction of αIg + IL-4 stimulated B cell treated with 35 μM C-9 was overloaded due to operational error with spotting instrument. Collectively these results demonstrate a reduction in [^{14}C]-U-glucose incorporation into lipid species in stimulated B cells with inhibition of ACL activity.

H. Fatty acid synthesis

Glucose through glycolysis provides citrate for the subsequent formation of acetyl-CoA and is the major route in providing carbons for *de novo* lipid synthesis (Figure 30). However, glutamine may also provide acetyl-CoA for *de novo* lipid synthesis through glutaminolysis or reductive carboxylation (129-131, 133). In a glioblastoma cell line, Deberardinis *et al*. (2007) demonstrated glutaminolysis provides oxaloacetate and citrate for the subsequent formation of acetyl-CoA (345).

Therein, glutamine was converted to oxaloacetate and formed acetyl-CoA by condensation with the glycolytic-derived citrate via ACL. Alternatively, oxaloacetate derived from glutamine can be converted to malate and then pyruvate to enter the TCA cycle, whereby the glutamine carbons may be incorporated into citrate and subsequently incorporated into acetyl-CoA (346). Additional, reports in hepatoma and adipocyte cell lines have demonstrated the metabolism of glutamine to α-ketoglutarate, an anaplerotic substrate to replenish tricarboxylic acid (TCA) cycle intermediates, that is converted to citrate (via isocitrate dehydrogenase and aconitase) to subsequently synthesize acetyl-CoA in lipid synthesis (347-352). In light of these reports and in collaboration with Drs. Richardson and Scott, I further evaluated *de novo* lipogenesis in B cells by gas chromatography-mass spectroscopy (GC-MS).

B cells were cultured in the presence of ^{13}C-U-glucose (50 %) or ^{13}C-U-glutamine (50 %) and stimulated with LPS for 24 hr and 48 hr. Cellular pellets were harvested and the amounts of acetyl-CoA were quantified by GC-MS (234). As the biosynthesis of fatty acids involves the condensation of acetyl-CoA, the labeling of acetyl-CoA from glucose and glutamine was first evaluated. Upon LPS stimulation, the incorporation of ^{13}C-label from glucose to acetyl-CoA increased substantially to 36 % (Figure 46). In addition the labeling of acetyl-CoA in B cells stimulated with LPS for 24 hr and 48 hr from ^{13}C-glutamine was not affected with stimulation. In B cells stimulated with LPS for 48 hr, the percent of contribution of ^{13}C-U-glucose (36 %) and glutamine (10 %) to acetyl-CoA pool combined to be equivalent to 92 % of

the total acetyl-CoA content (as input of ^{13}C is 50 % of either substrate). These results suggest that B cells in response to LPS primarily metabolize glucose for *de novo* lipid synthesis.

Labeling of free fatty acids (C14:0 myristic acid, C16:1 palmitoate, C16:0 palmitic acid, C18:2 linoleic acid, C18:1 oleic acid, C18:0 stearic acid, C20:0 arachidic acid) was then evaluated in prepared B cell extracts. The different synthetic pathways of these fatty acids (C16) are mainly synthesized by *de novo* lipogenesis, while C18-fatty acids result from elongation of palmitate. Palmitate can either be synthesized *de novo*, or originate from pre-existing sources (339). The total relative amount of free fatty acids synthesized *de novo* from ^{13}C-U-glucose and ^{13}C-U-glutamine increased with LPS stimulation at 24 hr and to a greater quantity at 48 hr (Figure 47A). The amount of ^{13}C-label that was converted to fatty acids was normalized to extracts of unstimulated B cells cultured with ^{13}C–U-glutamine for 24 hr. Free fatty acid synthesis in LPS stimulated B cells increased as *de novo* synthesis of C14:0 and C16:0 fatty acids from ^{13}C-U-glucose increased in relation to ^{13}C-U-glutamine (Figure 47B). Collectively these results demonstrate the flux of carbon for acetyl-CoA and free fatty acids is primarily from glucose rather than glutamine. Of note, glutamine contributions to acetyl-CoA and free fatty acids did not increase with LPS stimulation, remaining at quantities of incorporation illustrated in B cells cultured without stimulation.

I. The role of ACL activity in the *de novo* lipid synthesis in B cells

The role of ACL activity in the *de novo* lipid synthesis was next evaluated in B cells responding to LPS by GC-MS. In the presence of 50 % ^{13}C-U-glucose, B cells were stimulated with LPS for 6 hr before addition of 35 μM C-9 to culture for 36 hr. Cellular pellets were prepared and the amounts of fatty acids were quantified by GC-MS, as previously mentioned. The relative amounts of fatty acids (C14:0, C16:1, C18:2, C18:1, and C20:0) incorporating ^{13}C-label increased with LPS stimulation (Figure 48A). Treatment with C-9 prevented ^{13}C-U-glucose incorporation into fatty acid, despite LPS stimulation, incorporating equivalent ^{13}C-label as B cells cultured in the absence of stimulation. Together the percentage of free fatty acids synthesized by elongation was dramatically increased with LPS stimulation (Figure 48B). The inhibition of ACL by C-9 addition increases in incorporation of ^{13}C-label from glucose despite activation stimulus of LPS. Collectively these results suggest that ACL activity provides a significant contribution to *de novo* lipogenesis in B cells responding to LPS stimulation.

Figure 1. Glucose uptake increased in αIg stimulated B cells.

(A) B cells were cultured for 15 hr in the absence (Media) or presence of αIg (10 μg/mL). Glucose transport (cpm/10^6 cells/sec) was monitored by measuring the quantity of [^{3}H]-label uptake into cells after a [^{3}H]-2-deoxy-glucose pulse (60 sec) in Kreb's Ringer buffer. Specific transport was calculated by subtracting [^{3}H]-2-deoxy-glucose uptake in the presence of cytochalasin B (10 μM), an inhibitor of glucose transporters, from values obtained without cytochalasin.

(Inset) Rate of glucose uptake was assessed in αIg stimulated B cells (15 hr) in the presence and absence of cytochalasin B. Uptake of [^{3}H]-2-deoxy-glucose was determined in 30 sec intervals for 120 sec. No increase in uptake was seen in the presence of cytochalasin B (bottom line). Linear uptake of [^{3}H]-2-deoxy-glucose was observed from 30 sec to 90 sec without inhibitor (top line).

(B) Glucose uptake was measured in B cells cultured in the absence (Media) and presence of IL-4 (4 ng/mL), LPS (25 μg/mL), or αIg for 15 hr. Transport was measured after 60 sec exposure of [^{3}H]-2-deoxy-glucose in the presence and absence of cytochalasin B (10 μM).

Error bars reflect standard deviation from the mean of triplicate measurements, and the data are representative of 3 independent experiments.

Figure 1.

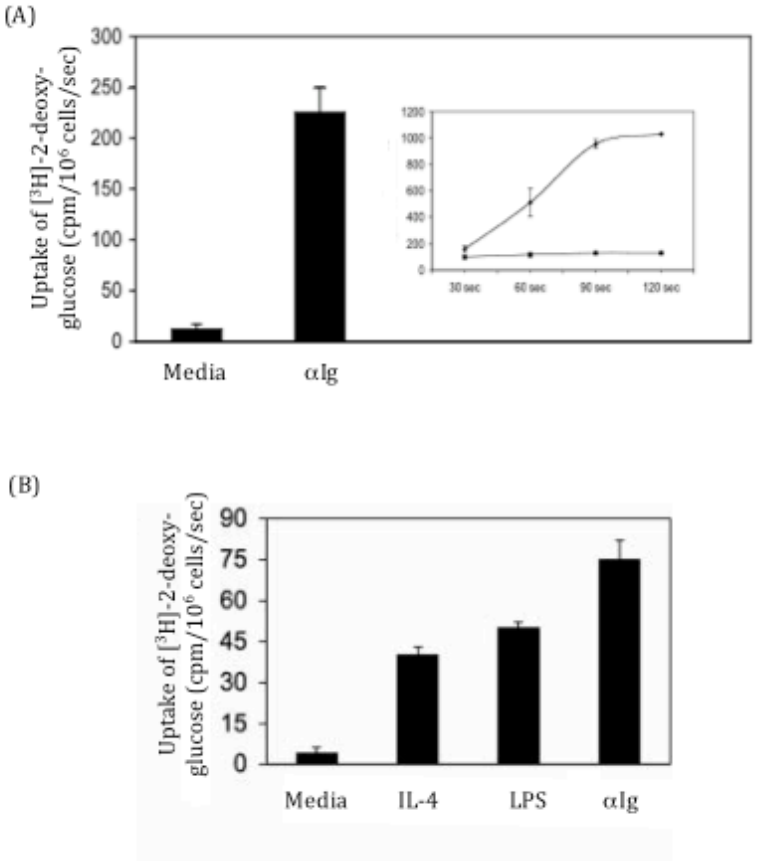
(A)
Uptake of [3H]-2-deoxy-glucose (cpm/10^6 cells/sec)
300
250
200
150
100
50
0
Media
αIg
1200
1000
800
600
400
200
0
30 sec
60 sec
90 sec
120 sec
(B)
Uptake of [3H]-2-deoxy-glucose (cpm/10^6 cells/sec)
90
75
60
45
30
15
0
Media
IL-4
LPS
αIg

Figure 2. Increased glucose transporter and sodium-potassium ATPase pump expression in response to receptor activation.

(A) B cells were cultured in the absence (Media) or presence of αIg (10 μg/mL), IL-4 (4 ng/mL) alone or in combination, or LPS (*S. typhosa* 25 μg/mL) for 3 hr, 9 hr, and 20 hr. Membrane protein was extracted and cell lysates were prepared in 2.5X glut-loading buffer and equivalent amounts of total protein were examined by Western blot for glut-1 protein levels. Glut-1 was detected as a smear in SDS-PAGE.

(B) B cells were cultured in the absence (Media) or presence of IL-4 (4 ng/mL) for 24 hr. Cell lysates were prepared in glut-1 lysis buffer and half the total volume was incubated with de-glycosylating enzyme PNGase F (50 U) for 8 hr at 37°C. Lysates of equivalent amounts of total cellular protein were examined by Western blot for glut-1, and subject to Western blot analysis. Extracts without PNGase F were analyzed in parallel and glut-1 was observed as a smear on the film. With enzymatic de-glycosylation, glut-1 was detected as a single band.

(C) B cells were cultured in the absence (Media) or presence of αIg (10 μg/mL), IL-4 (4 ng/mL) alone or in combination, or LPS (*S. typhosa,* 25 μg/mL) for 3 hr, 9 hr, and 20 hr. Cell lysates were prepared in glut-1 lysis buffer and equivalent amounts of total protein were examined by Western blot for Na^+K^+ ATPase pump. Lysates of B cells prepared as in (A) were evaluated for Na^+K^+ ATPase pump expression. The data are representative of 3 independent experiments.

Figure 2.

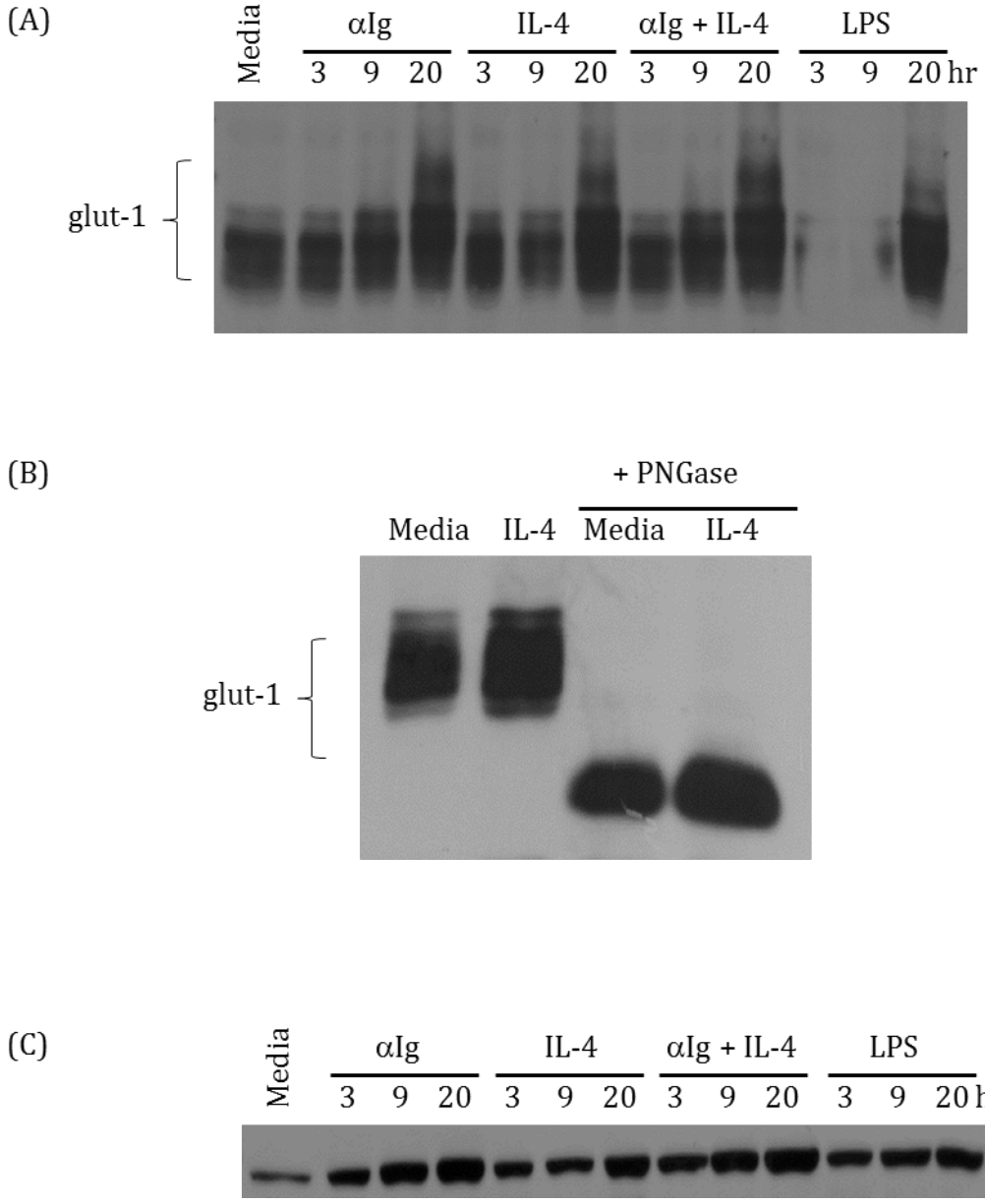
(A)
Media
αIg
IL-4
αIg + IL-4
LPS
3 9 20 3 9 20 3 9 20 3 9 20 hr
glut-1
(B)
+ PNGase
Media IL-4 Media IL-4
glut-1
(C)
Media
αIg
IL-4
αIg + IL-4
LPS
3 9 20 3 9 20 3 9 20 3 9 20 hr

Figure 3. Optimization of glut-1 detection of *ex vivo* B cells by immunocytochemistry.

B cells were cultured in medium alone (Media) or stimulated with αIg (10 μg/mL) and IL-4 (30 ng/mL) for 24 hr. Cells were then stained with increasing concentrations of anti-glut-1 antibody (indicated by ratios beneath images, dilutions are of Abcam ab14683) and FITC-conjugated secondary goat anti-rabbit IgG (1:1000), prepared as described in *Materials and methods*. The data are representative of 2 independent experiments.

Figure 3.

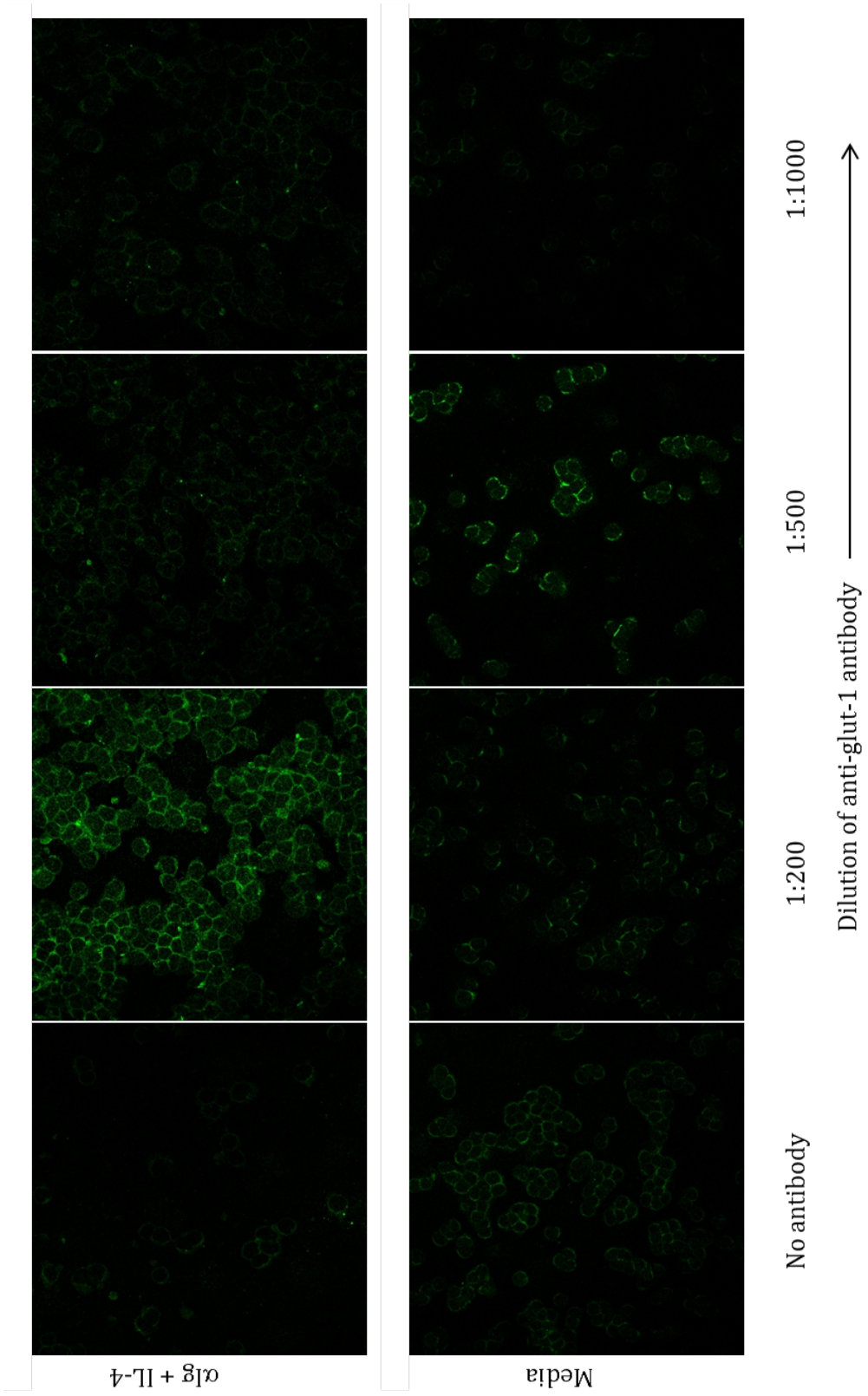
No antibody
1:200
1:500
1:1000
Dilution of anti-glut-1 antibody
Media
αIg + IL-4

Figure 4. Glut-1 expression in activated B cells.

B cells were cultured in medium alone (Media) or stimulated with αIg (10 μg/mL), IL-4 (30 ng/mL), CD40L (1:10), or αIg + IL-4 for 43 hr. B cells were prepared as described in *Materials and methods* and evaluated for glut-1 expression by ICC with incubation with anti-glut-1 antibody (1:200). The data are representative of 3 independent experiments.

Figure 4.

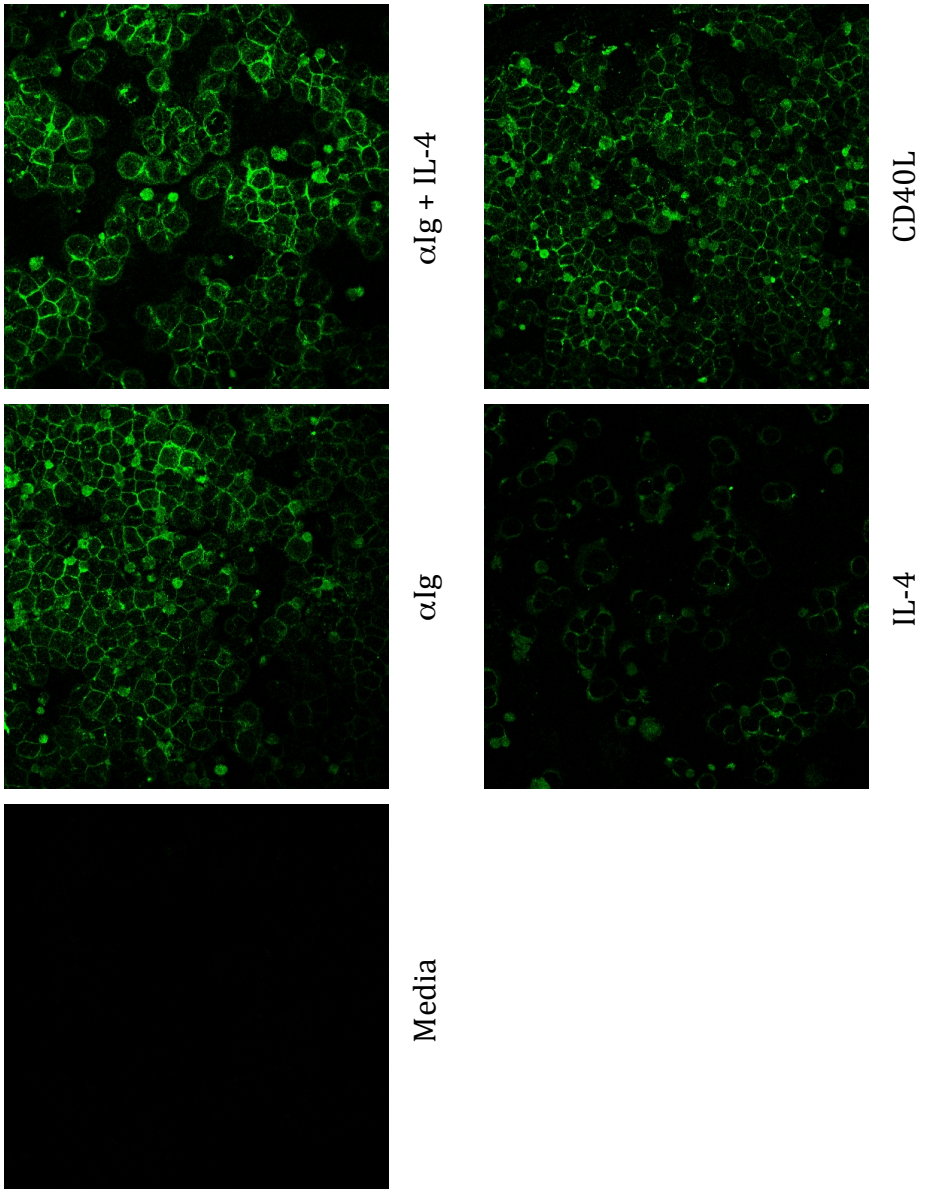

Figure 5. Glut-1 expression is induced with BCR cross-linking.

B cells were cultured in the absence (Media) (gray dashed line) or presence of 10 μg/mL αIg for 6 hr (blue line) and 12 hr (red line), and then glut-1 expression (PE-A) was determined by flow cytometry. Control Ab indicates an isotype-matched control staining of B cells stimulated with 10 μg/mL αIg for 12 hr. Data are representative of 10,000 cells (counts), completed in triplicate.

Figure 5.

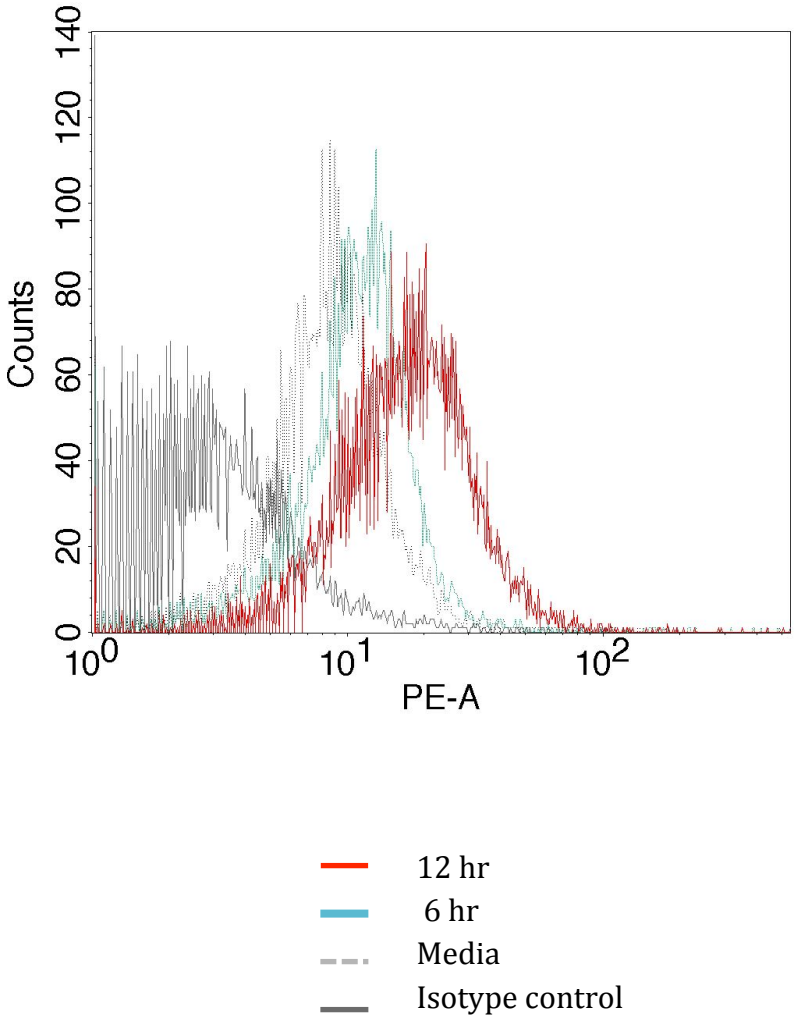
Counts
0
20
40
60
80
100
120
140
10^0
10^1
10^2
PE-A
12 hr
6 hr
Media
Isotype control

Figure 6. IL-4 induces glut-1 expression in B cells.

B cells were cultured in medium alone (gray line) or with 4 ng/mL IL-4 (black line) for 15 hr. Glut-1 staining (PE-A) was determined by flow cytometry as described in *Materials and methods*. Cells were also stained with an isotype control Ab (gray dashed line). Data are representative of 10,000 cells (counts), completed in triplicate.

Figure 6.

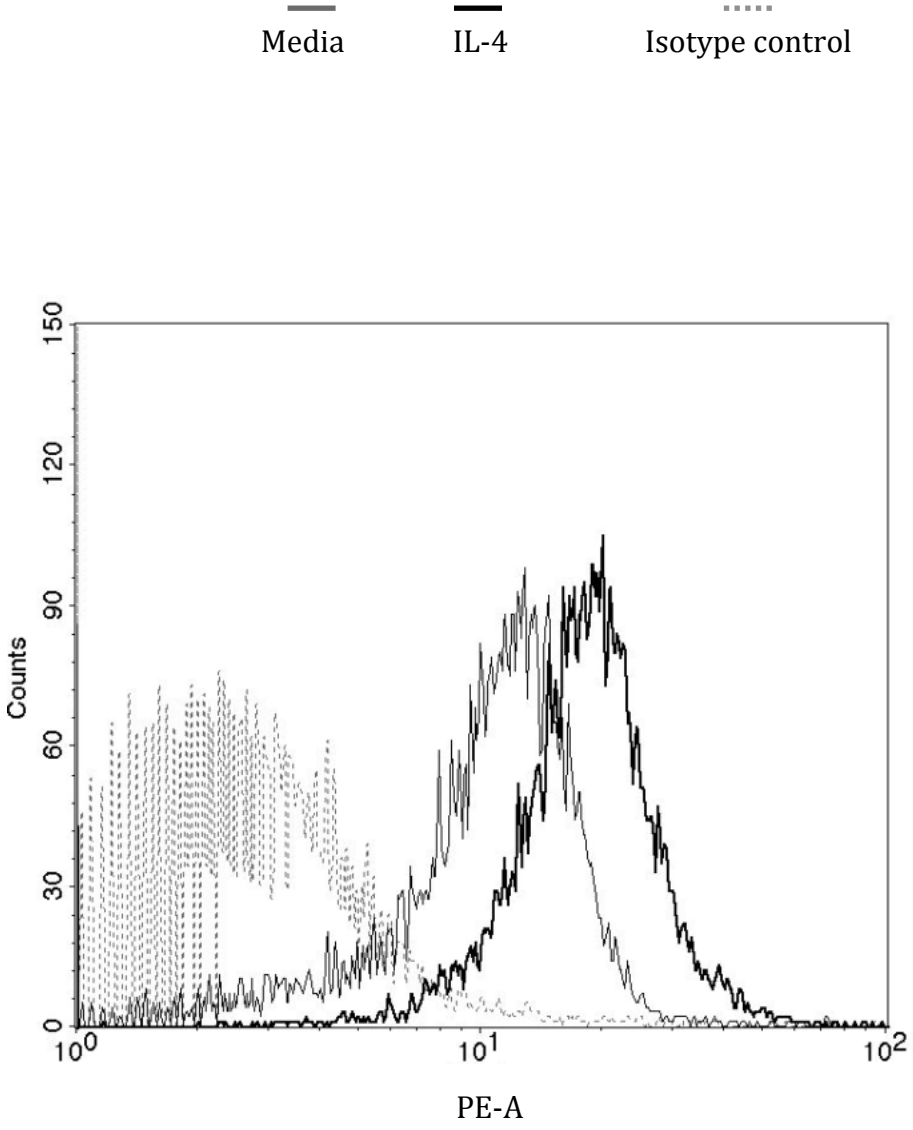
Media
IL-4
Isotype control
Counts
0
30
60
90
120
150
10^0
10^1
10^2
PE-A

Figure 7. Differential expression of *glut-1* in stimulated B cells.

B cells were cultured in medium alone (Media) or stimulated with αIg (10 μg/mL) or CD40L (1:10) for 6 hr, 11 hr, and 24 hr. At these time points, total RNA was isolated and *glut-1* expression was evaluated by semi-quantitative real-time PCR using SYBR green. Levels of expression of *glut-1* were normalized to *18S rRNA* and represent ratios of *glut-1*: *18S rRNA* relative to media *glut-1*: *18S rRNA*. Error bars reflect standard deviation from the mean of triplicate measurements, and the data are representative of 3 independent experiments.

Figure 7.

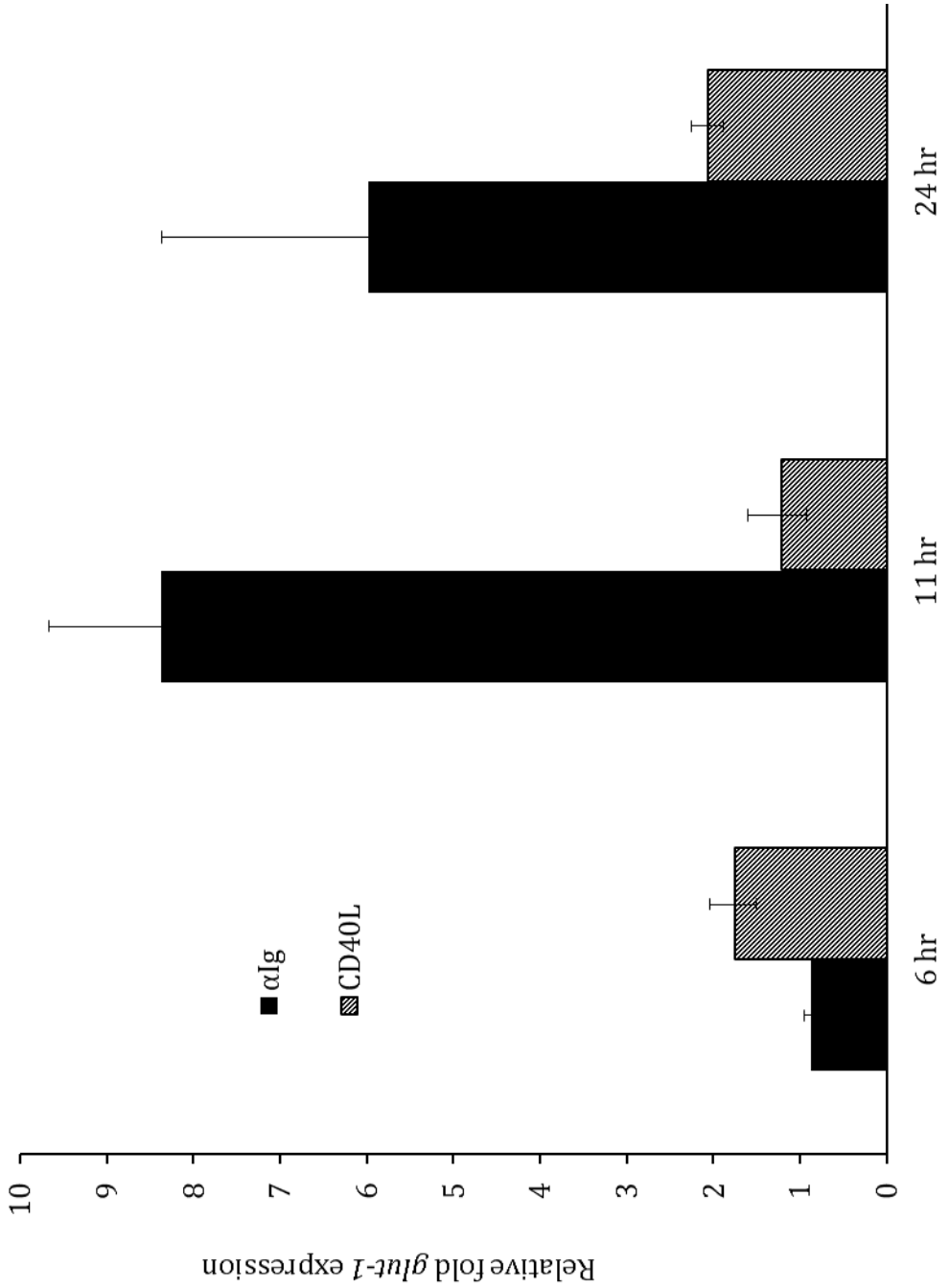
Relative fold glut-1 expression
0
1
2
3
4
5
6
7
8
9
10
αIg
CD40L
6 hr
11 hr
24 hr

Figure 8. Glucose uptake in activated B cells is reduced following inhibition of the PI3K pathway.

B cells were cultured in medium alone (Media) or with αIg (10 μg/mL) for 15 hr, in the absence (αIg) or presence of LY294002 (LY: 10 μM), wortmannin (Wort: 25 nM), or rapamycin (Rap: 50 nM). Cells were then harvested, and glucose transport (cpm/10^6 cells/sec) was monitored by measuring the quantity of [^{3}H]-label uptake into cells after a [^{3}H]-2-deoxy-glucose pulse (60 sec) in Kreb's Ringer buffer, as described in *Materials and methods*. Specific transport was calculated by subtracting [^{3}H]-2-deoxy-glucose uptake in the presence of cytochalasin B (10 μM), from values obtained without cytochalasin B. Error bars reflect standard deviation from the mean of triplicate measurements, and the data are representative of 3 independent experiments.

Figure 8.

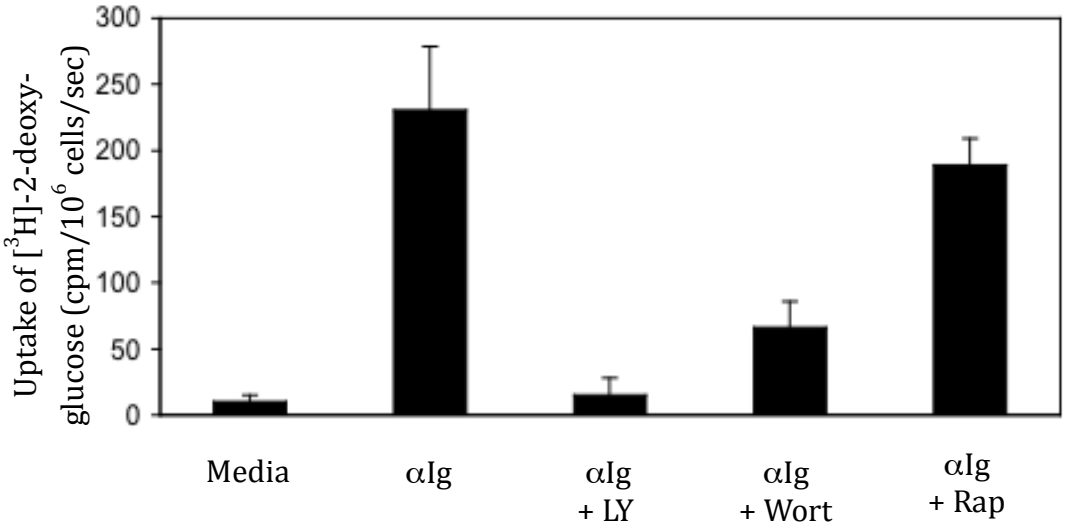
Uptake of [3H]-2-deoxy-glucose (cpm/10^6 cells/sec)
300
250
200
150
100
50
0
Media
αIg
αIg + LY
αIg + Wort
αIg + Rap

Figure 9. Glut-1 expression is not increased in B cells stimulated via the BCR in p85α-deficient mice.

B cells isolated from p85α-deficient mice were cultured in the absence (Media) (blue line) or presence of αIg (10 μg/mL) (red line) for 12 hr, and then glut-1 expression (PE-A) was determined by flow cytometry. Isotope control (gray dashed line) indicates an isotype-matched control staining of B cells stimulated with 10 μg/mL αIg for 12 hr. Data are representative of 10,000 cells (counts), completed in triplicate.

Figure 9.

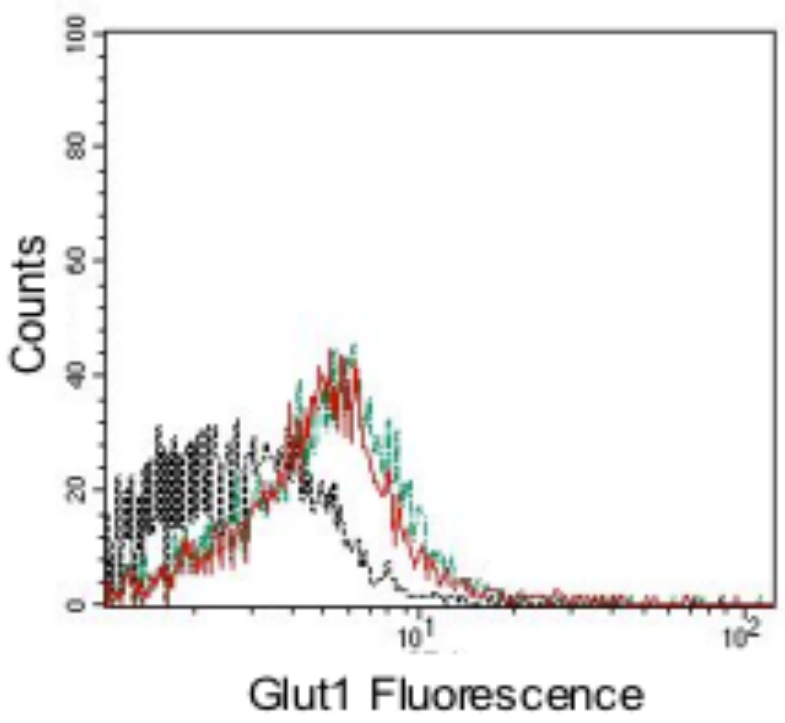
Counts
100
80
60
40
20
0
10^1
10^2
Glut1 Fluorescence
Isotype Control
Media
αIg 12 hr

Figure 10. B cells isolated from XID mice do not increase glut-1 expression in response to BCR cross-linking.

B cells were isolated from XID (bottom panel) or control wild-type (CBA/CaJ: lower panel) mice and cultured in the absence (Media) or presence of αIg (10 μg/mL) for 12 hr. B cells were prepared as described in *Materials and methods* and evaluated for glut-1 expression by ICC with incubation with anti-glut-1 antibody (1:200). The data are representative of 3 independent experiments.

Figure 10.

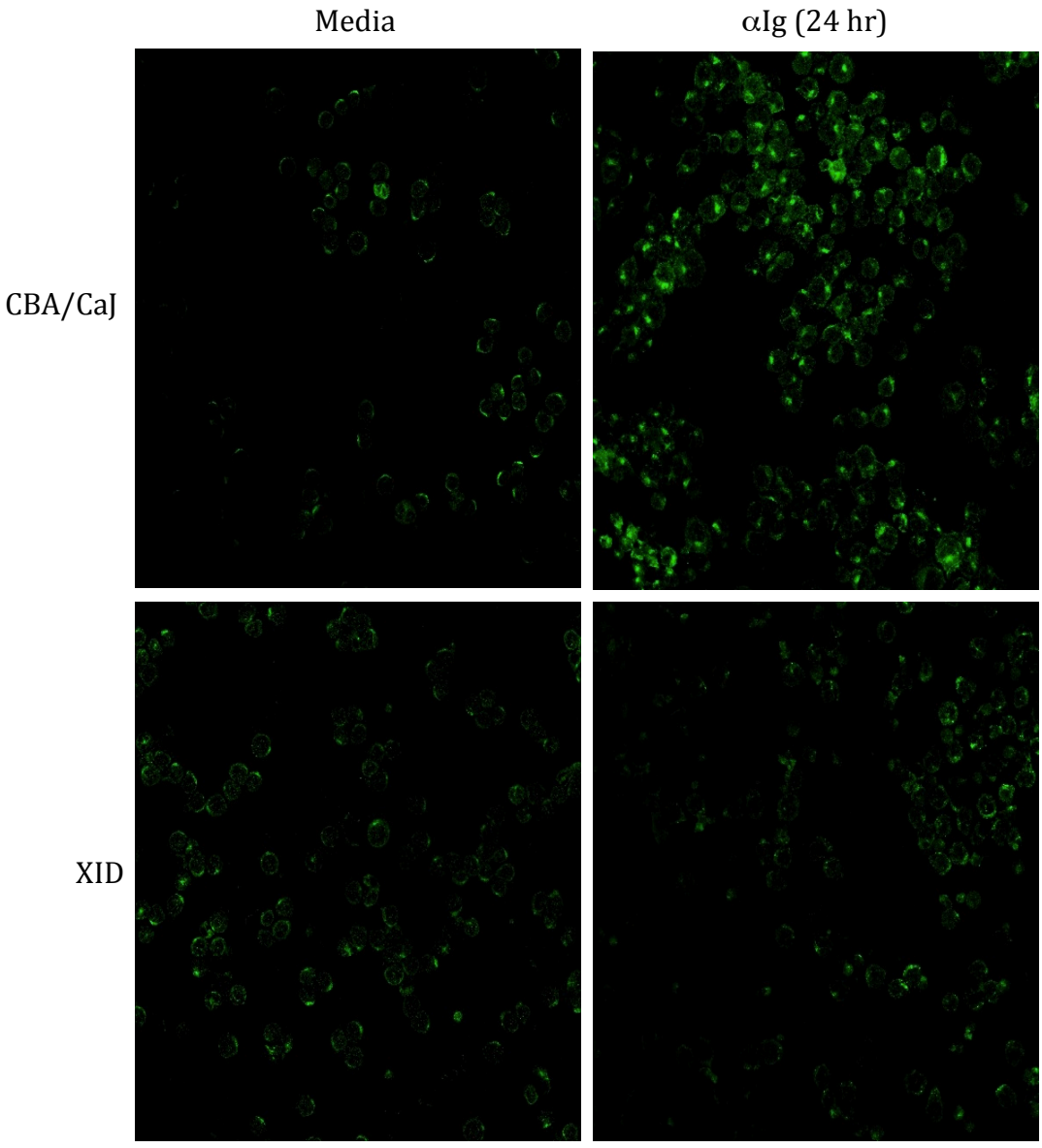

Figure 11. B cells increase cellular size and maintain viability in response to stimulation.

B cells were cultured in medium alone (Media) or stimulated with αIg (10 μg/mL), IL-4 (30 ng/mL), CD40L (1:10), LPS (25 μg/mL), or αIg + IL-4 for 0 hr, 20 hr, or 40 hr.

(A) At each time point, relative size of B cells was measured as function of mean forward scatter-area (FSC-A, arbitrary units) by flow cytometry. Error bars reflect standard deviation from the mean and the data are representative of 3 independent experiments.

(B) B cells were collected and viability measured as exclusion of propidium iodide by flow cytometry. The percent of cells that excluded PI are represented as viable. Histograms are representative of 10,000 cells, completed in triplicate.

Figure 11A.

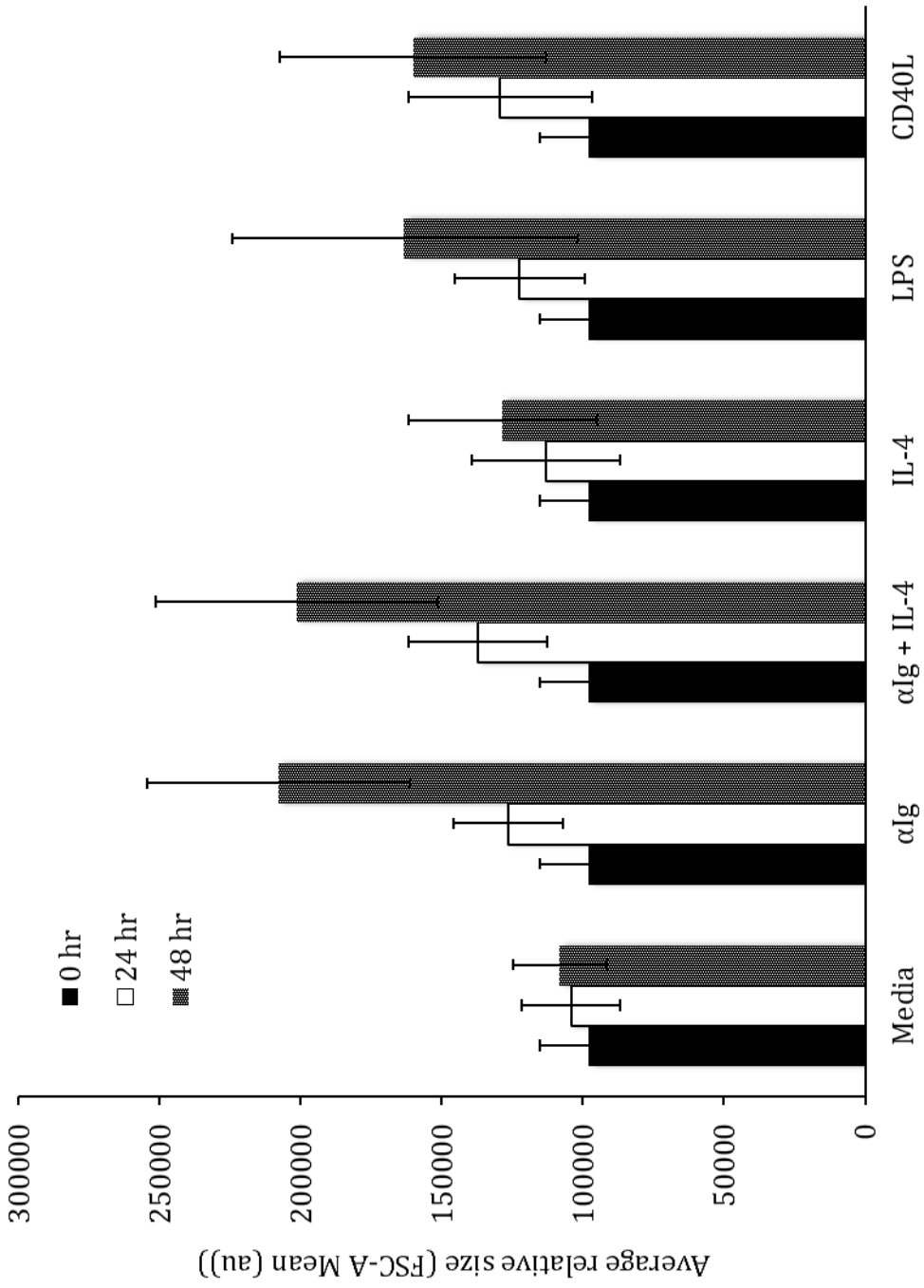
Average relative size (FSC-A Mean (au))
300000
250000
200000
150000
100000
50000
0
0 hr
24 hr
48 hr
Media
αIg
αIg + IL-4
IL-4
LPS
CD40L

Figure 11B.

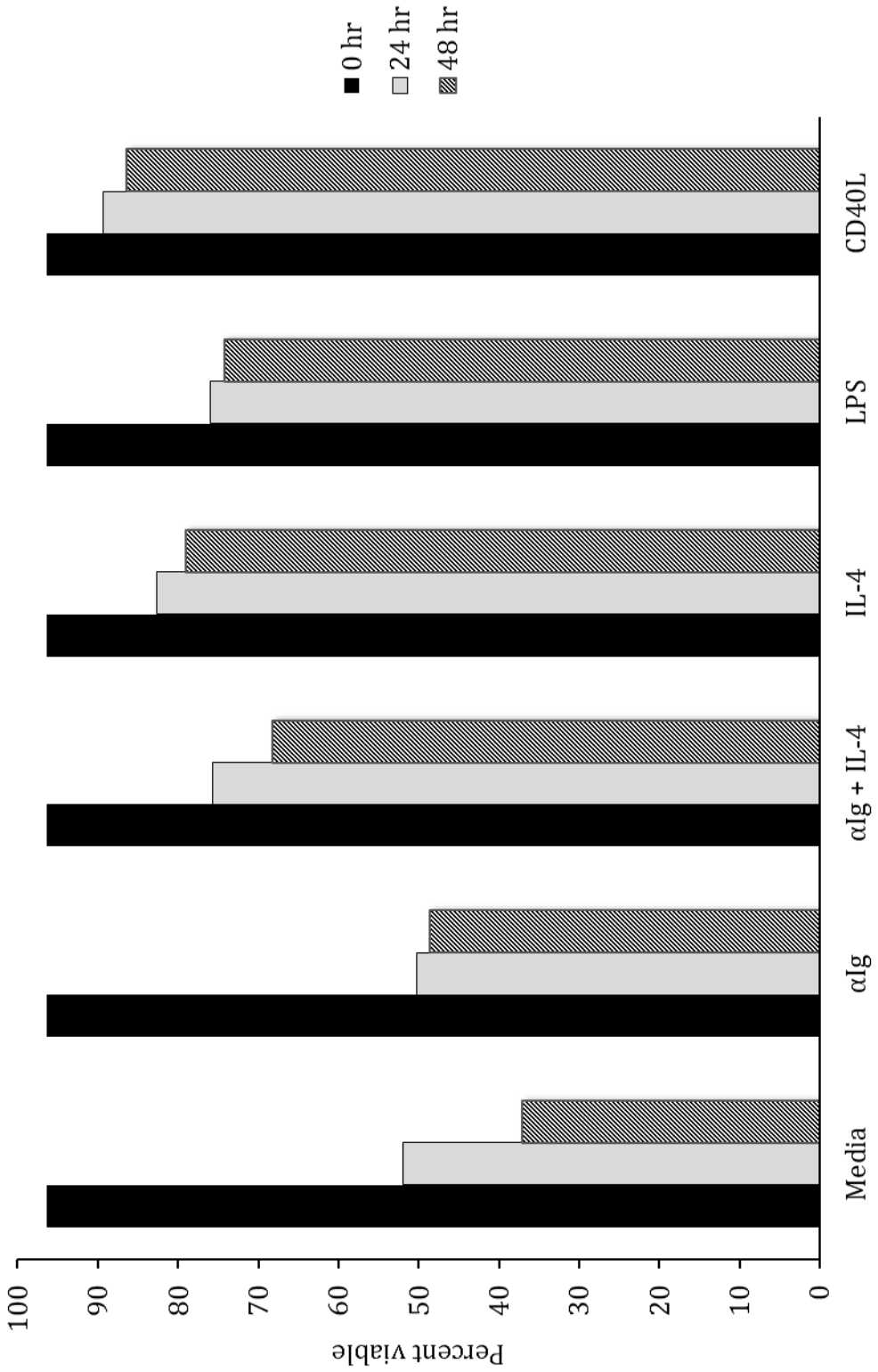
0 hr
24 hr
48 hr
Percent viable
0
10
20
30
40
50
60
70
80
90
100
Media
αIg
αIg + IL-4
IL-4
LPS
CD40L

Figure 12. Addition of glycolytic inhibitors reduces viability, not cellular size of IL-4 stimulated B cells.

B cells were cultured in medium alone (Media) or stimulated with IL-4 (30 ng/mL), in the absence (IL-4) or presence of 10 μM iodacetamide (IL-4 + 10 μM IAN) or 1 mM 2-deoxyglucose (IL-4 + 1 mM 2DG) for 18 hr.

(A) Relative size of B cells was measured as function of mean forward scatter-area (FSC-A, arbitrary units) by flow cytometry. Error bars reflect standard deviation from the mean and the data are representative of 3 independent experiments.

(B) B cells were collected and viability measured as exclusion of propidium iodide by flow cytometry. The percent of cells that excluded PI are represented as viable. Histograms are representative of 10,000 cells, completed in triplicate.

Figure 12A.

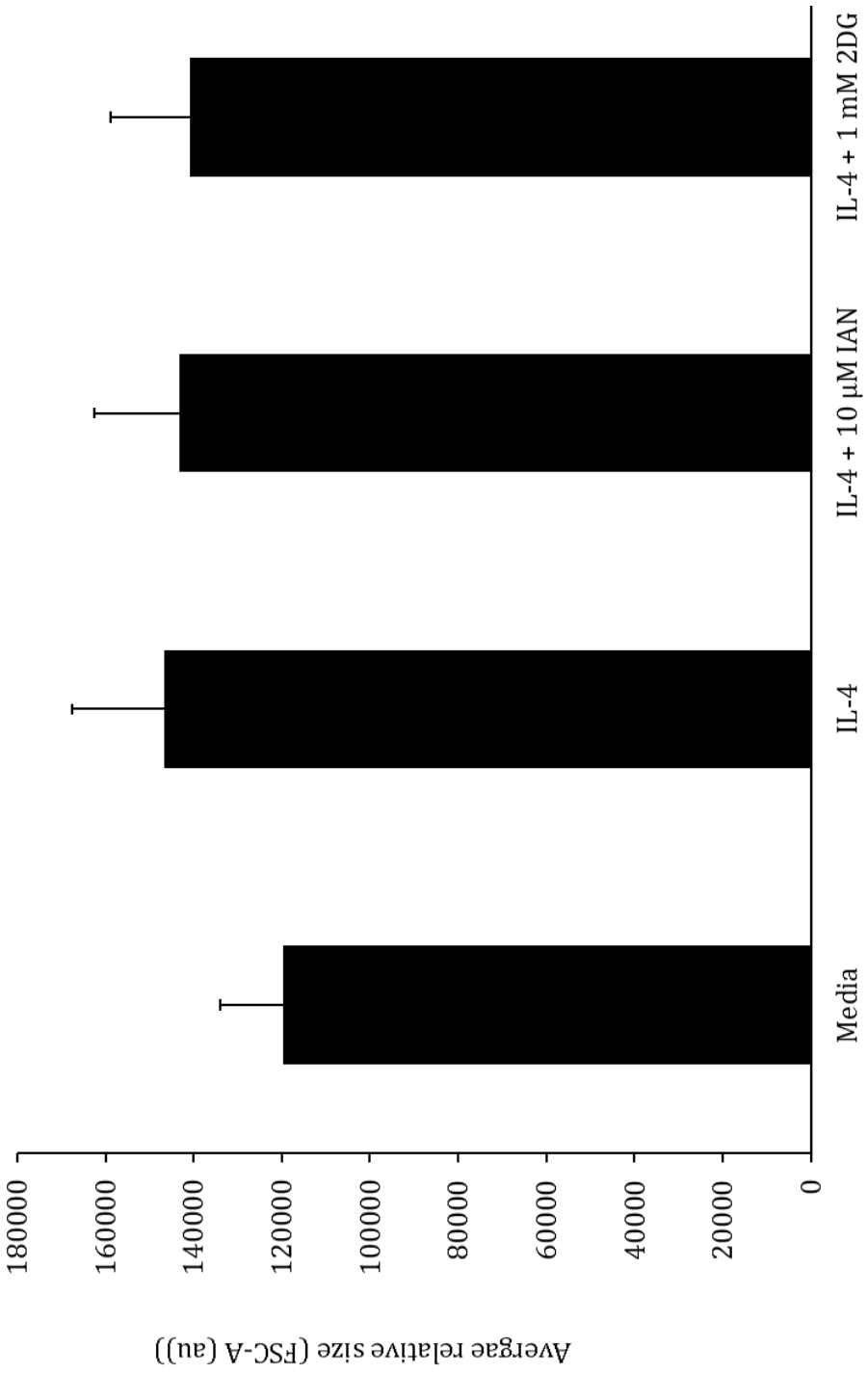
Average relative size (FSC-A (au))
180000
160000
140000
120000
100000
80000
60000
40000
20000
0
Media
IL-4
IL-4 + 10 μM IAN
IL-4 + 1 mM 2DG

Figure 12B.

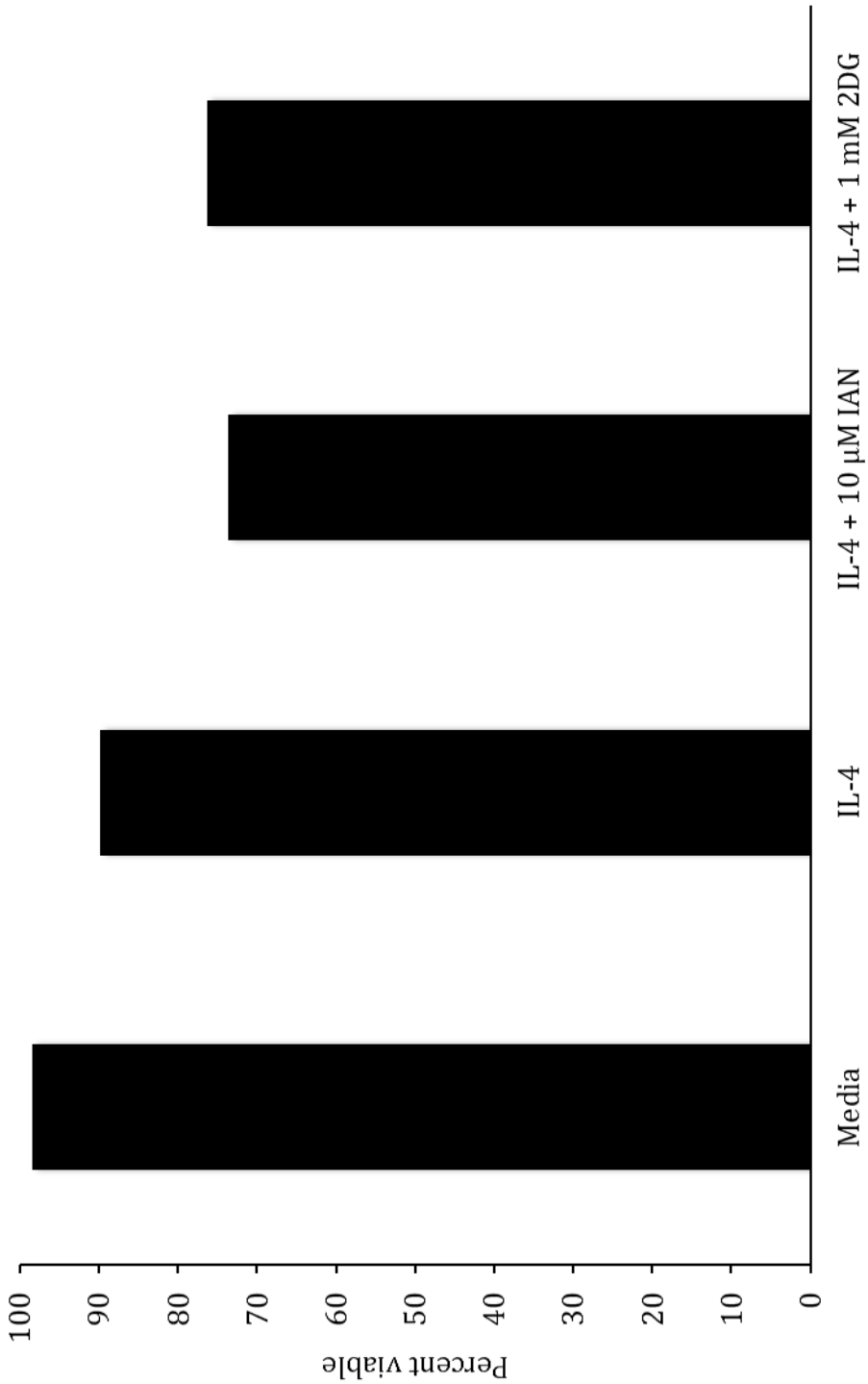
Percent viable
100
90
80
70
60
50
40
30
20
10
0
Media
IL-4
IL-4 + 10 µM IAN
IL-4 + 1 mM 2DG

Figure 13. Addition of 5TG does not reduce size or viability of IL-4 stimulated B cells.

B cells were cultured in medium alone (Media) or stimulated with IL-4 (30 ng/mL), in the absence (IL-4) or presence of 10 μM 5-thio-glucose (IL-4 +10 μM 5TG) or 1 mM 2-deoxyglucose (IL-4 + 1 mM 2DG) for 24 hr.

(A) Relative size of B cells was measured as function of mean forward scatter-area (FSC-A, arbitrary units) by flow cytometry. Error bars reflect standard deviation from the mean and the data are representative of 3 independent experiments.

(B) B cells were collected and viability measured as exclusion of propidium iodide by flow cytometry. The percent of cells that excluded PI are represented as viable. Histograms are representative of 10,000 cells, completed in triplicate.

Figure 13A.

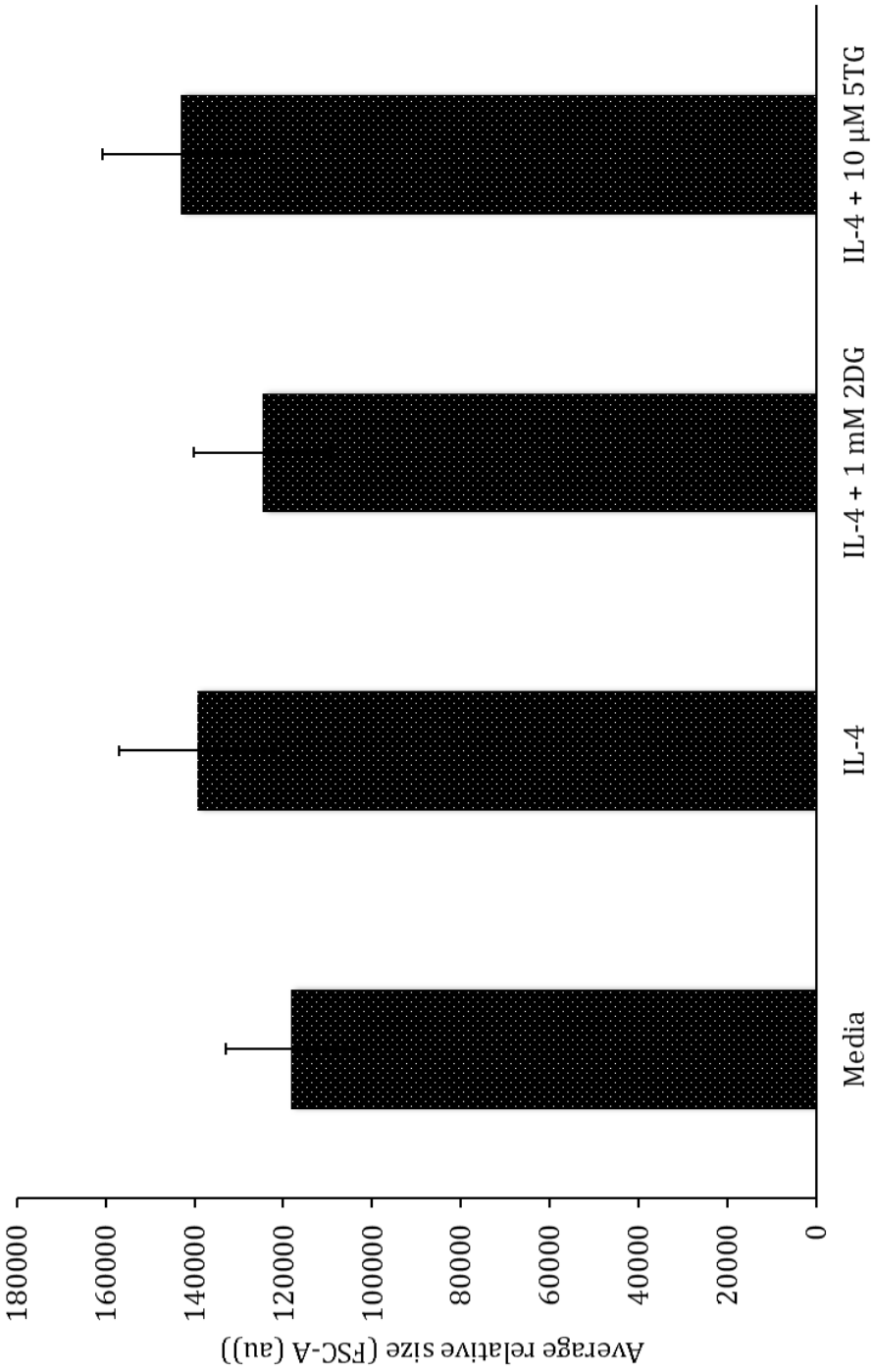
Average relative size (FSC-A (au))
0
20000
40000
60000
80000
100000
120000
140000
160000
180000
Media
IL-4
IL-4 + 1 mM 2DG
IL-4 + 10 µM 5TG

Figure 13B.

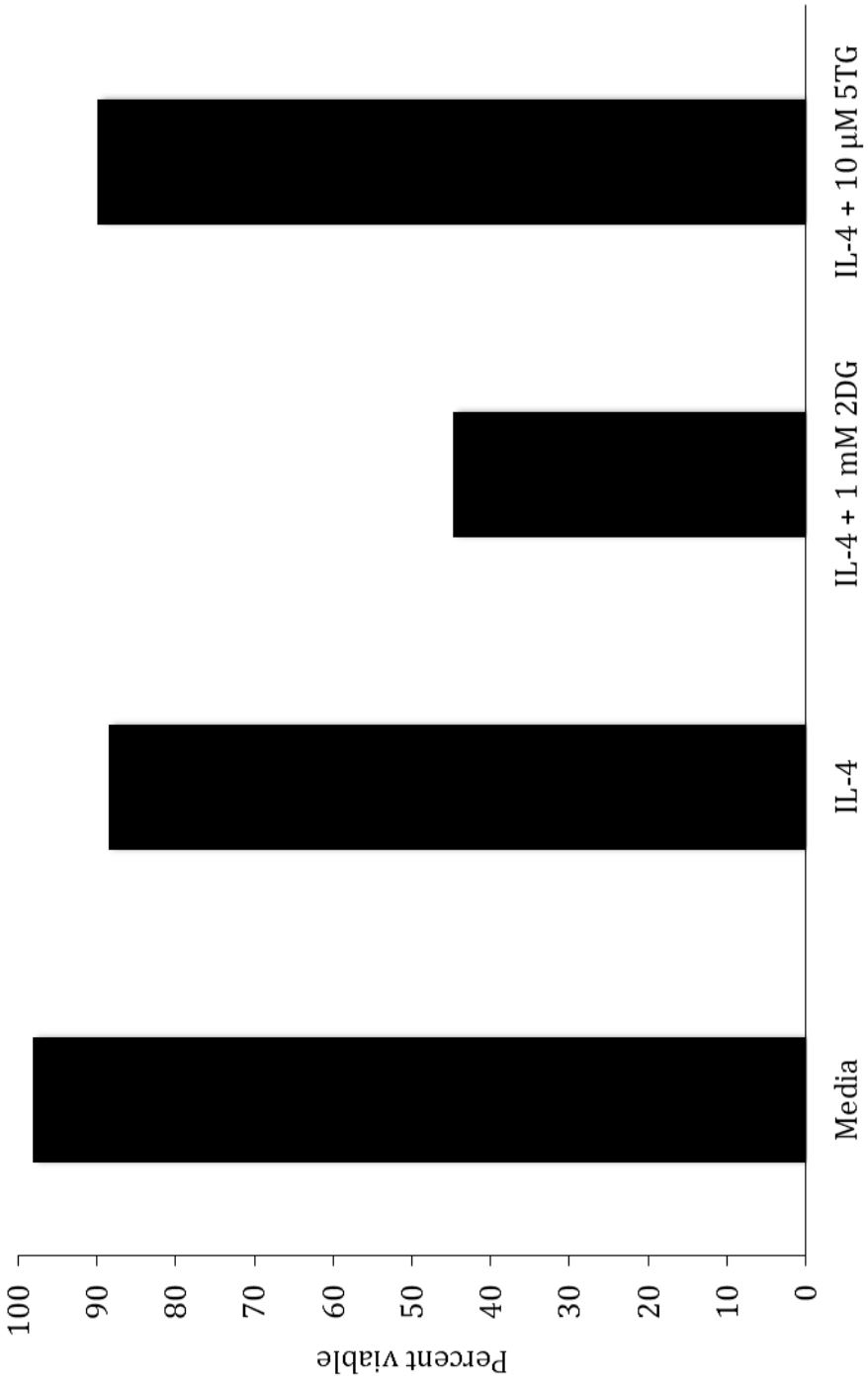
Percent viable
100
90
80
70
60
50
40
30
20
10
0
Media
IL-4
IL-4 + 1 mM 2DG
IL-4 + 10 μM 5TG

Figure 14. Addition of BP does not reduce size or viability of IL-4 stimulated B cells.

B cells were cultured in medium alone (Media) or stimulated with IL-4 (30 ng/mL), in the absence (IL-4) or presence of 10 μM 3-bromopyruvate (IL-4 + 10 μM BP), 1 μM 3-bromopyruvate (IL-4 + 1 μM BP), or 0.1 μM 3-bromopyruvate (IL-4 + 0.1 μM BP) for 23 hr.

(A) Relative size of B cells was measured as function of mean forward scatter-area (FSC-A, arbitrary units) by flow cytometry. Error bars reflect standard deviation from the mean and the data are representative of 3 independent experiments.

(B) B cells were collected and viability measured as exclusion of propidium iodide by flow cytometry. The percent of cells that excluded PI are represented as viable. Histograms are representative of 10,000 cells, completed in triplicate.

Figure 14A.

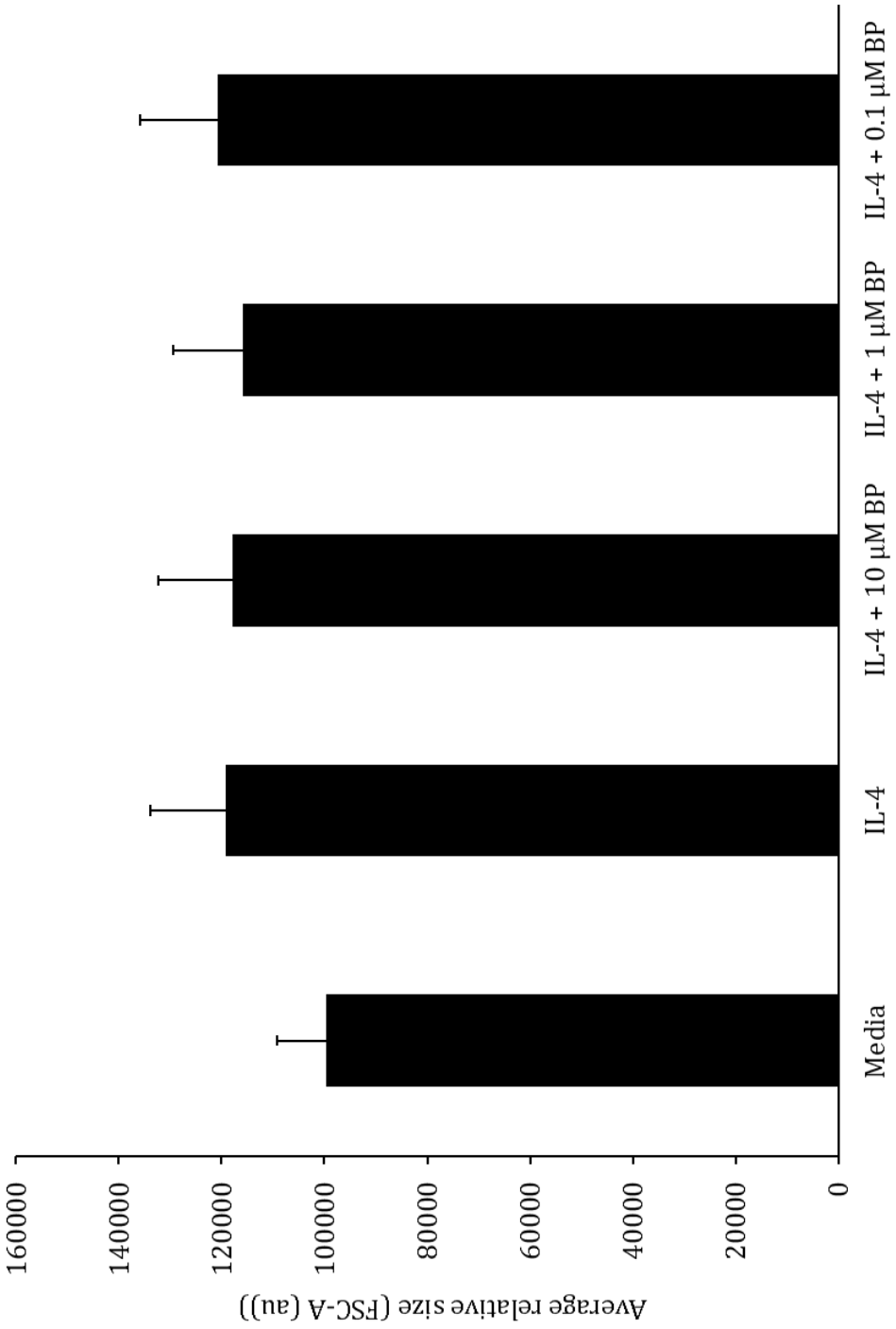
Average relative size (FSC-A (au))
160000
140000
120000
100000
80000
60000
40000
20000
0
Media
IL-4
IL-4 + 10 µM BP
IL-4 + 1 µM BP
IL-4 + 0.1 µM BP

Figure 14B.


Percent viable
100
90
80
70
60
50
40
30
20
10
0
Media
IL-4
IL-4 + 10 µM BP
IL-4 + 1 µM BP
IL-4 + 0.1 µM BP

Figure 15. BCR cross-linking induces glycolysis over time.

B cells (2 x 10^6/mL) were cultured in the absence (Media, 0 hr) or presence of αIg (10 μg/mL). At 180 minutes prior to the indicated times, B cell cultures were supplemented with 1 μCi/mL 5-[^{3}H]-glucose and glycolysis was then measured as described in *Materials and methods*. The data are represented as nanomoles of glucose converted to [^{3}H]OH per million cells per hour of 5-[^{3}H]-glucose pulse (nmol glucose/10^6/hr). The standard deviations for each time point are less than 5 % of the mean of triplicate measurements, and the data are representative of 3 independent experiments.

Figure 15.

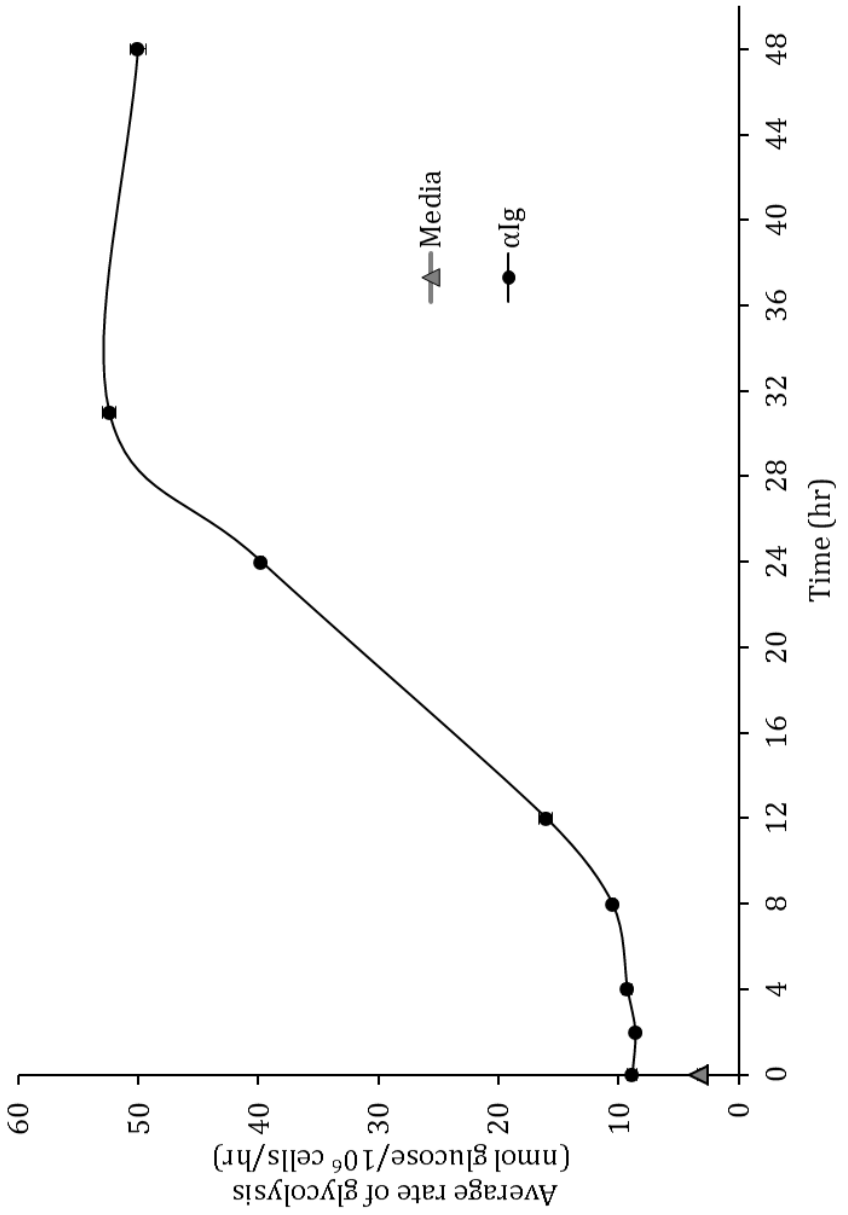
Average rate of glycolysis
(nmol glucose/10^6 cells/hr)
0
10
20
30
40
50
60
0
4
8
12
16
20
24
28
32
36
40
44
48
Time (hr)
Media
αIg

Figure 16. Glycolytic rate is differentially modulated in B cells in response to a variety of stimuli.

B cells (2 x 10^6/mL) were cultured in the absence (Media) or presence of αIg (10 μg/mL), IL-4 (30 ng/mL), CD40L (1:10), LPS (25 μg/mL), or αIg + IL-4 for 20 hr. At 180 minutes prior to the indicated time, B cell cultures were supplemented with 1 μCi/mL 5-[^{3}H]-glucose and glycolysis was then measured as described in *Materials and methods*. The data are represented as nanomoles of glucose converted to [^{3}H]OH per million cells per hour of 5-[^{3}H]-glucose pulse (nmol glucose/10^6/hr). Error bars reflect standard deviation from the mean of triplicate measurements, and the data are representative of 3 independent experiments.

Figure 16.

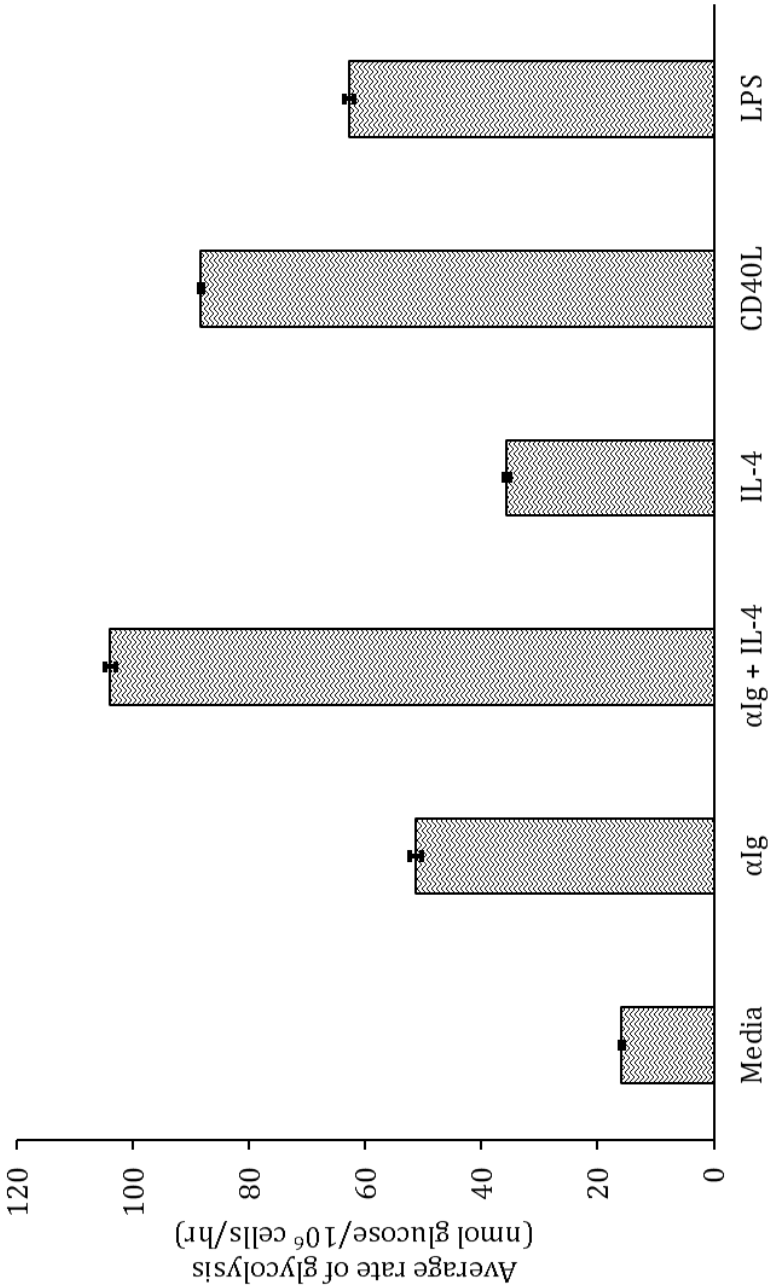
Average rate of glycolysis
(nmol glucose/10^6 cells/hr)
0
20
40
60
80
100
120
Media
αIg
αIg + IL-4
IL-4
CD40L
LPS

Figure 17. BCR cross-linking signals glycolytic flux via the PI3K signaling pathway.

B cells (2 x 10^6/mL) were cultured in the absence (Media) or stimulated with αIg (10 μg/mL) in the absence (αIg) or presence of 10 μM LY294002 (αIg + LY), 50 nM wortmannin (αIg + Wort), or 1.0 % vehicle alone (DMSO + αIg) for 12 hr. At 180 minutes prior to the indicated time, B cell cultures were supplemented with 1 μCi/mL 5-[^{3}H]-glucose and glycolysis was then measured as described in *Materials and methods*. The data are represented as nanomoles of glucose converted to [^{3}H]OH per million cells per hour of 5-[^{3}H]-glucose pulse (nmol glucose/10^6/hr). Error bars reflect standard deviation from the mean of triplicate measurements, and the data are representative of 3 independent experiments.

Figure 17.

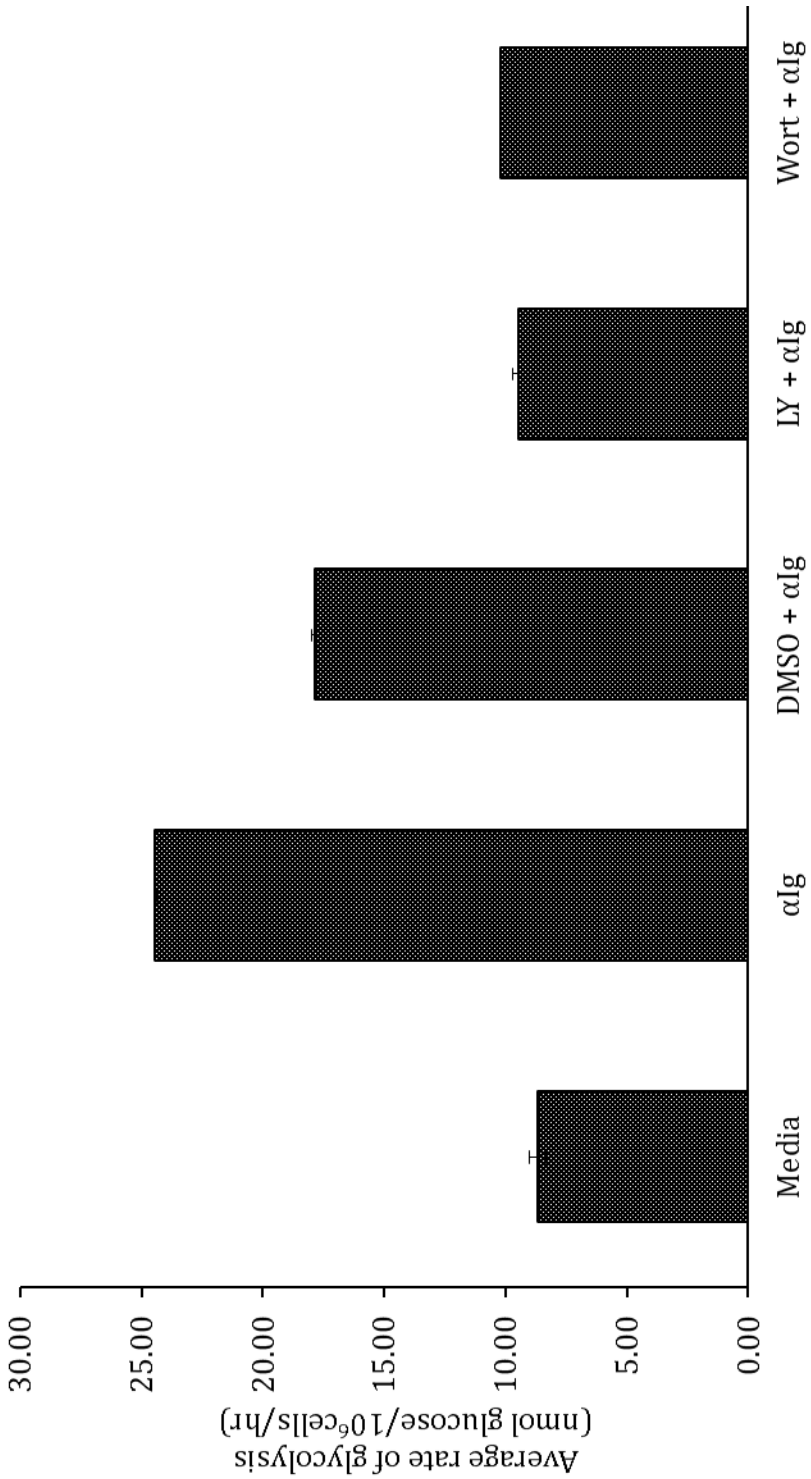
Average rate of glycolysis
(nmol glucose/1 0^6cells/hr)
30.00
25.00
20.00
15.00
10.00
5.00
0.00
Media
αIg
DMSO + αIg
LY + αIg
Wort + αIg

Figure 18. B cells deficient of p85α fail to increase glycolysis in response to BCR cross-linking.

B cells isolated from wild-type (WT) and p85α-deficient (KO) mice were cultured in the absence (Media) or presence of 10 μg/mL αIg for 18 hr and 28 hr. At 90 minutes prior to the indicated times, B cell cultures were supplemented with 1 μCi/mL 5-[^{3}H]-glucose and glycolysis was then measured as described in *Materials and methods*. The data are represented as nanomoles of glucose converted to [^{3}H]OH per million cells per hour of 5-[^{3}H]-glucose pulse (nmol glucose/10^6/hr). The standard deviations for each condition are less than 5 % of the mean.

Figure 18.

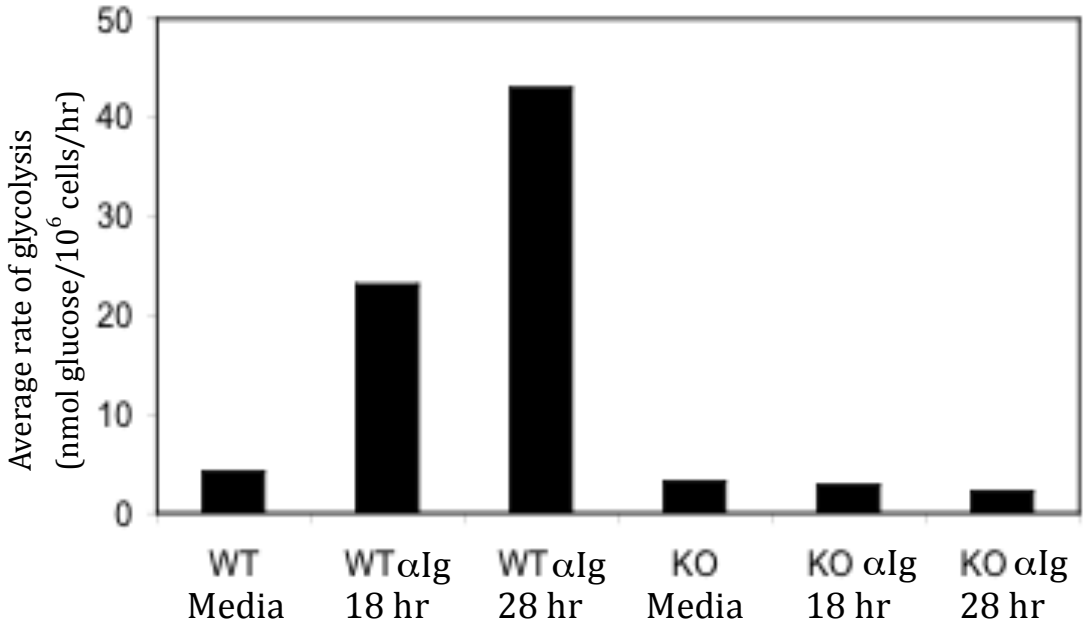
Average rate of glycolysis
(nmol glucose/10^6 cells/hr)
50
40
30
20
10
0
WT Media
WT αIg 18 hr
WT αIg 28 hr
KO Media
KO αIg 18 hr
KO αIg 28 hr

Figure 19. BTK activity is necessary for an enhanced glycolytic response to BCR cross-linking.

A) B cells were isolated from CBA/CaJ (WT) and XID mice were cultured in the absence (Media) or presence of αIg (10 μg/mL) or CD40L (1:10) for 3 hr, 6 hr, 12 hr and 22 hr. At 180 minutes prior to the indicated times, B cell cultures were supplemented with 1 μCi/mL 5-[^{3}H]-glucose and glycolysis was then measured as described in *Materials and methods*. The data are represented as nanomoles of glucose converted to [^{3}H]OH per million cells per hour of 5-[^{3}H]-glucose pulse (nmol glucose/10^6/hr). Error bars reflect standard deviation from the mean of triplicate measurements, and the data are representative of 3 independent experiments.

B) B cells were isolated from C57BL/6 (BL6) and BTK-deficient ($BTK^{-/-}$) mice were cultured in the absence (Media) or presence of αIg (10 μg/mL) for 6 hr, 12 hr, 23 hr, 44 hr, and 72 hr, or CD40L (1:10) for 6 hr, 12 hr, and 23 hr. At 180 minutes prior to the indicated times, B cell cultures were supplemented with 1 μCi/mL 5-[^{3}H]-glucose and glycolysis was then measured as described in *Materials and methods*. The data are represented as nanomoles of glucose converted to [^{3}H]OH per million cells per hour of 5-[^{3}H]-glucose pulse (nmol glucose/10^6/hr). Error bars reflect standard deviation from the mean of triplicate measurements, and the data are representative of 3 independent experiments.

Figure 19A.

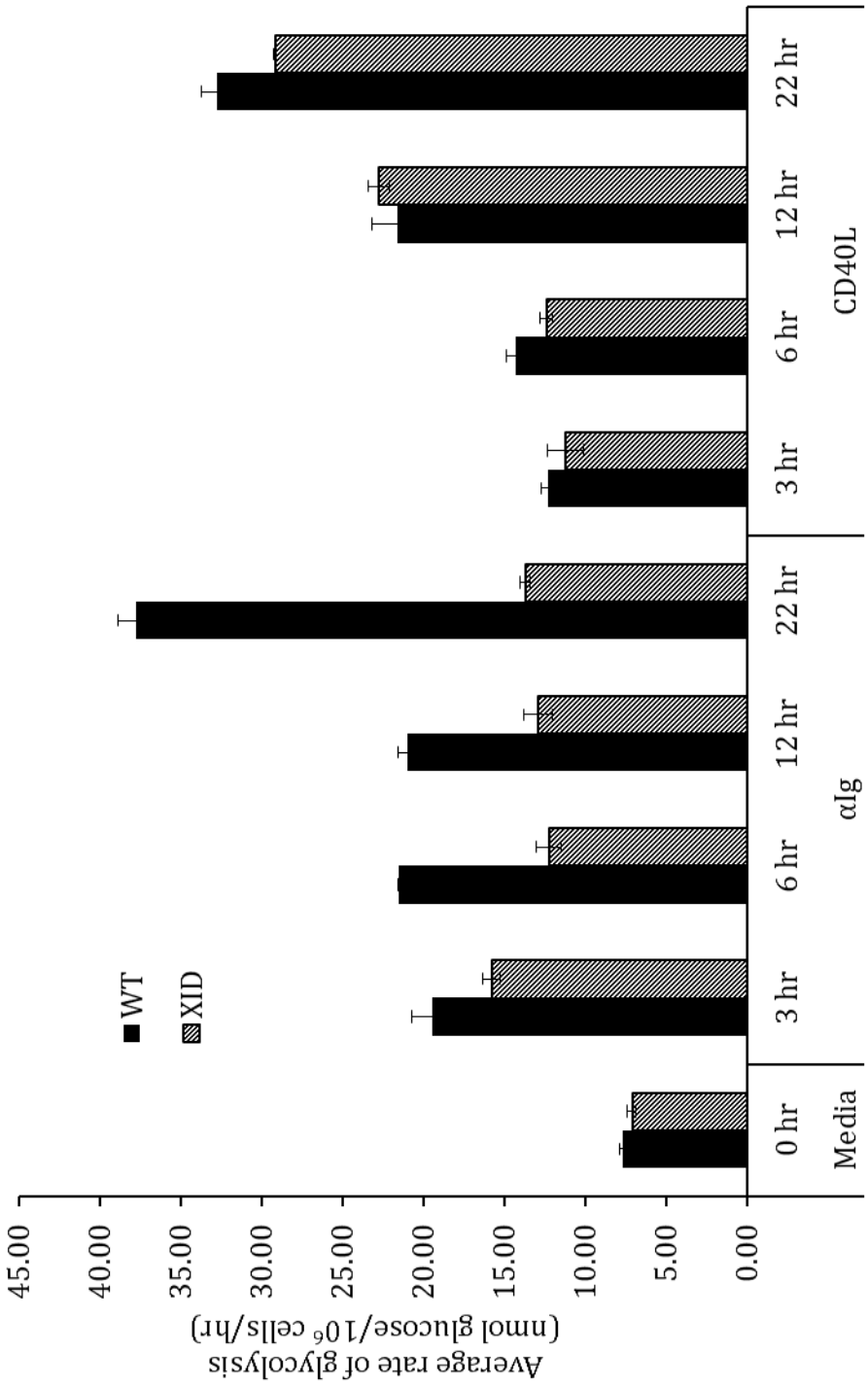
Average rate of glycolysis
(nmol glucose/10^6 cells/hr)
45.00
40.00
35.00
30.00
25.00
20.00
15.00
10.00
5.00
0.00
WT
XID
Media
0 hr
αIg
3 hr
6 hr
12 hr
22 hr
CD40L
3 hr
6 hr
12 hr
22 hr

Figure 19B.

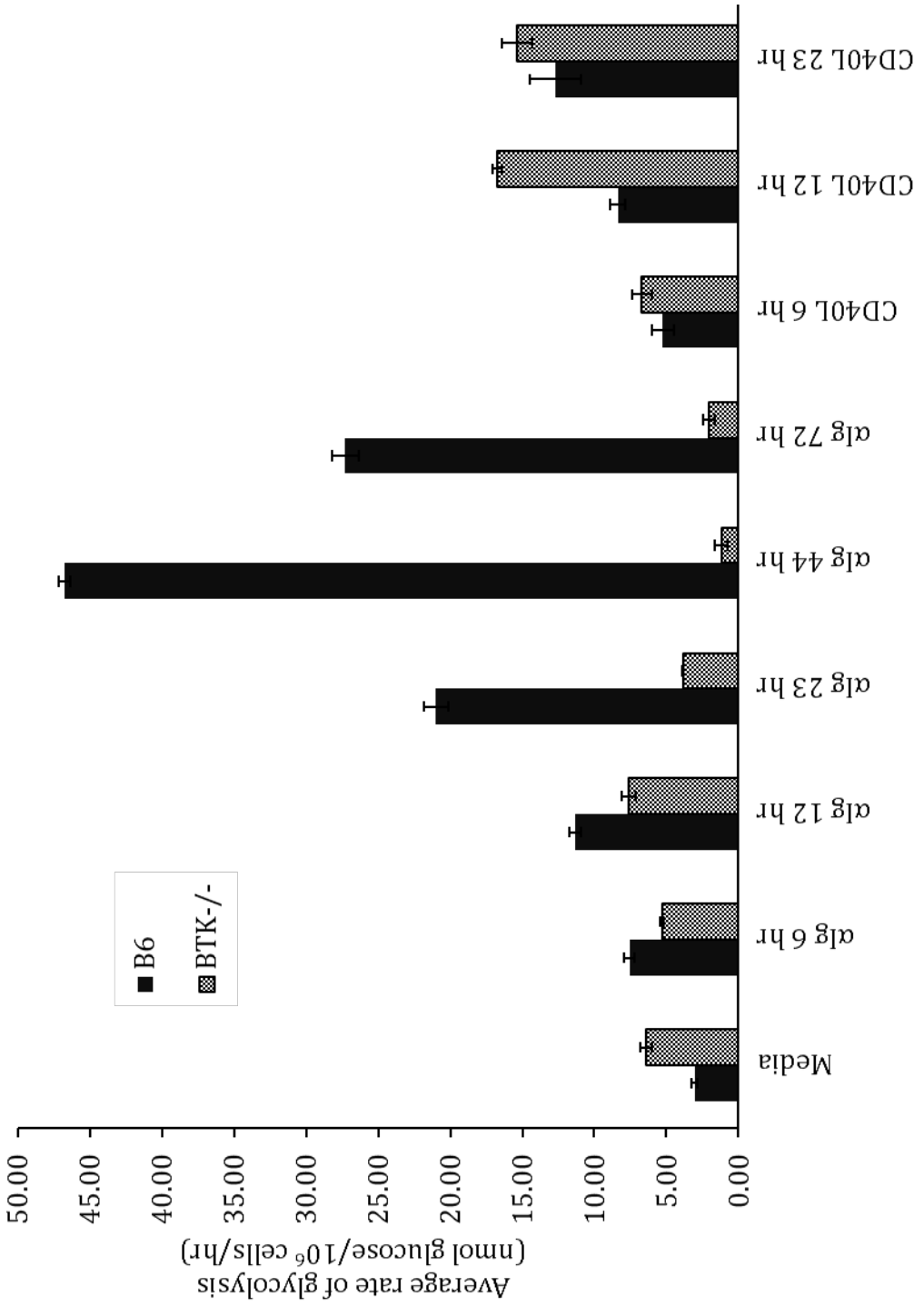
Average rate of glycolysis
(nmol glucose/10^6 cells/hr)
50.00
45.00
40.00
35.00
30.00
25.00
20.00
15.00
10.00
5.00
0.00
B6
BTK-/-
Media
αIg 6 hr
αIg 12 hr
αIg 23 hr
αIg 44 hr
αIg 72 hr
CD40L 6 hr
CD40L 12 hr
CD40L 23 hr

Figure 20. Deficiency in BLNK reduces the glycolytic response to BCR cross-linking.

B cells isolated from wild-type (129xSV) and BLNK-deficient ($BLNK^{-/-}$) mice were cultured in the absence (Media) or presence of αIg (10 μg/mL) or CD40L (1:10), LPS (25 μg/mL) for 5 hr. At 180 minutes prior to the indicated times, B cell cultures were supplemented with 1 μCi/mL 5-[^{3}H]-glucose and glycolysis was then measured as described in *Materials and methods*. The data are represented as nanomoles of glucose converted to [^{3}H]OH per million cells per hour of 5-[^{3}H]-glucose pulse (nmol glucose/10^6/hr). Error bars reflect standard deviation from the mean of triplicate measurements, and the data are representative of 3 independent experiments.

Figure 20.

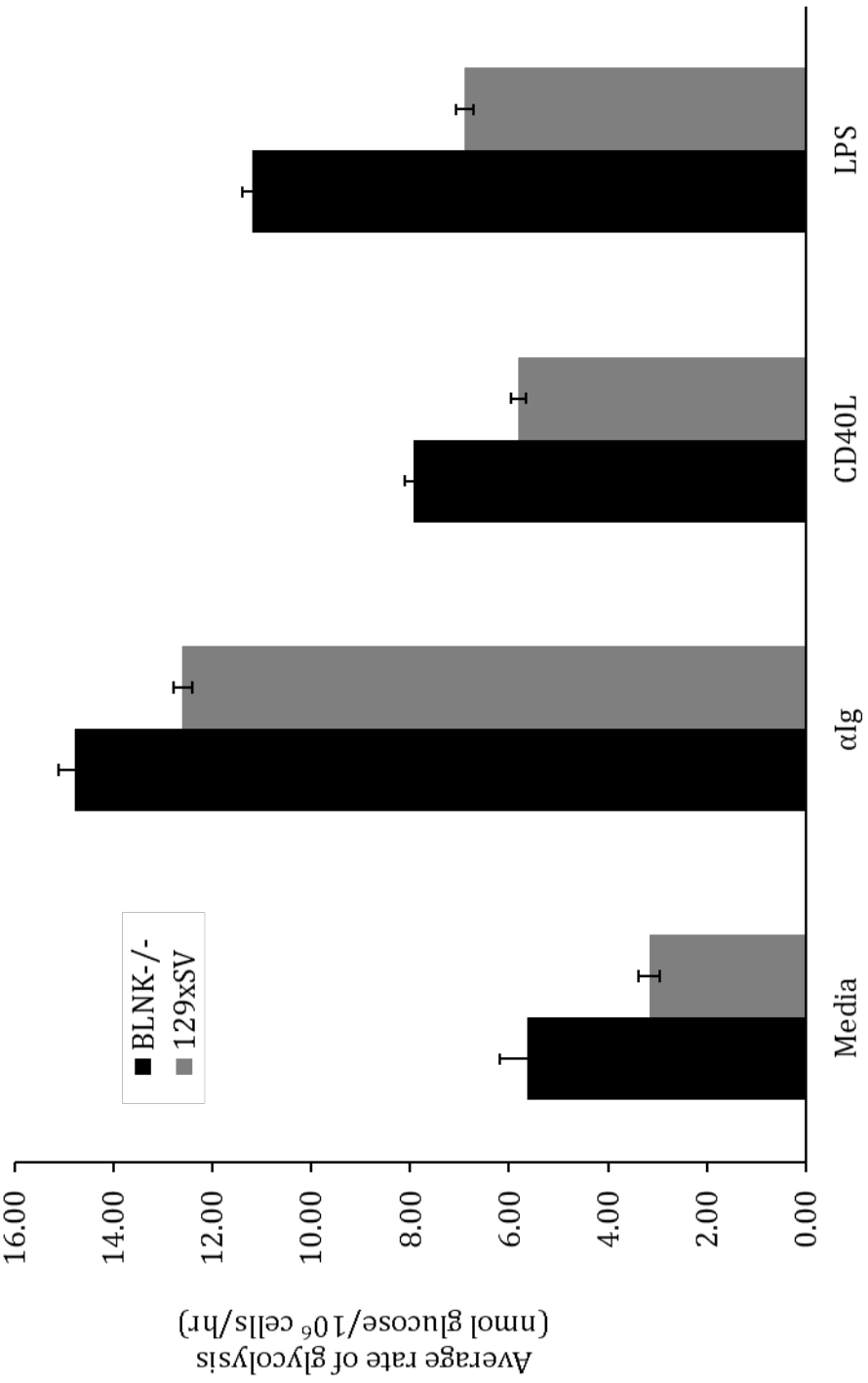
Average rate of glycolysis
(nmol glucose/10^6 cells/hr)
16.00
14.00
12.00
10.00
8.00
6.00
4.00
2.00
0.00
BLNK-/-
129xSV
Media
αIg
CD40L
LPS

Figure 21. Inhibition of PKCδ with rottlerin increases glycolysis independent of αIg stimulation.

B cells were cultured in the absence of stimulation (Media) with 10 μM rottlerin (Rottlerin) or in the presence of 10 μg/mL αIg (αIg) with rottlerin (αIg + Rottlerin) for 3 hr and 6 hr. At 180 minutes prior to the indicated time, B cell cultures were supplemented with 1 μCi/mL 5-[^{3}H]-glucose and glycolysis was then measured as described in *Materials and methods*. The data are represented as nanomoles of glucose converted to [^{3}H]OH per million cells per hour of 5-[^{3}H]-glucose pulse (nmol glucose/10^6/hr). Error bars reflect standard deviation from the mean of triplicate measurements, and the data are representative of 2 independent experiments.

Figure 21.

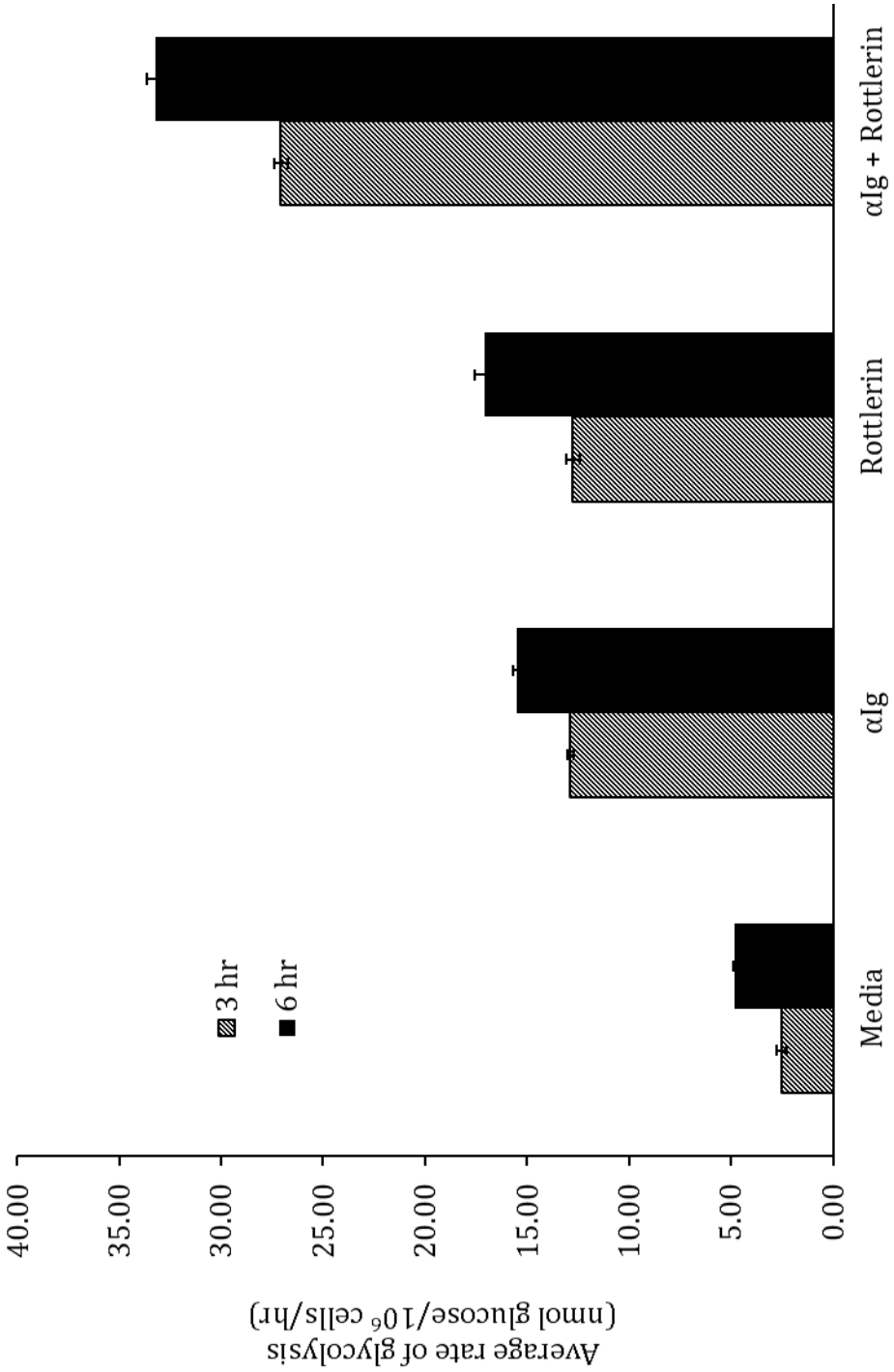
Average rate of glycolysis
(nmol glucose/10^6 cells/hr)
40.00
35.00
30.00
25.00
20.00
15.00
10.00
5.00
0.00
3 hr
6 hr
Media
αIg
Rottlerin
αIg + Rottlerin

Figure 22. PKCδ is not required for BCR-induced glycolytic flux in B cells.

B cells isolated from wild-type (C57BL/6x129x1/SvJ) and PKCδ-deficient ($PKC\delta^{-/-}$) mice were cultured in the absence (Media) or presence of αIg (10 μg/mL) for 24 hr. At 180 minutes prior to the indicated time, B cell cultures were supplemented with 1 μCi/mL 5-[^{3}H]-glucose and glycolysis was then measured as described in *Materials and methods*. The data are represented as nanomoles of glucose converted to [^{3}H]OH per million cells per hour of 5-[^{3}H]-glucose pulse (nmol glucose/10^6/hr). Error bars reflect standard deviation from the mean of triplicate measurements, and the data are representative of 3 independent experiments.

Figure 22.

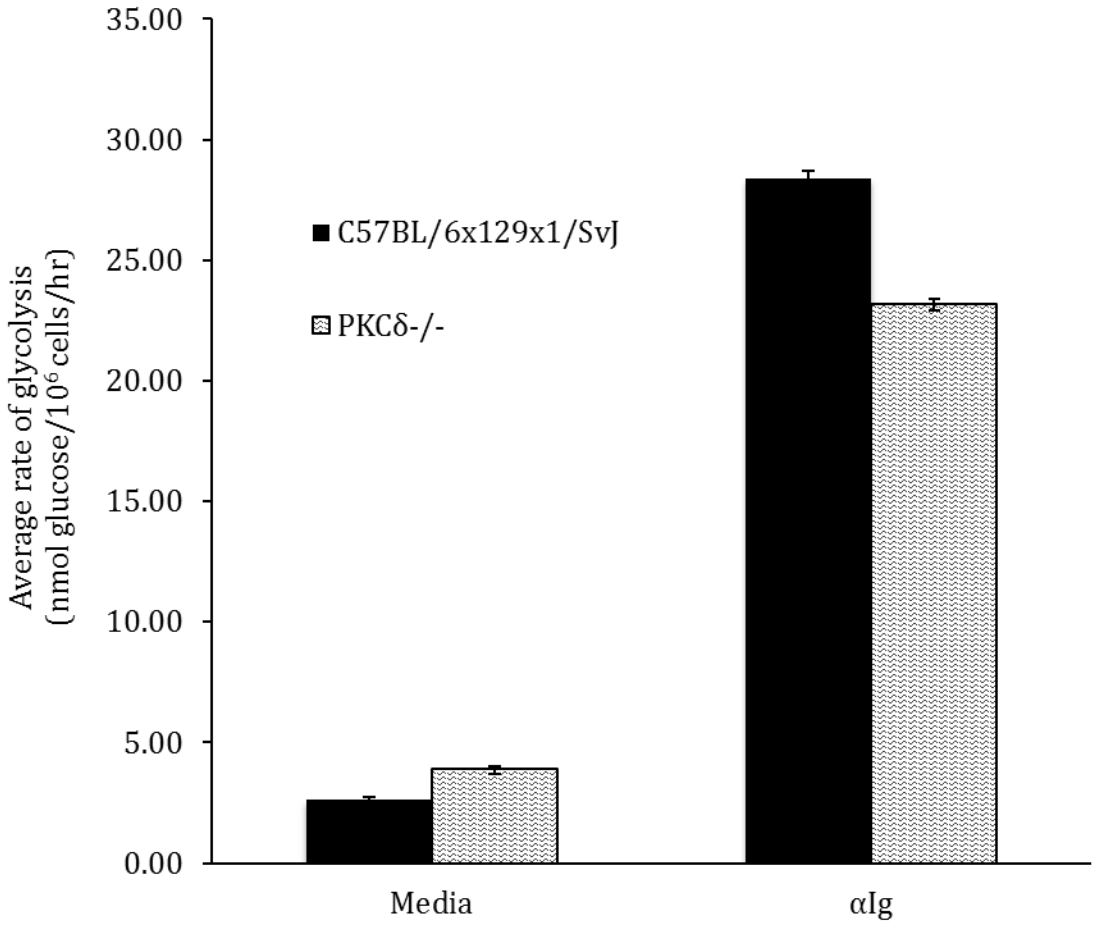
35.00
30.00
25.00
20.00
15.00
10.00
5.00
0.00
Average rate of glycolysis (nmol glucose/10^6 cells/hr)
C57BL/6x129x1/SvJ
PKCδ-/-
Media
αIg

Figure 23. IL-4 mediated increase in glycolysis requires STAT6 in B cells.

WT B cells were cultured in the absence (-) or presence of 4 ng/mL IL-4 (+) for 48 hr. STAT6-deficient (STAT6 KO) B cells were cultured in the absence (-) or presence of 4 ng/mL IL-4 (+) or cultured with cell-permeable forms (200 ng/mL) of WT TAT-Stat6 (WT-), WT TAT-Stat6 plus IL-4 (WT+), or constitutively active TAT-Stat6VT (VT) for 48 hr. At 180 minutes prior to the indicated time, B cell cultures were supplemented with 1 μCi/mL 5-[^{3}H]-glucose and glycolysis was then measured as described in *Materials and methods*. The data are represented as nanomoles of glucose converted to [^{3}H]OH per million cells per hour of 5-[^{3}H]-glucose pulse (nmol glucose/10^6/hr). Error bars reflect standard deviation from the mean of triplicate measurements, and the data are representative of 3 independent experiments.

Figure 23.

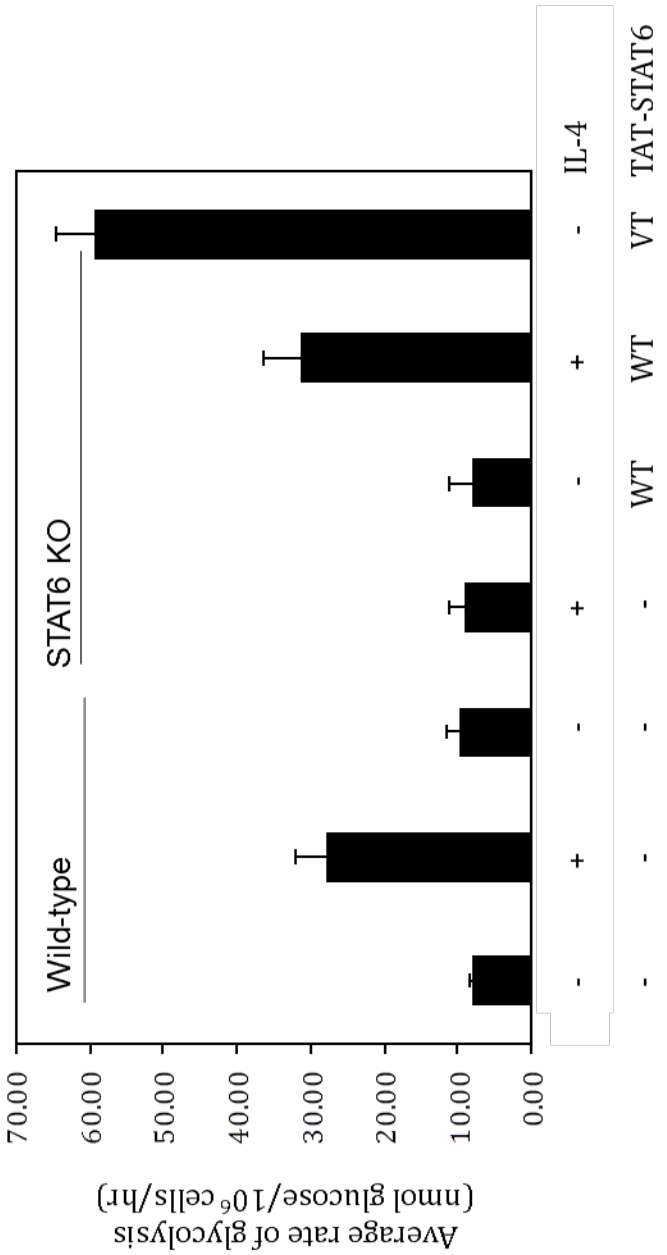
Wild-type
STAT6 KO
70.00
60.00
50.00
40.00
30.00
20.00
10.00
0.00
Average rate of glycolysis
(nmol glucose/10^6 cells/hr)
- - - - - - - -
- + - + - + - +
- - - - WT WT VT VT
IL-4
TAT-STAT6

Figure 24. Expression of key glycolytic enzymes increases in response to BCR cross-linking.

B cells were cultured in medium alone (media) or stimulated with αIg (15 μg/mL) for 24 hr. At these time points, total RNA was isolated and expression of *phosphofructose kinase* (*pfk*), *lactate dehydrogenase* (*ldh*), or *hexokinase* (*hk*) was assessed by semi-quantitative real time PCR with SYBR green. Levels of expression of the indicated gene were normalized to *18S rRNA* and represent ratios of the indicated gene: *18S rRNA* relative to media. Error bars reflect standard deviation from the mean of triplicate measurements, and the data are representative of 3 independent experiments.

Figure 24.

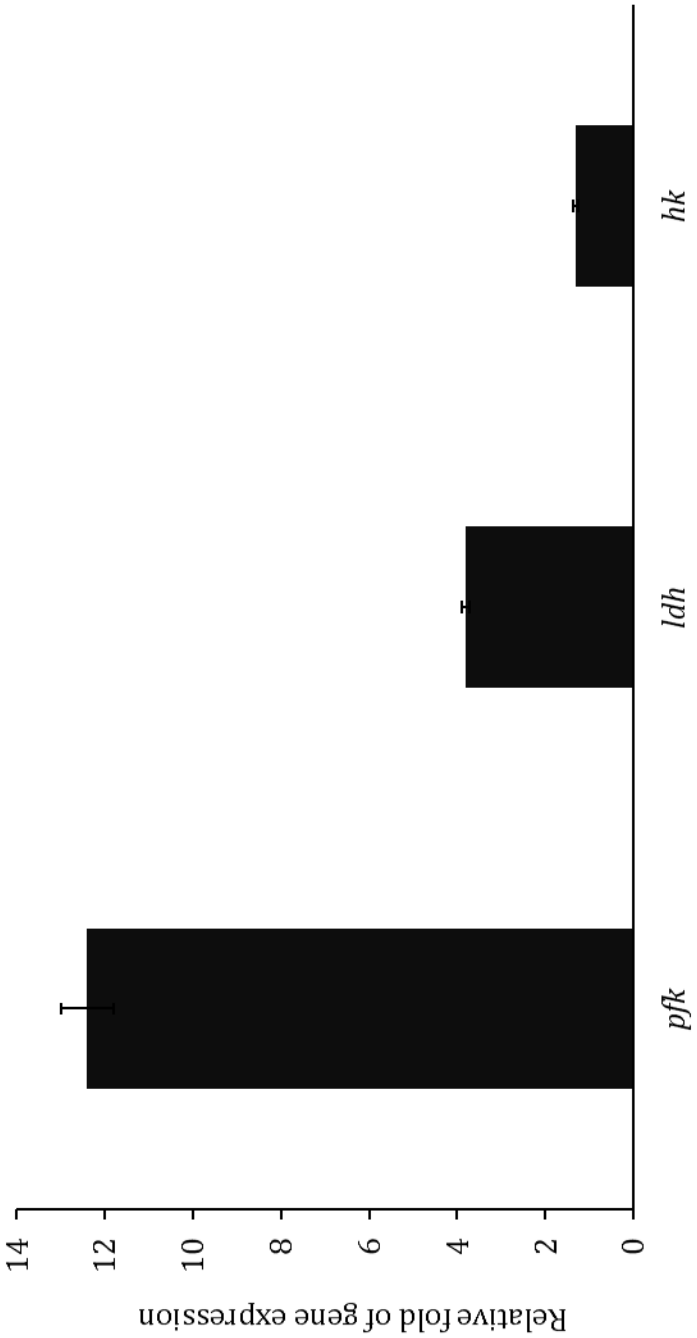

Figure 25. Lactate secretion is induced in response to BCR cross-linking.

B cells were cultured in medium alone (Media) or stimulated with αIg (10 μg/mL) for 16 hr, 24 hr, and 48 hr. The amount of lactate secreted into the tissue culture medium was then measured by colorimetric lactate oxidase method (Pointe Scientific). The data are represented as millimoles per liter (mmol/L). Error bars reflect standard deviation from the mean of triplicate measurements, and the data are representative of 3 independent experiments.

Figure 25.

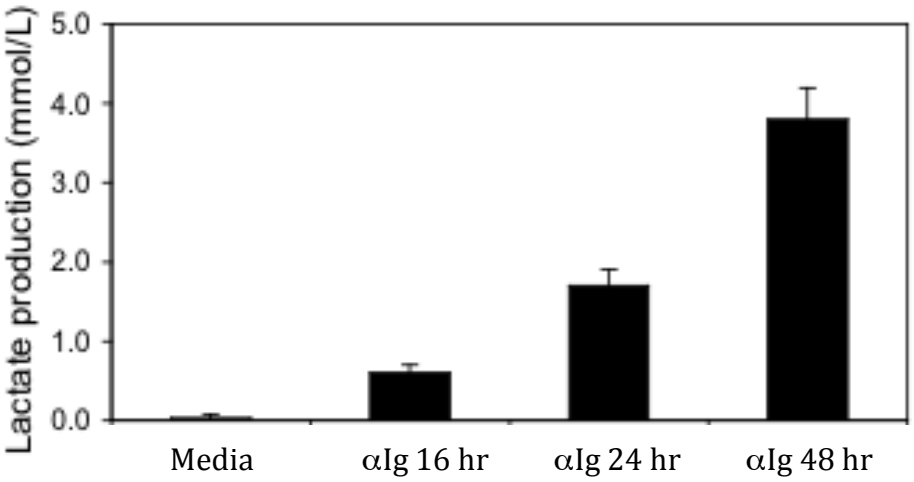
Lactate production (mmol/L)
5.0
4.0
3.0
2.0
1.0
0.0
Media
αIg 16 hr
αIg 24 hr
αIg 48 hr

Figure 26. ATP levels are reduced in B cells lacking functional BTK.

B cells of XID or wild-type (CBA/CaJ) were cultured in medium alone (Media) or stimulated with αIg (15 μg/mL) or IL-4 (30 ng/mL) for 23 hr. Concentrations of ATP (nM) in 1 x 10^6 B cells under each condition were determined by a bioluminescent assay. A standard curve for a series of standard ATP concentrations (0 nM to 1000 nM) was generated and the amount of ATP in the experimental samples was calculated from the standard curve. Error bars reflect standard deviation from the mean of triplicate measurements, and the data are representative of 3 independent experiments.

Figure 26.

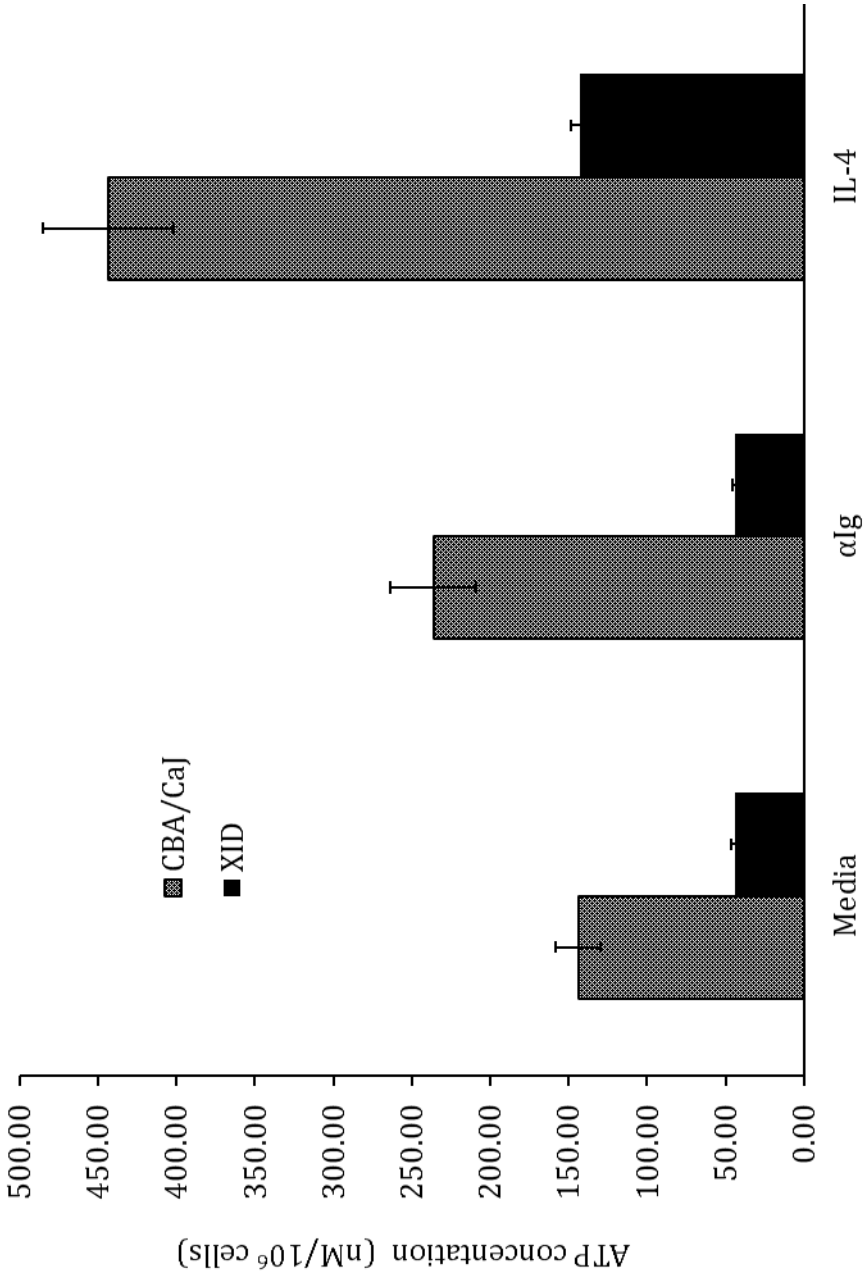
ATP concentration (nM/10^6 cells)
500.00
450.00
400.00
350.00
300.00
250.00
200.00
150.00
100.00
50.00
0.00
CBA/CaJ
XID
Media
αIg
IL-4

Figure 27. Stimulated B cells increase production of CO_2 levels.

B cells were cultured in medium alone (Media) or stimulated with αIg (15 μg/mL) or IL-4 (30 ng/mL) for 44 hr. The tissue culture medium contained bicarbonate-free RPMI-1640 supplemented with [^{14}C]-1-glucose or [^{14}C]-6-glucose. As a control for evaporation, cell-free RPMI-1640 with [^{14}C]-labeled glucose (RPMI-no cells) was included in our assay. Release of [^{14}C]O_2 into atmosphere was captured with saturated $Ba(OH)_2$ filter paper in sealed cell culture plate, as described in *Materials and methods*. Levels of [^{14}C]O_2 were determined by autoradiography and densitometry. Indicated numbers are representative of fold increase in average densitometric intensity values of the expired [^{14}C]O_2 from respective [^{14}C]-labeled glucose, captured from αIg or IL-4 stimulated B cells relative to unstimulated (Media). ImageJ software (v1.45) was used to obtain densitometric values. The data are representative of 2 independent experiments.

Figure 27.

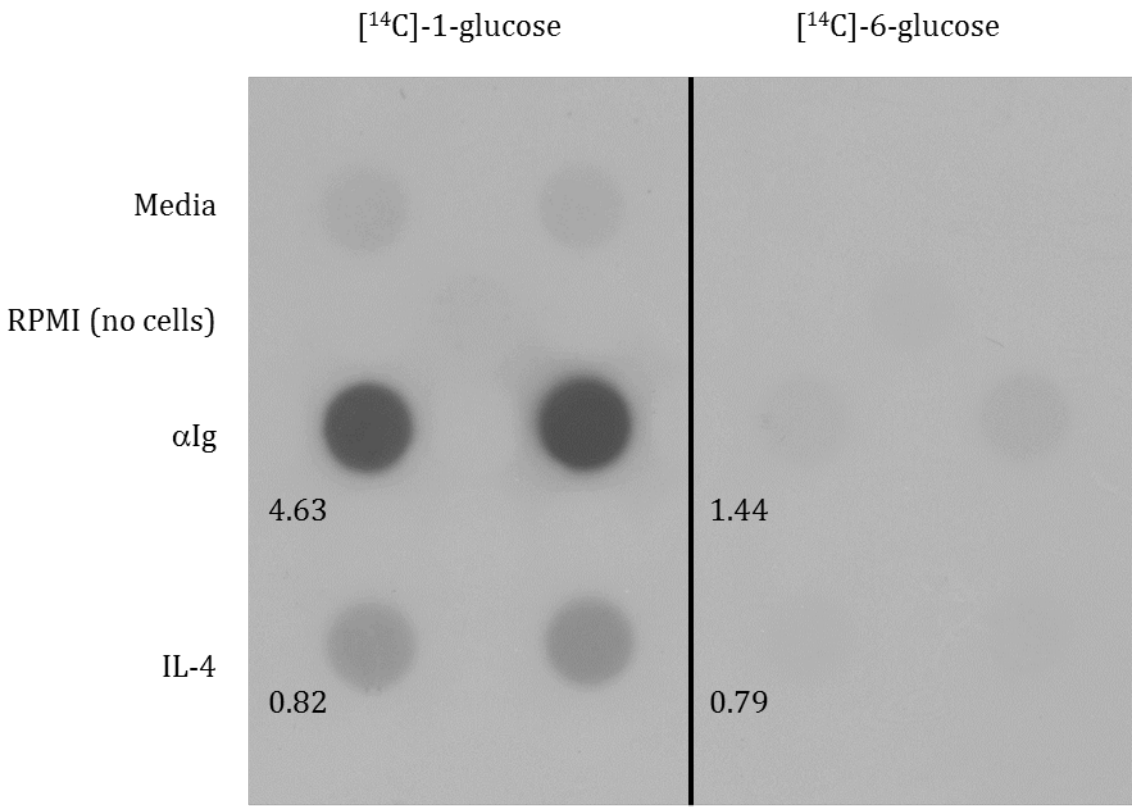
[14C]-1-glucose
[14C]-6-glucose
Media
RPMI (no cells)
αIg
4.63
1.44
IL-4
0.82
0.79

Figure 28. B cells increase [^{14}C]O_2 production in response to various stimuli.

B cells were cultured in medium alone (Media) or stimulated with αIg (15 μg/mL), IL-4 (30 ng/mL), αIg + IL-4, LPS (25 μg/mL), or phorbol myristate acetate (PMA: 300 ng/mL) and ionomycin (Iono: 400 ng/mL) for 24 hr. The tissue culture medium contained bicarbonate-free RPMI-1640 supplemented with [^{14}C]-1-glucose or [^{14}C]-6-glucose. As a control for evaporation, B cells were also cultured in RPMI-1640 without [^{14}C]-labeled glucose supplement (Unlabeled). Release of [^{14}C]O_2 into atmosphere was captured with saturated $Ba(OH)_2$ filter paper in sealed cell culture plate, as described in *Materials and methods*. Levels of [^{14}C]O_2 were determined by autoradiography and densitometry. Indicated numbers are representative of fold increase in average densitometric intensity values of the expired [^{14}C]O_2 from respective [^{14}C]-labeled glucose, captured from stimulated B cells relative to unstimulated (Media). ImageJ software (v1.45) was used to obtain densitometric values. The data are representative of 2 independent experiments.

Figure 28.

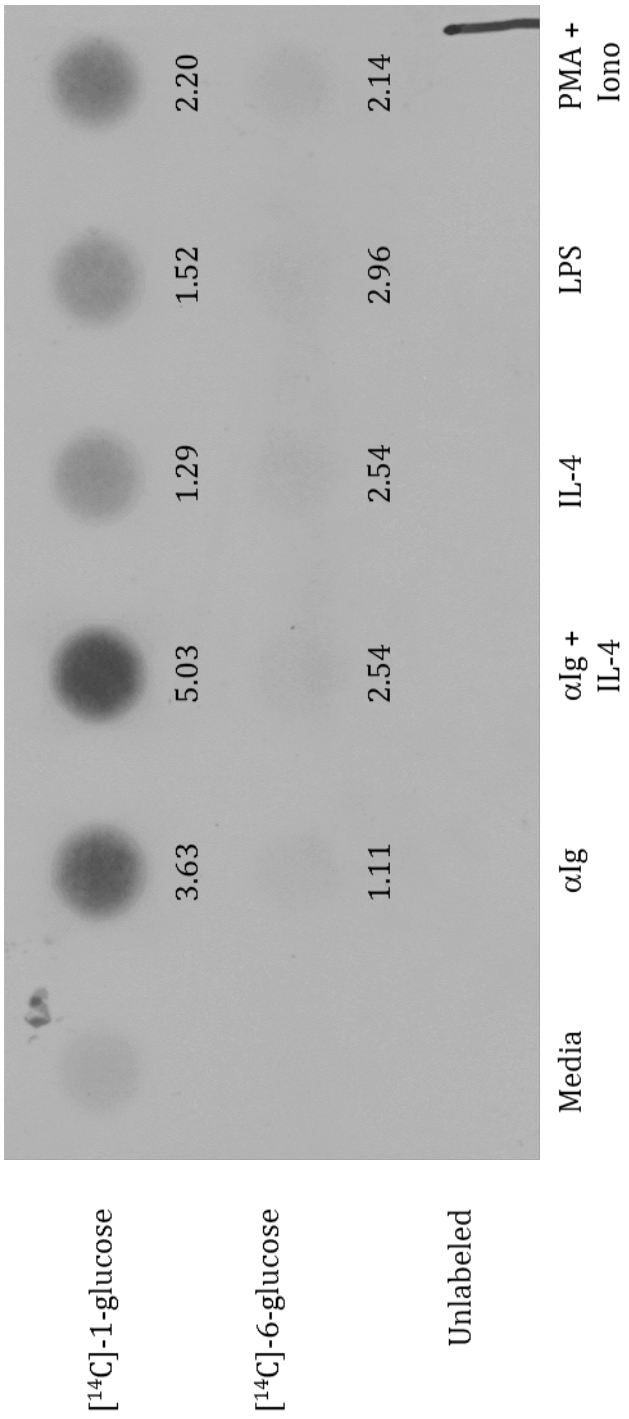
[14C]-1-glucose
[14C]-6-glucose
Unlabeled
Media
αIg
αIg + IL-4
IL-4
LPS
PMA + Iono
3.63
5.03
1.29
1.52
2.20
1.11
2.54
2.54
2.96
2.14

Figure 29. Inhibition of pentose phosphate pathway reduced production of $[^{14}C]O_2$ in B cells.

B cells were cultured in medium alone (Media) or stimulated with αIg (15 μg/mL) in the absence (no inhibitor) or presence of 100 μM 6-aminonicotinamide (6-ANA) for 18 hr. The tissue culture medium contained bicarbonate-free RPMI-1640 supplemented with $[^{14}C]$-1-glucose. As a control for evaporation, B cells in culture containing RPMI-1640 without $[^{14}C]$-labeled glucose (No $[^{14}C]$) was included in our assay. Release of $[^{14}C]O_2$ into atmosphere was captured with saturated $Ba(OH)_2$ filter paper in sealed cell culture plate, as described in *Materials and methods*. Levels of $[^{14}C]O_2$ were determined by autoradiography and densitometry. The data are representative of 1 independent experiment.

Figure 29.

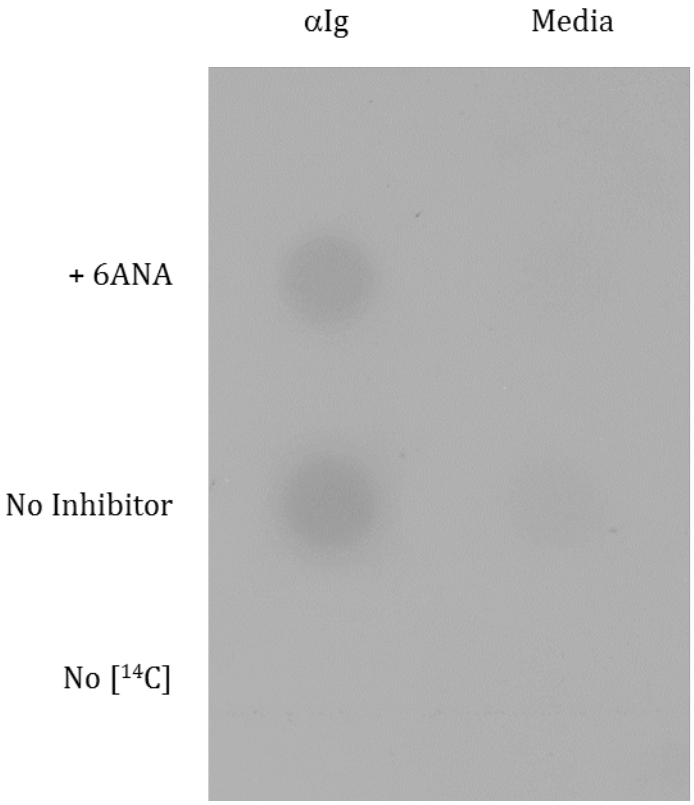

Figure 30. Pathway of glucose utilization into *de novo* lipogenesis.

Intracellular glucose can be metabolized through glycolysis to the end-product pyruvate. For further cellular utilization, pyruvate enters the mitochondria for processing through the TCA cycle. Truncation of this cycle occurs when citrate is exported out of the mitochondria and into the cytoplasm. The cytosolic enzyme, ATP citrate lyase (ACL) acts upon citrate to produce acetyl-CoA and oxaloacetate (not shown). The synthesis of lipids occurs through a series of enzymatic reactions utilizing the supply of acetyl-CoA subunits to form cholesterol, fatty acids and isoprenoids (not shown).

Figure 30.

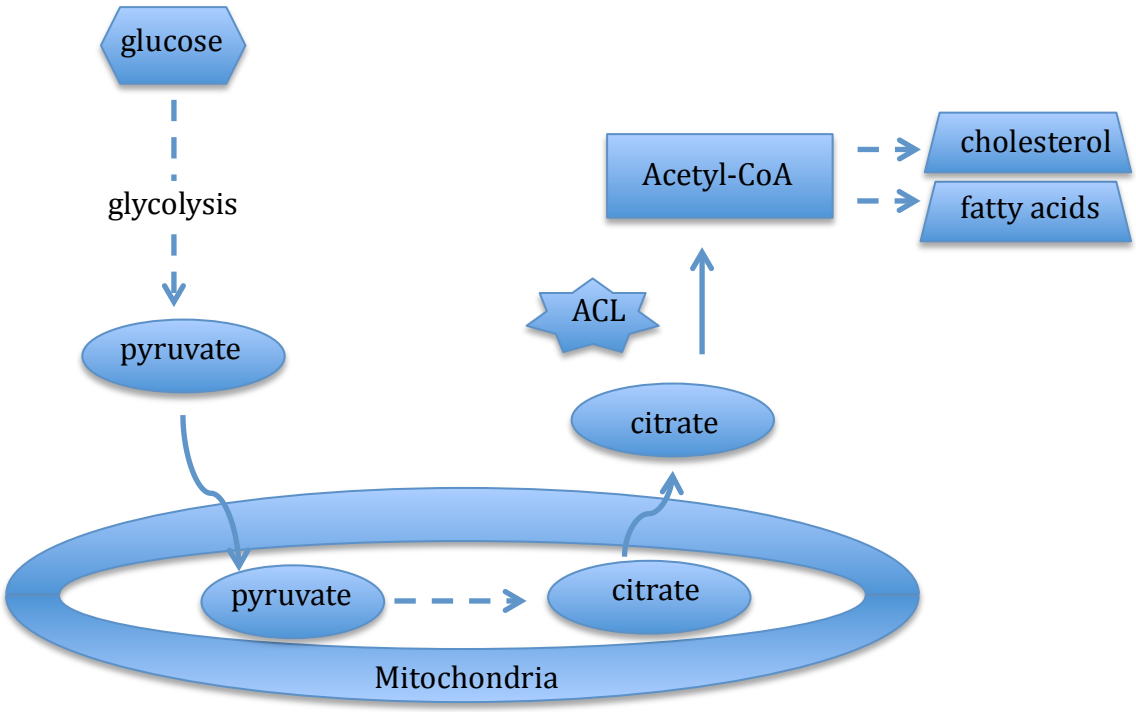
glucose
glycolysis
pyruvate
Acetyl-CoA
cholesterol
fatty acids
ACL
citrate
pyruvate
citrate
Mitochondria

Figure 31. Time course of ACL phosphorylation on serine^{454}.

(A) B cells were cultured in medium alone (Media) or stimulated with αIg (10 μg/mL), IL-4 (30 ng/mL), or αIg + IL-4 for 3 hr, 6 hr, 9 hr, 24 hr, 48 hr, and 72 hr. Cell lysates were prepared in Triton X-100 buffer, and equivalent amounts of total protein were examined by Western blot for phospho-serine^{454} ACL and hsp90 protein levels; the latter serves as a loading control.

(B) Quantification of the phospho-serine^{454} ACL bands was obtained through use of ImageJ software (v1.45). Both upper and lower band densities are listed as upper: lower for stimulated B cell extracts. Values represent fold increase of detected band in extracts of stimulated B cells above detected band density obtained in Media. The data are representative of 3 independent experiments.

Figure 31.

(A)

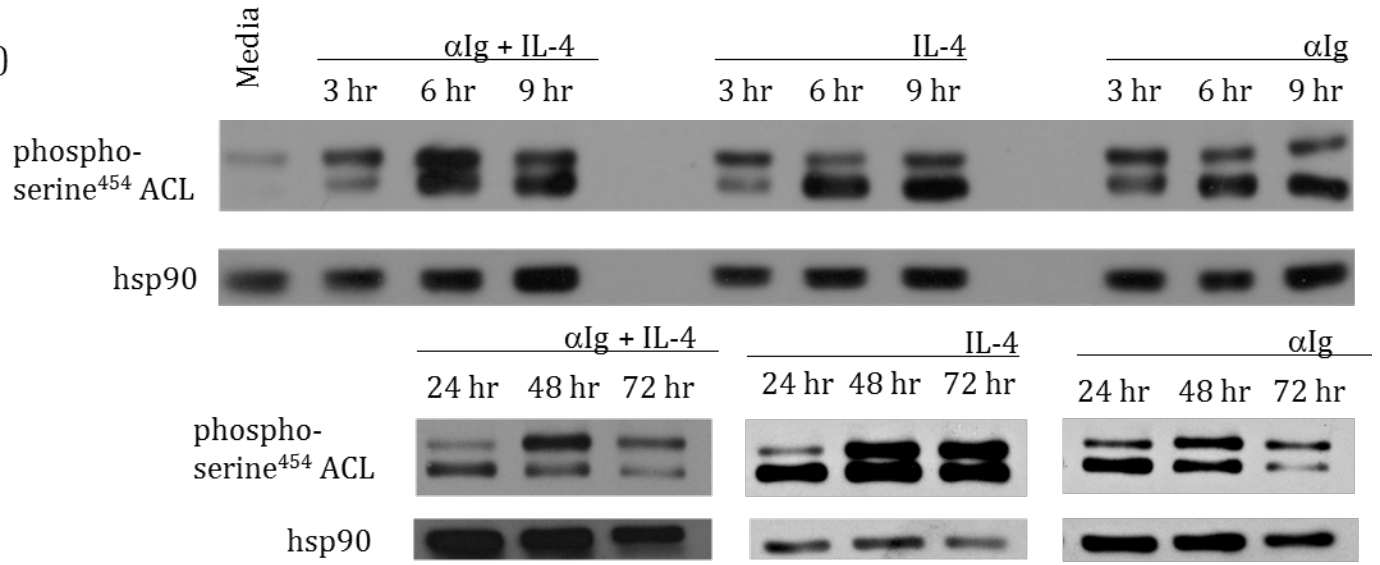

(B) Fold of phospho-serine^{454} ACL (top band: bottom band density)

	3 hr	6 hr	9 hr	24 hr	48 hr	72 hr
αIg + IL-4	2.6:2.6	5.7:15.3	4.4:17.7	1.6:7.4	11.5:4.9	5.1:2.2
IL-4	2.3:3.5	2.1:15.5	2.5:17.7	0.2:3.8	5.0:5.4	4.8:4.5
αIg	3.7:7.1	2.4:11.5	2.9:12.5	1.6:7.8	4.1:5.0	1.5:0.4

Figure 32. Phosphorylation of ACL at serine^{454} is dependent upon PI3K activity.

(A) B cells were cultured with αIg (10 μg/mL), IL-4 (30 ng/mL), αIg + IL-4, in the absence or presence of 25 μM LY294002 (LY), 50 nM wortmannin (Wort), or 50 nM rapamycin (Rap), or in medium alone with 1 % vehicle-only (DMSO) for 18 hr. Cells were then harvested, and cellular lysates prepared in Triton X-100 buffer, and equivalent amounts of total protein were examined by Western blot for phospho-serine^{454} ACL, phospho-serine^{473} Akt, total ACL, and hsp90 protein levels; the latter serves as a loading control.

(B) Quantification of the phospho-serine^{454} ACL band density was obtained through the use of ImageJ software (v1.45). Both upper and lower band densities are listed as upper: lower for stimulated B cell extracts. Values represent fold increase of detected band in extracts of stimulated B cells above detected band density obtained in DMSO-treated. The data are representative of 2 independent experiments.

Figure 32.

(A)

(B) Fold Stimulated over DMSO control of phospho-serine^{454} ACL (top band: bottom band density) or phospho-serine^{473} Akt

Phospho-serine^{454} ACL	No Inhibitor	+ LY	+ Wort	+ Rap
αIg + IL-4	1.8: 0.8	0.2: 0.3	1.1: 0.4	2.9: 0.2
IL-4	1.1: 0.3	-0.2: 0.1	0.2: 0.6	1.5: 0.6
αIg	1.4: 0.6	-0.4: -0.1	0.1: 0.3	1.4: 0.4

Phospho-serine^{473} Akt	No inhibitor	+ LY	+ Wort	+ Rap
αIg + IL-4	1.8	0.5	1.6	2.0
IL-4	0.6	-0.4	0.3	1.4
αIg	0.4	-0.6	-0.4	1.0

Figure 33. Deficiency of p85α decreases ACL phosphorylation.

(A) B cells were isolated from p85α$^{-/-}$ (Knockout), p85α$^{+/-}$ (Heterozygous), or p85α$^{+/+}$ (Wild-type) mice and cultured in the absence (Media) or presence of IL-4 (30 ng/mL), αIg (10 μg/mL), αIg + IL-4 for 3 hr and 6 hr. Cells were then harvested, cellular lysates prepared in Triton X-100 buffer, and equivalent amounts of total protein were examined by Western blot for phospho-serine^{454} ACL.

(B) Quantification of the phospho-serine^{454} ACL band density was obtained through use of ImageJ software (v1.45). Band density values represent fold increase of detected band in extracts of stimulated B cells above detected band density obtained in Media of the respective genotype. The data are representative of 3 independent experiments.

Figure 33.

(A)

(B) Fold Stimulated over Media of phospho-serine^{454} ACL (top band: bottom band density)

Knock-out	3 hr	6 hr	Heterozygous	3 hr	6 hr	Wild-type	3 hr	6 hr
αIg	0.1	-0.3	αIg	1.6	2.2	αIg	1.8	1.0
IL-4	-0.3	-0.3	IL-4	0.6	2.0	IL-4	1.3	0.9
αIg + IL-4	0.7	1.2	αIg + IL-4	2.2	2.1	αIg + IL-4	2.1	2.8
LPS	2.2	3.4	LPS	0.2	0.9	LPS	2.2	2.4

Figure 34. ACL activity is increased in response to αIg + IL-4 stimulation of B cells.

B cells were cultured in medium alone (0) or with αIg (10 μg/mL) and IL-4 (30 ng/mL) for the indicated time points. Whole cell extracts were then prepared and ACL activity was measured by coupled enzymatic reaction to malate dehydrogenase (MDH), as described in *Materials and methods*. ACL enzyme activity is expressed as the oxidation of NADH to $NAD^+ + H^+$, over time as measured by the change in absorbance (OD_{340}/min). The standard deviations for each condition are less than 5 % of the mean. This assay was conducted in duplicate by Dr. Maria Gumina (2009).

Figure 34.

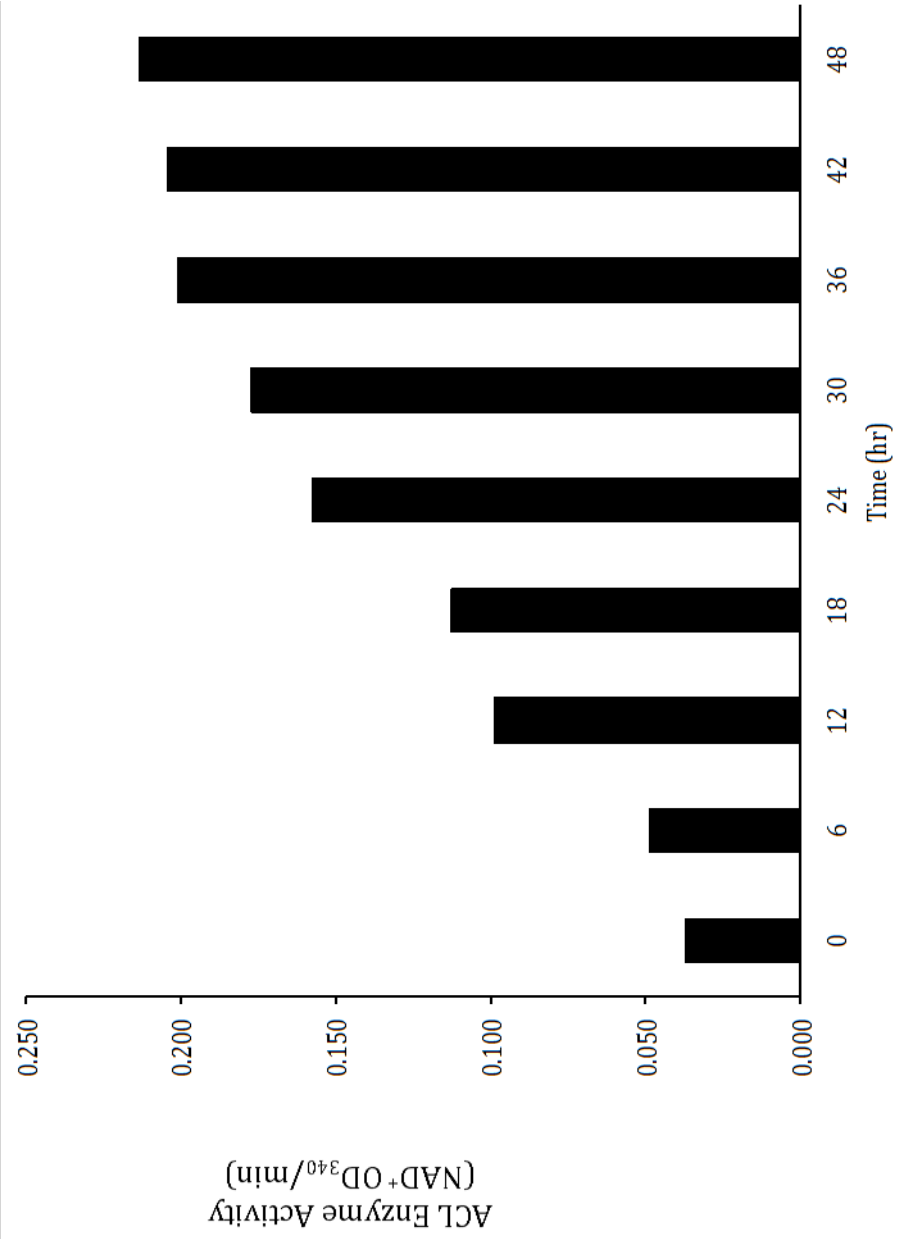
ACL Enzyme Activity
(NAD+ OD340/min)
0.250
0.200
0.150
0.100
0.050
0.000
0
6
12
18
24
30
36
42
48
Time (hr)

Figure 35. Deficiency of p85α reduces ACL enzyme activity.

B cells were isolated from $p85\alpha^{+/+}$, $p85\alpha^{+/-}$, or $p85^{-/-}$ mice cultured in the absence (Media) or presence of αIg (10 μg/mL) + IL-4 (30 ng/mL) for 18 hr. Whole cell extracts were then prepared and ACL activity was measured by coupled enzymatic reaction to malate dehydrogenase (MDH), as described in *Materials and methods*. ACL enzyme activity is expressed as the oxidation of NADH to $NAD^+ + H^+$, over time as measured by the change in absorbance (OD_{340}/min). Error bars reflect standard deviation from the mean of triplicate measurements. This assay was conducted in duplicate by Dr. Maria Gumina (2009).

Figure 35.

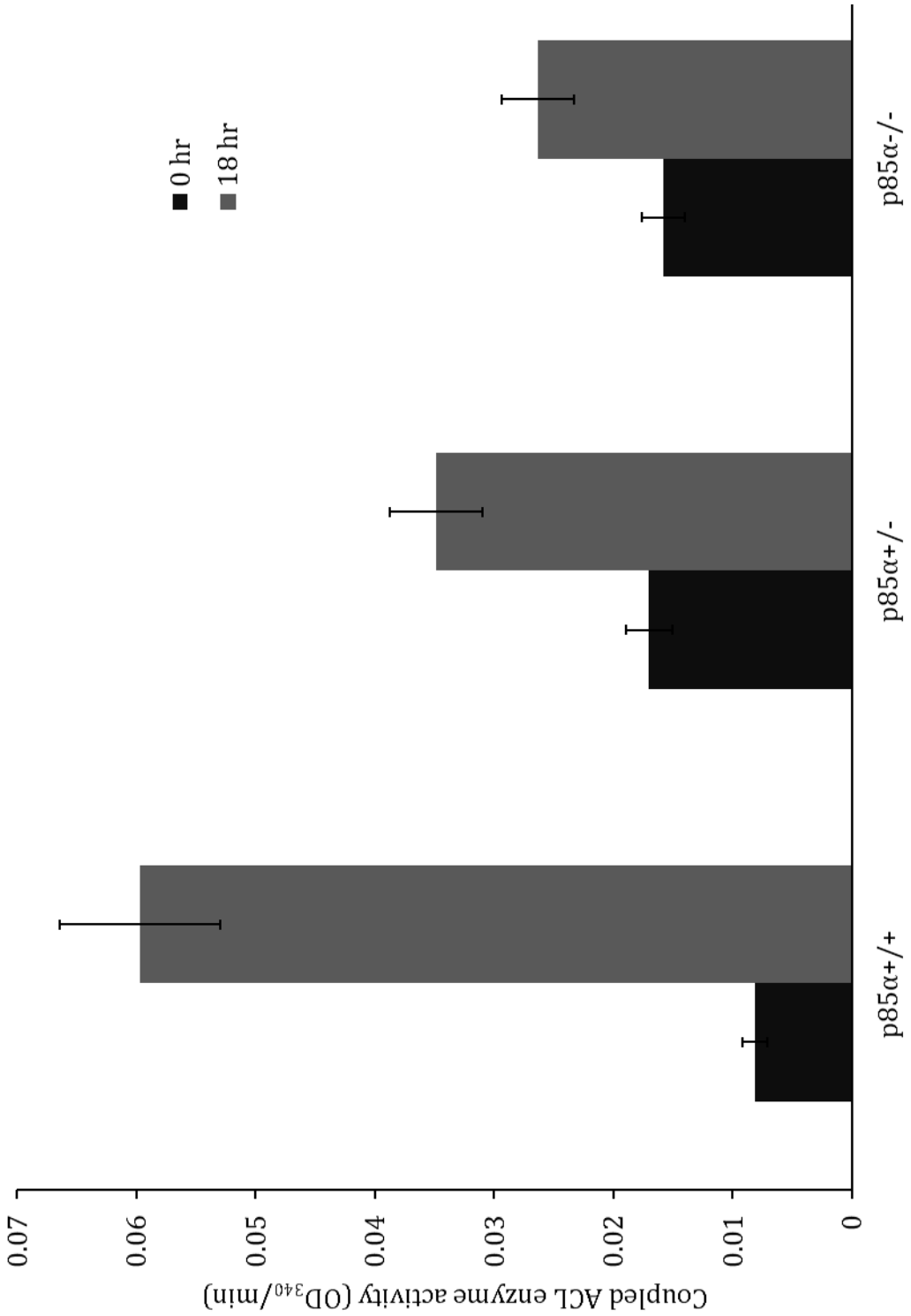
0 hr
18 hr
Coupled ACL enzyme activity (OD340/min)
0
0.01
0.02
0.03
0.04
0.05
0.06
0.07
p85α+/+
p85α+/-
p85α-/-

Figure 36. ACL activity in B cells following receptor stimulation.

B cells were cultured in medium alone (◆) or with 10 μg/mL αIg + 30 ng/mL IL-4 (Δ) or 50 μg/mL LPS (O111:B4) (✕) for the indicated time points. Whole cell extracts were then prepared and ACL activity was measured as the amount of [^{14}C]-acetyl-CoA (CPM) produced from incubation of extracts with [^{14}C]-citrate, as described in *Materials and methods*. Values represent the amount of [^{14}C]-acetyl-CoA (CPM) measured in MicroScintO by scintillation counting. For analysis, the measured average CPM was then plotted as a function of B cell culture time, and trendlines calculated by Microsoft Excel™. Error bars reflect standard deviation from the mean of triplicate measurements and the data are representative of 2 independent experiments.

Figure 36.

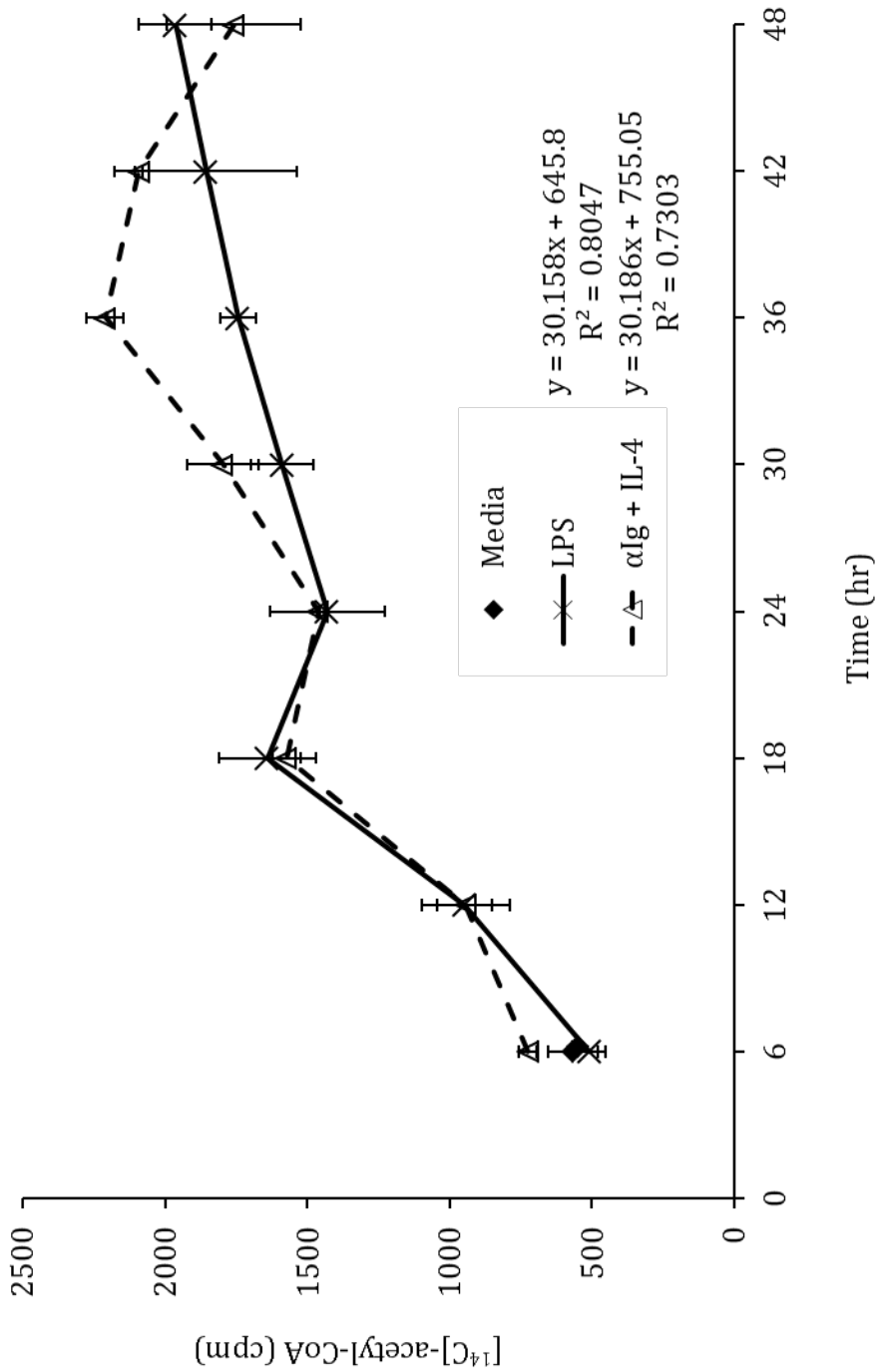
[14C]-acetyl-CoA (cpm)
2500
2000
1500
1000
500
0
0
6
12
18
24
30
36
42
48
Time (hr)
Media
LPS
αIg + IL-4
y = 30.158x + 645.8
R2 = 0.8047
y = 30.186x + 755.05
R2 = 0.7303

Figure 37. ACL activity is reduced in the presence of compound-9.

B cells were cultured in medium alone (Untreated) or with 10 μg/mL αIg + 30 ng/mL IL-4 or 50 μg/mL LPS (O111:B4) in the absence (0 μM) or presence of 25 μM, 35 μM, 50 μM compound-9 (C-9) for 24 hr. Whole cell extracts were then prepared and ACL enzyme activity assessed, as described in *Materials and methods*. The ACL enzyme activity is represented as the average [^{14}C]-acetyl-CoA (cpm) obtained through extraction in MicroScintO and scintillation counting. Values are expressed as cpm from ¼ total enzyme reaction volume and represent assay conducted in triplicate. The data are representative of 2 independent experiments.

Figure 37.

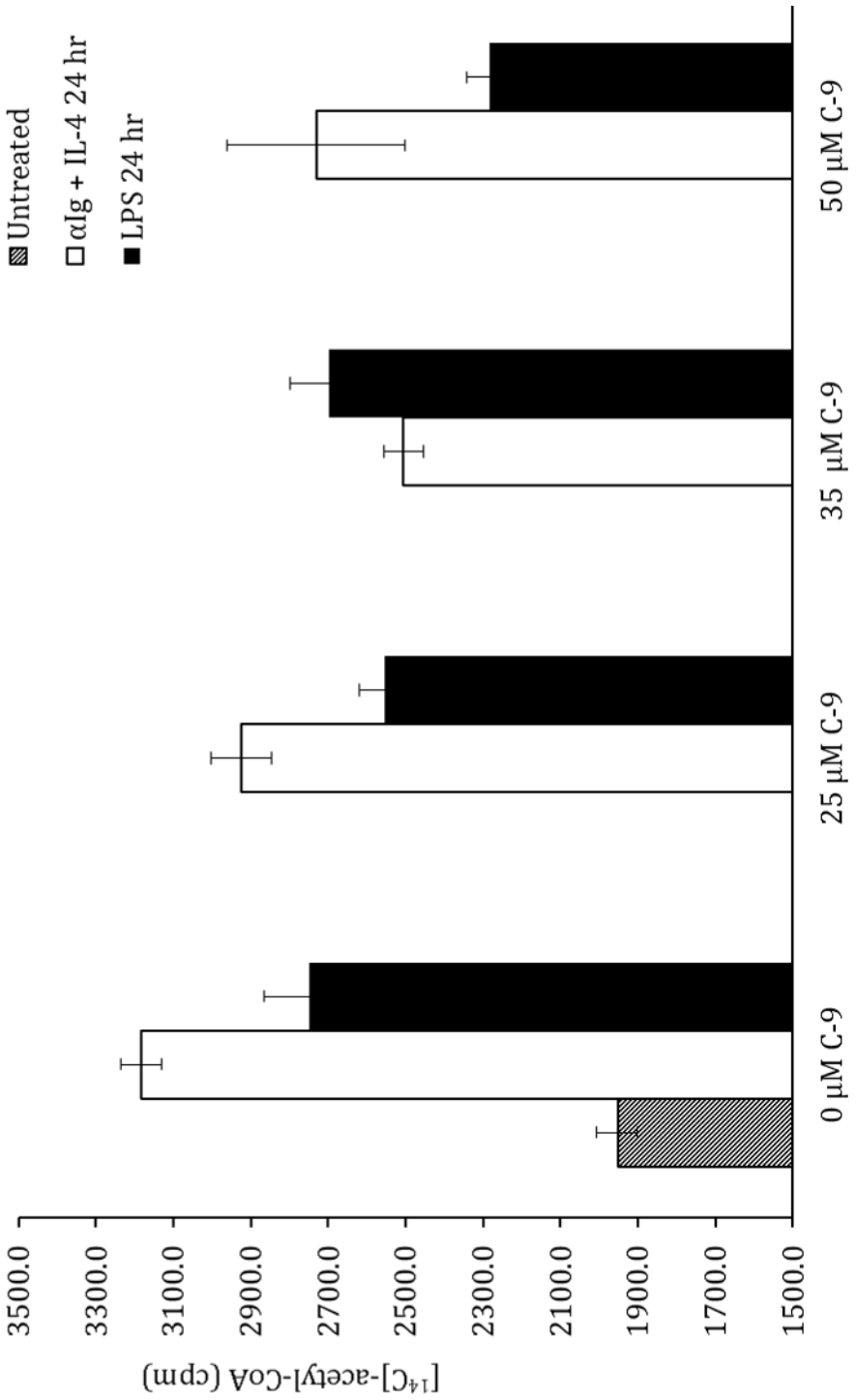
Untreated
αIg + IL-4 24 hr
LPS 24 hr
[14C]-acetyl-CoA (cpm)
3500.0
3300.0
3100.0
2900.0
2700.0
2500.0
2300.0
2100.0
1900.0
1700.0
1500.0
0 μM C-9
25 μM C-9
35 μM C-9
50 μM C-9

Table I. Inhibition of ACL activity does not significantly effect cellular size or volume of stimulated B cells.

B cells were cultured in medium alone (Untreated) or with 10 μg/mL αIg and 30 ng/mL IL-4 (αIg+ IL-4) or 50 μg/mL LPS (O111:B4) for 12 hr, 24 hr, and 48 hr. Compound-9 (C-9) at concentrations of 25 μM, 35 μM, or 50 μM was also co-incubated in B cells stimulated with LPS or αIg + IL-4. At the indicated time points, B cells were diluted 1/100 in PBS and both size (μ) and volume (pL) were measured by the Millipore Scepter™ instrument. The data are representative of 3 independent experiments.

Table I.

Volume (pL)	Initial	12 hr	24 hr	48 hr
Untreated	0.129			
LPS		0.170	0.275	0.386
LPS + 25 μM C-9		0.173	0.248	0.350
LPS + 35 μM C-9		0.183	0.265	0.358
LPS + 50 μM C-9		0.184	0.251	0.398
Size (microns)				
Untreated	6.265			
LPS		6.875	8.072	9.040
LPS + 25 μM C-9		6.917	7.791	8.741
LPS + 35 μM C-9		7.040	7.973	8.815
LPS + 50 μM C-9		7.060	7.824	9.129
Volume (pL)	Initial	12 hr	24 hr	48 hr
Untreated	0.129			
αIg + IL-4		0.174	0.281	0.384
αIg + IL-4, 25 μM C-9		0.178	0.278	0.377
αIg + IL-4, 35 μM C-9		0.178	0.256	0.365
αIg + IL-4, 50 μM C-9		0.168	0.286	0.369
Size (microns)				
Untreated	6.265			
αIg + IL-4		6.924	8.128	9.020
αIg + IL-4, 25 μM C-9		6.896	8.102	8.966
αIg + IL-4, 35 μM C-9		6.979	7.883	8.870
αIg + IL-4, 50 μM C-9		6.847	8.173	8.900

Table II. Stimulated B cell viability decreases with addition of compound-9.

B cells were cultured with LPS (50 μg/mL) or αIg (10 μg/mL) and IL-4 (30 ng/mL) (αIg + IL-4) and treated with indicated concentration of compound-9 (C-9) for 24 hr, 48 hr, and 72 hr. B cells were collected and viability measured as exclusion of propidium iodide by flow cytometry. The percent of cells that excluded PI are represented as viable. The data are representative of 3 independent experiments.

Table II.

Viability (% PI^-)	24 hr	48 hr	72 hr
αIg + IL-4	85.2	84.6	47.0
αIg + IL-4, 20 μM	86.4	82.6	48.4
αIg + IL-4, 35 μM	84.3	77.5	27.2
αIg + IL-4, 50 μM	75.9	60.0	24.2

Viability (% PI^-)	24 hr	48 hr	72 hr
LPS	93.2	87.8	81.6
LPS + 25 μM		75.6	71.0
LPS + 50 μM		31.2	13.5

Table III. Compound-9 treatment reduces B cell progression through the cell cycle.

B cells were cultured with LPS (50 μg/mL) or αIg (10 μg/mL) and IL-4 (30 ng/mL) (αIg + IL-4) and treated with indicated concentration of compound-9 (C-9) for 24 hr, 48 hr, and 72 hr. B cells were collected and sub G_0 DNA content measured via cell cycle analysis and flow cytometry. The percent of cells with sub G_0 DNA content PI are representative of 10,000 cells, completed in triplicate.

For BrdU incorporation, B cells were cultured with LPS (50 μg/mL) or αIg (10 μg/mL) and IL-4 (30 ng/mL) (αIg + IL-4) and treated with indicated concentration of compound-9 (C-9) for 24 hr, 48 hr, and 72 hr. Post 24 hr stimulation, BrdU was added to B cell culture. At 48 hr and 72 hr, B cells were collected and incorporation of BrdU was measured by flow cytometry, as described in *Materials and methods*. The percent of cells with incorporated BrdU are representative of 10,000 cells. The data are representative of 3 independent experiments.

Table III.

	Sub-G_0			% $BrdU^+$	
	24 hr	48 hr	72 hr	48 hr	72 hr
αIg + IL-4	5.4	1.3	4.8	10.3	21.4
αIg + IL-4 20 μM C-9	4.4	1.2	5.3	9.1	17.6
αIg + IL-4 35 μM C-9	6.0	2.5	23.5	2.2	4.1
αIg + IL-4 50 μM C-9	16.5	9.1	32.6	0.6	0.4
LPS	0.2	5.8	9.0	8.2	15.3
LPS + 25 μM C-9	0.2	6.5	6.2	9.1	13.4
LPS + 35 μM C-9	0.3	8.1	5.4	2.1	0.9
LPS + 50 μM C-9	2.7	35.0	28.3	0.9	0.4

Figure 38. Stimulation of B cells with αIg and IL-4 promotes an increase in bulk lipid synthesis.

B cells (10^7 cells) were cultured in the absence (Unstimulated) or presence of 10 μg/mL αIg and 30 ng/mL IL-4 (αIg + IL-4) for 24 hr, 48 hr, and 72 hr. Lipids were isolated and separated by HP-TLC, as described in *Materials and methods*. Lipids of murine brain tissue (Brain) were isolated and served as control for lipid species isolation. Standard lipid species (Standards: 1 μg) were separated on the chromatogram for comparison and identification of migrating lipid species in experimental samples. The data are representative of 2 independent experiments.

(A) Neutral lipids visualized by charring and

(B) Acidic lipids visualized by charring.

(C) Quantification of specific band density was obtained by Lamag Winscan software. Numbers represent fold increase in indicated lipid species' band density in comparison to identical lipid species in unstimulated.

Abbreviations for neutral lipid standards used are: CE (cholesterol esters), TG (triglycerides), C (cholesterol), CM (ceramide), CB (cerebrosides), PE (phosphatidylethanolamine), PC (phosphatidylcholine), SM (sphingomyelin), LPC (lysophosphatidylcholine). Abbreviations for acidic lipid standards used are: FFA (free fatty acids), CL (cardiolipin), PA (phosphatidic acid), S (sulfatides), PS (phosphatidylserine), PI (phosphatidylinositol).

Figure 38.

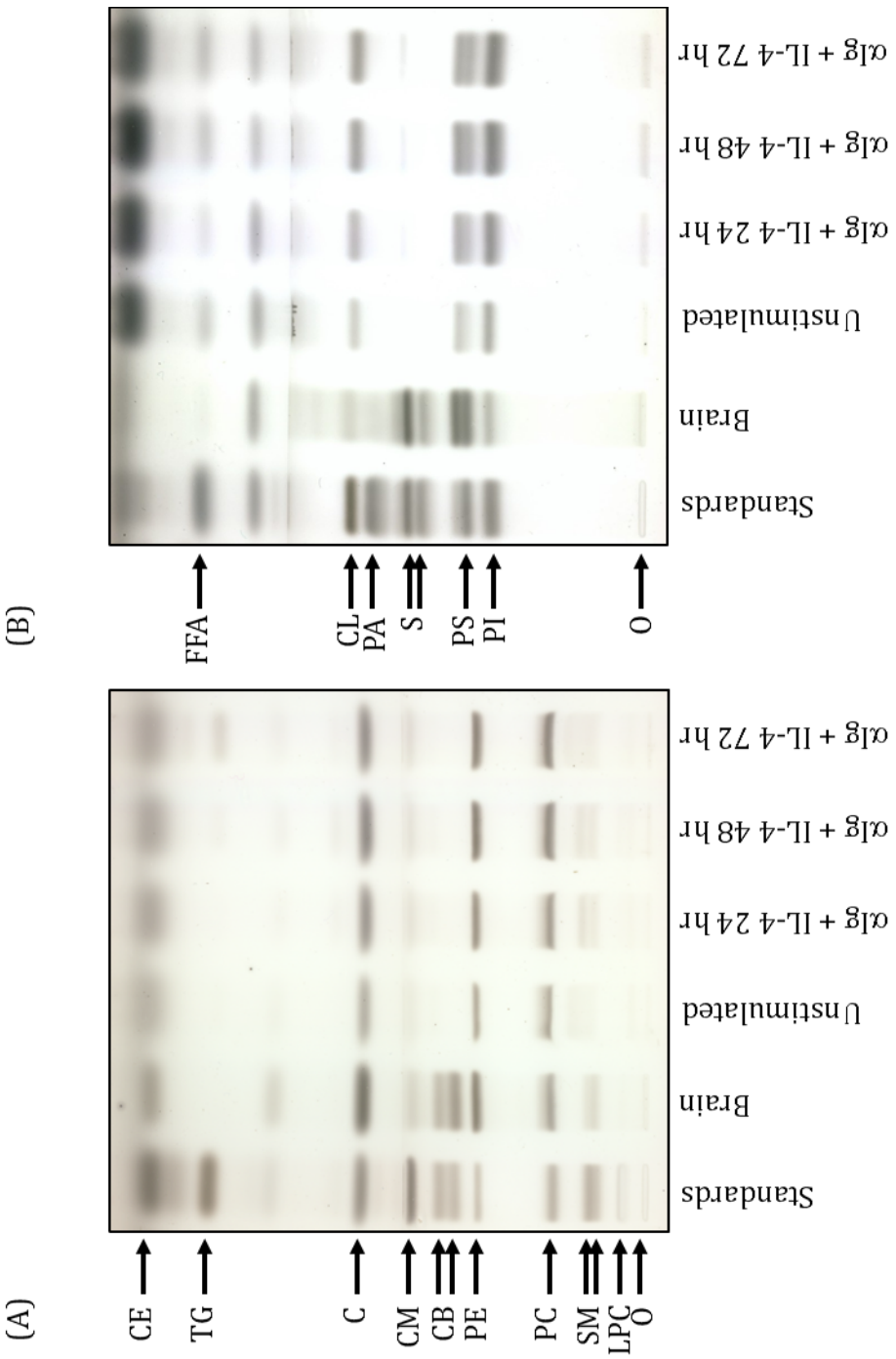
(A)
CE
TG
C
CM
CB
PE
PC
SM
LPC
O
Standards
Brain
Unstimulated
αIg + IL-4 24 hr
αIg + IL-4 48 hr
αIg + IL-4 72 hr
(B)
FFA
CL
PA
S
PS
PI
O
Standards
Brain
Unstimulated
αIg + IL-4 24 hr
αIg + IL-4 48 hr
αIg + IL-4 72 hr

Figure 38.

(C)

	αIg + IL-4 24 hr	αIg + IL-4 48 hr	αIg + IL-4 72 hr
C	0.6	0.9	0.7
CM	1.3	1.0	2.2
PE	0.8	1.4	1.3
PC	0.5	1.0	1.0

	αIg + IL-4 24 hr	αIg + IL-4 48 hr	αIg + IL-4 72 hr
CL	0.7	1.7	2.1
PG	0.0	0.9	1.1
PS	0.9	1.8	1.7
PI	0.9	1.7	1.9

Figure 39. LPS stimulation of B cells induces bulk lipid synthesis.

B cells (10^7 cells) were cultured in medium (Unstimulated) or stimulated with LPS (50 μg/mL) for 24 hr, 48 hr, and 72 hr. In addition, B cells (10^7 cells) were cultured in the presence of αIg (10 μg/mL) and IL-4 (30 ng/mL) for 24 hr. Lipids were then isolated and separated by HP-TLC, as described in *Materials and methods*. Lipids of murine brain tissue (Brain) were isolated and served as control for lipid species isolation. Standard lipid species (Standards: 1 μg) were separated on the chromatogram for comparison and identification of migrating lipid species in experimental samples. The data are representative of 2 independent experiments.

(A) Neutral lipids visualized by charring and

(B) Acidic lipids visualized by charring.

(C) Quantification of specific band density was obtained by Lamag Winscan software. Numbers represent fold increase in indicated lipid species' band density in comparison to identical lipid specie in unstimulated. Abbreviations for neutral lipid standards used are: CE (cholesterol esters), TG (triglycerides), C (cholesterol), CM (ceramide), CB (cerebrosides), PE (phosphatidylethanolamine), PC (phosphatidylcholine), SM (sphingomyelin), LPC (lysophosphatidylcholine). Abbreviations for acidic lipid standards used are: FFA (free fatty acids), CL (cardiolipin), PA (phosphatidic acid), S (sulfatides), PS (phosphatidylserine), PI (phosphatidylinositol).

Figure 39.

(C)

	LPS 24 hr	LPS 48 hr	LPS 72 hr
C	0.0	1.1	2.0
CM	0.9	0.4	2.3
PE	0.0	1.7	3.6
PC	0.0	1.1	2.1

	LPS 24 hr	LPS 48 hr	LPS 72 hr
CL	0.0	0.6	1.3
PG	0.0	0.0	1.0
PS	0.0	0.5	1.0
PI	0.0	0.8	1.4

Figure 40. Identification of neutral B cell lipids by colorimetric detection.

B cells (10^7 cells) were cultured in the presence of αIg (10 μg/mL) and IL-4 (30 ng/mL) for 48 hr. Lipids were isolated and separated by HP-TLC, as described in *Materials and methods*. Lipids of murine brain tissue (Brain) were isolated and served as control for lipid species isolation. Standard lipid species (Standards: 1 μg) were separated on the chromatogram for comparison and identification of migrating lipid species in experimental samples. The data are representative of 1 experiment.

Neutral fraction of 48 hr αIg + IL-4 stimulated B cells were separated by HP-TLC alongside indicated standard lipid species (1 μg) and isolated brain neutral fraction. The chromatogram was split and subsequently charred (A), or sprayed with orcinol-H_2SO_4 (B), ninhydrin (C), or Dittmer's ester (D), as described in *Materials and methods*. Abbreviations for neutral lipid standards used are: CE (cholesterol esters), TG (triglycerides), C (cholesterol), CM (ceramide), CB (cerebrosides), PE (phosphatidylethanolamine), PC (phosphatidylcholine), SM (sphingomyelin), LPC (lysophosphatidylcholine).

Figure 40.

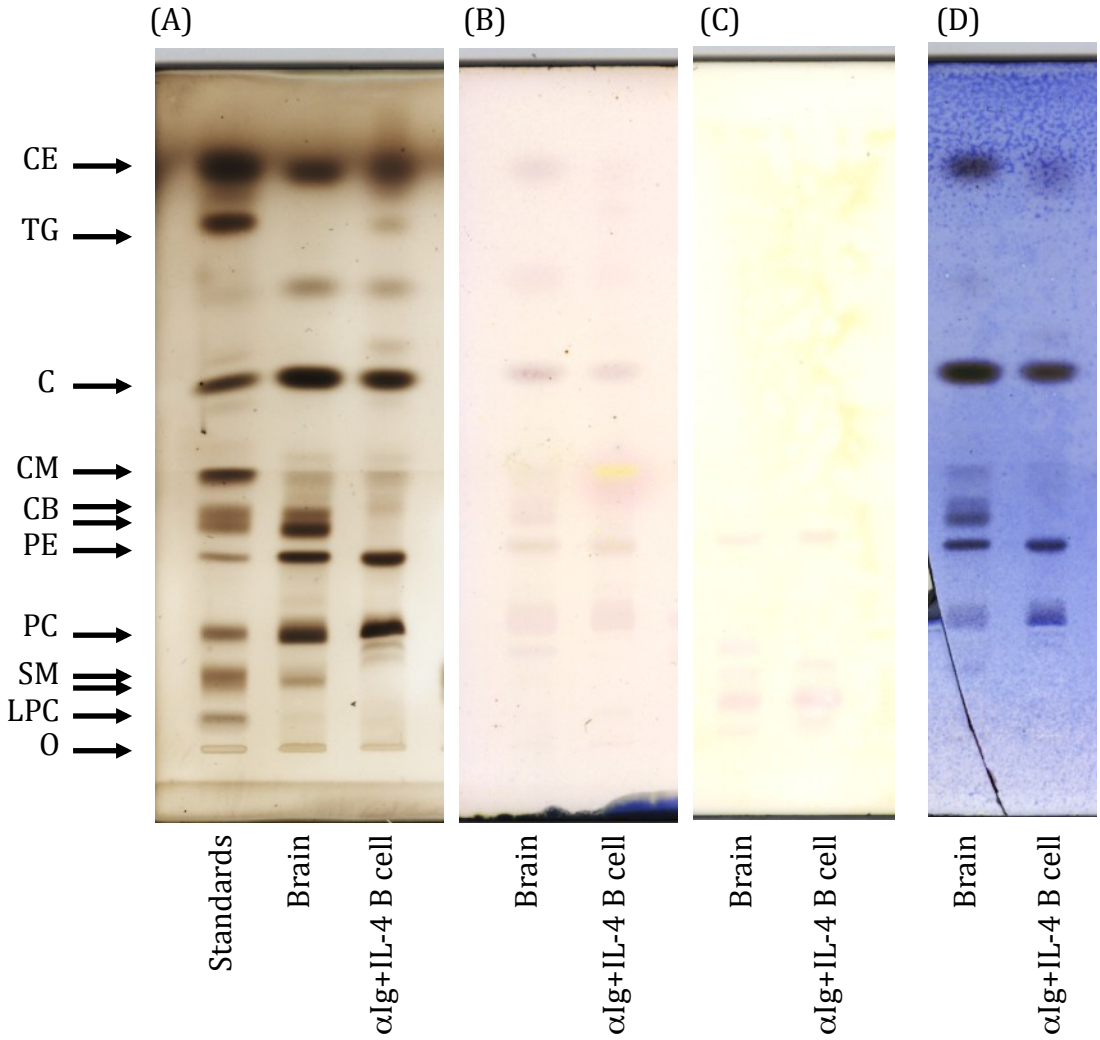
(A)
(B)
(C)
(D)
CE
TG
C
CM
CB
PE
PC
SM
LPC
O
Standards
Brain
αIg+IL-4 B cell
Brain
αIg+IL-4 B cell
Brain
αIg+IL-4 B cell
Brain
αIg+IL-4 B cell

Figure 41. Identification of acidic B cell lipids by colorimetric detection.

B cells (10^7 cells) were cultured in the presence of αIg (10 μg/mL) and IL-4 (30 ng/mL) for 48 hr. Acidic lipids were isolated and separated by HP-TLC, as described in *Materials and methods*. Acidic lipids of murine brain tissue (Brain) were isolated and served as control for lipid species isolation. Standard acidic lipid species (Standards: 1 μg) were separated on the chromatogram as well as phosphatidylglycerol (PG) for comparison and identification of migrating lipid species in experimental samples. The data are representative of 1 experiment.

The chromatogram was split and subsequently charred (A), or sprayed with orcinol-H_2SO_4 (B), ninhydrin (C), or Dittmer's ester (D). Abbreviations for acidic lipid standards used are: FFA (free fatty acids), CL (cardiolipin), PA (phosphatidic acid), PI (phosphatidylglycerol), S (sulfatides), PS (phosphatidylserine), PI (phosphatidylinositol).

Figure 41.

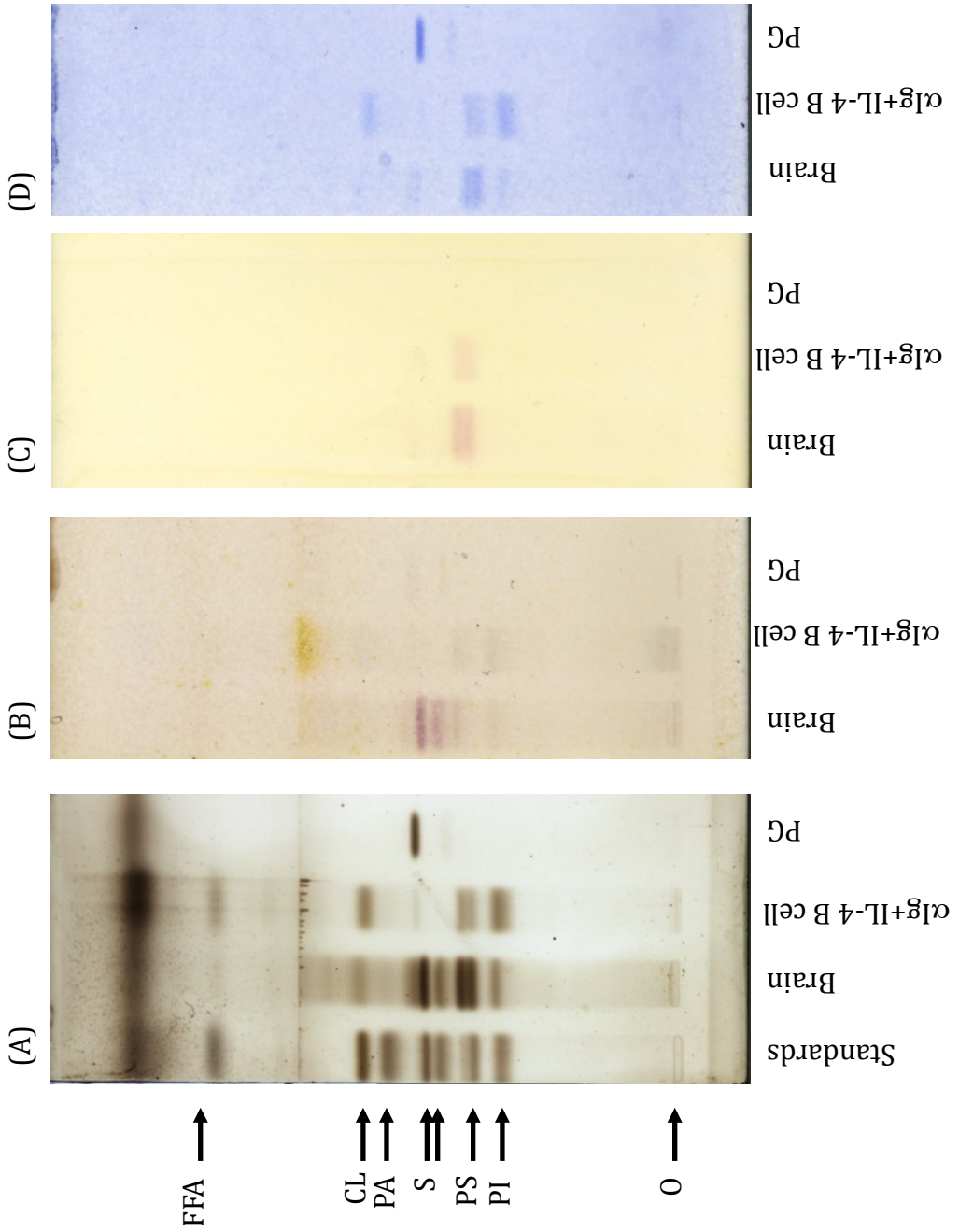
(A)
Standards
Brain
αIg+IL-4 B cell
PG
(B)
Brain
αIg+IL-4 B cell
PG
(C)
Brain
αIg+IL-4 B cell
PG
(D)
Brain
αIg+IL-4 B cell
PG
FFA
CL
PA
S
PS
PI
O

Figure 42. Glucose derived carbon is incorporated into *de novo* lipids in αIg + IL-4 stimulated B cells.

B cells (10^7 cells) were cultured in media supplemented with [^{14}C]-U-glucose (1 μCi/mL) in the absence (Unstimulated) or presence of 10 μg/mL αIg and 30 ng/mL IL-4 (αIg + IL-4) for 24 hr and 48 hr. Lipids were isolated and separated by HP-TLC, as described in *Materials and methods*. Standard lipid species (1 μg) were separated on the chromatogram for comparison and identification of migrating lipid species in experimental samples by charring. The data are representative of 2 independent experiments.

(A) Incorporation of [^{14}C]-U-glucose into neutral lipid species was first measured by autoradiography of the chromatogram (A.ii) and then the lipid species were visualized by charring (A.i), as described in *Materials and methods*. Quantification of specified band density was obtained by Lamag Winscan software; autoradiograms were quantified by ImageQuant software. Numbers charted (A.iii) were obtained by the following calculation, and PE is used for an example:

$$\frac{[^{14}\text{C}]\text{ dpm of PE in stimulated}}{\text{charred density of PE in stimulated}} - \frac{[^{14}\text{C}]\text{ dpm of PE in Unstimulated}}{\text{charred density of PE in Unstimulated}}$$

Abbreviations for neutral lipid standards used are: CE (cholesterol esters), TG (triglycerides), C (cholesterol), CM (ceramide), CB (cerebrosides), PE (phosphatidylethanolamine), PC (phosphatidylcholine), SM (sphingomyelin), LPC (lysophosphatidylcholine).

(B) Incorporation of [^{14}C]-U-glucose into acidic lipid species was first measured by autoradiography of the chromatogram (B.ii) and then the lipid species were

visualized by charring (B.i), as described in *Materials and methods*. Quantification of specified band density was obtained by Lamag Winscan software; autoradiograms were quantified by ImageQuant software. Numbers charted (B.iii) were obtained by the calculation described in (A.iii).

Abbreviations for acidic lipid standards used are: FFA (free fatty acids), CL (cardiolipin), PA (phosphatidic acid), PI (phosphatidylglycerol), S (sulfatides), PS (phosphatidylserine), PI (phosphatidylinositol).

Figure 42A.

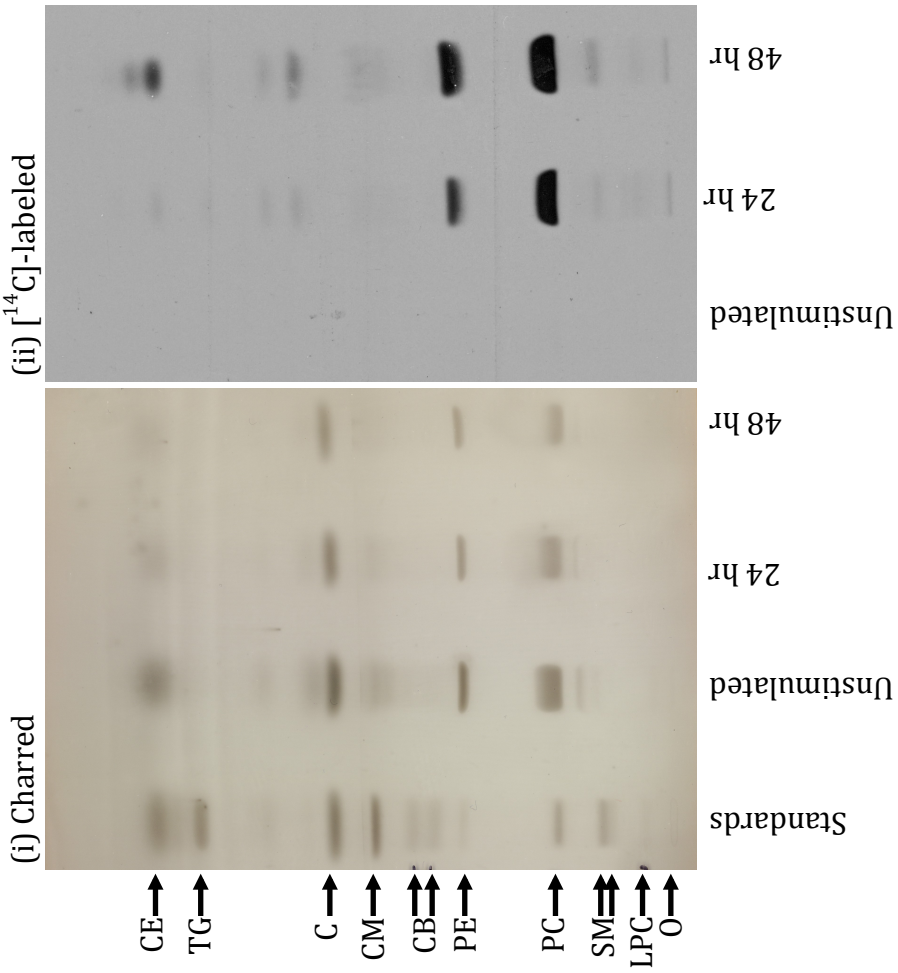

(iii)

	αIg + IL-4 24 hr	αIg + IL-4 48 hr
C	2.43	6.22
CM	16.06	208.67
PE	72.50	357.59
PC	142.98	999.80

Figure 42B.

	αIg + IL-4 24 hr	αIg + IL-4 48 hr
CL	118.85	327.95
PG	343.48	149.32
PS	137.41	367.80
PI	197.96	1456.70

Figure 43. B cells incorporate glucose-derived carbon into *de novo* lipids with LPS stimulation.

B cells (10^7 cells) were cultured in media supplemented with [^{14}C]-U-glucose (1 μCi/mL) in the absence (Unstimulated) or presence of 50 μg/mL LPS (O111:B4) for 24 hr, 48 hr, and 72 hr. Lipids were isolated and separated by HP-TLC, as described in *Materials and methods*. Standard lipid species (1 μg) were separated on the chromatogram for comparison and identification of migrating lipid species in experimental samples by charring. The data are representative of 2 independent experiments.

(A) Incorporation of [^{14}C]-U-glucose into neutral lipid species was first measured by autoradiography of the chromatogram (A.ii) and then the lipid species were visualized by charring (A.i), as described in *Materials and methods*. Quantification of specified band density was obtained by Lamag Winscan software; autoradiograms were quantified by ImageQuant software. Numbers charted (A.iii) were obtained by the following calculation, and PE is used for an example:

$$\frac{[^{14}\text{C}]\text{ dpm of PE in stimulated}}{\text{charred density of PE in stimulated}} - \frac{[^{14}\text{C}]\text{ dpm of PE in Unstimulated}}{\text{charred density of PE in Unstimulated}}$$

Abbreviations for neutral lipid standards used are: CE (cholesterol esters), TG (triglycerides), C (cholesterol), CM (ceramide), CB (cerebrosides), PE (phosphatidylethanolamine), PC (phosphatidylcholine), SM (sphingomyelin), LPC (lysophosphatidylcholine).

(B) Incorporation of [^{14}C]-U-glucose into acidic lipid species was first measured by autoradiography of the chromatogram (B.ii) and then the lipid species were

visualized by charring (B.i), as described in *Materials and methods*. Quantification of specified band density was obtained by Lamag Winscan software; autoradiograms were quantified by ImageQuant software. Numbers charted (B.iii) were obtained by the calculation described in (A.iii). Abbreviations for acidic lipid standards used are: FFA (free fatty acids), CL (cardiolipin), PA (phosphatidic acid), PI (phosphatidylglycerol), S (sulfatides), PS (phosphatidylserine), PI (phosphatidylinositol).

Figure 43A.

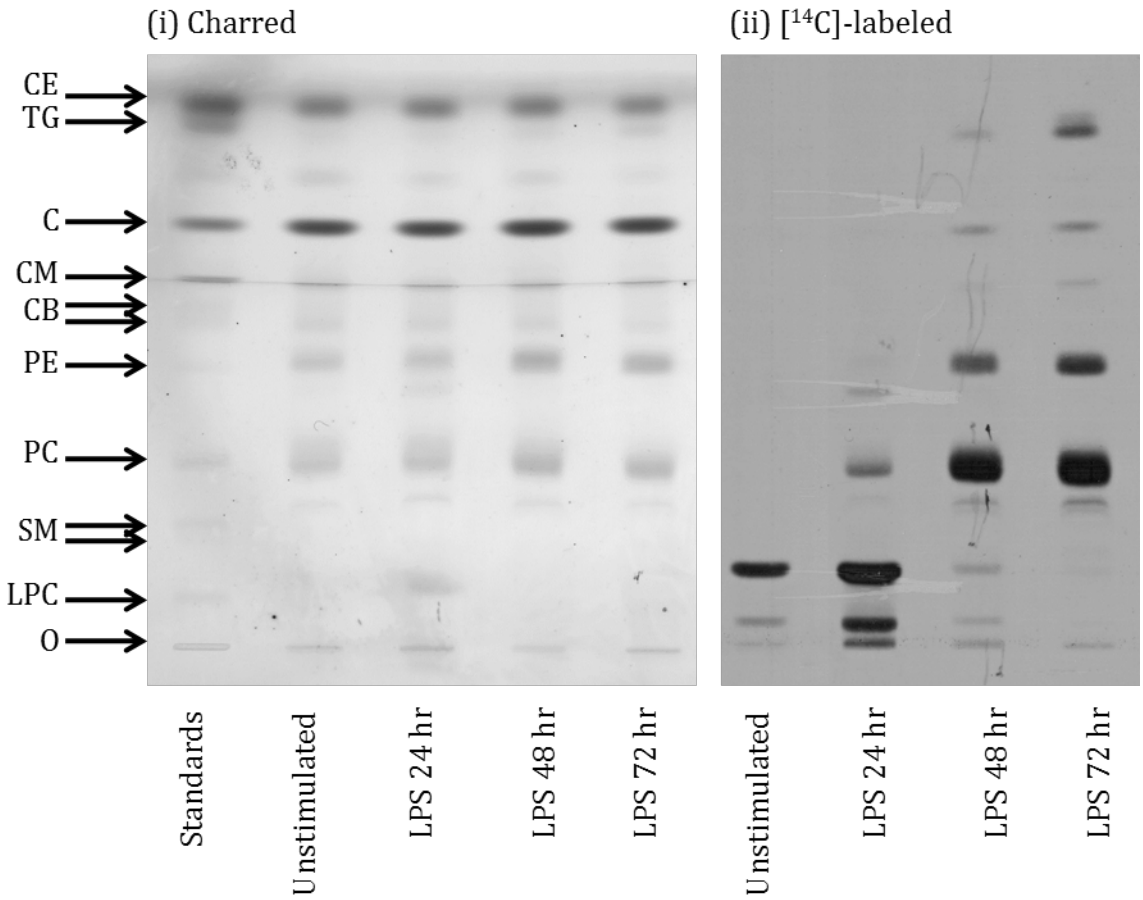

(iii)

	LPS 24 hr	LPS 48 hr	LPS 72 hr
C	3.05	9.84	11.27
CM	6.45	32.30	45.79
PE	17.04	75.39	101.96
PC	73.62	253.31	308.70

Figure 43B.

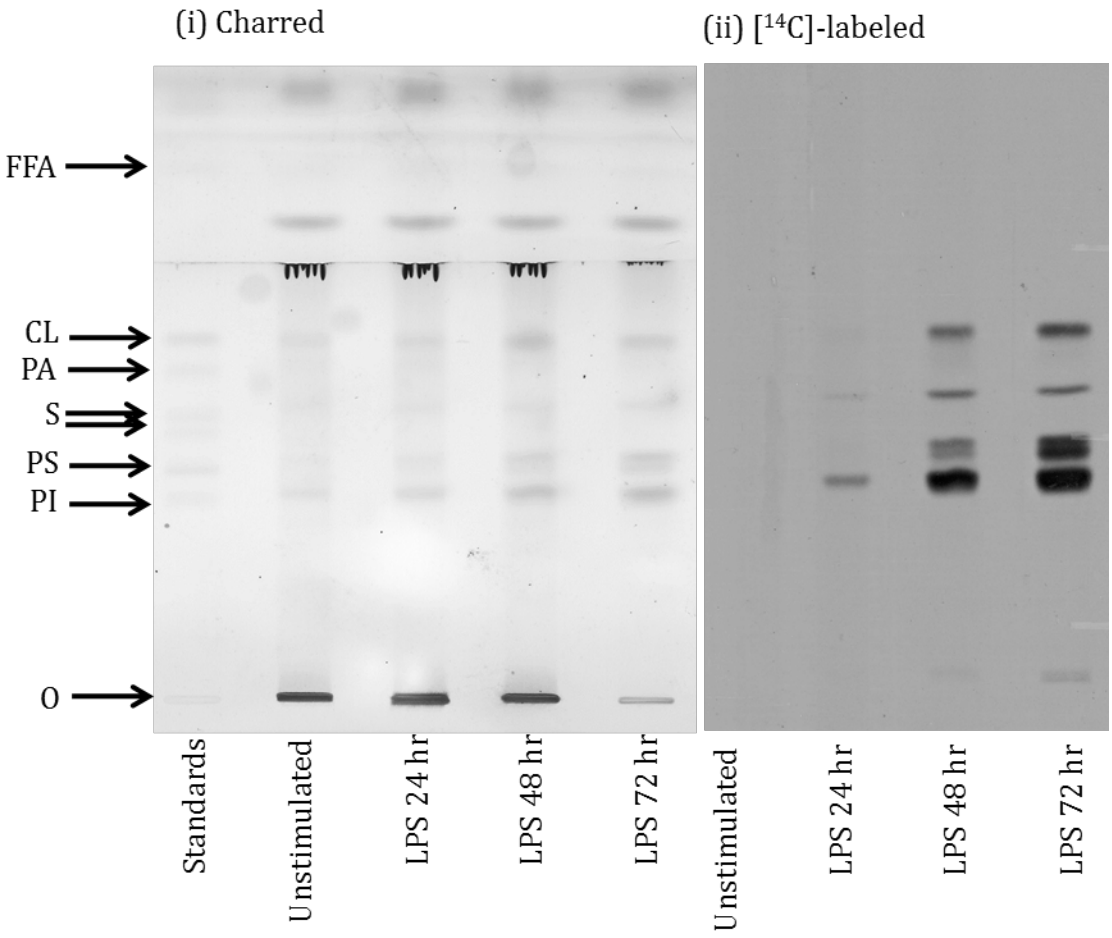

(iii)

	LPS 24 hr	LPS 48 hr	LPS 72 hr
CL	7.06	37.29	72.85
PG	28.70	85.02	66.78
PS	57.74	124.47	136.35
PI	174.16	227.74	189.79

Figure 44. Inhibition of ACL activity reduces incorporation of glucose-derived carbon into *de novo* lipids with LPS stimulation.

B cells were cultured in media alone (Unstimulated) or stimulated with 50 μg/mL LPS (O111:B4) in the absence (LPS) or presence of 25 μM, 35 μM, or 50 μM compound-9 (C-9) for 24 hr, 48 hr, and 72 hr, in media supplemented with [^{14}C]-U-glucose (1 μCi/mL). Lipids were isolated and neutral (A) and acidic (B) lipid fractions of equivalent number of cells (5.0 x 10^7, 7.5 x 10^7, respectively) were separated in each lane of the chromatogram by HP-TLC, as described in *Materials and methods*. Standard lipid species (1 μg) were separated on the chromatogram for comparison and identification of migrating lipid species in experimental samples by charring. The data are representative of 2 independent experiments.

(A) Incorporation of [^{14}C]-U-glucose into neutral lipid species was first visualized by autoradiography of the chromatogram (A.ii) and then the lipid species were visualized by charring (A.i), as described in *Materials and methods*. Quantification of specified band density was obtained by Lamag Winscan software; autoradiograms were quantified by ImageQuant software. Numbers charted (A.iii) were obtained by the following calculation, and PE is used for an example:

$$\frac{[^{14}\text{C}]\text{ dpm of PE in stimulated with C-9}}{\text{charred density of PE in stimulated with C-9}} - \frac{[^{14}\text{C}]\text{ dpm of PE in stimulated}}{\text{charred density of PE in stimulated}}$$

Abbreviations for neutral lipid standards used are: CE (cholesterol esters), TG (triglycerides), C (cholesterol), CM (ceramide), CB (cerebrosides), PE (phosphatidylethanolamine), PC (phosphatidylcholine), SM (sphingomyelin), LPC (lysophosphatidylcholine).

(B) Incorporation of [^{14}C]-U-glucose into acidic lipid species was first measured by autoradiography of the chromatogram (B.ii) and then the lipid species were visualized by charring (B.i), as described in *Materials and methods*. Quantification of specified band density was obtained by Lamag Winscan software; autoradiograms were quantified by ImageQuant software. Numbers charted (B.iii) were obtained by the calculation described in (A.iii).

Abbreviations for acidic lipid standards used are: FFA (free fatty acids), CL (cardiolipin), PA (phosphatidic acid), PI (phosphatidylglycerol), S (sulfatides), PS (phosphatidylserine), PI (phosphatidylinositol).

Figure 44A.

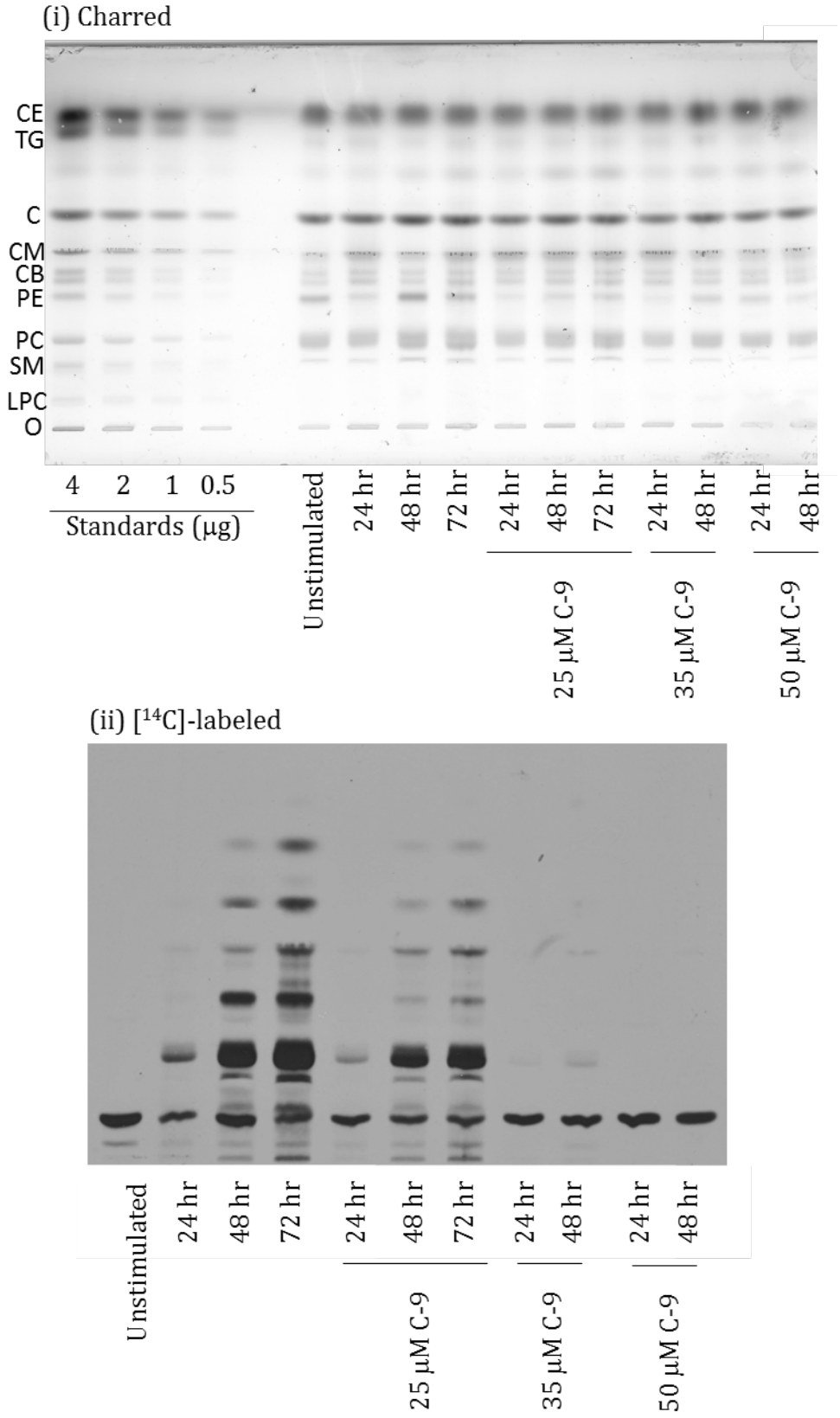
(i) Charred
CE
TG
C
CM
CB
PE
PC
SM
LPC
O
4
2
1
0.5
Standards (μg)
Unstimulated
24 hr
48 hr
72 hr
24 hr
48 hr
72 hr
24 hr
48 hr
24 hr
48 hr
25 μM C-9
35 μM C-9
50 μM C-9
(ii) [14C]-labeled
Unstimulated
24 hr
48 hr
72 hr
24 hr
48 hr
72 hr
24 hr
48 hr
24 hr
48 hr
25 μM C-9
35 μM C-9
50 μM C-9

Figure 44A.

(iii)

	LPS + 25 µM C-9 24 hr	LPS + 25 µM C-9 48 hr	LPS + 25 µM C-9 72 hr	LPS + 35 µM C-9 24 hr	LPS + 35 µM C-9 48 hr	LPS + 50 µM C-9 24 hr	LPS + 50 µM C-9 48 hr
C	13.87	6.53	1.73	21.85	9.15	4.61	-1.05
CM	11.70	5.53	1.97	48.87	65.76	8.85	-0.12
PE	279.38	147.66	30.37	1028.52	461.45	109.28	3.64
PC	9.88	8.13	2.01	27.12	14.29	4.91	1.13

Figure 44B.

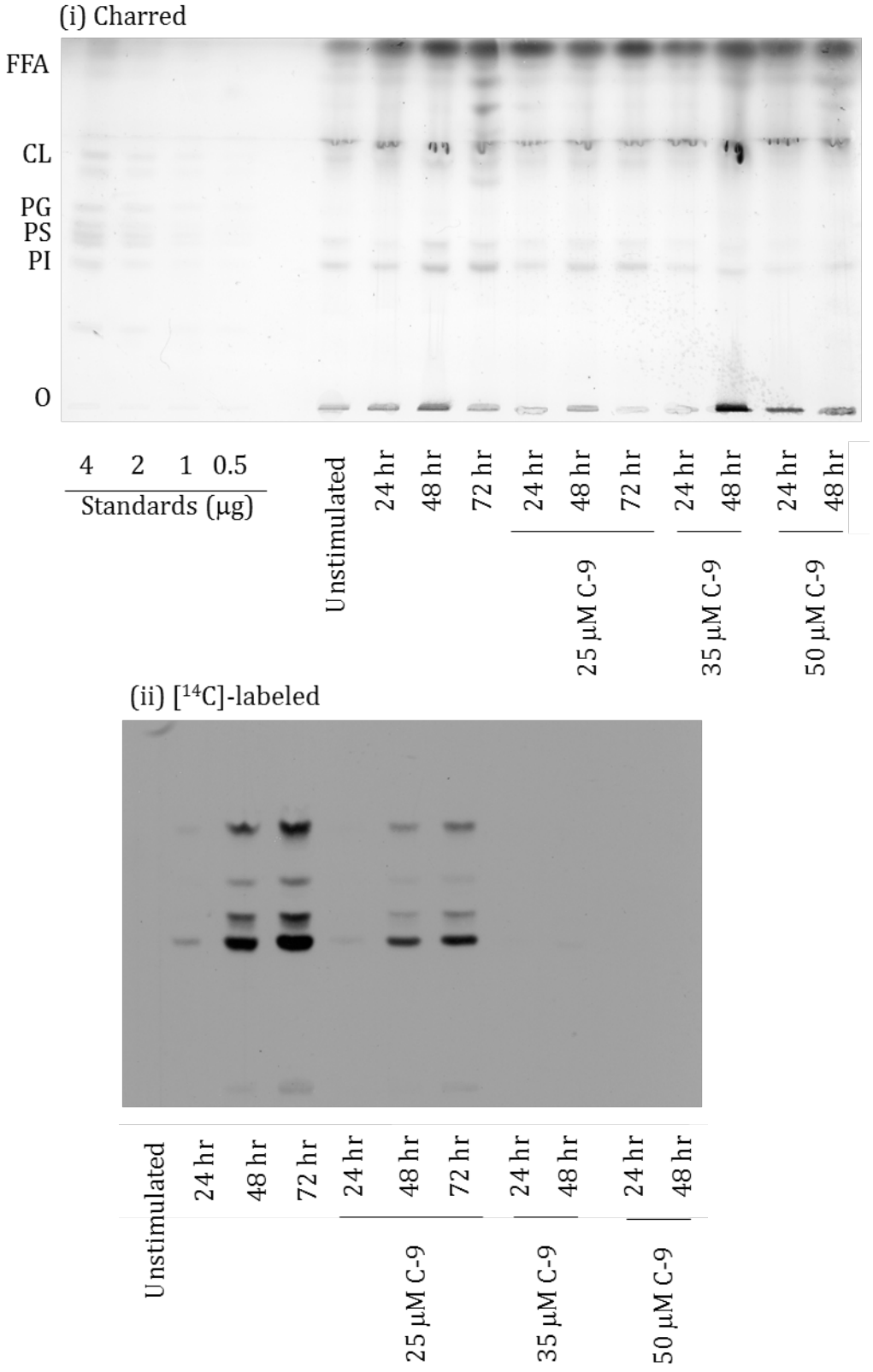
(i) Charred
FFA
CL
PG
PS
PI
O
4 2 1 0.5
Standards (µg)
Unstimulated
24 hr
48 hr
72 hr
24 hr
48 hr
72 hr
24 hr
48 hr
24 hr
48 hr
25 µM C-9
35 µM C-9
50 µM C-9
(ii) [14C]-labeled
Unstimulated
24 hr
48 hr
72 hr
24 hr
48 hr
72 hr
24 hr
48 hr
24 hr
48 hr
25 µM C-9
35 µM C-9
50 µM C-9

Figure 44B.

(iii)

	LPS + 25 µM C-9 24 hr	LPS + 25 µM C-9 48 hr	LPS + 25 µM C-9 72 hr	LPS + 35 µM C-9 24 hr	LPS + 35 µM C-9 48 hr	LPS + 50 µM C-9 24 hr	LPS + 50 µM C-9 48 hr
CL	16.81	4.73	-110.23	-37.11	-158.65	-55.55	-212.84
PG	844.86	261.00	-1855.37	-200.63	-475.38	-262.48	-691.20
PS	43.78	155.41	244.31	173.45	186.24	-30.61	-166.60
PI	61.96	23.29	68.82	91.14	-126.09	-68.23	-269.14

Figure 45. Inhibition of ACL activity reduces incorporation of glucose derived carbon into *de novo* lipids with αIg + IL-4 stimulation.

B cells were cultured in media alone (Unstimulated) or stimulated with 10 μg/mL αIg and 30 ng/mL IL-4 in the absence (αIg + IL-4) or presence of 25 μM, 35 μM, or 50 μM compound-9 (C-9) for 24 hr, 48 hr, and 72 hr, in media supplemented with [^{14}C]-U-glucose (1 μCi/mL). Lipids were then isolated and neutral (A) and acidic (B) lipid fractions of equivalent number of cells (5.0 x 10^7, 7.5 x 10^7, respectively) were separated in each lane of the chromatogram by HP-TLC, as described in *Materials and methods*. Standard lipid species (1 μg) were separated on the chromatogram for comparison and identification of migrating lipid species in experimental samples by charring. The data are representative of 2 independent experiments.

(A) Incorporation of [^{14}C]-U-glucose into neutral lipid species was first visualized by autoradiography of the chromatogram (A.ii) and then the lipid species were visualized by charring (A.i), as described in *Materials and methods*. Quantification of specified band density was obtained by Lamag Winscan software; autoradiograms were quantified by ImageQuant software. Numbers charted (A.iii) were obtained by the following calculation, and PE is used for an example:

$$\frac{[^{14}\text{C}]\text{ dpm of PE in stimulated with C-9}}{\text{charred density of PE in stimulated with C-9}} - \frac{[^{14}\text{C}]\text{ dpm of PE in stimulated}}{\text{charred density of PE in stimulated}}$$

Abbreviations for neutral lipid standards used are: CE (cholesterol esters), TG (triglycerides), C (cholesterol), CM (ceramide), CB (cerebrosides), PE

(phosphatidylethanolamine), PC (phosphatidylcholine), SM (sphingomyelin), LPC (lysophosphatidylcholine).

(B) Incorporation of [^{14}C]-U-glucose into acidic lipid species was first measured by autoradiography of the chromatogram (B.ii) and then the lipid species were visualized by charring (B.i), as described in *Materials and methods*. Quantification of specified band density was obtained by Lamag Winscan software; autoradiograms were quantified by ImageQuant software. Numbers charted (B.iii) were obtained by the calculation described in (A.iii).

Abbreviations for acidic lipid standards used are: FFA (free fatty acids), CL (cardiolipin), PA (phosphatidic acid), PI (phosphatidylglycerol), S (sulfatides), PS (phosphatidylserine), PI (phosphatidylinositol).

Figure 45A.

	αIg + IL-4 + 20 μM C-9 24 hr	αIg + IL-4 + 20 μM C-9 48 hr	αIg + IL-4 + 35 μM C-9 24 hr	αIg + IL-4 + 35 μM C-9 48 hr	αIg + IL-4 + 50 μM C-9 24 hr	αIg + IL-4 + 50 μM C-9 48 hr
C	-3.51	-37.25	-5.91	-80.92	-7.32	-92.54
CM	-9.95	66.88	-0.36	477.59	-23.62	-186.75
PE	-28.66	-387.04	-50.29	-729.43	-90.19	-695.31
PC	37.67	-4.62	70.71	-58.69	36.01	-63.51

Figure 45B.

	αIg + IL-4 + 20 μM C-9 24 hr	αIg + IL-4 + 20 μM C-9 48 hr	αIg + IL-4 + 35 μM C-9 24 hr	αIg + IL-4 + 35 μM C-9 48 hr	αIg + IL-4 + 50 μM C-9 24 hr	αIg + IL-4 + 50 μM C-9 48 hr
CL	10.05	10.69	-1.10	34.14	-2.95	-14.07
PG	-2.19	14.17	-5.67	43.10	-8.57	-3.50
PS	1.89	-20.39	-1.31	-49.64	-4.65	-52.72
PI	-20.16	-45.06	-29.49	-92.10	-33.47	-97.40

Figure 46. Contribution of glucose and glutamine to acetyl-CoA levels in B cells.

B cells were cultured in the presence of 50 % ^{13}C-U-glucose or ^{13}C-U-glutamine for 24 hr or 48 hr in the absence (−) or presence (+) of 50 μg/mL LPS (O111:B4). Cells were collected and labeling of constituent acetyl units analyzed in comparison to metabolite label by GC-MS, as described in *Materials and methods*. The average percent of ^{13}C-label incorporation into total acetyl-CoA was quantified and is represented on y-axis. Error bars reflect standard deviation from the mean of duplicate measurements.

Figure 46.

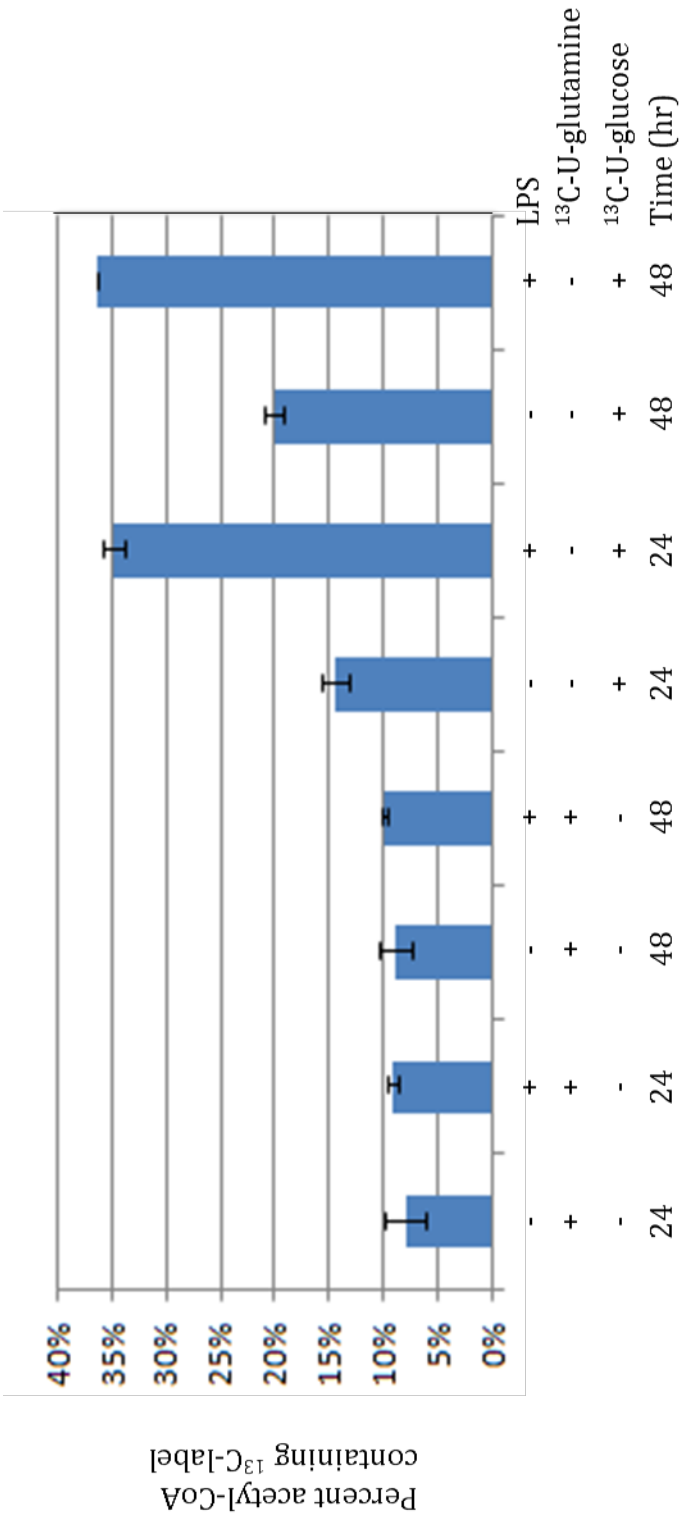
Percent acetyl-CoA containing 13C-label
40%
35%
30%
25%
20%
15%
10%
5%
0%
LPS
13C-U-glutamine
13C-U-glucose
Time (hr)
- + - + - + - + - + - +
+ + - - + + - - + + - -
- - + + - - + + - - + +
24 24 24 24 48 48 48 48 24 24 48 48

Figure 47. LPS stimulation increases glucose carbon incorporation into fatty acid synthesis in B cells.

B cells were cultured in the presence of 50 % ^{13}C-U-glucose or ^{13}C-U-glutamine for 24 hr or 48 hr in the absence (unstimulated) or presence of 50 μg/mL LPS (O111:B4, LPS). Cells were collected and fatty acids extracted. Samples were methylated to produce fatty acid methyl esters and subsequently analyzed by GC-MS, as described in *Materials and methods*.

(A) Relative amounts of fatty acid species were measured based on methyl ester ion signal and are presented normalized to values of 24 hr unstimulated B cells cultured in ^{13}C-glutamine.

(B) *De novo* fatty acid synthesis of C14:0 and C16:0, and elongation of C18:0 was evaluated in ^{13}C-U-glucose and ^{13}C-U-glutamine B cell extracts and the pooled percentage of *de novo* synthesis was calculated. Measurements were based on methyl ester ion signal. Error bars reflect standard deviation from the mean of duplicate measurements.

Figure 47A.

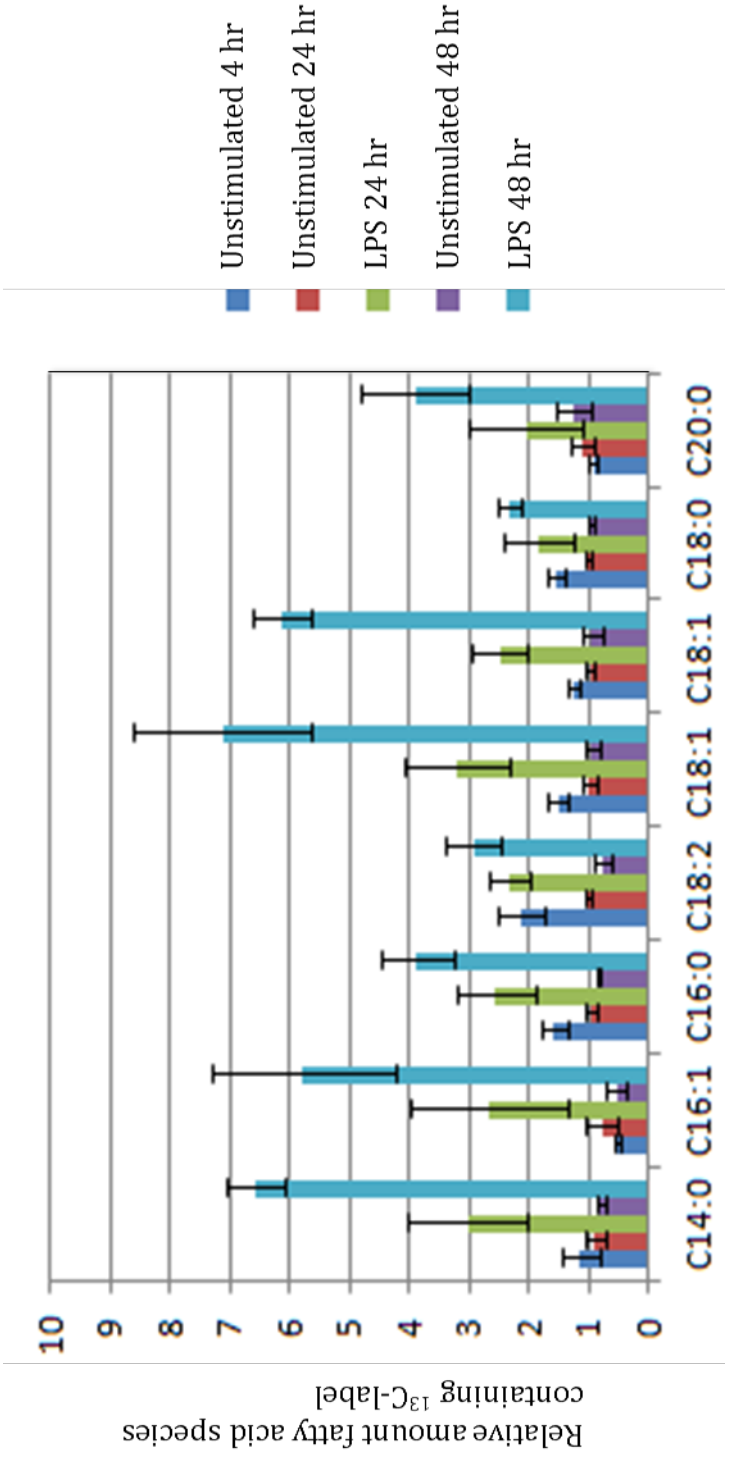
Unstimulated 4 hr
Unstimulated 24 hr
LPS 24 hr
Unstimulated 48 hr
LPS 48 hr
Relative amount fatty acid species containing 13C-label
0
1
2
3
4
5
6
7
8
9
10
C14:0
C16:1
C16:0
C18:2
C18:1
C18:1
C18:0
C20:0

Figure 47B.

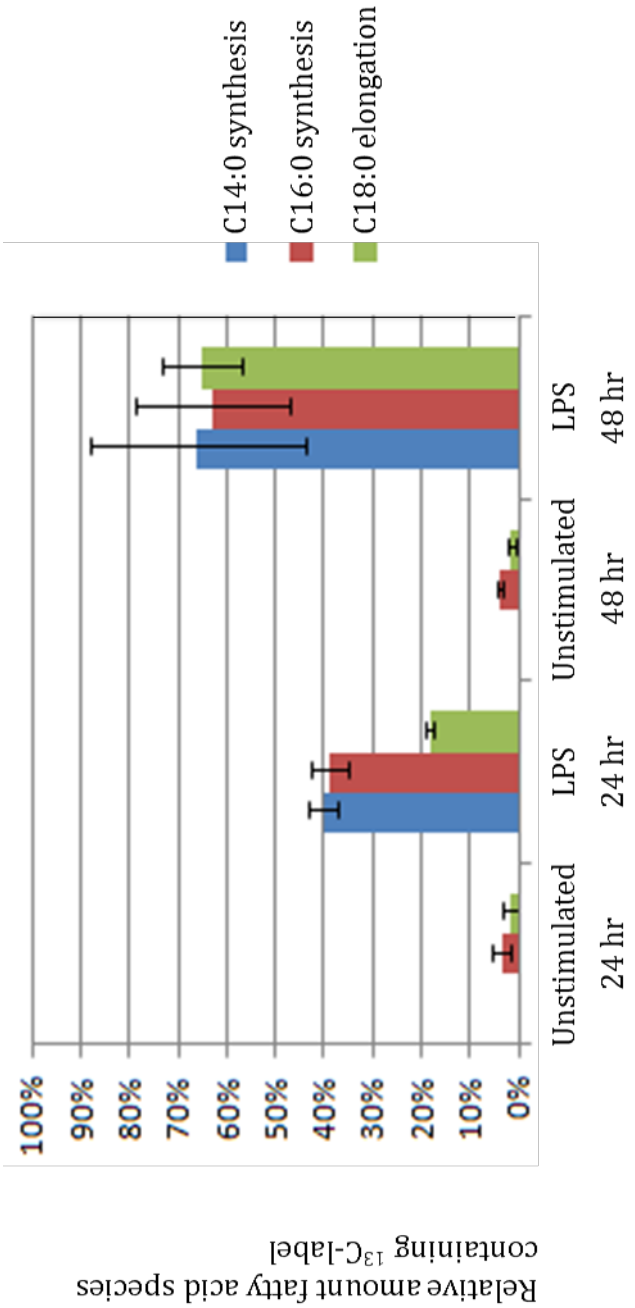
C14:0 synthesis
C16:0 synthesis
C18:0 elongation
100%
90%
80%
70%
60%
50%
40%
30%
20%
10%
0%
Unstimulated
24 hr
LPS
24 hr
Unstimulated
48 hr
LPS
48 hr
Relative amount fatty acid species containing 13C-label

Figure 48. Compound-9 addition reduces B cell lipid synthesis in response to LPS stimulation.

B cells were cultured in the presence of 50 % ^{13}C-U-glucose for 36 hr in the absence (unstimulated) or presence of 50 μg/mL LPS (O111:B4, LPS). Cells were collected and fatty acids extracted. Samples were methylated to produce fatty acid methyl esters and subsequently analyzed by GC-MS, as described in *Materials and methods*.

(A) Percent fatty acid content of C14:0, C16:1, C18:2, C18:1, and C20:0 was calculated based peak total ion counts by GC-MS.

(B) B cells were cultured in the presence of 50 % ^{13}C-U-glucose and LPS (50 μg/mL) for 6 hr pre-treatment of 35 μM compound-9 (C-9) for 30 hr. Cells were pelleted and fatty acids extracted with C17:0 fatty acid as an internal standard. Samples were methylated to produce fatty acid methyl esters and subsequently analyzed by GC-MS. Percent of elongated free fatty acids (C16:0, C18:0) synthesized was quantified by GC-MS.

Error bars reflect standard deviation from the mean of duplicate measurements.

Figure 48A.

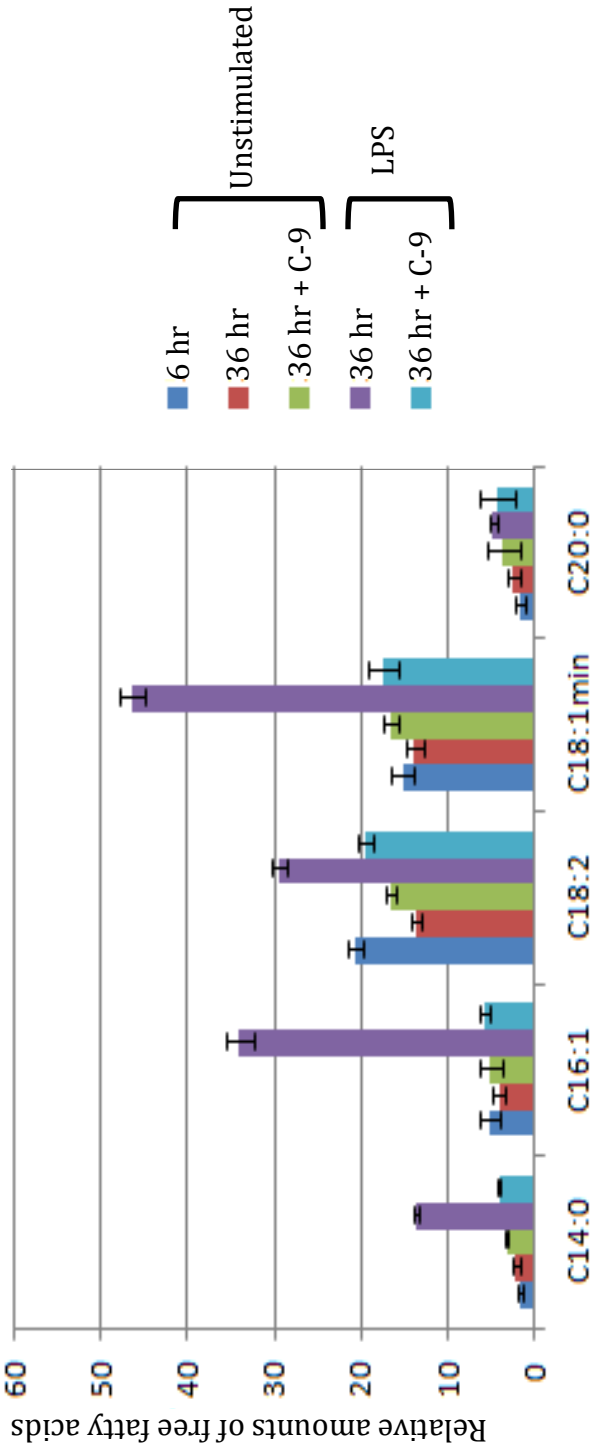
Unstimulated
LPS
6 hr
36 hr
36 hr + C-9
36 hr
36 hr + C-9
Relative amounts of free fatty acids
0
10
20
30
40
50
60
C14:0
C16:1
C18:2
C18:1min
C20:0

Figure 48B.

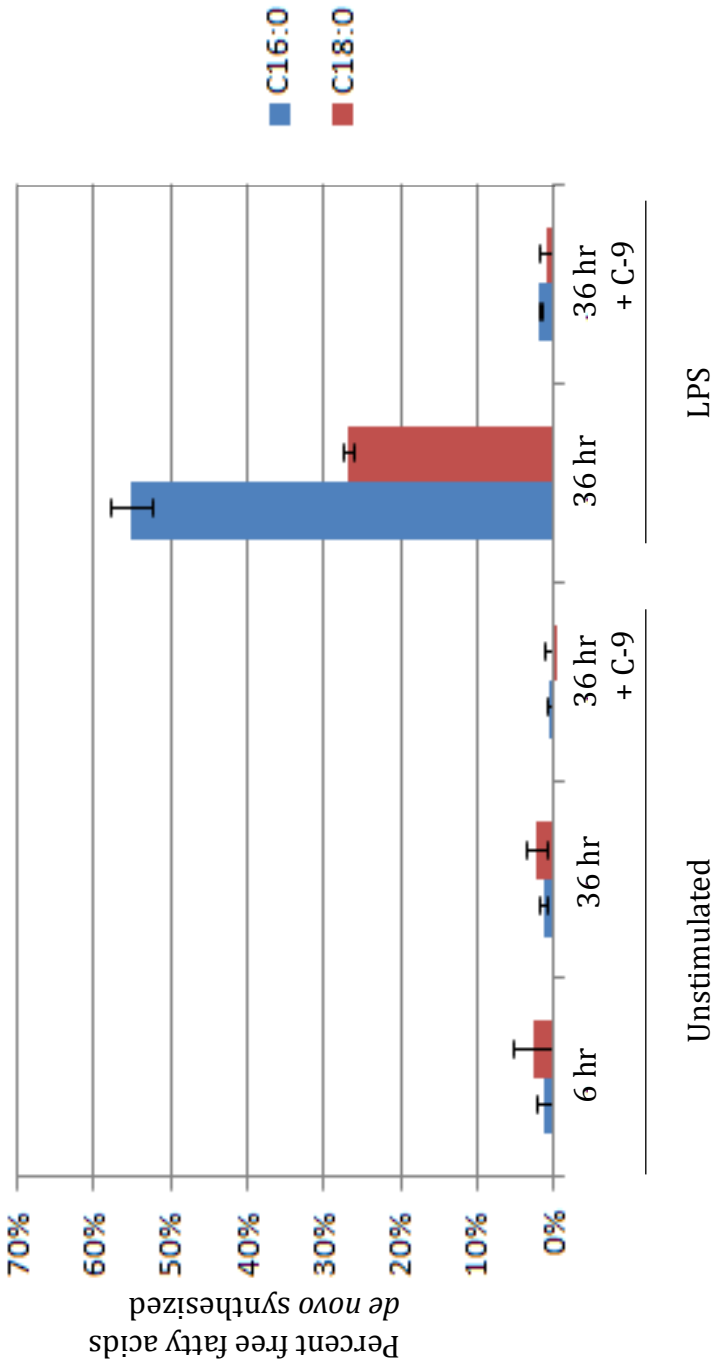
C16:0
C18:0
Percent free fatty acids
de novo synthesized
70%
60%
50%
40%
30%
20%
10%
0%
6 hr
36 hr
36 hr
+ C-9
36 hr
36 hr
+ C-9
Unstimulated
LPS

Discussion

Section 1

The regulation of cellular growth is an unresolved question in B cell biology. It is becoming clear that growth and survival rely on glucose metabolism, as glucose transport and utilization are necessary to provide for and support cellular growth. Long established in lymphocytes (*in vitro* and *in vivo*), upon encounter with antigen, cells increase in proliferation and change their metabolism by increasing glucose and glutamine utilization as well as the enzymes involved in their metabolism (92, 241, 353, 370). The induced alteration of cellular respiration and oxidative phosphorylation is termed the Crabtree effect. It has been commonly observed in tumor cells and has been attributed to normal lymphocytes which undergo rapid proliferation in response to antigen (313, 354-356). Immune reactions are important consumers of energy, especially in the form of ATP. Both the housekeeping functions (maintenance of ionic integrity, volume regulation, cell growth) and the specialized activities of immune cells (for example, cytokinesis, phagocytosis, signaling, antigen processing, effector functions) depend on their energy supply (115, 357). As reviewed by Hammerman *et al*., glucose metabolism may provide multiple purposes in cells, including generation of ATP and NADH for post-translational modification in the regulation of protein localization, trafficking, and enzyme activity, as well as providing intermediates for the *de novo* synthesis of macromolecules: amino acids, nucleotides, and lipids (38). Lymphocytes increase glycolytic flux and expression of glucose transporter-1 and glycolytic enzymes such as hexokinase, phosphofructose kinase, and ATP citrate lyase upon encounter with

antigen, initiating aerobic glycolysis (121, 150, 241,307, 309, 358). I evaluated the contribution of signal mediating events in the activation and growth responses of *ex vivo* B cells to various stimuli and defined those pathways involved in the propagation of regulatory signals at the level of glucose energy metabolism through the use of chemical inhibition and knockout murine models.

Upon engagement of the BCR, multiple receptor-associated kinases (RTK) are activated, which initiate multiple signal transduction pathways for an activation response in B cells (Figure 1) (15, 48). A central mediator of activation is the receptor kinase BTK. BTK transduces signals emanating from an engaged receptor (via SYK activation) to activate the PI3K and PLC pathways, two pathways evaluated for their contribution to growth, survival, and proliferation of B cells (5, 12, 47).

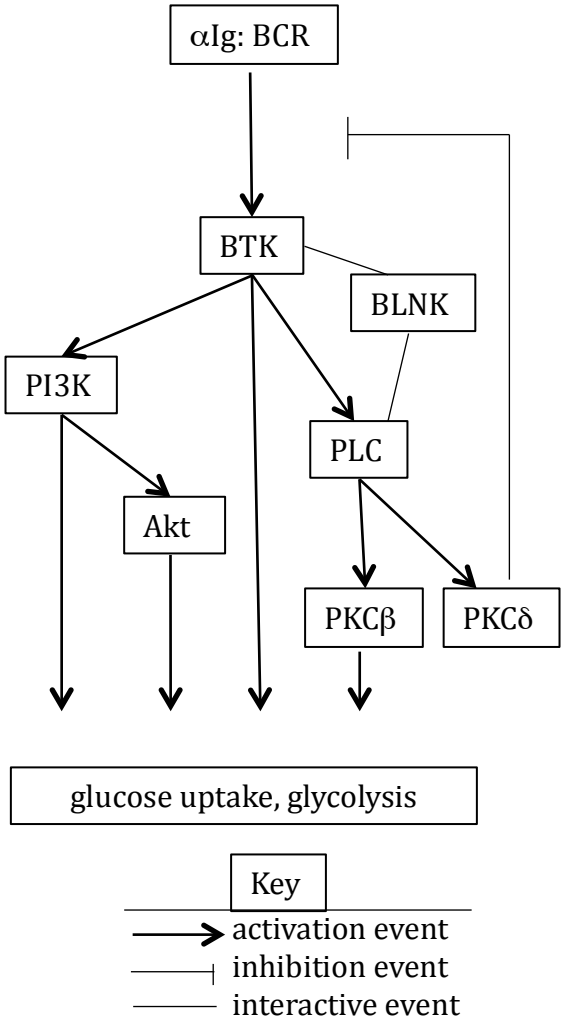

Figure 1: A simplified view of the examined pathways activated by BCR cross-linking, shown to contribute to the regulation of glucose uptake and glycolysis.

B cells deficient of active BTK (XID or $BTK^{-/-}$) demonstrate severe reductions in the activation response from BCR engagement (23, 30, 48). In confirmation with these published reports, this investigation demonstrated XID and $BTK^{-/-}$ B cells were unable to induce glycolysis at an increased rate upon αIg stimulation and contained limited concentrations of ATP and lactate, in comparison to normal murine B cells. In addition, XID B cells did not induce glycolytic gene or *glut-1* expression in response to αIg. The response of XID B cells to lipopolysaccharide (LPS) or cluster of differentiation 40 ligand (CD40L) was equivalent to wild-type B cells; LPS or CD40L stimulation increased glycolytic rate, ATP concentration, lactate production, as well as glycolytic enzyme and *glut-1* expression. Engaged to their cognate receptors (TNF-R and CD40, respectively), LPS and CD40L activate a glucose-mediated response independent of BTK activity. Therefore, active BTK is a necessary component for the glucose-mediated activation elicited by BCR, not TLR4 or CD40 receptor engagement.

Encounter with antigen activates the PI3K pathway leading to increased glycolytic flux (60, 114-117). Without functional PI3K, *e.g.* deletion of the p85α subunit in the murine model, animals contain low splenic B cell numbers, shorter life span, and smaller body mass (61, 62, 271). In this investigation, $p85\alpha^{-/-}$ B cells did not up-regulate glycolysis in response to αIg, which thereby limited the synthesis of cellular components required for growth and division. The inhibition of PI3K by p85α-deficiency or by chemical inhibition in wild-type B cells impaired glut-1 expression, as well as glucose transport and utilization, despite stimulation

with αIg. In addition, cellular size and viability were reduced. Therefore BCR engagement regulates glucose utilization in B cells through the activation of PI3K and BTK to elicit an activation response.

As previously described in the *Introduction*, the activation of B cells involves signal transduction events that promote PI3K and PLC (47). PI3K targets Akt for enhanced glycolysis in B cells. Active Akt has been shown to increase protein synthesis to support cellular growth by targeting eIF4e, eIF4e binding protein, S6 ribosomal protein, TSC2, and Foxo1 (359-363). Following BCR ligation, Akt also activates the transcription factors *c-myc* and NF-κB for survival and growth of B cells (56, 364-366). NF-κB induces expression of survival proteins, Bfl-1 and IAP1/2 to contribute to the anti-apoptotic effect of Akt activation (63,367-369), whereas *c-myc* putatively regulates glycolytic gene expression and mitochondrial biogenesis (114, 346, 369, 371). Regulated by *c-myc* and NF-κB, the transcription of cell cycle proteins (cyclin D, cdk, p27, bcl-2), nutrient transporters (glut-1, mcl-1) as well as glycolytic enzymes (phosphoglucose isomerase, phosphofructokinase, glyceraldehyde-3-phosphate dehydrogenase, phosphoglycerate kinase, enolase, ldh) are induced and their induction is necessary for growth and survival (112, 372-376). Of note, it is interesting that in many cancerous cells, the Akt pathway and its targets are active; and, whether by cause or effect, there is disregulated gene expression, increased cellular growth and proliferation, as well as mitochondrial suppression in tumor cells (118, 276, 356, 358).

Alternative to BCR engagement, the cytokine IL-4 stimulates B cells to promote

growth and survival (99, 169, 172, 290). In a recent published report from the Chiles' laboratory, B cells increased glucose uptake and glut-1 expression in response to IL-4 (377). Chemical inhibition of glycolysis through IAN or DG treatment limits the availability of glucose and its metabolites. The addition of these inhibitors to IL-4 stimulated B cells led to a minor reduction in size (FSC-A) and significant loss of viability. Similar to αIg stimulation, IL-4 not only promoted the glucose-mediated activation response, but without the supply of glucose and its metabolites, B cells are unable to support growth and undergo cellular death.

Upon IL-4 stimulation, the JAK-STAT pathway is activated in B cells (167). This investigation has shown STAT-6 in the IL-4 response to be required in glucose utilization. STAT-6-deficient B cells stimulated with IL-4 were unable to induce glycolytic flux. Through peptide reconstitution, B cells deficient of STAT-6 propagated the IL-4 activation signal, increasing glucose utilization. Alternative proteins involved in the IL-4 signal transduction pathway (IRS-2 and p85α) were also evaluated and determined to be dispensable for IL-4-induced glycolysis (170, 172, 377). Thus, a putative role for STAT-6 in modulating glycolytic metabolism by IL-4 is suggested through direct influence in enhancing glycolysis. In addition, STAT-6 may regulate glycolysis by inducing glycolytic enzyme expression as it is a transcription factor and putative STAT6-binding site have been located in the glycolytic enzyme phosphofructose kinase-2 promoter (300). Alternatively, members of the Pim family of serine/threonine kinases, which are downstream targets of IL-4-mediated STAT-6 signaling, may regulate glucose energy metabolism

via the phosphorylation of rate-limiting glycolytic enzymes (177, 300).

In a similar manner to αIg, LPS or CD40L engage their cognate receptors to promote B cell growth and survival; however unlike αIg, these stimuli are capable of promoting B cell maturation (87, 103, 106). Physiologically important, LPS is a bacterial membrane component that promotes differentiation of B cells to plasma cell stage (193). Also a stimulus for B cell differentiation, CD40L interacts with CD40 to induce B cells to mature and produce antibodies of different classes of immunoglobulin (103, 104). In brief, B cells responding to LPS or CD40L enhanced glucose utilization and expression of glut-1, similar to αIg stimulation, but independent of BTK activity and p85α. Therefore B cells trigger signal transduction pathways specific to the stimulating antigen to achieve similar growth and survival responses.

Another major signaling pathway activated in B cells responding to extracellular stimuli is PLC. Upon BCR cross-linking, the receptor tyrosine kinase, SYK, phosphorylates the adaptor protein BLNK (also known as SLP65) which recruits BTK and PLC, permitting the active BTK to phosphorylate and activate PLC (32, 49). This investigation demonstrated that αIg stimulation of BLNK-deficient B cells does induce glycolysis, similar to LPS or CD40L stimulation. In a manner independent of BLNK, enhanced glycolytic rates resembled wild-type B cells. These results are in conflict with previous published reports wherein BLNK deficiency perturbed survival and proliferation pathways activated by BCR engagement, *i.e.* $BLNK^{-/-}$ B cells have been shown to respond to stimuli in manner resembling XID or

BTK$^{-/-}$ B cells (33). This investigation demonstrated the initiation of the activation response (5 hr) elicited by αIg was not affected by the absence of BLNK. My results suggest that BLNK does not directly contribute to BCR-mediated increases in glucose metabolism. Further examination of the glucose-mediated activation response in BLNK$^{-/-}$ B cells (beyond 5hr) is needed.

Active PLC generates IP3 and DAG, two mediators that transduce an activation signal by promoting Ca^{2+} signaling and activation of PKCs (35, 47). The expression profile of PKCs in B cells includes conventional, novel, and atypical PKCs (43). PKCδ is a novel PKC activated through PLC activity that does not enhance the B cell activation response. Rather, PKCδ attenuates the signal through negative feedback of proximal BCR phosphorylation (36, 378). Published reports suggest the role of PKCδ is to inhibit the growth and proliferation of B cells to maintain tolerance in the immune response (151). In murine models, deficiency of PKCδ resulted in a large self-reactive B cell population; while, overexpression of PKCδ led to inhibited B cell growth, promoting auto-immunity and murine glomerulonephritis (45, 46). I demonstrated herein that stimulated with αIg, PKCδ$^{-/-}$ B cells enhanced glycolysis above levels observed in wild-type B cells. Also, the chemical inhibition of PKCδ by rottlerin was shown to enhance glycolysis in resting and αIg stimulated B cells. Together these results corroborate with published reports suggesting that PKCδ down-regulates the BCR-mediated activation response (43, 45, 46, 286, 287). Further studies are being conducted in the Chiles' laboratory to identify the contribution of the conventional isoform of PKC, PKCβ, in the αIg-

mediated activation response of B cells. In contrast to PKCδ, PKCβ is a target of PLC-generated DAG that promotes the signal pathways for activation; PKCβI/II-deficient mice demonstrate a XID-like phenotype (44, 50, 51). In preliminary results, PKCβ$^{-/-}$ B cells when stimulated with αIg are unable to increase glycolysis or glut-1 expression (manuscript submitted, 2012). In light of our ongoing investigation to assess PKC isoform specificity and significance, the activity of the PLC pathway to PKCβ, not PKCδ, in B cells contributes to the glucose-mediated activation response.

The proposed model of BCR regulated glycolysis based on my results and information gathered from literature integrates signal transduction pathways to modulate glycolysis to support B cell proliferation and differentiation (114, 300, 357). The engaged BCR recruits and activates PI3K as well as components of the PLC pathway to signal for the increased utilization of glucose in growth and survival of the B cell. In summary, I conclude that B cells are capable of multifaceted control of signal transduction pathways for modulation of glucose metabolism in the activation response to various extracellular stimuli.

Section 2

In normal immune cells, the response elicited by extracellular stimuli activates signal pathways for cellular growth, survival, and proliferation in a highly regulated fashion through signal transduction events. It is through the entry of the cell cycle from quiescence that B cells alter their metabolism to anaerobic glycolysis, permitting necessary cellular components to multiply for the development of daughter cells, including an increase in mitochondrial numbers (335, 336). Similar to tumor cells, in agreement with the Crabtree effect, activated B cells promote glycolysis through PI3K-Akt pathway which may decrease the cellular dependence upon the mitochondria, truncating the TCA cycle, to permit the promotion of *de novo* lipogenesis (313, 379). A large percentage of membrane-associated fatty acids of proliferating cells have been demonstrate to be synthesized *de novo* rather than from fatty acid degradation (380, 381). Akt has been shown to promote *de novo* lipid synthesis via myc-induced expression of glycerol-3-phosphate dehydrogenase and phosphatidylethanolamine-binding protein (382), the suppression of carnintine palmitoyl-transferase expression (an enzyme involved in lipid oxidation) (79), and the activation of transcription factor sterol-responsive enzyme binding peptide (SREBP) for the up-regulation of cellular fatty acid and cholesterol synthesis. Membrane expansion and mitochondrial biogenesis requires the SREBP-induced expression of fatty acid synthase (FAS), and cholesterol-synthesizing enzymes HMG-CoA synthase and HMG-CoA reductase (154, 383). Akt also directly activates second messenger and lipid synthesis by phosphorylation of ATP citrate lyase (ACL) for the production of acetyl-CoA (150, 384, 385). Additionally, it has been demonstrated in

normal and B cell lymphoma cells that proliferation and membrane expansion is regulated through activation of the PI3K-Akt signal pathway, which thereby promotes cell cycle entry and growth by induction of lipid synthesis and accumulation (205, 337, 386). The contribution of ACL activity for growth and survival of B cells in response to activation stimuli was addressed.

Glucose is an important nutrient that may be used as a source of energy and for components of cellular structure (121, 128, 313, 324). B cells in the process of differentiation to the plasma cell stage undergo a period of growth (*i.e.* cell mass accompanied with size and *de novo* macromolecular synthesis) and proliferation to expand intracellular membrane networks and undergo organelle biosynthesis for Ig synthesis and assembly (195, 196, 203, 218, 357). To support the synthesis of lipids and membranes, I hypothesized that B cells enhance nutrient metabolism, particularly the acquisition and utilization of glucose (shown in in Section 1 as increased glucose transport, glycolysis, and ATP concentration) through intracellular signaling to meet the metabolic requirements for generation of antibody-secreting plasma cells.

The cytoplasmic enzyme ATP-citrate lyase (ACL) is responsible for converting oxaloacetate and citrate to acetyl-CoA (127). In a committed step of the fatty-acid synthesis pathway, acetyl-CoA carboxylase (ACC) irreversibly carboxylates acetyl-CoA to generate malonyl-CoA (123, 124). Malonyl-CoA and acetyl-CoA combine to form long chain fatty acids, primarily palmitate (C16) or stearate (C18), by fatty acid synthase (FAS) that may be utilized in cholesterol synthesis or glycerolipid synthesis (212-215). Therefore, in *de novo* lipogenesis,

acetyl-CoA is the building block through which lipids such as cholesterol and fatty acids are synthesized. ACL is the essential and regulated enzyme, whose enzymatic function is vital for *de novo* lipogenesis and proliferation (77, 122, 126). The extent to which ACL contributes to the regulation of lipid biosynthesis in B cells is not known and was the subject of this investigation.

The signal transduction pathways emanating from an engaged BCR and IL-4R have been defined as they lead to growth, survival, and proliferation via PI3K activation. LPS stimulation however will promote the full development of quiescent splenic B cells through differentiation to plasma cells (100-102). As previously mentioned, *c-myc* activation through PI3K-Akt has been shown to be responsible for phosphatidylcholine (PC) synthesis and stimulates both PC and fatty acid (FA) synthesis for biogenesis of mitochondria (112, 113, 203, 209,369, 385). I examined the contribution of glucose to supply carbons for *de novo* lipogenesis occurring with LPS or αIg + IL-4 stimulation of splenic B cells to further elucidate the metabolic requirements for immune cell function.

In corroboration with previous reports about lymphocyte membrane and organelle biosynthesis, this investigation demonstrated an increase in *de novo* lipogenesis in B cells stimulated with LPS or αIg + IL-4 (120, 202, 203, 211, 219-221). Monitored via incorporation of radiolabeled glucose carbons, multiple lipid species were identified by [^{14}C]-HP-TLC. The identified lipids were phosphatidylcholine (PC), phosphatidylethanolamine (PE), cardiolipin (CL), and cholesterol (C). B cells also synthesized ceramides (CM) phosphatidylglycerol (PG),

phosphatidylserine (PS), phosphatidylinositol (PI) and sphingolipids (SM). Not surprisingly, multiple lipid species incorporated glucose carbon from [^{14}C]-labeled glucose metabolism, as the synthetic pathways are interconnected, as illustrated in the *Introduction* section (204, 223-225).

ACL enzyme activity has been shown to be dependent upon its phosphorylation status (149-153, 159); Berwick *et al.* (2002) reported the serine/threonine kinase Akt to direct phosphorylate ACL at its active site on serine 454, which in turn increased its enzymatic activity (150). Within 3 hr of stimulation in *ex vivo* B cells, I demonstrated that ACL was phosphorylated at serine 454 and this occurred in a PI3K-dependent manner. This phosphorylation correlated with an increase in ACL enzymatic activity, also PI3K-dependent. Therefore, B cells activated a lipogenic enzyme through the PI3K signal transduction pathway in the activation response for growth and differentiation.

Previously examined in cancer cell lines and in liver and adipose tissue, the inhibition of ACL activity by hydroxycitrate, SB-201076, and compound-9 (C-9) significantly reduced the generation of acetyl-CoA, cholesterol, and fatty acids (162, 163, 164, 340, 386). The most recently synthesized inhibitor of ACL, C-9 was used in my investigation because it has been shown to be cell-permeable and an efficient inhibitor of ACL (K_i is 0.13 μM) (164). The enzymatic activity of ACL was vital for *de novo* lipogenesis and proliferation of B cells. C-9 addition to activated B cell culture reduced the glucose-dependent generation of lipid precursors (acetyl-CoA and fatty acids) and *de novo* synthesis of membrane lipids. Concentrations of *de novo* free fatty acid species (oleate, palmitate, stearate) were reduced in LPS-stimulated B

cells treated with C-9. By examination of HP-TLC, [^{14}C]-glucose carbon incorporation into membrane lipid species decreased significantly in LPS or αIg + IL-4 stimulated B cells treated with C-9. These results suggested that ACL activity contributed significantly in the differentiation response of B cells via the modulation of glucose utilization in *de novo* synthesis of membrane lipids. In a previous report, Jacowski and co-workers (203, 337) demonstrated cell cycle progression of B cells correlated with membrane synthesis. My results suggest ACL regulates this process since LPS or αIg + IL-4 stimulated B cells with C-9 addition were unable to enter S-phase or remain viable. Inhibition of ACL activity with C-9 prevented membrane lipid synthesis and prevented cell cycle progression (Table I-III). Therefore, B cell proliferation and maturation to the plasma cell stage are dependent upon the function of ACL to synthesize glucose-derived acetyl-CoA for *de novo* lipogenesis.

Glutamine is an additional nutrient required for *in vitro* culture of lymphocytes (121, 128, 131,133, 241, 370, 375); thus, the possibility of glutamine as an alternative source of carbon for lipid synthesis in B cells was considered. In a glioblastoma cell line, Deberardinis *et al*. (2007) demonstrated glutaminolysis provides oxaloacetate and citrate for the subsequent formation of acetyl-CoA (345). Incorporation of glutamine or glucose carbons into acetyl-CoA or the major free fatty acids (C14:0 [myristic], C16:0 [palmitic], C18:0 [stearic], C18:1 [oleic], C18:2 [linoleic], and C20:0 [arachidic]) was evaluated in LPS stimulated B cells by GC-MS. The percentage of fatty acids containing glutamine-derived carbons remained at basal levels with LPS stimulation for 48 hr; whereas, the percentage of fatty acids

containing glucose-derived carbons increased with LPS stimulation. This suggested that LPS stimulation of B cells triggers the selective utilization of glucose, not glutamine, for lipid synthesis and lipid precursor generation as the free fatty acids may contribute to lipid tail moieties of PE, PG, and PC. This was not expected as I hypothesized that in addition to glucose-derived synthesis of acetyl-CoA and fatty acids, glutamine-derived synthesis of acetyl-CoA and fatty acids through glutaminolysis or reductive carboxylation would occur (232-234, 348, 349, 352, 387). The hypothesis however assumed an increase in glutamine carbons would occur similar to glucose carbons. The results presented here demonstrated that B cells enhance glucose not glutamine-derived synthesis of acetyl-CoA.

The role of ACL activity in the utilization of glucose or glutamine for acetyl-CoA and free fatty acid synthesis was also examined with the chemical inhibitor C-9. Previous *in vitro* studies of tumor cells reported that glutamine and glucose metabolism may be coupled and compensate for cellular survival (347-349, 351, 375). In the presence of C-9, LPS-stimulated B cells contained reduced percentages of glucose carbon incorporation in the *de novo* synthesized free fatty acids, further supporting [^{14}C]-HP-TLC data. The contribution of glutamine carbons to the *de novo* synthesis of free fatty acids in LPS-stimulated B cells was not reduced or enhanced with C-9 addition. These results suggested that B cells do not compensate for the loss of glucose-derived acetyl-CoA by generation of acetyl-CoA from glutamine. Therefore, glutamine was demonstrated to not be a major contributor of carbon for *de novo* lipogenesis via ACL activity. The purpose of glutamine uptake and

utilization in B cell homeostasis and response to B cell activation remains unknown; this is a new on-going project for the Chiles' laboratory.

Summary and future direction

B cells respond to antigen by activating growth, proliferation, maturation and differentiation pathways, in a glucose-dependent manner. This investigation demonstrated the dependency of BTK and PI3K activity in the growth and survival response of B cell to antigenic stimulation, contributing essentially to increased glucose uptake and utilization (203). Driven by αIg engagement of the BCR, the activation response included: increased glut-1, Na^+K^+ ATPase, and glycolytic enzyme expression, enhanced glycolysis, increased cellular size and viability, as well as increased ATP concentration, lactate production, and CO_2 production. Furthermore, the response in activation was demonstrated to be dependent upon the type of stimuli presented to the B cell; LPS and CD40L elicited induced glucose utilization through signal transduction pathways not dependent on BTK or PI3K activity. Further investigation and delineation of signal mediators involved under varied stimuli may provide insight to the role of enhanced glycolytic flux in the specificity of the B cell immune response.

Reports have suggested a central role for Akt and myc in the signal transduction events through which B cells respond to antigen (56, 66, 96, 113, 150, 154, 255, 310, 359, 369, 371). Interestingly, the synthesis of lipids and endomembrane expansion are among the many processes promoted in the B cell differentiation and requires glucose metabolism.

Results reported herein suggest that B cells proliferate and expand their cellular membranes predominantly through the activation of the PI3K-Akt pathway. In the activation response, B cells promote glucose utilization to supply fuel and the substrates for *de novo* macromolecular synthesis for growth, survival, and differentiation. The generation of acetyl-CoA from glucose (and to a lesser amount glutamine) through the activity of ACL was demonstrated herein to be vital in the process of B cell development from quiescent to the plasma cell stage. The contribution of glucose to growth, proliferation, maturation and differentiation pathways was essential and not only required the immediate activation of signal transduction pathways (PI3K and BTK via BCR engagement, STAT6 via IL-4 engagement), but also required the enzymatic activity of ACL for the growth and survival responses to antigenic stimulation.

Further investigation of glucose-dependent B cell function (Ig secretion) and the role glucose utilization and metabolism will illuminate the requirements and signal mediating events necessary for plasma cell generation. The murine B cell lymphoma cell line, CH12.lx, has been characterized for differentiation and production of IgM in response to LPS stimulation and may prove useful as a model system to examine ACL activity in B cell function as antibody-secreting plasma cells (203, 388). Preliminary results suggest that ACL is phosphorylated and its activity is required for IgM secretion. As primary murine B cells are not amenable to transfection, further studies in CH12.lx cells may also include siRNA knockdown of ACL to examine the role of this lipogenic enzyme in the formation and function of plasma cells mediated through *de novo* lipogenesis.

Investigation into the changes in lipid metabolism for the acceleration of membrane phospholipid synthesis in differentiating B-lymphoma cell lines may further current understandings of metabolic pathways which lead to the emergence of plasma cells and their malignant counterparts (*i.e.* multiple myeloma) (203, 389). Aberrant expression of ACL and constitutive activation of the PI3K-Akt pathway has been observed in many immortalized cells, lymphomas, and tumors (387, 390, 391). Targeted inhibition of ACL has shown promise in the treatment of pathological cell growth; ACL-specific RNAi or the ACL inhibitors SB-204990 and hydroxycitrate have prevented proliferation and survival *in vitro* of liver, colon, lung and prostate cancers (77, 122, 153, 160, 392, 393). This investigation illustrates the contribution of intracellular signaling and metabolic requirements involved in the acquisition and utilization of glucose to support bio-energetic needs for generation of antibody-secreting plasma cells in *ex vivo* B cells. The contribution of signal transduction pathways (STAT6, BTK, PI3K, and PLC) to enhance glucose transport and utilization for fuel and macromolecular synthesis connects the lipogenic enzyme- ACL to the activation response for B cell growth, survival, and differentiation.

Bibliography

1. Murphy K, Travers P, Walport M. *Janeway's Immunobiology.* New York: Garland Science, 2007.
2. Schamel WW, Reth M. Monomeric and oligomeric complexes of the B cell antigen receptor. Immunity. 2000 Jul;13(1):5-14.
3. Ernst P, Smale ST. Combinatorial regulation of transcription II: The immunoglobulin mu heavy chain gene. Immunity. 1995 May;2(5):427-38.
4. Reth M, Wienands J. Initiation and processing of signals from the B cell antigen receptor. Annu Rev Immunol. 1997;15:453-79.
5. Matsuuchi L, Gold MR. New views of BCR structure and organization. Curr Opin Immunol. 2001 Jun;13(3):270-7.
6. Kurosaki T. Genetic analysis of B cell antigen receptor signaling. Annu Rev Immunol. 1999;17:555-92.
7. Love PE, Hayes SM. ITAM-mediated signaling by the T-cell antigen receptor. Cold Spring Harb Perspect Biol. 2010 Jun;2(6):a002485.
8. Karnell FG, Brezski RJ, King LB, Silverman MA, Monroe JG. Membrane cholesterol content accounts for developmental differences in surface B cell receptor compartmentalization and signaling. J Biol Chem. 2005 Jul 8;280(27):25621-8.
9. Lankester AC, van Lier RA. Compartmentalization of B-cell antigen receptor functions. Mol Immunol. 1996 Jun;33(9):769-75.
10. DeFranco DB. Regulation of steroid receptor subcellular trafficking. Cell Biochem Biophys. 1999;30(1):1-24.
11. Sohn HW, Tolar P, Jin T, Pierce SK. Fluorescence resonance energy transfer in living cells reveals dynamic membrane changes in the initiation of B cell signaling. Proc Natl Acad Sci U S A. 2006 May 23;103(21):8143-8.
12. Campbell KS. Signal transduction from the B cell antigen-receptor. Curr Opin Immunol. 1999 Jun;11(3):256-64.
13. Gold MR. To make antibodies or not: signaling by the B-cell antigen receptor. Trends Pharmacol Sci. 2002 Jul;23(7):316-24.
14. Kurosaki T. Regulation of B cell fates by BCR signaling components. Curr Opin Immunol. 2002 Jun;14(3):341-7.
15. Dal Porto JM, Gauld SB, Merrell KT, Mills D, Pugh-Bernard AE, Cambier J. B cell antigen receptor signaling 101. Mol Immunol. 2004 Jul;41(6-7):599-613.
16. DeFranco AL, Chan VW, Lowell CA. Positive and negative roles of the tyrosine kinase Lyn in B cell function. Semin Immunol. 1998 Aug;10(4):299-307.
17. Pogue SL, Kurosaki T, Bolen J, Herbst R. B cell antigen receptor-induced activation of Akt promotes B cell survival and is dependent on Syk kinase. J Immunol. 2000 Aug 1;165(3):1300-6.
18. Satterthwaite AB, Li Z, Witte ON. Btk function in B cell development and response. Semin Immunol. 1998 Aug;10(4):309-16.

19. Mohamed AJ, Yu L, Bäckesjö CM, Vargas L, Faryal R, Aints A, Christensson B, Berglöf A, Vihinen M, Nore BF, Smith CI. Bruton's tyrosine kinase (Btk): function, regulation, and transformation with special emphasis on the PH domain. Immunol Rev. 2009 Mar;228(1):58-73.
20. Salim K, Bottomley MJ, Querfurth E, Zvelebil MJ, Gout I, Scaife R, Margolis RL, Gigg R, Smith CI, Driscoll PC, Waterfield MD, Panayotou G. Distinct specificity in the recognition of phosphoinositides by the pleckstrin homology domains of dynamin and Bruton's tyrosine kinase. EMBO J. 1996 Nov 15;15(22):6241-50.
21. Beitz LO, Fruman DA, Kurosaki T, Cantley LC, Scharenberg AM. SYK is upstream of phosphoinositide 3-kinase in B cell receptor signaling. J Biol Chem. 1999 Nov 12;274(46):32662-6.
22. Craxton A, Jiang A, Kurosaki T, Clark EA. Syk and Bruton's tyrosine kinase are required for B cell antigen receptor-mediated activation of the kinase Akt. J Biol Chem. 1999 Oct 22;274(43):30644-50.
23. Suzuki H, Matsuda S, Terauchi Y, Fujiwara M, Ohteki T, Asano T, Behrens TW, Kouro T, Takatsu K, Kadowaki T, Koyasu S. PI3K and Btk differentially regulate B cell antigen receptor-mediated signal transduction. Nat Immunol. 2003 Mar;4(3):280-6.
24. Li Z, Wahl MI, Eguinoa A, Stephens LR, Hawkins PT, Witte ON. Phosphatidylinositol 3-kinase-gamma activates Bruton's tyrosine kinase in concert with Src family kinases. Proc Natl Acad Sci U S A. 1997 Dec 9;94(25):13820-5.
25. Coffer PJ, Jin J, Woodgett JR. Protein kinase B (c-Akt): a multifunctional mediator of phosphatidylinositol 3-kinase activation. Biochem J. 1998 Oct 1;335 (Pt 1):1-13.
26. Cheng AM, Rowley B, Pao W, Hayday A, Bolen JB, Pawson T. Syk tyrosine kinase required for mouse viability and B-cell development. Nature. 1995 Nov 16;378(6554):303-6.
27. Turner M, Mee PJ, Costello PS, Williams O, Price AA, Duddy LP, Furlong MT, Geahlen RL, Tybulewicz VL. Perinatal lethality and blocked B-cell development in mice lacking the tyrosine kinase Syk. Nature. 1995 Nov 16;378(6554):298-302.
28. Khan WN. Regulation of B lymphocyte development and activation by Bruton's tyrosine kinase. Immunol Res. 2001;23(2-3):147-56.
29. Yokozeki T, Adler K, Lankar D, Bonnerot C. B cell receptor-mediated Syk-independent activation of phosphatidylinositol 3-kinase, Ras, and mitogen-activated protein kinase pathways. J Immunol. 2003 Aug 1;171(3):1328-35.
30. Rawlings DJ, Saffran DC, Tsukada S, Largaespada DA, Grimaldi JC, Cohen L, Mohr RN, Bazan JF, Howard M, Copeland NG. Mutation of unique region of Bruton's tyrosine kinase in immunodeficient XID mice. Science. 1993 Jul 16;261(5119):358-61.
31. Coggeshall KM. Positive and negative signaling in B lymphocytes. Curr Top Microbiol Immunol. 2000;245(1):213-60.

32. Kurosaki T, Maeda A, Ishiai M, Hashimoto A, Inabe K, Takata M. Regulation of the phospholipase C-gamma2 pathway in B cells. Immunol Rev. 2000 Aug;176:19-29.
33. Tan JE, Wong SC, Gan SK, Xu S, Lam KP. The adaptor protein BLNK is required for b cell antigen receptor-induced activation of nuclear factor-kappa B and cell cycle entry and survival of B lymphocytes. J Biol Chem. 2001 Jun 8;276(23):20055-63.
34. Hashimoto A, Takeda K, Inaba M, Sekimata M, Kaisho T, Ikehara S, Homma Y, Akira,S. Kurosaki T. Cutting edge: essential role of phospholipase C-gamma 2 in B cell development and function. J Immunol. 2000 Aug 15;165(4):1738-42.
35. Petro JB, Khan WN. Phospholipase C-gamma 2 couples Bruton's tyrosine kinase to the NF-kappaB signaling pathway in B lymphocytes. J Biol Chem. 2001 Jan 19;276(3):1715-9.
36. Barbazuk SM, Gold MR. Protein kinase C-delta is a target of B-cell antigen receptor signaling. Immunol Lett. 1999 Aug 3;69(2):259-67.
37. Weil R, Israël A. T-cell-receptor- and B-cell-receptor-mediated activation of NF-kappaB in lymphocytes. Curr Opin Immunol. 2004 Jun;16(3):374-81.
38. Hammerman PS, Fox CJ, Thompson CB. Beginnings of a signal-transduction pathway for bioenergetic control of cell survival. Trends Biochem Sci. 2004 Nov;29(11):586-92.
39. Stilo R, Liguoro D, Di Jeso B, Formisano S, Consiglio E, Leonardi A, Vito P. Physical and functional interaction of CARMA1 and CARMA3 with Ikappa kinase gamma-NFkappaB essential modulator. J Biol Chem. 2004 Aug 13;279(33):34323-31.
40. Moscat J, Diaz-Meco MT. The atypical PKC scaffold protein P62 is a novel target for anti-inflammatory and anti-cancer therapies. Adv Enzyme Regul. 2002;42:173-9.
41. Finco TS, Beg AA, Baldwin AS Jr. Inducible phosphorylation of I kappa B alpha is not sufficient for its dissociation from NF-kappa B and is inhibited by protease inhibitors. Proc Natl Acad Sci U S A. 1994 Dec 6;91(25):11884-8.
42. Zha J, Harada H, Yang E, Jockel J, Korsmeyer SJ. Serine phosphorylation of death agonist BAD in response to survival factor results in binding to 14-3-3 not BCL-X(L) Cell. 1996 Nov 15;87(4):619-28.
43. Way KJ, Chou E, King GL. Identification of PKC-isoform-specific biological actions using pharmacological approaches. Trends Pharmacol. Sci. 2000 May;21(5):181-7.
44. Leitges M, Scmedt C, Guinamard R, Davoust J, Schaal S, Stabel S, Tarakhovsky A. Immunodeficiency in protein kinase cbeta-deficient mice. Science. 1996 Aug 9;273(5276):788-91.
45. Mecklenbräuker I, Saijo K, Zheng NY, Leitges M, Tarakhovsky A. Protein kinase Cdelta controls self-antigen-induced B-cell tolerance. Nature. 2002 Apr 25;416(6883):860-5.

46. Miyamoto A, Nakayama K, Imaki H, Hirose S, Jiang Y, Abe M, Tsukiyama T, Nagahama H, Ohno S, Hatakeyama S, Nakayama KI. Increased proliferation of B cells and auto-immunity in mice lacking protein kinase Cdelta. Nature. 2002 Apr 25;416(6883):865-9.
47. Marshall AJ, Niiro H, Yun TJ, Clark EA. Regulation of B-cell activation and differentiation by the phosphatidylinositol 3-kinase and phospholipase Cgamma pathway. Immunol Rev. 2000 Aug;176:30-46.
48. Fruman DA, Satterthwaite AB, Witte ON. Xid-like phenotypes: a B cell signalosome takes shape. Immunity. 2000 Jul;13(1):1-3.
49. Kurosaki T, Tsukada S. BLNK: connecting Syk and Btk to calcium signals. Immunity. 2000 Jan;12(1):1-5. 196.
50. Saijo K, Mecklenbräuker I, Santana A, Leitger M, Schmedt C, Tarakhovsky A. Protein kinase C beta controls nuclear factor kappaB activation in B cells through selective regulation of the IkappaB kinase alpha. J Exp Med. 2002 Jun 17;195(12):1647-52.
51. Saijo K, Mecklenbräuker I, Schmedt C, Tarakhovsky A. B cell immunity regulated by the protein kinase C family. Ann N Y Acad Sci. 2003 Apr;987:125-34.
52. Donjerkovic D, Scott DW. Regulation of the G1 phase of the mammalian cell cycle. Cell Res. 2000 Mar;10(1):1-16.
53. Phillips RJ, Ghosh S. Regulation of IkappaB beta in WEHI 231 mature B cells. Mol Cell Biol. 1997 Aug;17(8):4390-6.
54. Lee H, Arsura M, Wu M, Duyao M, Buckler AJ, Sonenshein GE. Role of Rel-related factors in control of c-myc gene transcription in receptor-mediated apoptosis of the murine B cell WEHI 231 line. J Exp Med. 1995 Mar 1;181(3):1169-77.
55. Wen R, Chen Y, Xue L, Schuman J, Yang S, Morris SW, Wang D. Phospholipase Cgamma2 provides survival signals via Bcl2 and A1 in different subpopulations of B cells. J Biol Chem. 2003 Oct 31;278(44):43654-62.
56. Grumont RJ, Strasser A, Gerondakis S. B cell growth is controlled by phosphatidylinosotol 3-kinase-dependent induction of Rel/NF-kappaB regulated c-myc transcription. Mol Cell. 2002 Dec;10(6):1283-94.
57. Pohl T, Gugasyan R, Grumont RJ, Strasser A, Metcalf D, Tarlinton D, Sha W, Baltimore D, Gerondakis S. The combined absence of NF-kappa B1 and c-Rel reveals that overlapping roles for these transcription factors in the B cell lineage are restricted to the activation and function of mature cells. Proc Natl Acad Sci U S A. 2002 Apr 2;99(7):4514-9.
58. Donahue AC, Fruman DA. Proliferation and survival of activated B cells requires sustained antigen receptor engagement and phosphoinositide 3-kinase activation. J Immunol. 2003 Jun 15;170(12):5851-60.
59. Donahue AC, Fruman DA. PI3K signaling controls cell fate at many points in B lymphocyte development and activation. Semin Cell Dev Biol. 2004 Apr;15(2):183-97.
60. Okkenhaug K, Vanhaesebroeck B. PI3K in lymphocyte development, differentiation and activation. Nat Rev Immunol. 2003 Apr;3(4):317-30.

61. Fruman DA, Snapper SB, Yballe CM, Davidson L, Yu JY, Alt FW, Cantley LC. Impaired B cell development and proliferation in absence of phosphoinositide 3-kinase p85alpha. Science. 1999 Jan 15;283(5400):393-7.
62. Suzuki H, Terauchi Y, Fujiwara M, Aizawa S, Yazaki Y, Kadowaki T, Koyasu S. Xid-like immunodeficiency in mice with disruption of the p85alpha subunit of phosphoinositide 3-kinase. Science. 1999 Jan 15;283(5400):390-2.
63. del Peso L, González-García M, Page C, Herrera R, Nuñez G. Interleukin-3-induced phosphorylation of BAD through the protein kinase Akt. Science. 1997 Oct 24;278(5338):687-9.
64. Reuther-Madrid JY, Kashatus D, Chen S, Li X, Westwick J, Davis RJ, Earp HS, Wang CY, Baldwin Jr AS Jr. The p65/RelA subunit of NF-kappaB suppresses the sustained, antiapoptotic activity of Jun kinase induced by tumor necrosis factor. Mol Cell Biol. 2002 Dec;22(23):8175-83.
65. Sizemore N, Lerner N, Dombrowski N, Sakurai H, Stark GR. Distinct roles of the Ikappa B kinase alpha and beta subunits in liberating nuclear factor kappa B (NF-kappa B) from Ikappa B and in phosphorylating the p65 subunit of NF-kappa B. J Biol Chem. 2002 Feb 8;277(6):3863-9.
66. Gold MR, Scheid MP, Santos L, Dang-Lawson M, Roth RA, Matsuuchi L, Duronio V, Krebs DL. The B cell antigen receptor activates the Akt (protein kinase B)/glycogen synthase kinase-3 signaling pathway via phosphatidylinositol 3-kinase. J Immunol. 1999 Aug 15;163(4):1894-905.
67. Sears R, Nuckolls F, Haura E, Taya Y, Tamai K, Nevins JR. Multiple Ras-dependent phosphorylation pathways regulate Myc protein stability. Genes Dev. 2000 Oct 1;14(19):2501-14.
68. Piatelli MJ, Wardle C, Blois J, Doughty C, Schram BR, Rothstein TL, Chiles TC. Phosphatidylinositol 3-kinase-dependent mitogen-activated protein/extracellular signal-regulated kinase kinase 1/2 and NF-kappa B signaling pathways are required for B cell antigen receptor-mediated cyclin D2 induction in mature B cells. J Immunol. 2004 Mar 1;172(5):2753-62.
69. Kohn AD, Summers SA, Birnbaum MJ, Roth RA. Expression of a constitutively active Akt Ser/Thr kinase in 3T3-L1 adipocytes stimulates glucose uptake and glucose transporter 4 translocation. J Biol Chem. 1996 Dec 6;271(49):31372-8.
70. Wofford JA, Wieman HL, Jacobs SR, Zhao Y, Rathmell JC. IL-7 promotes Glut1 trafficking and glucose uptake via STAT5-mediated activation of Akt to support T-cell survival. Blood. 2008 Feb 15;111(4):2101-11.
71. Fingar DC, Blenis J. Target of rapamycin (TOR): an integrator of nutrient and growth factor signals and coordinator of cell growth and cell cycle progression.Oncogene. 2004 Apr 19;23(18):3151-71.
72. Hay N, Sonenberg N. Upstream and downstream of mTOR. Genes Dev. 2004 Aug 15;18(16):1926-45.
73. Edinger AL, Thompson CB. Akt maintains cell size and survival by increasing mTOR-dependent nutrient uptake. Mol Biol Cell. 2002 Jul;13(7):2276-88.
74. Kozma SC, Thomas G. Regulation of cell size in growth, development and human disease: PI3K, PKB and S6K. Bioessays. 2002 Jan;24(1):65-71.

75. Plas DR, Thompson CB. Akt activation promotes degradation of tuberin and FOXO3a via the proteasome. J Biol Chem. 2003 Apr 4;278(14):12361-6.
76. Rathmell JC, Elstrom RL, Cinalli RM, Thompson CB. Activated Akt promotes increased resting T cell size, CD28-independent T cell growth, and development of autoimmunity and lymphoma. Eur J Immunol. 2003 Aug;33(8):2223-32.
77. Bauer DE, Hatzivassiliou G, Zhao F, Andreadis C, Thompson CB. ATP citrate lyase is an important component of cell growth and transformation. Oncogene. 2005 Sep 15;24(41):6314-22.
78. Bauer DE, Harris MH, Plas DR, Lum JJ, Hammerman PS, Rathmell JC, Riley JL, Thompson CB. Cytokine stimulation of aerobic glycolysis in hematopoietic cells exceeds proliferative demand. FASEB J. 2004 Aug;18(11):1303-5.
79. Deberardinis RJ, Lum JJ, Thompson CB. Phosphatidylinositol 3-kinase-dependent modulation of carnitine palmitoyltransferase 1A expression regulates lipid metabolism during hematopoietic cell growth. J Biol Chem. 2006 Dec 8;281(49):37372-80.
80. Dummler B, Hemmings BA. Physiological roles of PKB/Akt isoforms in development and disease. Biochem Soc Trans 2007;35:231–5.
81. Chen WS, Xu PZ, Gottlob K, Chen ML, Sokol K, Shiyanova T, Roninson I, Weng W, Suzuki R, Tobe K, Kadowaki T, Hay N. Growth retardation and increased apoptosis in mice with homozygous disruption of the Akt1 gene. Genes Dev. 2001 Sep 1;15(17):2203-8.
82. Cho H, Thorvaldsen JL, Chu Q, Feng F, Birnbaum MJ. Akt1/PKBalpha is required for normal growth but dispensable for maintenance of glucose homeostasis in mice. J Biol Chem. 2001 Oct 19;276(42):38349-52.
83. Garofalo RS, Orena SJ, Rafidi K, Torchia AJ, Stock JL, Hildebrandt AL, Coskran T, Black SC, Brees DJ, Wicks JR, McNeish JD, Coleman KG. Severe diabetes, age-dependent loss of adipose tissue, and mild growth deficiency in mice lacking Akt2/PKB beta. J Clin Invest. 2003 Jul;112(2):197-208.
84. Easton RM, Cho H, Roovers K, Shineman DW, Mizrahi M, Forman MS, Lee VM, Szabolcs M, de Jong R, Oltersdorf T, Ludwig T, Efstratiadis A, Birnbaum MJ. Role for Akt3/protein kinase Bgamma in attainment of normal brain size. Mol Cell Biol. 2005 Mar;25(5):1869-78.
85. Tschopp O, Yang ZZ, Brodbeck D, Dummler BA, Hemmings-Mieszczak M, Watanabe T, Michaelis T, Frahm J, Hemmings BA. Essential role of protein kinase B gamma (PKB gamma/Akt3) in postnatal brain development but not in glucose homeostasis. Development. 2005 Jul;132(13):2943-54.
86. Kim DR. Proteomic changes during the B cell development. J Chromatogr B Analyt Technol Biomed Life Sci. 2005 Feb 5;815(1-2):295-303.
87. Burrows PD, Kearney JF, Schroeder HW Jr, Cooper MD. Normal B lymphocyte differentiation. Baillieres Clin Haematol. 1993 Dec;6(4):785-806.
88. Schram BR, Tze LE, Ramsey LB, Liu J, Najera L, Vegoe AL, Hardy RR, Hippen KL, Farrar MA, Behrens TW. B cell receptor basal signaling regulates antigen-induced Ig light chain rearrangements. J Immunol. 2008 Apr 1;180(7):4728-41.

89. Campana D, Janossy G, Bofill M, Trejdosiewicz LK, Ma D, Hoffbrand AV, Mason DY, Lebacq AM, Forster HK. Human B cell development. I. Phenotypic differences of B lymphocytes in the bone marrow and peripheral lymphoid tissue. J Immunol. 1985 Mar;134(3):1524-30.
90. Rolink A, Melchers F. B-cell development in the mouse. Immunol Lett. 1996 Dec;54(2-3):157-61.
91. Melchers, F. and A. Rolink, Ed. By William E. Paul, Lippincott-Raven Publishers, Philadelphia, PA. 1999. *Fundamental Immunology* 4th Ed, CH. 6 B-Lymphocyte Development and Biology. Pp. 183-217.
92. Maddaly R, Pai G, Balaji S, Sivaramakrishnan P, Srinivasan L, Sunder SS, Paul SF. Receptors and signaling mechanisms for B-lymphocyte activation, proliferation and differentiation--insights from both in vivo and in vitro approaches. FEBS Lett. 2010 Dec 15;584(24):4883-94.
93. Rolink AG, Schaniel C, Busslinger M, Nutt SL, Melchers F. Fidelity and infidelity in commitment to B-lymphocyte lineage development. Immunol Rev. 2000 Jun;175:104-11.
94. Oikawa T, Yamada T, Kihara-Negishi F, Yamamoto H, Kondoh N, Hitomi Y, Hashimoto Y. The role of Ets family transcription factor PU.1 in hematopoietic cell differentiation, proliferation and apoptosis. Cell Death Differ. 1999 Jul;6(7):599-608.
95. Nutt SL, Kee BL. The transcriptional regulation of B cell lineage commitment. Immunity. 2007 Jun;26(6):715-25.
96. Melchers F. B-lymphocyte-lineage cells from early precursors to Ig-secreting plasma cells: targets of regulation by the myc/mad/max families of genes? Curr Top Microbiol Immunol. 1997;224:19-30.
97. Raetz CR, Whitfield C. Lipopolysaccharide endotoxins. Annu Rev Biochem. 2002;71:635-700.
98. Gerondakis S, Grumont RJ, Banerjee A. Regulating B-cell activation and survival in response to TLR signals. Immunol Cell Biol. 2007 Aug-Sep;85(6):471-5.
99. Keegan AD, Zamorano J. Regulation of gene expression, growth, and cell survival by IL-4: contribution of multiple signaling pathways. Cell Res. 1998 Mar;8(1):1-13.
100. Parker DC. T cell-dependent B cell activation. Annu Rev Immunol. 1993;11:331-60.
101. Mills DM, Cambier JC. B lymphocyte activation during cognate interactions with CD4+ T lymphocytes: molecular dynamics and immunologic consequences. Semin Immunol. 2003 Dec;15(6):325-9.
102. Askonas BA. Immunoglobulin synthesis and its induction in B-lymphoid cells. Acta Endocrinol Suppl (Copenh). 1975;194:117-32.
103. Bishop GA, Hostager BS. The CD40-CD154 interaction in B cell-T cell liaisons. Cytokine Growth Factor Rev. 2003 Jun-Aug;14(3-4):297-309.
104. Elgueta R, Benson MJ, de Vries VC, Wasiuk A, Guo Y, Noelle RJ. Molecular mechanism and function of CD40/CD40L engagement in the immune system. Immunol Rev. 2009 May;229(1):152-72.

105. van Zelm MC, van der Burg M, van Dongen JJ. Homeostatic and maturation-associated proliferation in the peripheral B-cell compartment. Cell Cycle. 2007 Dec 1;6(23):2890-5.
106. Klein B, Tarte K, Jourdan M, Mathouk K, Moreaux J, Jourdan E, Legouffe E, De Vos J, Rossi JF. Survival and proliferation factors of normal and malignant plasma cells. Int J Hematol. 2003 Aug;78(2):106-13.
107. Yanaba K, Bouaziz JD, Matsushita T, Magro CM, St Clair EW, Tedder TF. B-lymphocyte contributions to human autoimmune disease. Immunol Rev. 2008 Jun;223:284-99.
108. Shaheen SP, Talwalkar SS, Medeiros LJ. Multiple myeloma and immunosecretory disorders: an update. Adv Anat Pathol. 2008 Jul;15(4):196-210.
109. Lorsbach RB, Hsi ED, Dogan A, Fend F. Plasma cell myeloma and related neoplasms. Am J Clin Pathol. 2011 Aug;136(2):168-82.
110. Bental M, Deutsch C. Metabolic changes in activated T cells: An NMR study of human peripheral blood lymphocytes. Magn Reson Med 1993;29:317–326.
111. Garcia-Manteiga JM, Mari S, Godejohann M, Spraul M, Napoli C, Cenci S, Musco G, Sitia R. Metabolomics of B to plasma cell differentiation. J Proteome Res. 2011 Sep 2;10(9):4165-76.
112. Osthus RC, Shim H, Kim S, Li Q, Reddy R, Mukherjee M, Xu Y, Wonsey D, Lee LA, Dang CV. Deregulation of glucose transporter 1 and glycolytic gene expression by c-Myc. J Biol Chem. 2000 Jul 21;275(29):21797-800.
113. Iritani BM, Eisenman RN. c-Myc enhances protein synthesis and cell size during B lymphocyte development. Proc Natl Acad Sci U S A. 1999 Nov 9;96(23):13180-5.
114. Doughty CA, Bleiman BF, Wagner DJ, Dufort FJ, Mataraza JM, Roberts MF, Chiles TC. Antigen receptor-mediated changes in glucose metabolism in B lymphocytes: role of phosphatidylinositol 3-kinase signaling in the glycolytic control of growth. Blood. 2006 Jun 1;107(11):4458-65.
115. Krauss S, Brand MD, Buttgereit F. Signaling takes a breath--new quantitative perspectives on bioenergetics and signal transduction. Immunity. 2001 Oct;15(4):497-502.
116. Fox CJ, Hammerman PS, Thompson CB. Fuel feeds function: energy metabolism and the T-cell response. Nat Rev Immunol. 2005 Nov;5(11):844-52.
117. Deberardinis RJ, Thompson CB. Cellular metabolism and disease: what do metabolic outliers teach us? Cell. 2012 Mar 16;148(6):1132-44.
118. DeBerardinis RJ, Lum JJ, Hatzivassiliou G, Thompson CB. The biology of cancer: metabolic reprogramming fuels cell growth and proliferation. Cell Metab. 2008 Jan;7(1):11-20.
119. MacIver NJ, Jacobs SR, Wieman HL, Wofford JA, Coloff JL, Rathmell JC. Glucose metabolism in lymphocytes is a regulated process with significant effects on immune cell function and survival. J Leukoc Biol. 2008 Oct;84(4):949-57.

120. Rush JS, Sweitzer T, Kent C, Decker GL, Waechter CJ. Biogenesis of the endoplasmic reticulum in activated B lymphocytes: temporal relationships between the induction of protein N-glycosylation activity and the biosynthesis of membrane protein and phospholipid. Arch Biochem Biophys. 1991 Jan;284(1):63-70.
121. Brand K. Glutamine and glucose metabolism during thymocyte proliferation. Pathways of glutamine and glutamate metabolism. Biochem J. 1985 Jun 1;228(2):353-61.
122. Hatzivassiliou G, Zhao F, Bauer DE, Andreadis C, Shaw AN, Dhanak D, Hingorani SR, Tuveson DA, Thompson CB. ATP citrate lyase inhibition can suppress tumor cell growth. Cancer Cell. 2005 Oct;8(4):311-21.
123. Ruderman NB, Saha AK, Vavvas D, Witters LA. Malonyl-CoA, fuel sensing, and insulin resistance. Am J Physiol. 1999 Jan;276(1 Pt 1):E1-E18.
124. Randle PJ, Garland PB, Hales CN, Newsholme EA. The glucose fatty-acid cycle. Its role in insulin sensitivity and the metabolic disturbances of diabetes mellitus. Lancet. 1963 Apr 13;1(7285):785-9.
125. Singh M, Richards EG, Mukherjee A, Srere PA. Structure of ATP citrate lyase from rat liver. Physicochemical studies and proteolytic modification. J Biol Chem. 1976 Sep 10;251(17):5242-50.
126. Abramson HN. The lipogenesis pathway as a cancer target. J Med Chem. 2011 Aug 25;54(16):5615-38.
127. Srere PA. The citrate enzymes: their structures, mechanisms, and biological functions. Curr Top Cell Regul. 1972;5:229-83.
128. Fitzpatrick L, Jenkins HA, Butler M. Glucose and glutamine metabolism of a murine B-lymphocyte hybridoma grown in batch culture. Appl Biochem Biotechnol. 1993 Nov;43(2):93-116.
129. Anastasiou D, 206. Cantley LC. Breathless cancer cells get fat on glutamine. Cell Res. 2012 Mar;22(3):443-6.
130. Joseph JW, Odegaard ML, Ronnebaum SM, Burgess SC, Muehlbauer J, Sherry AD, Newgard CB. Normal flux through ATP-citrate lyase or fatty acid synthase is not required for glucose-stimulated insulin secretion. J Biol Chem. 2007 Oct 26;282(43):31592-600.
131. Metallo CM, Vander Heiden MG. Metabolism strikes back: metabolic flux regulates cell signaling. Genes Dev. 2010 Dec 15;24(24):2717-22.
132. DeBerardinis RJ, Cheng T. Q's next: the diverse functions of glutamine in metabolism, cell biology and cancer. Oncogene. 2010 Jan 21;29(3):313-24.
133. Newsholme P, Lima MM, Procopio J, Pithon-Curi TC, Doi SQ, Bazotte RB, Curi R. Glutamine and glutamate as vital metabolites. Braz J Med Biol Res. 2003 Feb;36(2):153-63.
134. Watson JA, Lowenstein JM. Citrate and the conversion of carbohydrate into fat. Fatty acid synthesis by a combination of cytoplasm and mitochondria. J Biol Chem. 1970 Nov 25;245(22):5993-6002.

135. Pierce MW, Palmer JL, Keutmann HT, Avruch J. ATP-citrate lyase. Structure of a tryptic peptide containing the phosphorylation site directed by glucagon and the cAMP-dependent protein kinase. J Biol Chem. 1981 Sep 10;256(17):8867-70.
136. Whiteman EL, Cho H, Birnbaum MJ. Role of Akt/protein kinase B in metabolism. Trends Endocrinol Metab. 2002 Dec;13(10):444-51.
137. Inoue H, Honjo K, Takeda Y. Dietary response of the hepatic citrate-cleavage enzyme in hypophysectomized rats. J Biochem. 1966 Jul;60(1):93-5.
138. Cottam GL, Srere PA. Nature of the phosphorylated residue in citrate clevage enzyme. Biochem Biophys Res Commun. 1969 Jun 27;35(6):895-900.
139. Plowman DM, Cleland WW. Purification and kinetic studies of the citrate cleavage enzyme. J Biol Chem. 1967 Sep 25;242(18):4239-47.
140. Houston B, Nimmo HG. Purification and some kinetic properties of rat liver ATP citrate lyase. Biochem J. 1984 Dec 1;224(2):437-43.
141. Wells TN. ATP-citrate lyase from rat liver. Characterisation of the citryl-enzyme complexes. Eur J Biochem. 1991 Jul 1;199(1):163-8.
142. Hanson RW, Ballard FJ. The relative significance of acetate and glucose as precursors for lipid synthesis in liver and adipose tissue from ruminants. Biochem J. 1967 Nov;105(2):529-36.
143. Hallows WC, Lee S, Denu JM. Sirtuins deacetylate and activate mammalian acetyl-CoA synthetases. Proc Natl Acad Sci U S A. 2006 Jul 5;103(27):10230-5.
144. Huber H, Strieder N, Winnler H, Reiser G, Koppelstaetter K. Studies on the incorporation of 14-C-sodium acetate into the phospholipids of phytohaemagglutinin-stimulated and unstimulated lymphocytes. Br J Haematol. 1968 Aug;15(2):203-9.
145. Hynes MJ, Murray SL, Andrianopoulos A, Davis MA. Role of carnitine acetyltransferases in acetyl coenzyme A metabolism in Aspergillus nidulans. Eukaryot Cell. 2011 Apr;10(4):547-55.
146. Randle PJ, Priestman DA, Mistry SC, Halsall A. Glucose fatty acid interactions and the regulation of glucose disposal. J Cell Biochem. 1994;55 Suppl:1-11.
147. Hayashi H, Takahata S. Role of peroxisomal fatty acyl-CoA beta-oxidation in phospholipid biosynthesis. Arch Biochem Biophys. 1991 Feb 1;284(2):326-31.
148. Hayashi H, Miwa A. The role of peroxisomal fatty acyl-CoA beta-oxidation in bile acid biosynthesis. Arch Biochem Biophys. 1989 Nov 1;274(2):582-9.
149. Pentyala SN, Benjamin WB. Effect of oxaloacetate and phosphorylation on ATP-citrate lyase activity. Biochemistry. 1995 Sep 5;34(35):10961-9.
150. Berwick DC, Hers I, Heesom KJ, Moule SK, Tavare JM. The identification of ATP-citrate lyase as a protein kinase B (Akt) substrate in primary adipocytes. J Biol Chem. 2002 Sep 13;277(37):33895-900.
151. Ramakrishna S, Benjamin WB. Phosphorylation of different sites of acetyl CoA carboxylase by ATP-citrate lyase kinase and cyclic AMP-dependent protein kinase. Biochem Biophys Res Commun. 1983 Dec 16;117(2):435-43.

152. Potapova IA, El-Maghrabi MR, Doronin SV, Benjamin WB. Phosphorylation of recombinant human ATP:citrate lyase by cAMP-dependent protein kinase abolishes homotropic allosteric regulation of the enzyme by citrate and increases the enzyme activity. Allosteric activation of ATP:citrate lyase by phosphorylated sugars. Biochemistry. 2000 Feb 8;39(5):1169-79.
153. Migita T, Narita T, Nomura K, Miyagi E, Inazuka F, Matsuura M, Ushijima M, Mashima T, Seimiya H, Satoh Y, Okumura S, Nakagawa K, Ishikawa Y. ATP citrate lyase: activation and therapeutic implications in non-small cell lung cancer. Cancer Res. 2008 Oct 15;68(20):8547-54.
154. Porstmann T, Griffiths B, Chung YL, Delpuech O, Griffiths JR, Downward J, Schulze A. PKB/Akt induces transcription of enzymes involved in cholesterol and fatty acid biosynthesis via activation of SREBP. Oncogene. 2005 Sep 29;24(43):6465-81.
155. Sato R, Okamoto A, Inoue J, Miyamoto W, Sakai Y, Emoto N, Shimano H, Maeda M. Transcriptional regulation of the ATP citrate-lyase gene by sterol regulatory element-binding proteins. J Biol Chem. 2000 Apr 28;275(17):12497-502.
156. Beigneux AP, Kosinski C, Gavino B, Horton JD, Skarnes WC, Young SG. ATP-citrate lyase deficiency in the mouse. J Biol Chem. 2004 Mar 5;279(10):9557-64.
157. Williams SP, Sykes BD, Bridger WA. Phosphorus-31 nuclear magnetic resonance study of the active site phosphohistidine and regulatory phosphoserine residues of rat liver ATP-citrate lyase. Biochemistry. 1985 Sep 24;24(20):5527-31.
158. Hughes K, Ramakrishna S, Benjamin WB, Woodgett JR. Identification of multifunctional ATP-citrate lyase kinase as the alpha-isoform of glycogen synthase kinase-3. Biochem J. 1992 Nov 15;288 (Pt1):309-14.
159. Pierce MW, Palmer JL, Keutmann HT, Hall TA, Avruch J. The insulin-directed phosphorylation site on ATP-citrate lyase is identical with the site phosphorylated by the cAMP-dependent protein kinase in vitro. J Biol Chem. 1982 Sep 25;257(18):10681-6.
160. Hanai J, Doro N, Sasaki AT, Kobayashi S, Cantley LC, Seth P, Sukhatme VP. Inhibition of lung cancer growth: ATP citrate lyase knockdown and statin treatment leads to dual blockade of mitogen-activated protein kinase (MAPK) and phosphatidylinositol-3-kinase (PI3K)/AKT pathways. J Cell Physiol. 2012 Apr;227(4):1709-20.
161. Guay C, Madiraju SR, Aumais A, Joly E, Prentki M. A role for ATP-citrate lyase, malic enzyme, and pyruvate/citrate cycling in glucose-induced insulin secretion. J Biol Chem. 2007 Dec 7;282(49):35657-65.
162. Pearce NJ, Yates JW, Berkhout TA, Jackson B, Tew D, Boyd H, Camilleri P, Sweeney P, Gribble AD, Shaw A, Groot PH. The role of ATP citrate-lyase in the metabolic regulation of plasma lipids. Hypolipidaemic effects of SB-204990, a lactone prodrug of the potent ATP citrate-lyase inhibitor SB-201076. Biochem J. 1998 Aug 15;334 (Pt 1):113-9.

163. Watson JA, Fang M, Lowenstein JM. Tricarballylate and hydroxycitrate: substrate and inhibitor of ATP: citrate oxaloacetate lyase. Arch Biochem Biophys. 1969 Dec;135(1):209-17.
164. Li JJ, Wang H, Tino JA, Robl JA, Herpin TF, Lawrence RM, Biller S, Jamil H, Ponticiello R, Chen L, Chu CH, Flynn N, Cheng D, Zhao R, Chen B, Schnur D, Obermeier MT, Sasseville V, Padmanabha R, Pike K, Harrity T. 2-hydroxy-N-arylbenzenesulfonamides as ATP-citrate lyase inhibitors. Bioorg Med Chem Lett. 2007 Jun 1;17(11):3208-11.
165. Dolle RE, McNair D, Hughes MJ, Kruse LI, Eggelston D, Saxty BA, Wells TN, Groot PH. ATP-citrate lyase as a target for hypolipidemic intervention. Sulfoximine and 3-hydroxy-beta-lactam containing analogues of citric acid as potential tight-binding inhibitors. J Med Chem. 1992 Dec 25;35(26):4875-84.
166. Gribble AD, Dolle RE, Shaw A, McNair D, Novelli R, Novelli CE, Slingsby BP, Shah VP, Tew D, Saxty BA, Allen M, Groot PH, Pearce N, Yates J. ATP-citrate lyase as a target for hypolipidemic intervention. Design and synthesis of 2-substituted butanedioic acids as novel, potent inhibitors of the enzyme. J Med Chem. 1996 Aug 30;39(18):3569-84.
167. Nelms K, Keegan AD, Zamorano J, Ryan JJ, Paul WE. The IL-4 receptor: signaling mechanisms and biologic functions. Annu Rev Immunol. 1999;17:701-38.
168. Illera VA, Perandones CE, Stunz LL, Mower DA Jr, Ashman RF. Apoptosis in splenic B lymphocytes. Regulation by protein kinase C and IL-4. J Immunol. 1993 Sep 15;151(6):2965-73.
169. Wurster AL, Rodgers VL, White MF, Rothstein TL, Grusby MJ. Interleukin-4-mediated protection of primary B cells from apoptosis through Stat6-dependent up-regulation of Bcl-xL. J Biol Chem. 2002 Jul 26;277(30):27169-75.
170. Kelly-Welkech A, Hanson EM, Keegan AD. Interleukin-4 (IL-4) pathway. Sci STKE. 2005 Jul 19;2005(293):cm9.
171. Wurster AL, Tanaka T, Grusby MJ. The biology of Stat4 and Stat6. Oncogene. 2000 May 15;19(21):2577-84.
172. Zamorano J, Wang HY, Wang LM, Pierce JH, Keegan AD. IL-4 protects cells from apoptosis via the insulin receptor substrate pathway and a second independent signaling pathway. J Immunol. 1996 Dec 1;157(11):4926-34.
173. Morris SC, Dragula NL, Finkelman FD. IL-4 promotes Stat6-dependent survival of autoreactive B cells in vivo without inducing autoantibody production. J Immunol. 2002 Aug 15;169(4):1696-704.
174. Rathmell JC, Farkash EA, Gao W, Thompson CB. IL-7 enhances the survival and maintains the size of naive T cells. J Immunol. 2001 Dec 15;167(12):6869-76.
175. Gupta S, Jiang M, Anthony A, Pernis AB. Lineage-specific modulation of interleukin 4 signaling by interferon regulatory factor 4. J Exp Med. 1999 Dec 20;190(12):1837-48.

176. Monticelli S, Ghittoni R, Kabesch M, Vercelli D. Myb proteins repress human Ig epsilon germline transcription by inhibiting STAT6-dependent promoter activation. Mol Immunol. 2002 Jun;38(15):1129-38.
177. Schroder AJ, Pavlidis P, Arimura A, Capece D, Rothman PB. Cutting edge: STAT6 serves as a positive and negative regulator of gene expression in IL-4-stimulated B lymphocytes. J Immunol. 2002 Feb 1;168(3):996-1000.
178. Spencer L, Shultz L, Rajan TV. Interleukin-4 receptor-Stat6 signaling in murine infections with a tissue-dwelling nematode parasite. Infect Immun. 2001 Dec;69(12):7743-52.
179. Venkataraman C, Shankar G, Sen G, Bondada S. Bacterial lipopolysaccharide induced B cell activation is mediated via a phosphatidylinositol 3-kinase dependent signaling pathway. Immunol Lett. 1999 Aug 3;69(2):233-8.
180. Hoshino K, Takeuchi O, Kawai T, Sanjo H, Ogawa T, Takeda Y, Takeda K, Akira S. Cutting edge: Toll-like receptor 4 (TLR4)-deficient mice are hyporesponsive to lipopolysaccharide: evidence for TLR4 as the Lps gene product. J Immunol. 1999 Apr 1;162(7):3749-52.
181. Dasari P, Nicholson IC, Hodge G, Dandie GW, Zola H. Expression of toll-like receptors on B lymphocytes. Cell Immunol. 2005 Jul-Aug;236(1-2):140-5.
182. Bonefeld CM, Haks M, Nielsen B, von Essen M, Boding L, Hansen AK, Larsen JM, Odum N, Krimpenfort P, Kruisbeek A, Christensen JP, Thomsen AR, Geisler C. TCR down-regulation controls virus-specific CD8+ T cell responses. J Immunol. 2008 Dec 1;181(11):7786-99. 55.
183. Sultzer BM, Castagna R, Bandekar J, Wong P. Lipopolysaccharide nonresponder cells: the C3H/HeJ defect. Immunobiology. 1993 Apr;187(3-5):257-71.
184. Meyer-Bahlburg A, Khim S, Rawlings DJ. B cell intrinsic TLR signals amplify but are not required for humoral immunity. J Exp Med. 2007 Dec 24;204(13):3095-101.
185. Suzuki N, Suzuki S, Millar DG, Unno M, Hara H, Calzascia T, Yamasaki S, Yokosuka T, Chen NJ, Elford AR, Suzuki J, Takeuchi A, Mirtsos C, Bouchard D, Ohashi PS, Yeh WC, Saito T. A critical role for the innate immune signaling molecule IRAK-4 in T cell activation. Science. 2006 Mar 31;311(5769):1927-32.
186. Peng SL. Signaling in B cells via Toll-like receptors. Curr Opin Immunol. 2005 Jun;17(3):230-6.
187. Takeda K, Akira S. TLR signaling pathways. Semin Immunol. 2004 Feb;16(1):3-9.
188. Kang SM, Yoo DG, Kim MC, Song JM, Park MK, O E, Quan FS, Akira S, Compans RW. MyD88 plays an essential role in inducing B cells capable of differentiating into antibody-secreting cells after vaccination. J Virol. 2011 Nov;85(21):11391-400.

189. Neves P, Lampropoulou V, Calderon-Gomez E, Roch T, Stervbo U, Shen P, Kühl AA, Loddenkemper C, Haury M, Nedospasov SA, Kaufmann SH, Steinhoff U, Calado DP, Fillatreau S. Signaling via the MyD88 adaptor protein in B cells suppresses protective immunity during Salmonella typhimurium infection. Immunity. 2010 Nov 24;33(5):777-90.
190. Peck-Palmer OM, Unsinger J, Chang KC, Davis CG, McDunn JE, Hotchkiss RS. Deletion of MyD88 markedly attenuates sepsis-induced T and B lymphocyte apoptosis but worsens survival. J Leukoc Biol. 2008 Apr;83(4):1009-18.
191. Bolland S. An innate path to human B cell tolerance. Immunity. 2008 Nov 14;29(5):667-9.
192. Isnardi I, Ng YS, Srdanovic I, Motaghedi R, Rudchenko S, von Bernuth H, Zhang SY, Puel A, Jouanguy E, Picard C, Garty BZ, Camcioglu Y, Doffinger R, Kumararatne D, Davies G, Gallin JI, Haraguchi S, Day NK, Casanova JL, Meffre E. IRAK-4- and MyD88-dependent pathways are essential for the removal of developing autoreactive B cells in humans. Immunity. 2008 Nov 14;29(5):746-57.
193. Kearney JF, Klein J, Bockman DE, Cooper MD, Lawton AR. B cell differentiation induced by lipopolysaccharide. V. Suppression of plasma cell maturation by anti-mu: mode of action and characteristics of suppressed cells. J Immunol. 1978 Jan;120(1):158-66.
194. Brewer JW, Hendershot LM. Building an antibody factory: a job for the unfolded protein response. Nat Immunol. 2005 Jan;6(1):23-9.
195. Wiest DL, Burkhardt JK, Stockdale AM, Argon Y. Expression of intracisternal A-type particles is increased when a B-cell lymphoma differentiates into an immunoglobulin-secreting cell. J Virol. 1989 Feb;63(2):659-68.
196. Kirk SJ, Cliff JM, Thomas JA, Ward TH. Biogenesis of secretory organelles during B cell differentiation. J Leukoc Biol. 2010 Feb;87(2):245-55.
197. Fagone P, Gunter C, Sage CR, Gunn KE, Brewer JW, Jackowski S. CTP:phosphocholine cytidylyltransferase alpha is required for B-cell proliferation and class switch recombination. J Biol Chem. 2009 Mar 13;284(11):6847-54.
198. McGehee AM, Dougan SK, Klemm EJ, Shui G, Park B, Kim YM, Watson N, Wenk MR, Ploegh HL, Hu CC. XBP-1-deficient plasmablasts show normal protein folding but altered glycosylation and lipid synthesis. J Immunol. 2009 Sep 15;183(6):3690-9.
199. Brewer JW, Jackowski S. UPR-Mediated Membrane Biogenesis in B Cells. Biochem Res Int. 2012;2012:738471.
200. Shaffer AL, Shapiro-Shelef M, Iwakoshi NN, Lee AH, Qian SB, Zhao H, Yu X, Yang L, Tan BK, Rosenwald A, Hurt EM, Petroulakis E, Sonenberg N, Yewdell JW, Calame K, Glimcher LH, Staudt LM. XBP1, downstream of Blimp-1, expands the secretory apparatus and other organelles, and increases protein synthesis in plasma cell differentiation. Immunity. 2004 Jul;21(1):81-93.
201. Shaffer AL, Emre NC, Romesser PB, Staudt LM. IRF4: Immunity. Malignancy! Therapy? Clin Cancer Res. 2009 May 1;15(9):2954-61.

202. van Meer G, Voelker DR, Feigenson GW. Membrane lipids: where they are and how they behave. Nat Rev Mol Cell Biol. 2008 Feb;9(2):112-24.
203. Fagone P, Sriburi R, Ward-Chapman C, Frank M, Wang J, Gunter C, Brewer JW, Jackowski S. Phospholipid biosynthesis program underlying membrane expansion during B-lymphocyte differentiation. J Biol Chem. 2007 Mar 9;282(10):7591-605.
204. Jackowski S, Fagone P. CTP: Phosphocholine cytidylyltransferase: paving the way from gene to membrane. J Biol Chem. 2005 Jan 14;280(2):853-6.
205. Sriburi R, Jackowski S, Mori K, Brewer JW. XBP1: a link between the unfolded protein response, lipid biosynthesis, and biogenesis of the endoplasmic reticulum. J Cell Biol. 2004 Oct 11;167(1):35-41.
206. Banchio C, Schang LM, Vance DE. Phosphorylation of Sp1 by cyclin-dependent kinase 2 modulates the role of Sp1 in CTP:phosphocholine cytidylyltransferase alpha regulation during the S phase of the cell cycle. J Biol Chem. 2004 Sep 17;279(38):40220-6.
207. Vance DE, Vance JE. Physiological consequences of disruption of mammalian phospholipid biosynthetic genes. J Lipid Res. 2009 Apr;50 Suppl:S132-7.
208. Vance DE. Role of phosphatidylcholine biosynthesis in the regulation of lipoprotein homeostasis. Curr Opin Lipidol. 2008 Jun;19(3):229-34.
209. Leventis PA, Grinstein S. The distribution and function of phosphatidylserine in cellular membranes. Annu Rev Biophys. 2010 Jun 9;39:407-27.
210. Merrill AH Jr. Sphingolipid and glycosphingolipid metabolic pathways in the era of sphingolipidomics. Chem Rev. 2011 Oct 12;111(10):6387-422.
211. Fagone P, Jackowski S. Membrane phospholipid synthesis and endoplasmic reticulum function. J Lipid Res. 2009 Apr;50 Suppl:S311-6.
212. Heiniger HJ, Marshall JD. Cholesterol synthesis in polyclonally activated cytotoxic lymphocytes and its requirement for differentiation and proliferation. Proc Natl Acad Sci U S A. 1982 Jun;79(12):3823-7.
213. Sumi S, Beauchamp RD, Townsend CM Jr, Uchida T, Murakami M, Rajaraman S, Ishizuka J, Thompson JC. Inhibition of pancreatic adenocarcinoma cell growth by lovastatin. Gastroenterology. 1992 Sep;103(3):982-9.
214. Heiniger HJ. Cholesterol and its biosynthesis in normal and malignant lymphocytes. Cancer Res. 1981 Sep;41(9 Pt 2):3792-4.
215. Menendez JA, Lupu R. Fatty acid synthase-catalyzed de novo fatty acid biosynthesis: from anabolic-energy-storage pathway in normal tissues to jack-of-all-trades in cancer cells. Arch Immunol Ther Exp (Warsz). 2004 Nov-Dec;52(6):414-26.
216. Kuhajda FP, Jenner K, Wood FD, Hennigar RA, Jacobs LB, Dick JD, Pasternack GR. Fatty acid synthesis: a potential selective target for antineoplastic therapy. Proc Natl Acad Sci U S A. 1994 Jul 5;91(14):6379-83.
217. Alli PM, Pinn ML, Jaffee EM, McFadden JM, Kuhajda FP. Fatty acid synthase inhibitors are chemopreventive for mammary cancer in neu-N transgenic mice. Oncogene. 2005 Jan 6;24(1):39-46.

218. Calame KL, Lin KI, Tunyaplin C. Regulatory mechanisms that determine the development and function of plasma cells. Annu Rev Immunol. 2003;21:205-30.
219. Kenny JJ, Martínez-Maza O, Fehniger T, Ashman RF. Lipid synthesis: an indicator of antigen-induced signal transduction in antigen-binding cells. J Immunol. 1979 Apr;122(4):1278-84.
220. Yaqoob P. Fatty acids as gatekeepers of immune cell regulation. Trends Immunol. 2003 Dec;24(12):639-45.
221. Goldfinger M, Laviad EL, Hadar R, Shmuel M, Dagan A, Park H, Merrill AH Jr, Ringel I, Futerman AH, Tirosh B. De novo ceramide synthesis is required for N-linked glycosylation in plasma cells. J Immunol. 2009 Jun 1;182(11):7038-47.
222. Hannun YA, Obeid LM. Principles of bioactive lipid signalling: lessons from sphingolipids. Nat Rev Mol Cell Biol. 2008 Feb;9(2):139-50.
223. Hermansson M, Hokynar K, Somerharju P. Mechanisms of glycerophospholipid homeostasis in mammalian cells. Prog Lipid Res. 2011 Jul;50(3):240-57.
224. Nohturfft A, Zhang SC. Coordination of lipid metabolism in membrane biogenesis. Annu Rev Cell Dev Biol. 2009;25:539-66.
225. Voelker DR. Phosphatidylserine functions as the major precursor of phosphatidylethanolamine in cultured BHK-21 cells. Proc Natl Acad Sci U S A. 1984 May;81(9):2669-73.
226. Nishizuka Y. Intracellular signaling by hydrolysis of phospholipids and activation of protein kinase C. Science. 1992 Oct 23;258(5082):607-14.
227. Powell KA, Valova VA, Malladi CS, Jensen ON, Larsen MR, Robinson PJ. Phosphorylation of dynamin I on Ser-795 by protein kinase C blocks its association with phospholipids. J Biol Chem. 2000 Apr 21;275(16):11610-7.
228. Nagai Y, Aoki J, Sato T, Amano K, Matsuda Y, Arai H, Inoue K. An alternative splicing form of phosphatidylserine-specific phospholipase A1 that exhibits lysophosphatidylserine-specific lysophospholipase activity in humans. J Biol Chem. 1999 Apr 16;274(16):11053-9.
229. Hamilton RL, Fielding PE. Nascent very low density lipoproteins from rat hepatocytic Golgi fractions are enriched in phosphatidylethanolamine. Biochem Biophys Res Commun. 1989 Apr 14;160(1):162-73.
230. Agren JJ, Hallikainen M, Vidgren H, Miettinen TA, Gylling H. Postprandial lipemic response and lipoprotein composition in subjects with low or high cholesterol absorption efficiency. Clin Chim Acta. 2006 Apr;366(1-2):309-15.
231. Emoto K, Toyama-Sorimachi N, Karasuyama H, Inoue K, Umeda M. Exposure of phosphatidylethanolamine on the surface of apoptotic cells. Exp Cell Res. 1997 May 1;232(2):430-4.
232. Richardson AD, Yang C, Osterman A, Smith JW. Central carbon metabolism in the progression of mammary carcinoma. Breast Cancer Res Treat. 2008 Jul;110(2):297-307.

233. Scott DA, Richardson AD, Filipp FV, Knutzen CA, Chiang GG, Ronai ZA, Osterman AL, Smith JW. Comparative metabolic flux profiling of melanoma cell lines: beyond the Warburg effect. J Biol Chem. 2011 Dec 9;286(49):42626-34.
234. Lee WN, Bassilian S, Ajie HO, Schoeller DA, Edmond J, Bergner EA, Byerley LO. In vivo measurement of fatty acids and cholesterol synthesis using D2O and mass isotopomer analysis. Am J Physiol. 1994 May;266(5 Pt 1):E699-708.
235. Folch J, Lees M, Sloane Stanely GH. A simple method for the isolation and purification of total lipides from animal tissues. J Biol Chem. 1957 May;226(1):497-509.
236. Baek RC, Martin DR, Cox NR, Seyfried TN. Comparative analysis of brain lipids in mice, cats, and humans with Sandhoff disease. Lipids. 2009 Mar;44(3):197-205.
237. Macala LJ, Yu RK, Ando S. Analysis of brain lipids by high performance thin-layer chromatography and densitometry. J Lipid Res. 1983 Sep;24(9):1243-50.
238. Ma Z, Chu CH, Cheng D. A novel direct homogeneous assay for ATP citrate lyase. J Lipid Res. 2009 Oct;50(10):2131-5.
239. Linn TC, Srere PA. Identification of ATP citrate lyase as a phosphoprotein. J Biol Chem. 1979 Mar 10;254(5):1691-8.
240. Tabor H, Tabor CW, Hafner EW. Convenient method for detecting [^{14}C]O_2 in multiple samples: application to rapid screening for mutants. J Bacteriol. 1976 Oct;128(1):485-6.
241. Ardawi MS, Newsholme EA. Maximum activities of some enzymes of glycolysis, the tricarboxylic acid cycle and ketone-body and glutamine utilization pathways in lymphocytes of the rat. Biochem J. 1982 Dec 15;208(3):743-8.
242. Cambier JC, Monroe JG. B cell activation. V. Differentiation signaling of B cell membrane depolarization, increased I-A expression, G0 to G1 transition, and thymidine uptake by anti-IgM and anti-IgD antibodies. J Immunol. 1984 Aug;133(2):576-81.
243. Mizel SB, Wilson L. Inhibition of the transport of several hexoses in mammalian cells by cytochalasin B. J Biol Chem. 1972 Jun 25;247(12):4102-5.
244. Ebstensen RD, Plagemann PG. Cytochalasin B: inhibition of glucose and glucosamine transport. Proc Natl Acad Sci U S A. 1972 Jun;69(6):1430-4.
245. Banchereau J, Brière F, Liu YJ, Rousset F. Molecular control of B lymphocyte growth and differentiation. Stem Cells. 1994 May;12(3):278-88.
246. Ales-Martinez JE, Cuenda E, Gaur A, Scott DW. Prevention of B cell clonal deletion and anergy by activated T cells and their lymphokines. Sem in Immunol 1992; 4 (3):195–205.
247. Mueckler M. Facilitative glucose transporters. Eur J Biochem. 1994 Feb 1;219(3):713-25.

248. Samih N, Hovsepian S, Notel F, Prorok M, Zattara-Cannoni H, Mathieu S, Lombardo D, Fayet G, El-Battari A. The impact of N- and O-glycosylation on the functions of Glut-1 transporter in human thyroid anaplastic cells. Biochim Biophys Acta. 2003 Apr 7;1621(1):92-101.
249. Hresko RC, Kruse M, Strube M, Mueckler M. Topology of the Glut 1 glucose transporter deduced from glycosylation scanning mutagenesis. J Biol Chem. 1994 Aug 12;269(32):20482-8.
250. Devraj K, Klinger ME, Myers RL, Mokashi A, Hawkins RA, Simpson IA. GLUT-1 glucose transporters in the blood-brain barrier: differential phosphorylation. J Neurosci Res. 2011 Dec;89(12):1913-25.
251. Kaplan JH. Biochemistry of Na,K-ATPase. Annu Rev Biochem. 2002;71:511-35.
252. Marakhova I, Karitskaya I, Aksenov N, Zenin V, Vinogradova T. Interleukin-2-dependent regulation of Na/K pump in human lymphocytes. FEBS Lett. 2005 May 23;579(13):2773-80.
253. Ueyama A, Yaworsky KL, Wang Q, Ebina Y, Klip A. GLUT-4myc ectopic expression in L6 myoblasts generates a GLUT-4-specific pool conferring insulin sensitivity. Am J Physiol. 1999 Sep;277(3 Pt 1):E572-8.
254. Kaliman P, Viñals F, Testar X, Palacín M, Zorzano A. Disruption of GLUT1 glucose carrier trafficking in L6E9 and Sol8 myoblasts by the phosphatidylinositol 3-kinase inhibitor wortmannin. Biochem J. 1995 Dec 1;312 (Pt 2):471-7.
255. Wieman HL, Wofford JA, Rathmell JC. Cytokine stimulation promotes glucose uptake via phosphatidylinositol-3 kinase/Akt regulation of Glut1 activity and trafficking. Mol Biol Cell. 2007 Apr;18(4):1437-46.
256. Wieman HL, Horn SR, Jacobs SR, Altman BJ, Kornbluth S, Rathmell JC. An essential role for the Glut1 PDZ-binding motif in growth factor regulation of Glut1 degradation and trafficking. Biochem J. 2009 Mar 1;418(2):345-67.
257. The Jackson Laboratory. Major histocompatibility complex (MHC) H2 haplotypes for 56 inbred strains of mice. MPD:Jax2. Mouse Phenome Database web site, The Jackson Laboratory, Bar Harbor, Maine USA. http://phenome.jax.org, Feb, 2012.
258. Barata JT, Silva A, Brandao JG, Nadler LM, Cardoso AA, Boussiotis VA. Activation of PI3K is indispensable for interleukin 7-mediated viability, proliferation, glucose use, and growth of T cell acute lymphoblastic leukemia cells. J Exp Med. 2004 Sep 6;200(5):659-69.
259. Kan O, Baldwin SA, Whetton AD. Apoptosis is regulated by the rate of glucose transport in an interleukin 3 dependent cell line. J Exp Med. 1994 Sep 1;180(3):917-23.
260. Werner M, Hobeika E, Jumaa H. Role of PI3K in the generation and survival of B cells. Immunol Rev. 2010 Sep;237(1):55-71.
261. Vlahos CJ, Matter WF, Hui KY, Brown RF. A specific inhibitor of phosphatidylinositol 3-kinase, 2-(4-morpholinyl)-8-phenyl-4H-1-benzopyran-4-one (LY294002). J Biol Chem. 1994 Feb 18;269(7):5241-8.

262. Jacobs MD, Black J, Futer O, Swenson L, Hare B, Fleming M, Saxena K. Pim-1 ligand-bound structures reveal the mechanism of serine/threonine kinase inhibition by LY294002. J Biol Chem. 2005 Apr 8;280(14):13728-34
263. Davies SP, Reddy H, Caivano M, Cohen P. Specificity and mechanism of action of some commonly used protein kinase inhibitors. Biochem J. 2000 Oct 1;351(Pt 1):95-105.
264. Brunn GJ, Williams J, Sabers C, Wiederrecht G, Lawrence JC Jr, Abraham RT. Direct inhibition of the signaling functions of the mammalian target of rapamycin by the phosphoinositide 3-kinase inhibitors, wortmannin and LY294002. EMBO J. 1996 Oct 1;15(19):5256-67.
265. Powis G, Bonjouklian R, Berggren MM, Gallegos A, Abraham R, Ashendel C, Zalkow L, Matter WF, Dodge J, Grindey G, Vlahos CJ. Wortmannin, a potent and selective inhibitor of phosphatidylinositol-3-kinase. Cancer Res. 1994 May 1;54(9):2419-23.
266. Wymann MP, Bulgarelli-Leva G, Zvelebil MJ, Pirola L, Vanhaesebroeck B, Waterfield MD, Panayotou G. Wortmannin inactivates phosphoinositide 3-kinase by covalent modification of Lys-802, a residue involved in the phosphate transfer reaction. Mol Cell Biol. 1996 Apr;16(4):1722-33.
267. Srinivasan L, Sasaki Y, Calado DP, Zhang B, Paik JH, DePinho RA, Kutok JL, Kearney JF, Otipoby KL, Rajewsky K. PI3 kinase signals BCR-dependent mature B cell survival. Cell. 2009 Oct 30;139(3):573-86.
268. Vanhaesebroeck B, Leevers SJ, Ahmadi K, Timms J, Katso R, Driscoll PC, Woscholski R, Parker PJ, Waterfield MD. Synthesis and function of 3-phosphorylated inositol lipids. Annu Rev Biochem. 2001;70:535-602.
269. Ikezoe T, Nishioka C, Bandobashi K, Yang Y, Kuwayama Y, Adachi Y, Takeuchi T, Koeffler HP, Taguchi H. Longitudinal inhibition of PI3K/Akt/mTOR signaling by LY294002 and rapamycin induces growth arrest of adult T-cell leukemia cells. Leuk Res. 2007 May;31(5):673-82.
270. Fruman DA, Bismuth G. Fine tuning the immune response with PI3K. Immunol Rev. 2009 Mar;228(1):253-72.
271. Fruman DA, Snapper SB, Yballe CM, Alt FW, Cantley LC. Phosphoinositide 3-kinase knockout mice: role of p85alpha in B cell development and proliferation. Biochem Soc Trans. 1999 Aug;27(4):624-9.
272. Tsukada S, Baba Y, Watanabe D. Btk and BLNK in B cell development. Adv Immunol. 2001;77:123-62.
273. Wortis HH, Teutsch M, Higer M, Zheng J, Parker DC. B-cell activation by crosslinking of surface IgM or ligation of CD40 involves alternative signal pathways and results in different B-cell phenotypes. Proc Natl Acad Sci U S A. 1995 Apr 11;92(8):3348-52.
274. Tumang JR, Owyang A, Andjelic S, Jin Z, Hardy RR, Liou ML, Liou HC. c-Rel is essential for B lymphocyte survival and cell cycle progression. Eur J Immunol. 1998 Dec;28(12):4299-312.

275. Woodland RT, Fox CJ, Schmidt MR, Hammerman PS, Opferman JT, Korsmeyer SJ, Hilbert DM, Thompson CB. Multiple signaling pathways promote B lymphocyte stimulator dependent B-cell growth and survival. Blood. 2008 Jan 15;111(2):750-60.
276. Pelicano H, Martin DS, Xu RH, Huang P. Glycolysis inhibition for anticancer treatment. Oncogene. 2006 Aug 7;25(34):4633-46.
277. Pedersen PL. Warburg, me and Hexokinase 2: Multiple discoveries of key molecular events underlying one of cancers' most common phenotypes, the "Warburg Effect", i.e., elevated glycolysis in the presence of oxygen. J Bioenerg Biomembr. 2007 Jun;39(3):211-22.
278. Schmidt MM, Dringen R. Differential effects of iodoacetamide and iodoacetate on glycolysis and glutathione metabolism of cultured astrocytes. Front Neuroenergetics. 2009;1:1.
279. Davis B, Lazarus NR. An in vitro system for studying insulin release: effects of glucose and glucose-6-phosphate. J Physiol. 1977 Sep;271(1):273-88.
280. Ashcroft SJ, Weerasinghe LC, Bassett JM, Randle PJ. The pentose cycle and insulin release in mouse pancreatic islets. Biochem J. 1972 Feb;126(3):525-32.
281. Chiu CW, Dalton M, Ishiai M, Kurosaki T, Chan AC. BLNK: molecular scaffolding through 'cis'-mediated organization of signaling proteins. EMBO J. 2002 Dec 2;21(23):6461-72.
282. Imai C, Ross ME, Reid G, Coustan-Smith E, Schultz KR, Pui CH, Downing JR, Campana D. Expression of the adaptor protein BLNK/SLP-65 in childhood acute lymphoblastic leukemia. Leukemia. 2004 May;18(5):922-5.
283. Ying H, Li Z, Yang L, Zhang J. Syk mediates BCR- and CD40-signaling integration during B cell activation. Immunobiology. 2011 May;216(5):566-70.
284. Mizuno T, Rothstein TL. B cell receptor (BCR) cross-talk: CD40 engagement creates an alternate pathway for BCR signaling that activates I kappa B kinase/I kappa B alpha/NF-kappa B without the need for PI3K and phospholipase C gamma. J Immunol. 2005 May 15;174(10):6062-70.
285. Scharenberg AM, Kinet JP. PtdIns-3,4,5-P3: a regulatory nexus between tyrosine kinases and sustained calcium signals. Cell. 1998 Jul 10;94(1):5-8.
286. Gschwendt M, Müller HJ, Kielbassa K, Zang R, Kittstein W, Rincke G, Marks F. Rottlerin, a novel protein kinase inhibitor. Biochem Biophys Res Commun. 1994 Feb 28;199(1):93-8.
287. Kontny E, Kurowska M, Szczepańska K, Maśliński W. Rottlerin, a PKC isozyme-selective inhibitor, affects signaling events and cytokine production in human monocytes. J Leukoc Biol. 2000 Feb;67(2):249-58.
288. Soltoff SP. Rottlerin: an inappropriate and ineffective inhibitor of PKCdelta. Trends Pharmacol Sci. 2007 Sep;28(9):453-8.
289. Takeda K, Tanaka T, Shi W, Matsumoto M, Minami M, Kashiwamura S, Nakanishi K, Yoshida N, Kishimoto T, Akira S. Essential role of Stat6 in IL-4 signalling. Nature. 1996 Apr 18;380(6575):627-30.

290. Mori M, Morris SC, Orekhova T, Marinaro M, Giannini E, Finkelman FD. IL-4 promotes the migration of circulating B cells to the spleen and increases splenic B cell survival. J Immunol. 2000 Jun 1;164(11):5704-12.
291. Hirayama T, Dai S, Abbas S, Yamanaka Y, Abu-Amer Y. Inhibition of inflammatory bone erosion by constitutively active STAT-6 through blockade of JNK and NF-kappaB activation. Arthritis Rheum. 2005 Sep;52(9):2719-29.
292. Schwarze SR, Hruska KA, Dowdy SF. Protein transduction: unrestricted delivery into all cells? Trends Cell Biol. 2000 Jul;10(7):290-5.
293. Frankel AD, Pabo CO. Cellular uptake of the tat protein from human immunodeficiency virus. Cell. 1988 Dec 23;55(6):1189-93.
294. Mathupala SP, Rempel A, Pedersen PL. Glucose catabolism in cancer cells. Isolation, sequence, and activity of the promoter for type II hexokinase. J Biol Chem. 1995 Jul 14;270(28):16918-25.
295. Mathupala SP, Rempel A, Pedersen PL. Glucose catabolism in cancer cells: identification and characterization of a marked activation response of the type II hexokinase gene to hypoxic conditions. J Biol Chem. 2001 Nov 16;276(46):43407-12.
296. Wilson JE. Isozymes of mammalian hexokinase: structure, subcellular localization and metabolic function. J Exp Biol. 2003 Jun;206(Pt 12):2049-57.
297. Chehtane M, Khaled AR. Interleukin-7 mediates glucose utilization in lymphocytes through transcriptional regulation of the hexokinase II gene. Am J Physiol Cell Physiol. 2010 Jun;298(6):C1560-71.
298. Markert CL. Lactate dehydrogenase. Biochemistry and function of lactate dehydrogenase. Cell Biochem Funct. 1984 Jul;2(3):131-4.
299. Alcazar O, Tiedge M, Lenzen S. Importance of lactate dehydrogenase for the regulation of glycolytic flux and insulin secretion in insulin-producing cells. Biochem J. 2000 Dec 1;352 Pt 2:373-80.
300. Zhu X, Hart R, Chang MS, Kim JW, Lee SY, Cao YA, Mock D, Ke E, Saunders B, Alexander A, Grossoehme J, Lin KM, Yan Z, Hsueh R, Lee J, Scheuermann RH, Fruman DA, Seaman W, Subramaniam S, Sternweis P, Simon MI, Choi S. Analysis of the major patterns of B cell gene expression changes in response to short-term stimulation with 33 single ligands. J Immunol. 2004 Dec 15;173(12):7141-9.
301. Pan L, Beverley PC, Isaacson PG. Lactate dehydrogenase (LDH) isoenzymes and proliferative activity of lymphoid cells--an immunocytochemical study. Clin Exp Immunol. 1991 Nov;86(2):240-5.
302. Boag JM, Beesley AH, Firth MJ, Freitas JR, Ford J, Hoffmann K, Cummings AJ, de Klerk NH, Kees UR. Altered glucose metabolism in childhood pre-B acute lymphoblastic leukaemia. Leukemia. 2006 Oct;20(10):1731-7.
303. Rambotti P, Davis S. Lactic dehydrogenase in normal and leukemia lymphocyte subpopulations: evidence for the presence of abnormal T cells and B cells in chronic lymphocytic leukemia. Blood. 1981 Feb;57(2):324-7.

304. Blenk S, Engelmann J, Weniger M, Schultz J, Dittrich M, Rosenwald A, Müller-Hermelink HK, Müller T, Dandekar T. Germinal center B cell-like (GCB) and activated B cell-like (ABC) type of diffuse large B cell lymphoma (DLBCL): analysis of molecular predictors, signatures, cell cycle state and patient survival. Cancer Inform. 2007 Dec 12;3:399-420.
305. Bustin SA, Benes V, Nolan T, Pfaffl MW. Quantitative real-time RT-PCR--a perspective. J Mol Endocrinol. 2005 Jun;34(3):597-601.
306. Krejci O, Prouzova Z, Horvath O, Trka J, Hrusak O. Cutting edge: TCR delta gene is frequently rearranged in adult B lymphocytes. J Immunol. 2003 Jul 15;171(2):524-7.
307. Gottlob K, Majewski N, Kennedy S, Kandel E, Robey RB, Hay N. Inhibition of early apoptotic events by Akt/PKB is dependent on the first committed step of glycolysis and mitochondrial hexokinase. Genes Dev. 2001 Jun 1;15(11):1406-18.
308. Pastorino JG, Shulga N, Hoek JB. Mitochondrial binding of hexokinase II inhibits Bax-induced cytochrome c release and apoptosis. J Biol Chem. 2002 Mar 1;277(9):7610-8.
309. Majewski N, Nogueira V, Bhaskar P, Coy PE, Skeen JE, Gottlob K, Chandel NS, Thompson CB, Robey RB, Hay N. Hexokinase-mitochondria interaction mediated by Akt is required to inhibit apoptosis in the presence or absence of Bax and Bak. Mol Cell. 2004 Dec 3;16(5):819-30.
310. Majewski N, Nogueira V, Robey RB, Hay N. Akt inhibits apoptosis downstream of BID cleavage via a glucose-dependent mechanism involving mitochondrial hexokinases. Mol Cell Biol. 2004 Jan;24(2):730-40.
311. Arora KK, Pedersen PL. Functional significance of mitochondrial bound hexokinase in tumor cell metabolism. Evidence for preferential phosphorylation of glucose by intramitochondrially generated ATP. J Biol Chem. 1988 Nov 25;263(33):17422-8.
312. Nista A, De Martino C, Malorni W, Marcante ML, Silvestrini B, Floridi A. Effect of lonidamine on the aerobic glycolysis of normal and phytohemagglutinin-stimulated human peripheral blood lymphocytes. Exp Mol Pathol. 1985 Apr;42(2):194-205.
313. Guppy M, Greiner E, Brand K. The role of the Crabtree effect and an endogenous fuel in the energy metabolism of resting and proliferating thymocytes. Eur J Biochem. 1993 Feb 15;212(1):95-9.
314. Katz J, Wood HG. The use of C14O2 yields from glucose-1- and -6-C14 for the evaluation of the pathways of glucose metabolism. J Biol Chem. 1963 Feb;238:517-23.
315. Stryer L. *Biochemistry* 4th Ed, W.H. Freeman 1995
316. Segal S, Berman M, Blair A. The metabolism of variously C14-labeled glucose in man and an estimation of the extent of glucose metabolism by the hexose monophosphate pathway. J Clin Invest. 1961 Jul;40:1263-79.
317. Schuit F, De Vos A, Farfari S, Moens K, Pipeleers D, Brun T, Prentki M. Metabolic fate of glucose in purified islet cells. Glucose-regulated anaplerosis in beta cells. J Biol Chem. 1997 Jul 25;272(30):18572-9.

318. Lagoo A, Tseng CK, Sell S. Molecular signals in B cell activation. II. IL-2-mediated signals are required in late G1 for transition to S phase after ionomycin and PMA treatment. Cell Immunol. 1990 May;127(2):497-505.
319. Rothstein TL, Baeker TR, Miller RA, Kolber DL. Stimulation of murine B cells by the combination of calcium ionophore plus phorbol ester. Cell Immunol. 1986 Oct 15;102(2):364-73.
320. Castagna M, Takai Y, Kaibuchi K, Sano K, Kikkawa U, Nishizuka Y. Direct activation of calcium-activated, phospholipid-dependent protein kinase by tumor-promoting phorbol esters. J Biol Chem. 1982 Jul 10;257(13):7847-51.
321. Miller RA. Calcium signals in T lymphocytes from old mice. Life Sci. 1996;59(5-6):469-75.
322. Hunting D, Gowans B, Henderson JF. Effects of 6-aminonicotinamide on cell growth, poly(ADP-ribose) synthesis and nucleotide metabolism. Biochem Pharmacol. 1985 Nov 15;34(22):3999-4003.
323. Wiest DL, Burkhardt JK, Hester S, Hortsch M, Meyer DI, Argon Y. Membrane biogenesis during B cell differentiation: most endoplasmic reticulum proteins are expressed coordinately. J Cell Biol. 1990 May;110(5):1501-11.
324. Icard P, Poulain L, Lincet H. Understanding the central role of citrate in the metabolism of cancer cells. Biochim Biophys Acta. 2012 Jan;1825(1):111-6.
325. Towle HC, Kaytor EN, Shih HM. Regulation of the expression of lipogenic enzyme genes by carbohydrate. Annu Rev Nutr. 1997;17:405-33.
326. Ki SW, Ishigami K, Kitahara T, Kasahara K, Yoshida M, Horinouchi S. Radicicol binds and inhibits mammalian ATP citrate lyase. J Biol Chem. 2000 Dec 15;275(50):39231-6.
327. Ramakrishna S, Benjamin WB. Cyclic nucleotide-independent protein kinase from rat liver. Purification and characterization of a multifunctional protein kinase. J Biol Chem. 1985 Oct 5;260(22):12280-6.
328. Ramakrishna S, D'Angelo G, Benjamin WB. Sequence of sites on ATP-citrate lyase and phosphatase inhibitor 2 phosphorylated by multifunctional protein kinase (a glycogen synthase kinase 3 like kinase). Biochemistry. 1990 Aug 21;29(33):7617-24.
329. Price DJ, Nemenoff RA, Avruch J. Purification of a hepatic S6 kinase from cycloheximide-treated rats. J Biol Chem. 1989 Aug 15;264(23):13825-33.
330. Alessi DR, Andjelkovic M, Caudwell B, Cron P, Morrice N, Cohen P, Hemmings BA. Mechanism of activation of protein kinase B by insulin and IGF-1. EMBO J. 1996 Dec 2;15(23):6541-51.
331. Laplante M, Sabatini DM. An emerging role of mTOR in lipid biosynthesis. Curr Biol. 2009 Dec 1;19(22):R1046-52.
332. Terauchi Y, Tsuji Y, Satoh S, Minoura H, Murakami K, Okuno A, Inukai K, Asano T, Kaburagi Y, Ueki K, Nakajima H, Hanafusa T, Matsuzawa Y, Sekihara H, Yin Y, Barrett JC, Oda H, Ishikawa T, Akanuma Y, Komuro I, Suzuki M, Yamamura K, Kodama T, Suzuki H, Yamamura K, Kodama T, Suzuki H, Koyasu S, Aizawa S, Tobe K, Fukui Y, Yazaki Y, Kadowaki T. Increased insulin sensitivity and hypoglycaemia in mice lacking the p85 alpha subunit of phosphoinositide 3-kinase. Nat Genet. 1999 Feb;21(2):230-5.

333. Dye JR, Palvanov A, Guo B, Rothstein TL. B cell receptor cross-talk: exposure to lipopolysaccharide induces an alternate pathway for B cell receptor-induced ERK phosphorylation and NF-kappa B activation. J Immunol. 2007 Jul 1;179(1):229-35.
334. Hebeis BJ, Vigorito E, Turner M. The p110delta subunit of phosphoinositide 3-kinase is required for the lipopolysaccharide response of mouse B cells. Biochem Soc Trans. 2004 Nov;32(Pt 5):789-91.
335. DeFranco AL, Raveche ES, Paul WE. Separate control of B lymphocyte early activation and proliferation in response to anti-IgM antibodies. J Immunol. 1985 Jul;135(1):87-94.
336. Sieckmann DG. The use of anti-immunoglobulins to induce a signal for cell division in B lymphocytes via their membrane IgM and IgD. Immunol Rev. 1980;52:181-210.
337. Jackowski S. Coordination of membrane phospholipid synthesis with the cell cycle. J Biol Chem. 1994 Feb 4;269(5):3858-67.
338. Carpenter CL. Btk-dependent regulation of phosphoinositide synthesis. Biochem Soc Trans. 2004 Apr;32(Pt 2):326-9.
339. Kent C. Eukaryotic phospholipid biosynthesis. Annu Rev Biochem. 1995;64:315-43.
340. Sullivan AC, Triscari J, Hamilton JG, Miller ON, Wheatley VR. Effect of (-)-hydroxycitrate upon the accumulation of lipid in the rat. I. Lipogenesis. Lipids. 1974 Feb;9(2):121-8.
341. Patel MS, Owen OE. Lipogenesis from ketone bodies in rat brain. Evidence for conversion of acetoacetate into acetyl-coenzyme A in the cytosol. Biochem J. 1976 Jun 15;156(3):603-7.
342. Neskovic N, Sarlieve L, Nussbaum JL, Kostic D, Mandel P. Quantitative thin-layer chromatography of glycolipids in animal tissues. Clin Chim Acta. 1972 Apr;38(1):147-53.
343. Valls JE, Bello RA, Kodaira MS. Semiquantitative analysis by thin-layer chromatography (TLC) of biogenic amines in dried, salted and canned fish products. J Food Quality 2002 May;25(2):165–176.
344. Dittmer JC, Lester RL. A simple, specific spray for the detection of phospholipids on thin-layer chromatograms. J Lipid Res. 1964 Jan;15:126-7.
345. DeBerardinis RJ, Mancuso A, Daikhin E, Nissim I, Yudkoff M, Wehrli S, Thompson CB. Beyond aerobic glycolysis: transformed cells can engage in glutamine metabolism that exceeds the requirement for protein and nucleotide synthesis. Proc Natl Acad Sci U S A. 2007 Dec 4;104(49):19345-50.
346. Gao P, Tchernyshyov I, Chang TC, Lee YS, Kita K, Ochi T, Zeller KI, De Marzo AM, Van Eyk JE, Mendell JT, Dang CV. c-Myc suppression of miR-23a/b enhances mitochondrial glutaminase expression and glutamine metabolism. Nature. 2009 Apr 9;458(7239):762-5.
347. Yang C, Sudderth J, Dang T, Bachoo RM, McDonald JG, DeBerardinis RJ. Glioblastoma cells require glutamate dehydrogenase to survive impairments of glucose metabolism or Akt signaling. Cancer Res. 2009 Oct 15;69(20):7986-93.

348. Wellen KE, Lu C, Mancuso A, Lemons JM, Ryczko M, Dennis JW, Rabinowitz JD, Coller HA, Thompson CB. The hexosamine biosynthetic pathway couples growth factor-induced glutamine uptake to glucose metabolism. Genes Dev. 2010 Dec 15;24(24):2784-99.
349. Holleran AL, Briscoe DA, Fiskum G, Kelleher JK. Glutamine metabolism in AS-30D hepatoma cells. Evidence for its conversion into lipids via reductive carboxylation. Mol Cell Biochem. 1995 Nov 22;152(2):95-101.
350. Yoo H, Antoniewicz MR, Stephanopoulos G, Kelleher JK. Quantifying reductive carboxylation flux of glutamine to lipid in a brown adipocyte cell line. J Biol Chem. 2008 Jul 25;283(30):20621-7.
351. Metallo CM, Gameiro PA, Bell EL, Mattaini KR, Yang J, Hiller K, Jewell CM, Johnson ZR, Irvine DJ, Guarente L, Kelleher JK, Vander Heiden MG, Iliopoulos O, Stephanopoulos G. Reductive glutamine metabolism by IDH1 mediates lipogenesis under hypoxia. Nature. 2011 Nov 20;481(7381):380-4.
352. Hiller K, Metallo CM, Kelleher JK, Stephanopoulos G. Nontargeted elucidation of metabolic pathways using stable-isotope tracers and mass spectrometry. Anal Chem. 2010 Aug 1;82(15):6621-8.
353. Jacobs SR, Michalek RD, Rathmell JC. IL-7 is essential for homeostatic control of T cell metabolism in vivo. J Immunol. 2010 Apr 1;184(7):3461-9.
354. Rodríguez-Enríquez S, Juárez O, Rodríguez-Zavala JS, Moreno-Sánchez R. Multisite control of the Crabtree effect in ascites hepatoma cells. Eur J Biochem. 2001 Apr;268(8):2512-9.
355. Dell' Antone P. Energy metabolism in cancer cells: How to explain the Warburg and Crabtree effects? Med Hypotheses. 2012 Jul 5.
356. Diaz-Ruiz R, Rigoulet M, Devin A. The Warburg and Crabtree effects: On the origin of cancer cell energy metabolism and of yeast glucose repression. Biochim Biophys Acta. 2011 Jun;1807(6):568-76.
357. Buttgereit F, Burmester GR, Brand MD. Bioenergetics of immune functions: fundamental and therapeutic aspects. Immunol Today. 2000 Apr;21(4):192-9.
358. Elstrom RL, Bauer DE, Buzzai M, Karnauskas R, Harris MH, Plas DR, Zhuang H, Cinalli RM, Alavi A, Rudin CM, Thompson CB. Akt stimulates aerobic glycolysis in cancer cells. Cancer Res. 2004 Jun 1;64(11):3892-9.
359. Patke A, Mecklenbräuker I, Erdjument-Bromage H, Tempst P, Tarakhovsky A. BAFF controls B cell metabolic fitness through a PKC beta- and Akt-dependent mechanism. J Exp Med. 2006 Oct 30;203(11):2551-62.
360. Minich WB, Balasta ML, Goss DJ, Rhoads RE. Chromatographic resolution of in vivo phosphorylated and nonphosphorylated eukaryotic translation initiation factor eIF-4E: increased cap affinity of the phosphorylated form. Proc Natl Acad Sci U S A. 1994 Aug 2;91(16):7668-72.
361. Ruggero D, Sonenberg N. The Akt of translational control. Oncogene. 2005 Nov 14;24(50):7426-34.
362. Brunet A, Bonni A, Zigmond MJ, Lin MZ, Juo P, Hu LS, Anderson MJ, Arden KC, Blenis J, Greenberg ME. Akt promotes cell survival by phosphorylating and inhibiting a Forkhead transcription factor. Cell. 1999 Mar 19;96(6):857-68.

363. Potter CJ, Pedraza LG, Xu T. Akt regulates growth by directly phosphorylating Tsc2. Nat Cell Biol. 2002 Sep;4(9):658-65.
364. Bone H, Williams NA. Antigen-receptor cross-linking and lipopolysaccharide trigger distinct phosphoinositide 3-kinase-dependent pathways to NF-kappa B activation in primary B cells. Int Immunol. 2001 Jun;13(6):807-16.
365. Glynne R, Ghandour G, Rayner J, Mack DH, Goodnow CC. B-lymphocyte quiescence, tolerance and activation as viewed by global gene expression profiling on microarrays.Immunol Rev. 2000 Aug;176:216-46.
366. Romashkova JA, Makarov SS. NF-kappaB is a target of AKT in anti-apoptotic PDGF signalling. Nature. 1999 Sep 2;401(6748):86-90.
367. Wang D, Sul HS. Insulin stimulation of the fatty acid synthase promoter is mediated by the phosphatidylinositol 3-kinase pathway. Involvement of protein kinase B/Akt. J Biol Chem. 1998 Sep 25;273(39):25420-6.
368. Zong WX, Edelstein LC, Chen C, Bash J, Gélinas C. The prosurvival Bcl-2 homolog Bfl-1/A1 is a direct transcriptional target of NF-kappaB that blocks TNFalpha-induced apoptosis. Genes Dev. 1999 Feb 15;13(4):382-7.
369. Habib T, Park H, Tsang M, de Alborán IM, Nicks A, Wilson L, Knoepfler PS, Andrews S, Rawlings DJ, Eisenman RN, Iritani BM. Myc stimulates B lymphocyte differentiation and amplifies calcium signaling. J Cell Biol. 2007 Nov 19;179(4):717-31.
370. Newsholme EA, Crabtree B, Ardawi MS. The role of high rates of glycolysis and glutamine utilization in rapidly dividing cells. Biosci Rep. 1985 May;5(5):393-400.
371. Kim JW, Zeller KI, Wang Y, Jegga AG, Aronow BJ, O'Donnell KA, Dang CV. Evaluation of myc E-box phylogenetic footprints in glycolytic genes by chromatin immunoprecipitation assays. Mol Cell Biol. 2004 Jul;24(13):5923-36.
372. Lewis JT, Dayanandan B, Habener JF, Kieffer TJ. Glucose-dependent insulinotropic polypeptide confers early phase insulin release to oral glucose in rats: demonstration by a receptor antagonist. Endocrinology. 2000 Oct;141(10):3710-6.
373. Eilers M, Eisenman RN. Myc's broad reach. Genes Dev. 2008 Oct 15;22(20):2755-66.
374. Dang CV. Links between metabolism and cancer. Genes Dev. 2012 May 1;26(9):877-90.
375. Le A, Lane AN, Hamaker M, Bose S, Gouw A, Barbi J, Tsukamoto T, Rojas CJ, Slusher BS, Zhang H, Zimmerman LJ, Liebler DC, Slebos RJ, Lorkiewicz PK, Higashi RM, Fan TW, Dang CV. Glucose-independent glutamine metabolism via TCA cycling for proliferation and survival in B cells. Cell Metab. 2012 Jan 4;15(1):110-21.
376. Kim JW, Gao P, Liu YC, Semenza GL, Dang CV. Hypoxia-inducible factor 1 and dysregulated c-Myc cooperatively induce vascular endothelial growth factor and metabolic switches hexokinase 2 and pyruvate dehydrogenase kinase 1. Mol Cell Biol. 2007 Nov;27(21):7381-93. 320.

377. Dufort FJ, Bleiman BF, Gumina MR, Blair D, Wagner DJ, Roberts MF, Abu-Amer Y, Chiles TC. Cutting edge: IL-4-mediated protection of primary B lymphocytes from apoptosis via Stat6-dependent regulation of glycolytic metabolism. J Immunol. 2007 Oct 15;179(8):4953-7.
378. Pracht C, Minguet S, Leitges M, Reth M, Huber M. Association of protein kinase C-delta with the B cell antigen receptor complex. Cell Signal. 2007 Apr;19(4):715-22.
379. Parlo RA, Coleman PS. Enhanced rate of citrate export from cholesterol-rich hepatoma mitochondria. The truncated Krebs cycle and other metabolic ramifications of mitochondrial membrane cholesterol. J Biol Chem. 1984 Aug 25;259(16):9997-10003.
380. Kannan R, Learn DB, Baker N, Elovson J. Fatty acid synthesis in vivo and hepatic contribution to whole-body lipogenic rates in obese Zucker rats. Lipids. 1980 Dec;15(12):993-8.
381. Ookhtens M, Kannan R, Lyon I, Baker N. Liver and adipose tissue contributions to newly formed fatty acids in an ascites tumor. Am J Physiol. 1984 Jul;247(1 Pt 2):R146-53.
382. Schuhmacher M, Kohlhuber F, Hölzel M, Kaiser C, Burtscher H, Jarsch M, Bornkamm GW, Laux G, Polack A, Weidle UH, Eick D. The transcriptional program of a human B cell line in response to Myc. Nucleic Acids Res. 2001 Jan 15;29(2):397-406.
383. Morrish F, Neretti N, Sedivy JM, Hockenbery DM. The oncogene c-Myc coordinates regulation of metabolic networks to enable rapid cell cycle entry. Cell Cycle. 2008 Apr 15;7(8):1054-66.
384. Hunt AN, Fenn HC, Clark GT, Wright MM, Postle AD, McMaster CR. Lipidomic analysis of the molecular specificity of a cholinephosphotransferase in situ. Biochem Soc Trans. 2004 Dec;32(Pt 6):1060-2.
385. Morrish F, Isern N, Sadilek M, Jeffrey M, Hockenbery DM. c-Myc activates multiple metabolic networks to generate substrates for cell-cycle entry. Oncogene. 2009 Jul 9;28(27):2485-91.
386. Berkhout TA, Havekes LM, Pearce NJ, Groot PH. The effect of (-)-hydroxycitrate on the activity of the low-density-lipoprotein receptor and 3-hydroxy-3-methylglutaryl-CoA reductase levels in the human hepatoma cell line Hep G2. Biochem J. 1990 Nov 15;272(1):181-6.
387. Mosca E, Barcella M, Alfieri R, Bevilacqua A, Canti G, Milanesi L. Systems biology of the metabolic network regulated by the Akt pathway. Biotechnol Adv. 2012 Jan;30(1):131-41.
388. Stockdale AM, Dul JL, Wiest DL, Digel M, Argon Y. The expression of membrane and secreted immunoglobulin during the in vitro differentiation of the murine B cell lymphoma CH12. J Immunol. 1987 Nov15;139(10):3527-35.
389. Klein B, Tarte K, Jourdan M, Mathouk K, Moreaux J, Jourdan E, Legouffe E, De Vos J, Rossi JF. Survival and proliferation factors of normal and malignant plasma cells. Int J Hematol. 2003 Aug;78(2):106-13.

390. Swinnen JV, Brusselmans K, Verhoeven G. Increased lipogenesis in cancer cells: new players, novel targets. Curr Opin Clin Nutr Metab Care. 2006 Jul;9(4):358-65.
391. Tong X, Zhao F, Thompson CB. The molecular determinants of de novo nucleotide biosynthesis in cancer cells. Curr Opin Genet Dev. 2009 Feb;19(1):32-7.
392. Beckner ME, Fellows-Mayle W, Zhang Z, Agostino NR, Kant JA, Day BW, Pollack IF. Identification of ATP citrate lyase as a positive regulator of glycolytic function in glioblastomas. Int J Cancer. 2010 May 15;126(10):2282-95.
393. Zu XY, Zhang QH, Liu JH, Cao RX, Zhong J, Yi GH, Quan ZH, Pizzorno G. ATP citrate lyase inhibitors as novel cancer therapeutic agents. Recent Pat Anticancer Drug Discov. 2012 May 1;7(2):154-67.